CTE / NCDOT
Joint Environmental Research Program

Final Report

Methodology to Assess Soil, Hydrologic, and Site Parameters that Affect Wetland Restoration: Phase 2

Prepared By

M.J. Vepraskas, J.G. White, A. Amoozegar, D.L. Hesterberg, R.L. Huffman, R.W. Skaggs, J.D. Gregory, S.W. Broome, P.V. Caldwell, K.M. Davis, S. Abit, H.C. Smith, A.J. Zelasko, and C.S. Brownfield.

North Carolina State University
Departments of Soil Science, Biological and Agricultural Engineering, and Forestry
Box 7619
Raleigh, NC 27695-7619

August 2007

1. Report No.
FHWA/NC/2006-47

2. Government Accession No.

3. Recipient's Catalog No.

4. Title and Subtitle
Methodology to Assess Soil, Hydrologic, and Site Parameters that Affect Wetland Restoration: Phase 2

5. Report Date
August 2007

6. Performing Organization Code

7. Author(s)
M. J. Vepraskas et al.

8. Performing Organization Report No.

9. Performing Organization Name and Address
North Carolina State University
Dep. of Soil Science
Box 7619
Raleigh, NC 27695-7619

10. Work Unit No. (TRAIS)

11. Contract or Grant No.

12. Sponsoring Agency Name and Address
North Carolina Department of Transportation
Research and Analysis Group
1 South Wilmington Street
Raleigh, North Carolina 27601

13. Type of Report and Period Covered
Final Report
July 1, 2003 to June 30, 2007

14. Sponsoring Agency Code
2004-19

Supplementary Notes:

16. Abstract

Juniper Bay is a 750 acre Carolina Bay that was purchased by the NC Department of Transportation for wetland restoration. The experimental results reported here were completed at the site between 2003 and 2007, that were completed at Juniper Bay and at three reference bays. Hydrologic studies showed that a Pond Pine Woodland plant community is growing in reference bays where water ponds above the surface for 45 to 135 days per year. At Juniper Bay, such conditions may occur in the mineral soils along the bay's perimeter. The Nonriverine Swamp Forest community is found in organic soils that have water ponded on the surface for 300-320 days per year. This community may develop in the central portion of Juniper Bay. Because soil organic carbon levels in Juniper Bay soils generally exceed 3%, the soils should become anaerobic within a week after saturating. Other related biogeochemical reactions necessary for wetland functions should occur in Juniper Bay soils as well. Large storms (greater than 2 in. per day) cause relatively large quantities of dissolved organic carbon, phosphorus, calcium and magnesium to enter surface and ground waters at Juniper Bay. These chemical may be transported offsite in ditch water leaving the site. The quantity of phosphorus can exceed 1 ppm in organic soils because of the large amount of dissolved organic carbon produced in the soils. These phosphorus concentrations should be monitored because they may be large enough to contribute to eutrophication of downstream waters.

17. Key Words
Natural resources, ecosystems, environmental quality, land use

18. Distribution Statement

19. Security Classif. (of this report)
Unclassified

20. Security Classif. (of this page)
Unclassified

21. No. of Pages
241

22. Price

Form DOT F 1700.7 (8-72) **Reproduction of completed page authorized**

DISCLAIMER

ACKNOWLEGEMENTS

We would like to thank the Technical Advisory Committee for assisting in this research. The committee members include: James Hauser (chair), Gordon Cashin, Matt Flint, David Henderson, LeiLani Paugh, Jason Elliott, Randy Griffin, Elizabeth Lusk, Phil Harris, Elizabeth Lusk, Moy Biswas, Dennis Pipkin, and Mustan Kadibhai.

From NC State University, this project was conducted by a number of graduate students and technicians. Alex Adams led the support initially, and he was followed by Gary Kreiser and Chris Niewoehner. Without their leadership and service this project would not have been completed. James Cox and Bryan Roberts were also essential in supporting numerous field efforts.

EXECUTIVE SUMMARY

Juniper Bay is a 750 acre Carolina Bay that was purchased by the NC Department of Transportation for wetland restoration. This report summarizes studies done on the soils and hydrology at Juniper Bay as well as at three reference bays that contain target plant communities. A previous report reviewed Juniper Bay's history, geology, hydrology, soils, and also provides data on the target or reference areas that the Bay will be restored to. Principle findings from this study are summarized below with implications for management of Juniper Bay noted.

Three reference bays in Bladen County, NC were studied to document the hydrologies needed to reestablish the target vegetation at Juniper Bay. The references bays had four three different plant communities that were evaluated: Pond Pine Woodland, Nonriverine Swamp Forest, and Bay Forest. It was found from the reference bay investigations that the hydrologies for these plant communities are as follows:

a. Where the thickness of organic soil layers is less than 16 in. (40 cm) and the median hydroperiod (i.e. when the water table is above the land surface) is 45-135 days per water year, then tree species typical of the Pond Pine Woodland community should be planted there.

b. Where organic soil layers between approximately 8 and 31 in. (20 and 80 cm) thick, phosphorus levels greater than 18 mg dm^{-3}, and a median hydroperiod of 300-320 days per water year, the Nonriverine Swamp Forest community would be a good choice for restoration.

c. Where soils have similar hydroperiods to those of "b", but with organic layer thicknesses greater than 31 in. (80 cm) and phosphorus levels below 18 mg dm^{-3}, the Bay Forest community would be recommended.

At this time, it appears that the Pond Pine Woodland community will tend to grow in the mineral soils near the edge of the bay, with the Nonriverine Swamp Forest community growing in the organic soils at the center of the bay that are ponded for extended periods.

Field and laboratory studies showed that the time for anaerobic conditions (and and other critical wetland chemical reactions) to develop after saturation begins (Lag time) was related to soil organic C percentage but not to average daily temperature. When soil organic carbon was <3%, the Lag values ranged from 3 to 48 d. Soils containing higher soil organic carbon concentrations had Lag values being 5 d or less in most cases. These results suggest that in created wetlands the minimum amount of soil organic C needed to ensure wetland biogeochemical functions occur is 3%. There appears to be little advantage to having higher organic C levels, although higher levels pose no problems. When soil organic C percentages are below 3%, soils must remain saturated for longer periods for wetland biogeochemical reactions to occur. The soil organic C levels at Juniper Bay are generally >3% and reducing reactions appear to occur within a week of saturation.

Surface drainage water exiting Juniper Bay from the main ditch following a storm event has higher concentrations of total organic carbon (TOC), P, Ca, and Mg compared to concentrations measured during baseflow conditions. During major storm events, organic carbon is dissolved near the surface and displaces Ca, Mg and P that is sorbed onto soil particles. The displaced elements dissolve into the groundwater which then drains into ditches and is taken offsite. This process will increase the chance that relatively high levels of P will be released to surface waters draining from Juniper Bay.

Laboratory experiments confirmed that “large” amounts of dissolved reactive P will be released from Juniper Bay soils following saturation. In the experiments, P dissolution was highly correlated with dissolved organic carbon concentrations, possibly because the dissolved organic C displaces P held on soil particles. Therefore, dissolution of P is predicted to be greatest in the organic soils, where dissolved organic carbon concentrations are likely to be highest.   The dissolved P concentrations were > 1 ppm, and while these numbers appear small, current data from the literature indicate they are high enough to contribute to eutrophication of surface waters. This could lead to fish kills in rivers receiving water draining from restored wetlands. Further work should be done to monitor P outputs from Juniper Bay.

TABLE OF CONTENTS

Chapter 1

INTRODUCTION

M.J. Vepraskas

Many wetland restoration efforts in North Carolina have failed to meet the relatively limited restoration goals imposed by US Army Corps of Engineers (Corps) permits. On such sites that have been reviewed by the principal investigators, it is obvious that failures result from multiple shortcomings in site assessment, identification of potential functions, methodologies to restore wetland functions, and effective assessment of the progress of functional restoration. The research proposed here is designed to address those shortcomings in a study of restoration success in Juniper Bay, a converted Carolina Bay depressional wetland in Robeson County, NC.

Juniper Bay was developed for agriculture several decades ago and currently has about 300 ha of drained and intensively managed agricultural land that is not jurisdictional wetland due to its status as prior converted agricultural land. The drainage system in Juniper Bay not only removes excess surface and ground water, but it directs runoff to a different location in the watershed than under previous natural conditions. The overall goal of the research is to evaluate the strategy and performance of the restoration of wetland functions in Juniper Bay and to test alternative restoration methods. The restoration efforts will include:

- plugging or filling the drainage ditches as necessary to restore historical hydrologic functions and the directions and rates of surface and subsurface runoff
- re-establishing the forest community in accordance with community types located in the reference ecosystem
- soil management as needed to assist in hydrologic function restoration, forest community establishment, and nutrient cycling processes.

This research will evaluate whether these strategies are sufficient to restore appropriate wetland functions in Juniper Bay, and will identify other factors and methods that must be addressed in implementing wetland restoration in depressional wetlands that have been converted to agriculture.

BACKGROUND

A. *Wetland Restoration Requirements* – Wetland mitigation as practiced by the North Carolina Department of Transportation (NCDOT) is the restoration of wetlands to replace those altered or destroyed in the course of road construction and maintenance. The type of wetland ecosystem that must be replaced is specified by the Corps permit that authorized wetland alteration in a particular road project in accordance with Section 404 of the Clean Water Act. To get full credit for wetland restoration efforts, Corps permits usually specify that wetland hydrology, hydric soils, and a plant community similar to the reference ecosystem be restored. The reference ecosystem is a functioning wetland located in the vicinity of the restoration site that has minimal alteration and that is judged to represent the prior natural condition of the restoration site. However, most wetlands have key hydrologic and soil characteristics, such that if the hydrology is restored to cause key soil processes to occur, then it is likely that the most important wetland functions will be restored.

B. *Reasons Restoration Efforts can Fail –* All of the principal investigators have been involved with creating and restoring wetlands in both the southeastern and Midwestern U.S. While restoration is simple in concept, it can be difficult to implement for a variety of reasons. These include:

1. **Variability in Soils and Sediments**: In most of the natural wet flat, organic flat, and depressional wetlands in North Carolina, slowly permeable soil or sediment layers near the surface that limit vertical or lateral drainage are instrumental in the maintenance of wetland hydrology. Drainage ditches often penetrate such layers and provide subsurface flow connections to geologic sediments consisting of layers of sand or gravel. Such connections can cause water ponded in a wetland to leak out. This causes the wetland to be drier than normal, and in extreme cases can limit establishment and growth of wetland plants and the development of hydric soils. The locations and depths of both permeable and impermeable layers must be known prior to beginning restoration, and hydrologic restoration methods on the site must restore the functional impact of slowly permeable layers.

2. **Regional Alteration of Hydrology**: If ground water levels in areas outside the restoration site have been lowered by ditching or pumping, then these modified levels will often affect the ground water levels within the restoration site. Regional subsurface hydraulic gradients that are much higher than historical ones can subvert restoration of wetland hydrology by contributing to relatively high rates of subsurface lateral flow in near-surface soil layers with relatively high hydraulic conductivity. Simply filling ditches within the site itself may not restore wetland hydrology if water is able to leak out the wetland’s bottom or subsurface perimeter. Therefore, regional hydrology must be assessed and restoration methods must account for restoration of historical regional surface and subsurface hydraulic gradients.

3. **Excessive Levels of Soil Nutrients**: While all plants need certain nutrients to grow, the natural plant communities of Carolina Bays are adapted to soils that are acidic and contain few nutrients. Fields used for agriculture were fertilized and limed regularly, so the nutrient levels in the soils are high and the acidity low. When wetlands are created in fields used for agriculture, the high levels of nutrients can cause undesired plants to flourish at the expense of the desired plants of the reference ecosystem. Conversely, restored areas of bottomland hardwood forest fail to grow adequately when grading and soil alteration leave soils at the surface that contain inadequate nutrient levels.

4. **Alteration of Soil Physical Properties**: Wetland restoration often requires extensive grading of the soil surface. For example, the typical restoration procedure for drained agricultural land includes filling the ditches by pushing soil from the inter-ditch fields into the ditches. That process destroys the soil profile. Top soil is pushed into the ditches, subsoil remains at the surface, and the structure of the soil at the surface is

severely degraded by the soil movement and compaction that occurs. The soil remaining at the surface has much lower site quality potential for plant community restoration than the previous agricultural field. Restoration methods must be developed (and approved by the Corps) that can restore hydrology while minimizing such adverse impacts on the soil.

Successful restoration will require that potential limiting conditions such as those described above be identified in the planning process. Then the site will have to be managed during the construction phase and establishment phases to prevent limiting conditions and or apply management practices that ameliorate them.

PROBLEM NEED AND DEFINITION

Restored wetlands must perform the hydrologic, biogeochemical, and plant and animal habitat functions that are found in natural wetlands. Limited assessment of those functions is normally conducted in accordance with Corps permits that specify monitoring of certain parameters of hydrology, hydric soil indicators, and plant community structure. While wetlands may perform many ecological functions, the likelihood of their occurrence can be estimated by monitoring key soil and hydrologic properties. In current wetland restoration practice, there is often a lack of detailed pre- and post-restoration monitoring and assessment that documents the progress of the recovery of wetland functions on restoration sites. This leads to conflicts between agencies restoring wetlands and those regulating them, and delays issuance of permits until the regulatory agencies are certain the restoration efforts will be successful.

RESEARCH OBJECTIVES

1. Document the variability in the properties of soils and sediments and the water table regime across Juniper Bay and the reference bay that will affect restoration success.

2. Assess the recovery rate of key hydrologic, biogeochemical, and plant community functions that are necessary for a sustainable wetland ecosystem.

3. Identify soil chemical and physical properties and hydrologic requirements for optimum growth of Carolina Bay vegetation.

4. Evaluate the dynamics of the critical biogeochemical processes needed for functioning of restored wetlands.

LITERATURE REVIEW

Geographic Extent

Carolina Bays are oval, NW-SE oriented depressions with sand rims that are located in upland landscapes in the southeastern Coastal Plain and occasionally in the lower

Piedmont in certain areas. They range in size from a few acres to more than 7000 acres. Though most numerous in North and South Carolina, Carolina Bays have been identified as far south as north Georgia and as far north as Maryland and Delaware (Melton, 1938; Frey, 1950; Prouty, 1952; and Bliley and Pettry, 1979;). Prouty (1952) estimated the total number of Carolina Bays at 500,000 with about 80% of that number occurring in the Carolinas. In North Carolina, bays are most numerous in the southern portion of the middle Coastal Plain, including the counties of Bladen, Columbus, Cumberland, Hoke, Robeson, Sampson, and Scotland. However, they occur in most of the counties of the southern and central Coastal Plain and occasionally in the northeastern Coastal Plain.

Character of Soils

The bay floor may have organic soils or poorly drained or very poorly drained sandy to clayey mineral soils that are also found in irregularly shaped wet areas outside the bays (Table 1.1). The northwest ends of many bays merge imperceptibly with the surrounding upland, but the northeast, southeast, and part of the southwest rims are moderately to distinctly prominent landscape features. The prominent, nearly white, sandy rims with Kureb or Wakulla soils on the southeast ends commonly rise 1-3 m above the bay bottom and usually are eolian (wind transported and deposited) sand. The rims on the northeast and southwest sides are sandy, but many of the sands are the result of normal soil development on materials of the uplands as well as from eolian materials (Daniels et al., 1999).

Table 1.1. Major soils in the Carolina Bay System (Daniels et al., 1999)

Textural Family	**Drainage Class**				
	Well	**Moderately well**	**Poorly**	**Very poorly**	**Organic soils**
Bay Interiors					
Fine			Coxville McColl	Byars	
Fine-loamy	Norfolk Noboco	Goldsboro	Rains	Pantego	
Coarse-loamy			Woodington	Torhunta	
Sandy			Lynn Haven	Murville Rutlege	Mattamuskeet Pamlico
Rims					
Loamy	Wagram Autryville	Bonneau			
Sandy	Wakulla Lakeland Cainhoy Rimini Kershaw Kureb Centenary	Chipley Pactolus			

Hydrology

The hydroperiod of Carolina Bays ranges from permanently flooded to seasonally saturated. Due to the topographic gradient in bays, there is a soil drainage class gradient from excessively drained on the highest portions of the sandy rims to poorly drained or very poorly drained in the lowest elevation portions. Most have significant areas of jurisdictional wetlands, though some of the driest bays may have wetland in the lower elevation portion surrounded by nonwetland area. Many Carolina Bays contain natural lakes, the largest located in Columbus and Bladen Counties, NC. Bays vary significantly in types of connections to surface waters. Few have surface flow input, a notable exception being Lake Waccamaw in Columbus County. Some bays have surface runoff outlets, but the majority likely do not. The types of surface outlets range from dispersed overland flow during large rainfall events to well-developed stream channels.

Hydrologists have long theorized that the hydrology of Carolina Bays is influenced by subsurface flow inputs and fine-textured soil or parent material layers that restrict downward flux of stored water in the bay. Early limited studies of Carolina Bay hydroperiods showed that the hydroperiod was dominated by rainfall inputs and evaporation outputs (Sharitz and Gibbons, 1982). Only relatively recently, however, have detailed hydrology studies begun to elucidate the complex hydrology of Carolina Bays and shown the complex subsurface interactions with the surrounding area (Knight et al., 1989; Newman and Schalles, 1990; Lide et al., 1995; O'ney et al., 1999). In the bays studied by these authors, there was local depressional hydrology superimposed on the regional subsuface hydraulic gradients of the landscape in which the bay occurred. Both Lide et al. (1995) and O'ney et al. (1999) found that the topography of subsurface layers was similar to the surface topography. Sedimentary layers sloped downward from the surrounding uplands to lows under the lower elevation portions of the bay. Hydraulic gradients into the bays resulted in subsurface flows along sandy layers overlying fine-textured layers with upward gradients into the bays during the wet season. In both bays, water accumulated in the bay during the wet season of the year and then was depleted during the dry season. Lide et al. (1995) concluded that Thunder Bay in Barnwell County, SC provided significant ground water recharge during the drying period of late spring/early summer. O'ney et al. (1999) concluded that Chapel Bay in Bamberg County, SC likely provided some recharge but that drying was dominated by evaporation losses.

Geomorphology

Stratigraphy of the lacustrine bay-fill sediment and the fossil pollen in the sediment indicates water levels have fluctuated in the past. In most bays a series of alternating organic and inorganic zones can be identified, and most bays were more lake-like at one time (Whitehead, 1965). Inorganic sediments consist of sandy or clayey loam, lenses of gravel, sand, or iron-cemented sand, and marl and clay. The clay and silt zones represent lacustrine depositional periods after bay formation, and as such did not influence water levels early in bay history. Original bay water levels probably reflected regional hydrology. Surface water levels have decreased in time because bays are infilling with sediment and peat and surrounding groundwater levels are decreasing because of local stream excision (Schalles et al., 1989). Ditching and channelization, for primarily agricultural drainage, have also lowered groundwater levels in their vicinity.

Some bays contain extensive organic deposits, while others are clay based. Significant peat reflects a more stable hydrology with almost continuous groundwater recharge. Chemistry of water and soils in clay-based Carolina bays indicates a rainwater-dominated system characteristic of perched-water settings (Schalles et al., 1989). Water levels are related to precipitation, but variable responses are common.

Sediments on the coastal plain were deposited by both coastal and fluvial processes (and surfaces have been reworked by wind). Consequently, coastal plain stratigraphic units can consist of sands, silts, or clays, reflecting the energy present in the environment at the time of their deposition. Surficial sands often overlie clay layers; these finer-textured sediments perch water and may be important to maintaining the bays.

The original surface of these coastal plain sediments was most likely undulating. Water tables on broad interfluves would have been high; as stream incision progressed, water tables would become lower near interfluve edges. Undulations in the region where water could pond because of poor surface or subsurface drainage resulted in bays (Kaczorowski, 1977).

Bays have been reported to form on saprolite and clayey Coastal Plain sediments (Bliley and Burney, 1988), over impervious humate (Thom, 1970; Kaczorowski, 1977), clay (Gamble et al., 1977; Schalles et al., 1989), and in poorly drained depressions in sandy surficial sediments (Bliley and Pettry, 1979). Landscape position, water table fluctuations, and impervious layers interact to produce differences in individual bay hydrology and response to rainwater inputs. Bays are likely both recharge and discharge features depending on bay water levels in relation to the regional water table (Schalles, 1979). Understanding the hydrology of a particular bay requires an understanding of the nature, continuity, and depth of underlying sediments and their interactions with regional hydrology.

Vegetation

The vegetative communities of Carolina Bays in the Carolinas are diverse among bays and usually complex within bays (Sharitz and Gibbons, 1982; Schafale and Weakley, 1990). That diversity and complexity is related to topography, soils, hydrology, and disturbance history. Schafale and Weakley recognize nine natural community types that commonly occur in Carolina Bays in North Carolina: low pocosin, high pocosin, small depression pocosin, pond pine woodland, peatland Atlantic white cedar forest, bay forest, cypress savanna, small depression pond, and natural lake shoreline. However, examples of most common forest or emergent wetland vegetation types that occur in the Coastal Plain may be found in the complex vegetation mixes of Carolina Bays. All bays have a vegetation gradient from the xeric communities of the sandy rims to the wetland or aquatic communities of the lowest elevation area of the bay, usually in the southeastern quadrant (Sharitz and Gibbons, 1982).

The long-term success of the Juniper Bay restoration project will be evaluated partly by the similarity of the species composition and structure of its future stable plant community to that at reference Carolina bay sites. Certain key wetland functions (e.g. duration of anaerobic conditions) at Juniper Bay should also be compared with functions at reference sites. In the early years following restoration at Juniper Bay, before a stable community is attained, successional changes in the community structure and wetland functions should be monitored to try to determine if they are progressing toward their desired future states. Clearly, evaluating the success of the Juniper Bay restoration requires characterization of reference sites.

Carolina bay lengths range from 50 m to 8 km (Frey, 1949). There appears to be no consistent relationship with particular geological formations or topography (Prouty, 1952). Some bays remain dry nearly all of the time; some contain permanent water;

others are seasonally inundated (Sharitz and Gibbons, 1982). Many bays have been disturbed by forestry or agricultural practices while some remain in relatively pristine condition. Fire is a natural disturbance that has probably affected all bays, but to varying extents.

Against the background of extremely heterogeneous environmental influences, it is not surprising that plant community types vary widely among Carolina bays. Major community types previously reported at bays include pine forests, herbaceous marshes, shrub bogs, deciduous forests, evergreen bay forests, pond cypress swamps, prairies, and submerged aquatic beds (Buell, 1946; Penfound, 1952; Whitehead and Tan, 1969; Porcher, 1966; Wharton, 1978; Schalles and Shure, 1989). This vegetation variation suggests that the stable community type that will eventually develop at Juniper Bay is difficult to predict, and that several reference sites should be selected. These sites should be located close to Juniper Bay and have soils, hydrology, and disturbance histories similar to those at Juniper Bay prior to its conversion to agriculture. It is expected that the plant community types and wetland functions will vary among these reference sites. The range of structural and functional variability in the plant communities of these reference sites is the target for Juniper Bay.

Wetland Soils or Hydric Soils

Hydric soils are defined as those that are saturated, flooded, or ponded long enough during the growing season to develop anaerobic conditions in the upper part. Hydric soils must be anaerobic. Many water quality functions that wetlands perform occur because the soils have become anaerobic and chemically reduced.

Wetland restoration efforts are successful when the soils in the restored wetlands become anaerobic for extended periods of time. Development of anaerobic conditions can be monitored by analyzing water chemistry or by measuring the oxidation-reduction potential, which is also called the redox potential (Ponnamperuma, 1972). Water chemistry measurements are used to determine concentrations of reduced chemical species such as NH_4^+, and Fe(II). The presence of Fe(II) is considered proof that the soils are anaerobic.

Redox potential measurements are electrical measurements that determine the voltage developed between a Pt wire and a reference electrode buried in the soil. (Patrick et al., 1996). They are used to determine whether soils are developing the anaerobic conditions necessary for them to be considered as hydric soils. Redox potential measurements are probably the single most important measurements to be made on soils to confirm that a wetland restoration has been successful.

The time required to restore wetland functions is site specific. However, it has been found that some soils regain their hydric soil processes within years of construction (Vepraskas et al., 1999). In a study of created wetlands in the midwestern U.S., Vepraskas et al. found that hydric soil field indicators developed within 3 yrs of wetland creation, and appeared to reach full development within 5 yrs. To develop the necessary low redox potential required for anaerobic conditions, soil organic matter levels apparently had to exceed 4% in the midwestern U.S. The hydric soil field indicators adopted for use throughout the U.S. have been presented in USDA-NRCS (1998).

ORGANIZATION OF THE REPORT

The following chapters summarize the principal findings of the research done to date. Each chapter covers a separate topic and was written by the researchers involved. The chapters were written to be "self-contained" and can be read without referring to other chapters. This format was selected to make reading of the report easier.

PREVIOUS WORK

This report summarizes the work done at Juniper Bay and three reference bays from 2003 to 2007. A previous report (report no. FHWA/NC/2003-06) documented work done from 2001 to 2003 by our research group. Wetland trees were planted in 2004 at Juniper Bay prior to the time hydrology was restored. Ditches were filled in 2005 and hydrology restored in 2006 at Juniper Bay.

REFERENCES

Bliley, D. J. and D. A. Burney (1988). "Late Pleistocene climatic factors in the genesis of a Carolina bay." Southeastern Geology **29**(2): 83-101.

Bliley, D. J. and D. E. Pettry. 1979. Carolina bays on the eastern shore of Virginia. Soil Sci. Soc. Am. Jour. 43:558-564.

Buell, M.F. 1946. Jerome Bog, a peat-filled "Carolina bay." Bull. Torrey Bot. Club 73: 24-33.

Daniels, R. B., S. W. Buol, H. J. Kleiss, and C. A. Ditzler. 1999. Soil systems in North Carolina. Tech. Bull. 314, Soil Science Dept., NC State Univ., Raleigh, NC.

Estes, J.E., M.R. Mel, and J.D. Hooper. 1977. Measuring soil moisture with an airborne imaging passive microwave radiometer. Photogrammetric Engineering and Remote Sensing 43:1273-1281.

Frey, D.G. 1949. Morphometry and hydrography of some natural lakes of the North Carolina coastal plain: the bay lake as a morphometric type. J. Elisha Mitchell Sci. Soc. 65: 1-37.

Frey, D. G. 1950. Carolina bays in relation to the North Carolina Coastal Plain. J. Elisha Mitchell Sci. Soc. 66:44-52.

Gamble, E. E., R. B. Daniels, et al. (1977). "Primary and secondary rims of Carolina Bays." Southeastern Geology 18: 199-212.

Houser, P.R., W.J. Shuttleworth, J.S. Famiglietti, H.V. Gupta, K.H. Syed, and D.C. Goodrich. 1998. Integration of soil moisture remote sensing and hydrologic modeling using data assimilation. Water Resour. 34 (12):3405-3420.

Kaczorowski, R. T. (1977). The Carolina Bays: a comparison with modern oriented lakes. Columbia, South Carolina, Coastal Research Division, Department of Geology, University of South Carolina.

Knight, R. L., J. S. Bays, and F. R. Richardson. 1989. Floral composition, soil relations, and hydrology of a Carolina bay in South Carolina. p. 219-234, *In* R. R. Sharitz and J. W. Gibbons (eds.). Freshwater wetlands and wildlife symposium: perspectives on natural, managed, and degraded ecosystems. US Dept. of Energy, Off. of Sci. and Tech. Info., Oak Ridge, TN. Conf. 8603101, DOE Symposium Series No. 61.

Lide, R. F., V. G. Meentemeyer, J. E. Pinder, III, and L. M. Beatty. 1995. Hydrology of a Carolina bay located on the upper Coastal Plain of western South Carolina. Wetlands 15(1):47-57.

Melton, F. A. 1938. Possible late Cretaceous origin of the Carolina “bays.” Geol. Soc. Am. Bull. 49:1954.

Newman, M. C. and J. F. Schalles. 1990. The water chemistry of Carolina bays. Archiv für Hydrobiologie 118:147-168.

O’ney, S. E., M. H. Eisenbies, and M. Miwa. 1999. Hydrologic processes in the vicinity of a Carolina bay affecting water quality: an assessment in association with a hardwood fiber farm. Unpublished progress report. USDA Forest Service, Center for Forested Wetlands Research, Charleston, SC.

Penfound, W.T. 1952. Southern swamps and marshes. Bot. Rev. 18: 413-446.

Poe, G.A and A.T. Edgerton. 1971. Determination of soil moisture content with airborne microwave radiometry. Summary report. U.S. National Oceanic and Atmospheric Administration & Aerojet-General Corporation Microwave Division, El Monte, CA.

Porcher, R.D., Jr. 1966. A floristic study of the vascular plants in nine selected Carolina Bays in Berkeley County, S.C. MS thesis. Univ. SC, Columbia.

Prouty, W. F. 1952. Carolina bays and their origin. Bull. Geol. Soc. Am. 63:167-224.

Richter, J.C. 1981. Ground registration of data from an airborne multifrequency microwave radiometer (MFMR).USDA. Lyndon B. Johnson Space Center (JSC) # 17152, NASA/JSC. AgRISTARS . Lockheed Engineering and Management Services Company. National Technical Information Service, 1981. 29 p.

Schafale, M. P. and A. S. Weakley. 1990. Classification of the natural communities of North Carolina: Third approximation. North Carolina Natural Heritage Program, NC Dept. of Environment, Health, and Natural Resources, Raleigh, NC.

Schalles, J. R. (1979). Comparative limnology and ecosystem analysis of Carolina bay ponds on the upper coastal plain of South Carolina. Ph.D. Dissertation, Emory University, Atlanta, GA.

Schalles, J. F., R. R. Sharitz, et al. (1989). Carolina bays of the Savannah River Plant. Aiken, S. C., Savannah River Plant National Environmental Research Park.

Schalles, J.F. and D.J. Shure. 1989. Hydrology, community structure, and productivity patterns of a dystrophic Carolina bay wetland. Ecol. Monog. 59(4): 365-385.

Schmugge, T. 1976. Microwave radiometry for soil moisture sensing. p. 184-205 *in* Remote Sensing of Soil Moisture and Groundwater, Workshop Proceedings, 1976.

Sharitz, R. R. and J. W. Gibbons. 1982. The ecology of southeastern shrub bogs (pocosins) and Carolina bays: a community profile. FWS/OBS-82/04. Division of Biological Services, US Fish and Wildlife Service, Washington, DC.

Thom, B. G. (1970). "Carolina bays in Horry and Marion Counties, South Carolina." Geological Society of America Bulletin 81: 783-814.

Wharton, C.H. 1978. The natural environments of Georgia. Geol. And Water Res. Div. Res. Planning Sect., Office of Planning and Research, Ga. Dept. of Nat. Res., Atlanta, Ga. 227 pp.

Whitehead, D. R. 1965. Palynology and Pleistocene phytogeography of unglaciated eastern North America. *In* The Quaternary of the United States. H. E. Wright, Jr. and D. G. Frey. Princeton, N. J., Princeton University Press**:** 417-432.

Whitehead, D.R. and K.W. Tan. 1969. Modern vegetation and pollen rain in Bladen County, North Carolina. Ecology 50: 235-248.

Chapter 2

SAMPLING DEVICE TO EXTRACT INTACT CORES IN SATURATED ORGANIC SOILS

P.V. Caldwell, A. A. Adams, C.P. Niewoehner, M.J. Vepraskas, and J.D. Gregory

INTRODUCTION

Hydrologic computer models are powerful tools for predicting water table levels in soils. Most models require soil property data such as saturated hydraulic conductivity and soil water characteristic curves to simulate the movement and storage of water in the soil profile (Skaggs, 1978; McDonald and Harbaugh, 1988). These properties are frequently measured on undisturbed soil cores in the laboratory. Various mechanical devices have been developed for the collection of undisturbed soil cores. Many samplers are attached to tractors and use hydraulic pressure to either pound or push the sampler into the soil (Abu-Hamdeh and Al-Jalil, 1999; Janssen et al., 1998; Vepraskas et al., 1990). Others have used more portable, manual means to push or pound the sampler into the soil profile (Chong et al., 1982; Jackson, 1987; Seaby, 2000; Swanson, 1950; Stolt et al., 1991). Most of these methods work well only in soil of sufficient strength to withstand compaction or disturbance during sample collection.

Little data are available for the saturated hydraulic conductivity or soil water characteristic of saturated organic soils under forest vegetation, because it is difficult to collect undisturbed samples from these soils. Organic soils in forested settings have a dense, interconnected mat of roots at the surface that must be severed when collecting core samples. These organic soil materials are usually saturated and have very low soil strength. Collecting undisturbed cores using traditional methods virtually destroys the sample during the collection process. Additional problems are encountered when collecting samples in flooded conditions. When a sampler is successfully inserted into a saturated organic soil, the action of lifting it out of the ground induces suction at the bottom of the sampler that causes the soil core to be pulled from the sampler.

The objective of this study was to develop a sampler that could be used in saturated organic soils to collect undisturbed soil cores suitable for laboratory measurements of saturated hydraulic conductivity and the soil water characteristic curves.

SAMPLER DESIGN AND CONSTRUCTION

The sampling device was made from a section of 3-in.-diam. schedule 40 PVC pipe that was 39.4 in. (100 cm) long (Fig. 2.1). Diameters of all parts of the apparatus are 3 in. (7.6 cm) unless otherwise noted. Two female-threaded adapters were glued to the ends of the PVC pipe using PVC cement. A cutting head was fashioned from a threaded male PVC adapter with a short piece of PVC pipe glued into the slip-fit end (Fig. 2.2). The edge of the male adapter and PVC pipe were tapered to a 45° angle using a belt sander to facilitate easier penetration into the soil. The arbor end of a hole-saw was removed using a pneumatic cut-off wheel, resulting in a 3-in.-diam. diameter saw-toothed ring that was 1.5 in (3.8 cm) long. This ring was glued into the PVC pipe in the male adapter using epoxy cement such that the saw teeth extended approximately 0.5 in (1.3 cm) from the end of the PVC pipe. Additional supplies included a 47.2 in (120-cm) length of 0.5-in.-diam. galvanized-steel tubing, a plastic funnel that fit into the galvanized tube, and two PVC male threaded caps.

SAMPLER OPERATION

To collect samples, the sampler cutting head was threaded onto one end of the PVC pipe. The cutting head was then placed on the soil surface and slowly rotated by hand using gentle downward pressure. The saw cut through fibric organic soil material as well as the numerous roots encountered in the profile. Once the sampler reached the desired depth, the remaining air space in the top of the sampler was filled with water. The pipe was then capped on the top with one of the threaded PVC caps using sealant on the threads. Capping the top of the sampler helped maintain suction inside the sampler to prevent loss of the core when it was raised from the ground, similar to holding one's finger over the end of a drinking straw and lifting it out of the glass. Next, the galvanized tubing was pounded into the ground immediately adjacent to the sampler such that the end of the tube was at the same depth as the cutting head of the sampler. The tube was cleared of debris with a length of steel rod, and was then attached to the sampler using duct tape. A small hole was then dug into the soil next to the sampler with a spade to allow removal of the saw adapter just before the bottom of the sampler was raised above the water table.

Before the sampler was raised from the soil, water was poured through the funnel into the galvanized tube until the tube was full. At this point, the sampler and galvanized tube were lifted from the soil either manually or with a tripod/winch arrangement. As the sampler was lifted, the void created beneath it was filled with water from the galvanized tube to relieve the suction that would otherwise draw the sample out of the pipe. Cuttle and Malcolm (1979) suggested inserting a tube adjacent to the sampler to allow air into the area below the sampler to relieve the suction. However, we found that due to the weight of the saturated organic soil sample and the low friction between the sample and the sampler tube, it was necessary to fill the void below with water to prevent loss of the core. Depending on the depth of sampling, it may be necessary to add water to the funnel as the sampler is being raised. When the sampler was lifted to within a few centimeters of the top of the water table, the cutting head was removed and a threaded cap installed in its place using sealant on the threads. By keeping the bottom of the sampler below the water table, pressure was maintained on the bottom of the core to minimize the possibility of losing the sample. With both ends capped, the sampler was completely raised from the soil surface and stored. The sampler could then be transported to the laboratory in a vertical orientation to prevent damage to the saturated soil material inside. The soil core can be removed from the sampler by either cutting the PVC pipe lengthwise to expose the sample, or by pushing it out of the PVC pipe using a plunger-type device.

Short core samples (e.g. 3 in. (7.6 cm) long) can also be prepared by cutting the PVC pipe cross-wise and leaving the soil surrounded by a PVC ring.

EXAMPLE OF USE

Samples were collected from organic soils using this device in three Carolina Bays in NC located approximately at 34°40’59” N and 78°34’54” W. The organic soils were members of the Croatan series (loamy, siliceous, dysic, thermic Terric Haplosaprists) and Pamlico series (sandy or sandy-skeletal, siliceous, dysic, thermic Terric Haplosaprists). The dominant vegetation at these sites consist of pocosin plant species, with trees such as pond pine (*Pinus serotina* L.), swamp red bay (*Persea palustris* L.), loblolly bay (*Gordonia lasianthus* L.), and sweetbay (*Magnolia virginiana* L.), and shrub species including fetterbush (*Lyonia lucida* L.), ti-ti (*Cyrilla racemiflora* L.), inkberry (*Ilex glabra* L.), and blaspheme vine (*Smilax laurifolia* L.). Hydrologic models of the three bays were to be developed, requiring soil data such as saturated hydraulic conductivity and soil water characteristic curves to be measured from intact soil cores. Three cores were taken in each of the three bays.

The apparatus that was used to measure hydraulic conductivity and soil water characteristic required samples of approximately 3 in. (7.6 cm) diam. and 3 in. (7.6 cm) in height. The 39.4 in. (100 cm) long soil core was cut into 3 in. (7.6 cm) long sections by first setting the PVC pipe into a bucket while maintaining its vertical orientation. The top threaded cap was removed, and the water above the core surface was siphoned out. The location of the upper core surface was marked on the outside of the sampler, and marks were made at 3 in. (7.6 cm) intervals to the bottom of the pipe. A wheel-type PVC pipe cutter was used to gently cut through the pipe at the marked locations while leaving the soil sample intact.

When the PVC pipe was cut completely through, a 4-in. wide, sharpened spatula was inserted into the cut and gently worked across the sample. Any roots in the sample were cut using razor blades or thin saws to minimize damage to the sample. The PVC section containing the sample was then removed while being supported on the bottom by a spatula. The sample was then inverted onto another spatula, and a piece of cheesecloth was secured to the bottom of the sample using a rubber band. The sample was then flipped back over and placed in a pan of water to maintain saturation.

The saturated hydraulic conductivity was measured using the constant head method (Klute and Dirksen, 1986). The soil water characteristic curve was also determined using a pressure cell apparatus (Klute, 1986). At the completion of these tests, the samples were placed in cans, weighed, oven-dried at 221° F (105° C) for 24 hours, and reweighed to determine water content. Bulk density was computed using the oven-dry weight and inner volume of the PVC ring.

The saturated hydraulic conductivity and bulk density for the Oi, Oe, and Oa horizons in the organic soils sampled are shown in Table 2.1. The organic soil horizons had very low bulk densities (< 12.5 lb ft^{-3} (0.2 g cm^{-3})) due to the lack of mineral soil material in the matrix. The surface (Oi) horizons, composed mostly of undecomposed leaves and fibrous roots, generally had saturated hydraulic conductivities too high to be measured with the laboratory apparatus (Table 2.1). The soil water characteristic data (Fig. 2.3) showed that the organic soils had a porosity of approximately 0.9 ft^3 ft^{-3}. Most of the water drained from the cores at soil water pressures >-19.7 in (-50 cm). These pores had equivalent cylindrical diameters >0.0039 in (0.1 mm) as estimated from the capillary rise equation (Hillel, 2004).

DISCUSSION

The sampler successfully removed intact cores from the sites in most cases. The surface Oi horizon, which consisted of loose leaves and some fibrous roots, was occasionally compressed during the coring process. Extreme care should be taken not to exert excessive downward force when taking the sample, which can destroy the fragile structure of the organic surface horizons. Samples collected from Oe and Oa horizons showed no apparent compaction in that the surface of the samples remained at a constant elevation as the sampler was pushed into the ground. Despite the slightly smaller (0.08 in (2 mm)) inner diameter of the hole saw, no gaps between the sample and core wall were visible to the naked eye.

This sampling device was also applied to saturated sandy mineral soils at some sites. For these soils, 3-in.-diam. thin-walled steel tubing replaced the PVC piping. No cutting head was necessary in these soils, but the leading edge of the steel tubing was sharpened using a grinder to facilitate cutting through roots during the sampling process. The steel tubing was pounded into the soil using a fence-post driver until it reached the desired depth. In this case, rubber end caps with gear clamps were used on either end of the sampler to secure the core inside. No apparent compaction of samples was observed in these soils. Extraction of the cores from the soil and sample preparation was performed as described previously for the organic soils.

The sampler has proven reliable in collecting virtually undisturbed samples from saturated Oe and Oa horizons in over 30 plots. The undisturbed samples can be used to determine soil bulk density, saturated and unsaturated hydraulic conductivity, soil water characteristic curves, among others. The samples can also be used to evaluate root growth and soil micromorphology. The same cutting head apparatus was used for all organic soil cores without the need to replace or re-glue the hole-saw. Soil data collected by this method have successfully been used in hydrologic models predicting water table levels with a high degree of accuracy, with typical average absolute deviations between simulated and measured water table depths of less than 2 in. (5 cm). Distinct advantages of this sampler are its low cost, ease of construction, lightweight, and the ability to section the core into samples that can be tested in the laboratory.

REFERENCES

Abu-Hamdeh, N.H., and H.F. Al-Jalil. 1999. Hydraulically powered soil core sampler and its application to soil density and porosity estimation. Soil Till. Res. 52:113-120.

Chong, S.K., M.A. Khan, and R.E. Green. 1982. Portable hand-operated soil core sampler. Soil Sci. Soc. Am. J. 46:433-434.

Cuttle, S.P., and D.C. Malcolm. 1979. A corer for taking undisturbed peat samples. Plant Soil. 51:297-300.

Hillel, D. 2004. Introduction to environmental soil physics. Elsevier Academic Press, Amsterdam, Netherlands.

Jackson, D. 1987. A description of a manually operated soil core-sampler. Commun. Soil Sci. Plant Anal. 18:781-787.

Janssen, K.A., J.L. Havlin, and E.H. Horstick. 1998. Hydraulic device for transect sampling soil. Soil Sci. Soc. Am. J. 62:480-486.

Klute, A. 1986. Water retention: laboratory methods. p. 635-662. *In* A. Klute (ed.) Methods of soil analysis, part 1. 2nd ed. Agron. Monogr. 9, ASA and SSSA, Madison, WI.

Klute, A., and C. Dirksen. 1986. Hydraulic conductivity and diffusivity: laboratory methods. p. 687-734. *In* A. Klute (ed.) Methods of soil analysis, part 1. 2nd ed. Agron. Monogr. 9, ASA and SSSA, Madison, WI.

McDonald, M.G. and A.W. Harbaugh. 1988. A modular three-dimensional finite difference ground water flow model. Techniques of water resources investigations of the U.S. Geol. Surv., Book 6, Chap. A1. U.S. Geological Survey, Washington, DC.

Seaby, D.A. 2000. Portable, two-stage sampler for "difficult" soils. Soil Sci. Soc. Am. J. 64:1327-1329.

Skaggs, R.W. 1978. A water management model for shallow water table soils. Tech. Rep. 134. Water Res. Instit., Raleigh, NC.

Stolt, M.H., J.C. Baker, and T.W. Simpson. 1991. Bucket auger modification for obtaining undisturbed samples of deep saprolite. Soil Sci. 151:179-182.

Swanson, C.L. 1950. A portable soil core sampler and penetrometer. Agron. J. 42:447-451.

Vepraskas, M.J., M.T. Hoover, J.L. Beeson, M.S. Carpenter, and J.B. Richards. 1990. Sampling device to extract inclined, undisturbed soil cores. Soil Sci. Soc. Am. J. 54:1192-1195.

ACKNOWLEDGEMENT

This chapter was published in the Soil Science Society of America Journal (2005, 69:2071-2075). It was also used as a portion of P.V. Caldwell's Ph.D. dissertation (2005) entitled "Characterization of the hydrologic regime of four Carolina Bay plant communities" that was earned through NC State University and is available through the university's library.

Table 2.1. Laboratory bulk density and hydraulic conductivity measurements conducted on organic soils across all three Carolina Bays.

		Bulk density			Saturated hydraulic conductivity		
Horizon	Organic soil material	Number of samples	Mean	Standard error	Number of samples	Mean	Standard error
			----lb ft^{-3}----			----in h^{-1}----	
Oi	Fibric (Peat)	4	6.24	0.62	1	7.1	ND[†]
Oe	Hemic (Mucky Peat)	10	6.86	0.62	6	5.9	2.6
Oa	Sapric(Muck)	14	8.11	0.62	14	0.1	0.3

[†] ND Saturated hydraulic conductivity of Oi horizon generally exceeded capability of laboratory apparatus to measure.

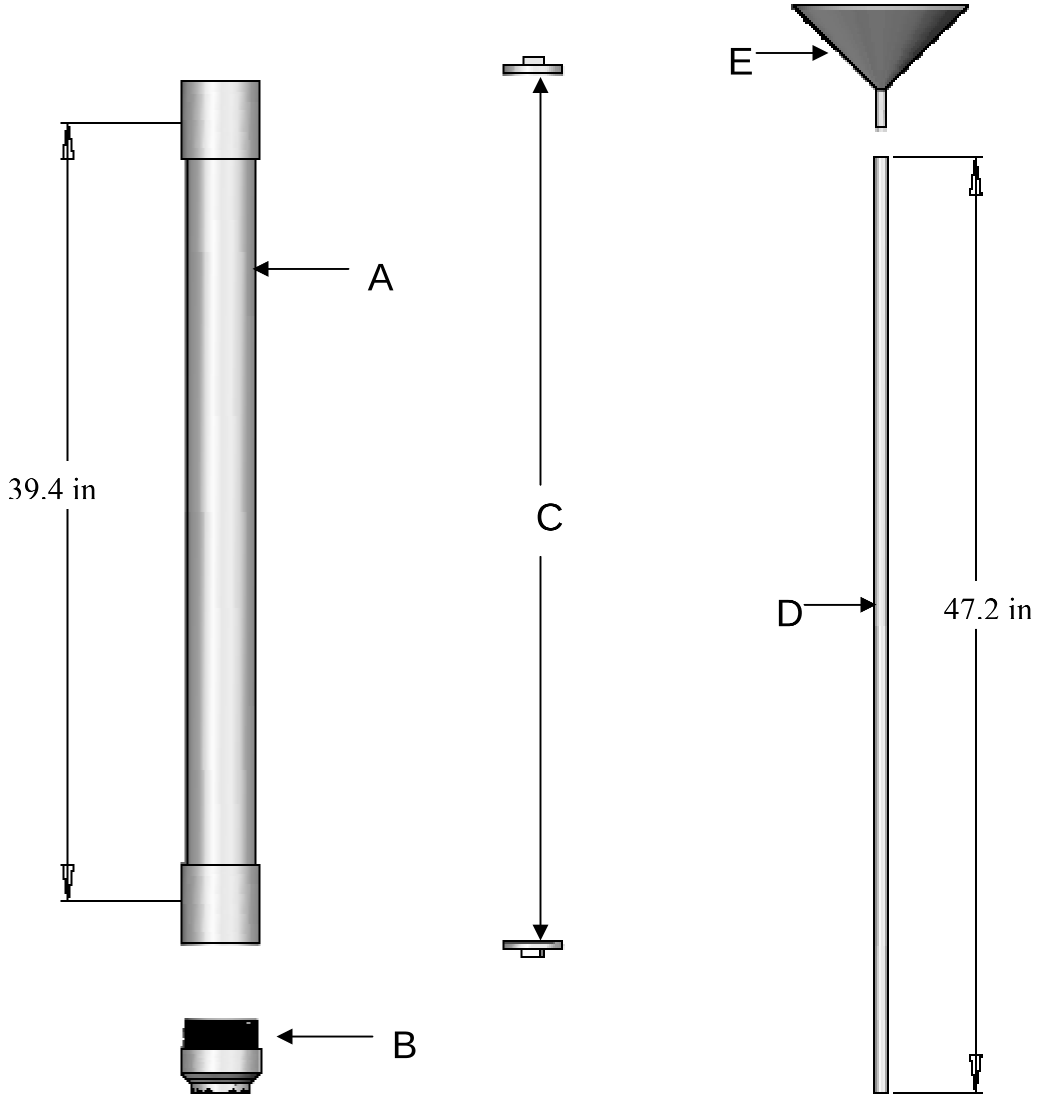

Figure 2.1. Schematic diagram of the core sampler. Components are: A) a 39.4 in (100 cm) long 3 in diam. schedule 40 PVC pipe with female threaded adapters on each end, B) a sampler cutting head, C) two 3 in. diam. male threaded PVC caps, D) a 47.2 in (120 cm) long, 0.5 in diam. galvanized pipe, and E) a plastic funnel.

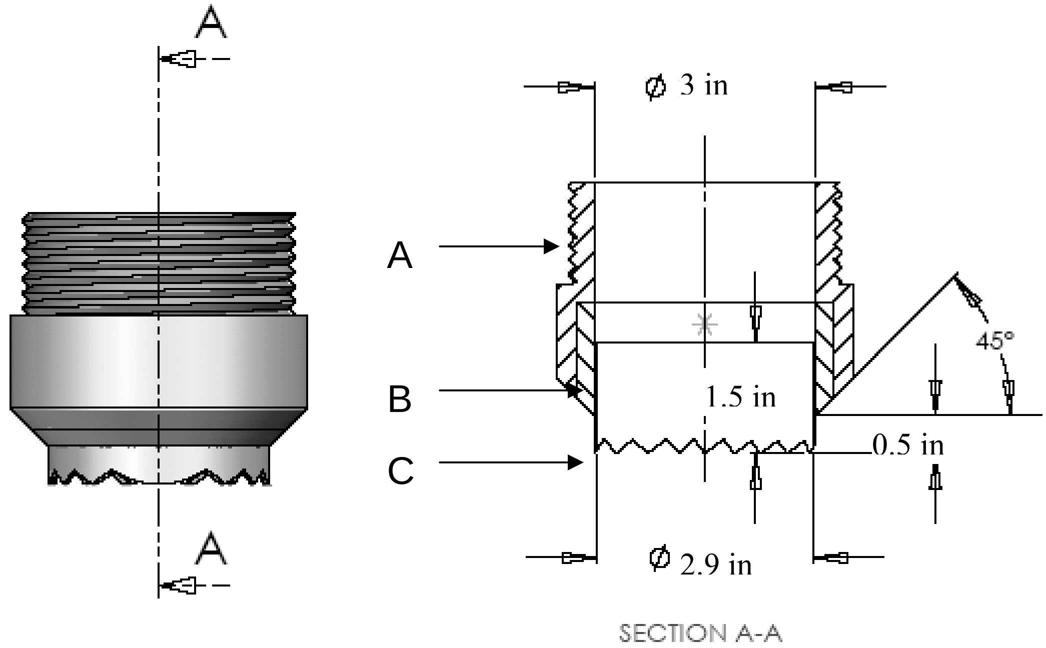

Figure 2.2. Drawing and relevant dimensions of the sampler cutting head. Components are: A) a 3 in diam. male threaded adapter, B) a 3 in diam. section of PVC pipe glued into (A), C) a 3 in diam. hole-saw with arbor end removed.

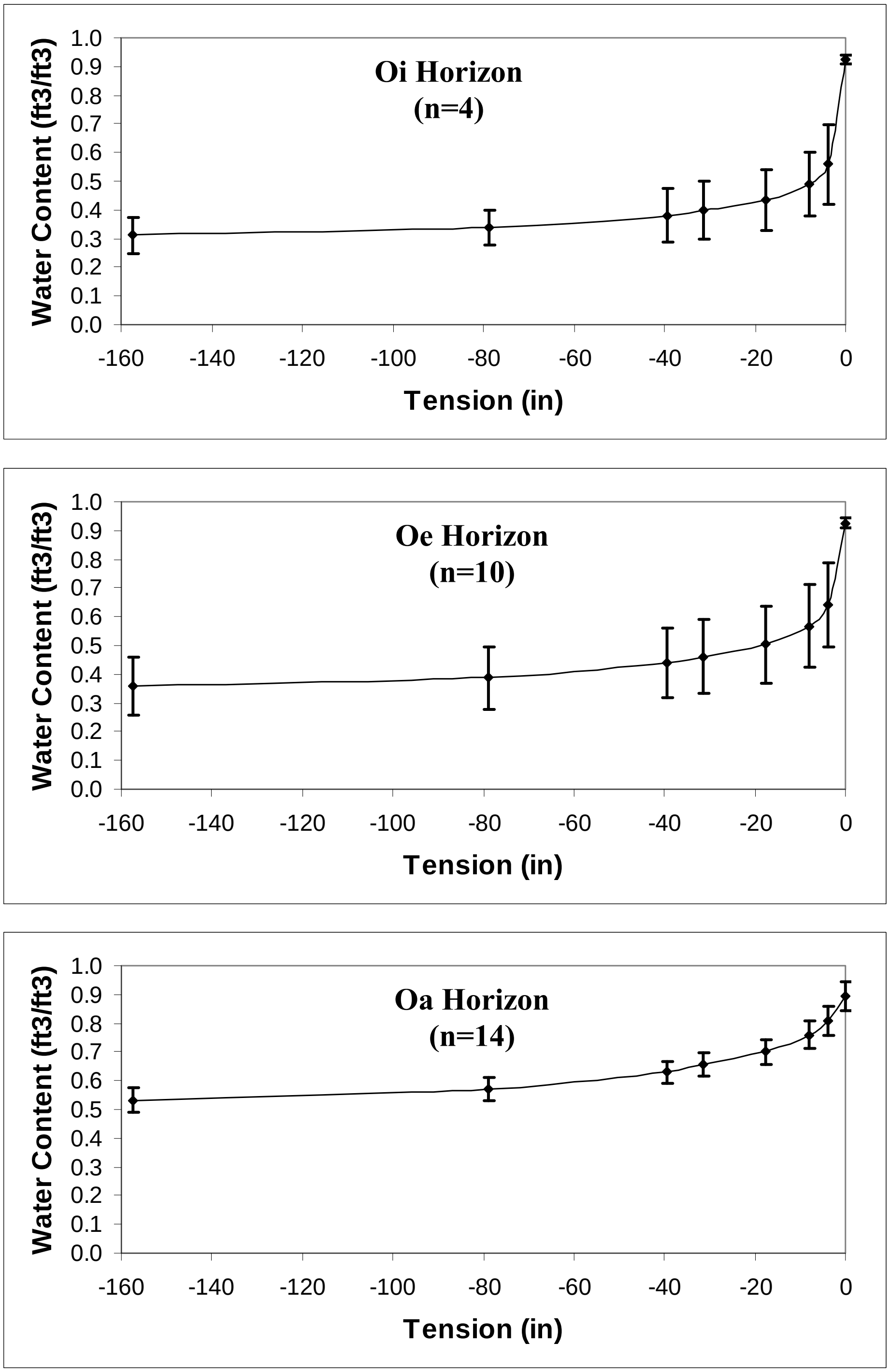

Figure 2.3. Mean soil water characteristic curves for the Oi, Oe, and Oa horizons of organic soils.

Chapter 3

PHYSICAL PROPERTIES OF NATURAL ORGANIC SOILS IN CAROLINA BAYS OF THE SOUTHEASTERN UNITED STATES

P.V. Caldwell, M.J. Vepraskas, and J.D. Gregory

INTRODUCTION

One of the environments in which organic soils form is one that is saturated with water at or above the surface for most or nearly all of the year (Collins and Kuehl, 2001). Under these conditions, microbial decomposition of plant matter is usually limited, causing organic material to accumulate on top of the underlying mineral strata. Areas containing organic soils in their natural, undrained state, are wetlands known as bogs, fens, swamps, pocosins, marshes, and peatlands (Mitsch and Gosselink, 2000). Organic soils have a long history of uses, including agricultural crop production, forest timber production, and they have even been mined as an energy source (Lilly, 1981). In more recent years, many developed areas containing these organic soils have been restored to approximate the original wetland hydrology and vegetation.

By definition, organic soil materials have an organic carbon content of 18% or more with 60% or more clay-sized mineral particles, or 12% or more organic carbon with 0% clay (Soil Survey Staff, 1993). The USDA classifies organic soil horizons (O horizons) on the basis of the relative volume of plant fibers in the horizons (Soil Survey Staff, 2003). Fibers are pieces of plant tissue (excluding live roots) that have diameters between 0.006 in (0.15 mm) and 0.8 in (2 cm). The Oi horizons consist of fibric soil material (texturally known as peat) such as undecomposed leaves, roots, stems, etc., with 75% of their volumes containing plant fibers. The Oa horizons contain sapric material (texturally known as muck), with less than 17% of their volumes containing plant fibers. The Oe horizons are composed of hemic organic material (texturally known as mucky peat) that has a state of decomposition in between that of Oi and Oa horizons.

The hydrologic regimes required for the development of organic soils as well as the establishment of wetland plant communities under which they develop are not completely understood. This is partly because these processes occur over a very long period of time, longer than the scope of most scientific studies. Hydrologic models are powerful tools used to predict the present and long-term hydrology of wetland sites with organic soils. They can also be used to evaluate the hydrology of naturally vegetated wetlands to determine the hydrology needed by specific plant communities that will be established in restored wetlands. Models such as DRAINMOD (Skaggs, 1978) and MODFLOW (McDonald and Harbaugh, 1988) require soil property data such as saturated hydraulic conductivity (K_{sat}) and soil water characteristic curves to simulate the movement and storage of water in the soil profile. Unfortunately, published soil property data for natural organic soils are lacking, particularly in the southeastern U.S. This is largely due to the difficulty in obtaining the undisturbed soil samples required to estimate these properties. Dense vegetation, fragile surface horizons, woody debris in the soil profile, and flooded conditions all serve to complicate the sample collection process.

Organic soils in the United States (excluding Alaska and Hawaii) are concentrated in the upper Midwest and along the southeastern Atlantic Coastal Plain. Numerous studies have been conducted to estimate soil physical properties of natural organic soils in the midwestern U.S. as well as in northern Europe (Boelter, 1964, 1965, 1969; Rycroft et al., 1975). However, the kind and amount of the mineral fraction of the soil, vegetation type, degree of decomposition, and hydrology can affect soil properties (Soil Survey Staff, 1993). As a result, these soil data may not be applicable to natural organic soils of the southeastern U.S., such as those found in Carolina Bay wetlands. Carolina Bays are elliptical depressions oriented on the landscape such that the major axis of the bay is in the northwest-to-southeast direction (Prouty, 1952). They are formed in poorly drained Coastal Plain sediments, and occur along the Atlantic seaboard from northern Florida to New Jersey, but are concentrated in the Carolinas. Their estimated numbers range from 100,000 to 500,000 (Nifong 1998; Prouty 1952), and they can be as small as 295 ft (90 m) along the major axis or as large as 6.8 mi (11 km) (Prouty, 1952).

Some studies have estimated the physical properties of drained and managed organic soils in the southeastern U.S. that were in agriculture or forest timber production (McCarthy et al., 1992; Amatya, 1993; Amatya and Skaggs, 2001; Ewing, 2003). However, the physical properties of these soils (e.g. bulk density and pore size distribution) are different from their undrained and unmanaged counterparts due to the effects of drainage and other management practices that compact the soil and increase the rate of decomposition of organic matter. When organic soils are drained for agriculture, the undecomposed fibric organic (Oi) surface horizons and the moderately decomposed hemic organic (Oe) horizons are stripped from the surface, and any accessible buried logs are removed (Ewing et al., 2005; Lilly, 1981). These horizons tend to have higher porosities and K_{sat} values than the highly decomposed sapric organic horizons that are left after development (Boelter, 1969). Once the organic soils are drained, further irreversible changes to the porosity and hydraulic conductivity occur to the remaining sapric soil horizons (Ilnicki and Zeitz, 2003).

The objective of this study was to estimate the physical properties of natural organic soils in Carolina Bay wetlands of the southeastern U.S. so that hydrologic models of these sites could be developed. Because of the inherent difficulty in physically extracting intact soil cores from the ground under the conditions present at these types of sites, a secondary objective of this study was to develop means for estimating some of these physical properties based on more easily collected data.

MATERIALS AND METHODS

As part of a Carolina Bay wetland restoration project, three undrained and naturally vegetated Carolina Bays were selected as reference sites for the restoration. DRAINMOD hydrologic models (Skaggs, 1978) were developed to simulate the long-term hydrologic regime of the various plant communities found at these sites. DRAINMOD requires estimates of soil physical properties such as K_{sat} and soil water characteristic curves to simulate water table depths in the area of interest.

The reference sites were: Charlie Long Millpond Bay (504 ac, 204 ha), Tatum Millpond Bay (1997 ac, 808 ha), and Causeway Bay (358 ac, 145 ha) in Bladen County NC. All are in or near Bladen Lakes State Forest, at approximately 34^{o}40’59” N and 78^{o}34’54” W. The area has a high density of Carolina Bays on terraces of the Cape Fear River. The average annual air temperature in this region is 62.2^{o} F (16.8^{o} C) and average annual rainfall is 48.4 in (123 cm) per year (USDA, 2002).

The three reference sites represent natural conditions for organic soils in the southeastern US. Tatum Millpond Bay and Charlie Long Millpond Bay have both been managed by the NC Division of Forest Resources since 1938, and have not been extensively burned in the last 65 to 70 yr (Ewing, 2003). Causeway Bay, which is located on privately owned land, also has not been burned in the last 65 to 70 yr. In the past, Tatum Millpond Bay was selectively logged for Atlantic White Cedar (*Chamaecyparis thyoides* L.) between 1938 and 1954 (Lees, 2004). Charlie Long Millpond Bay reportedly has never been logged, though it was used to practice fireline construction in the 1970s. Past management practices in Causeway Bay are unclear, but it is known that the last timber harvest occurred in the northeast section in the 1960s (Ewing, 2003). None of the bays have had their hydrology altered by extensive drainage.

Soil types at the sites typically transition from mineral soils near the bay perimeter to organic soils in the center. Torhunta (coarse-loamy, siliceous, active, acid, thermic, Typic Humaquepts), Lynn Haven (sandy, siliceous, thermic, Typic Alaquods), and Leon (sandy, siliceous, thermic, Aeric, Alaquods) soil series are found along the perimeter, while Pamlico (Sandy or Sandy-skeletal, siliceous, dysic, thermic, Terric Haplosaprists) and Croatan (Loamy, siliceous, dysic, thermic, Terric Haplosaprists) soil series can be found near the centers of the bays (Leab, 1990).

Typical vegetation found at the reference sites included tree species such as Pond Pine (*Pinus serotina* L.), Swamp Tupelo (*Nyssa Biflora* L.), Loblolly Bay (*Gordonia lasianthus* L.), Sweetbay (*Magnolia virginiana* L.), and Swamp Red Bay (*Persea palustris* L.) The understory consisted of Gallberry (*Ilex coriacea* L.), Giant Cane (*Arundinaria gigantean* L.), Fetterbush (*Lyonia lucida* L.), Coastal Sweet-pepperbush (*Clethera alnifolia* L.), Highbush Blueberry (*Vaccinium corymbosum* L.), and Green Briar (*Smilax laurifolia* L.) (Lees, 2004).

Transects 1000 to 1500 ft (300 to 460 m) long were cut by hand through the dense vegetation along the minor axes of the three bays. Along each transect, 15 to 20 plots (16 ft by 16 ft, 5 m by 5 m square) were established approximately every 33 yd (30 m) for soil and vegetation classification. The soils were described by Ewing (2003), and divided into four classes based on the depth of organic soil material. Organic (O) horizons less than 8 in (20 cm) thick were found in the mineral soils. The O horizons that were 8 to 16 in (20 to 40 cm) thick were in soils with histic epipedons. Shallow organic soils had O horizons 16 to 24 in (40-60 cm) thick, and deep organic soils had O horizons greater than 24 in (60 cm) thick. Soils were classified in this manner because these groups could be applied across all three sites, whereas soil series varied from site to site due to textural variation in underlying mineral horizons.

An undisturbed soil core was collected from each of 15 plots: four plots at Charlie Long Millpond Bay, four plots at Causeway Bay, and seven plots at Tatum Millpond Bay. These 15 plots were distributed across the four soil classes as shown in Figure 3.1. Locations of sampling points were selected based on the relative abundance of each soil class at each site. These samples were collected using the sampling device of Caldwell et al. (2005) that could remove an intact soil core (3 in. diam. x 39 in. long) in organic soils from beneath the water table. The soil core was then cut into 3 in. (7.6 cm) long sections for laboratory analysis using a wheel-type PVC pipe cutter to cut through the sampler body. Sharpened spatulas and razor blades were used to gently cut through the soil core.

Vertical saturated hydraulic conductivity (K_{sat}) was measured on each soil core sample in the laboratory using the constant head method (Klute and Dirksen, 1986). The soil water characteristic curve was then measured for each core sample on a volume basis with a Tempe cell apparatus using the methods of Klute (1986) for soil water pressures ranging from 0 TO –0.4 bar (0 to -400 cm) as measured at the bottom of the core sample. At the completion of these measurements, the samples were placed in cans, weighed, oven-dried at 221^{o} F (105^{o} C) for 24 hours, and reweighed to determine water content. Bulk density was computed using the oven-dry weight and the initial apparent volume of each core sample. Initial volumes were used in bulk density calculations since these organic soils exhibited extensive shrinkage upon oven drying. Total porosity was calculated as the water content at zero soil water pressure as measured on the pressure cell apparatus. Particle density was measured using an air pycnometer (Flint and Flint, 2002).

For each of the 15 plots, horizontal K_{sat} (as opposed to the vertical K_{sat} measured on the laboratory samples) was measured in situ for soil horizons below the water table using the piezometer method and calculations described by Luthin and Kirkham (1949). This procedure consisted of placing a 4-in.-diam. PVC pipe on the soil surface. The lower 4 to 6 in (10 to 15 cm) of the PVC pipe was screened to allow water to flow freely through the pipe. A 4-in.-diam. bucket auger was inserted into the PVC pipe, and was used to bore down into the soil profile. As the bore hole deepened, the PVC pipe was pushed downward into the hole. This process was repeated until the screened section of the pipe was positioned in the soil horizon of interest. A "slug" consisting of a 12 in (30 cm) long, 2-in.-diam. PVC pipe filled with gravel and capped on both ends was carefully dropped into the 4-in.diam. PVC pipe, and the rate of water level decline inside the pipe was recorded and used to calculate K_{sat}. Three replications of conductivity measurements were made before boring down to the next soil horizon.

Repeated two-sample t tests were conducted using the TTEST procedure in SAS (SAS Institute, 2002) to determine the significance of differences in the mean physical properties of the Oi, Oe, and Oa horizons at $p \leq 0.05$. The distribution of K_{sat} values was found to be log-normal at the 0.05 level. As a result, geometric means and standard deviations are reported and were used to determine the significance of differences among horizon types and measurement methods. All other soil physical properties were found to have normal distributions.

RESULTS AND DISCUSSION

A typical profile description for a deep organic soil in the reference sites is shown in Table 3.1 to illustrate the morphological features of the major types of organic soil horizons. The Oi horizons were at the soil surface and contained a dense, interconnected mat of plant roots. In this root mat, needles and leaves were found in layers creating a coarse platy structure. The layers may have formed in autumn when the trees shed their leaves or needles. The Oe horizons occurred below a depth of 8 in (20 cm) and were up to 12 in (30 cm) thick. They contained fewer roots than in the Oi horizon, and had a massive structure. Fibers in the Oe horizons were more decomposed than in the Oi horizons. The Oa horizons were deepest in the soil profile and also had a massive structure and fewer roots than found in the Oi horizons.

Measured Soil Physical Properties

Bulk density, particle density, and total porosity data are shown in Table 3.2, where data were averaged for each horizon type across the three sites. The number of samples varied for each soil horizon type (i.e. Oi, Oe, and Oa). This was due in part to the relative abundance of the three soil horizons, but it is primarily an indication of the difficulty in obtaining intact samples from the fragile Oi horizons. Standard errors were very low for all soil properties and horizons measured indicating very little difference among reference sites. The bulk density of the organic soil horizons averaged approximately 9.98 lb ft^{-3} (0.16 g cm^{-3}) with no significant difference between the three horizon types ($p > 0.763$). Total porosity values were high (0.90 ft^3 ft^{-3}) and were also virtually the same among the three organic horizon types ($p > 0.531$).

Particle densities were virtually identical among horizon types ($p > 0.728$), averaging approximately 93.6 lb ft^{-3} (1.5 g cm^{-3}). Cellulose and lignin, the primary constituents of cell walls in woody plant material, are the last components to be decomposed (Fioretto et al., 2004). These decomposition-resistant components have a density of about 93.6 lb ft^{-3} (1.5 g cm^{-3}) (Kellogg and Wangaard, 1969), which is identical to the particle density of the organic soils studied here. Ewing (2003) found the carbon to nitrogen ratios to range from 25:1 for Oi horizons to 50:1 for Oa horizons, indicating a loss of nitrogen compounds relative to carbon compounds during the decomposition process. As an Oi horizon is decomposed to the state of an Oe or Oa horizon, the loss of the more easily decomposed nitrogen-bearing materials such as sugars, starches, and simple proteins apparently did not have a dramatic impact on the soil particle density. The decomposition processes that create Oa and Oe horizons apparently serve to reduce the size of the organic particles without altering the particle density to a measurable extent.

Despite the similarities in bulk density, particle density, and total porosity among the three horizon types, K_{sat} decreased ($p < 0.030$) from the Oi surface horizons to the Oa horizons below (Table 3.3). While the conductivities were virtually the same between laboratory and in situ measurements for Oe and Oa horizons ($p > 0.767$), the laboratory-measured conductivities were less than those measured in situ for Oi horizons ($P = 0.002$). This difference suggested that large, water-conducting pores in the Oi horizons (possibly root channels) were severed in the core collection process and became non-conducting. Given the platy, layered structure of the Oi horizons (Table 3.1), most pores in these materials were likely oriented horizontally along layers of relatively undecomposed organic material, and were evidently longer than the 3-in.-diam. size of the soil cores. Conversely, due to the massive structure of the Oe and Oa horizons, most of the pores in these materials likely occurred in the space between well decomposed organic soil particles. These pores apparently were sufficiently interconnected within the 3-in.-diam. soil cores so as to have similar K_{sat} values between in situ and laboratory measurement methods. The K_{sat} was more variable across the study sites for the less decomposed organic layers near the surface, and less variable for the more decomposed subsurface organic layers.

Differences in pore sizes among the organic soil horizons were apparent in the soil water characteristic curves (Fig. 3.2). For Oi horizons, over 35% of the water held in the saturated samples drained at soil water pressure heads greater than –4 in (–10 cm), while for Oa horizons, only about 20% of the water drained at similar pressure heads. Conversely, over half of the water held at saturation was still retained in Oa horizons at soil water pressure heads of –157 in (–400 cm), whereas in Oi horizons only approximately 35% of the water was retained.

Equivalent cylindrical pore diameters were estimated using the capillary rise equation (Hillel, 2004) for each organic soil horizon as shown in Figure 3.3, under the assumption that the pores were fully wet. Over 30% of the pores in Oi horizons had diameters exceeding approximately 0.012 in (0.3 mm). This horizon is located at the soil surface, where the bulk of plant roots occur. Vepraskas et al. (1991) found that the average diameters of root channels were 0.013 in (0.32 mm) in a southeastern forested site. It is likely that the large pores found in the Oi horizon are root channels that act as the primary conduits for water flow, contributing to the relatively high K_{sat} for these horizons. There was still an abundance of smaller pores in the Oi horizon (38% were less than 0.0003 in. (0.007 mm) in diam.) but the larger pores control the rate at which water moves through saturated soil. In Oa horizons, more than half the pores (by volume) had diameters less than 0.0003 in (0.007 mm). Further, the Oa horizons contained approximately half the volume of large pores (greater than 0.012 in (0.3 mm)) as found in the Oi horizons ($p = 0.024$). These results are reflected in the K_{sat} measurements for these horizons. The Oa horizons, with a greater volume of smaller pores, had lower conductivities than did the Oi horizons with a greater volume of larger pores.

Estimating Organic Soil Hydrologic Properties From More Easily Obtained Data

Due to the difficulty in obtaining undisturbed soil samples in natural organic soils as well as the expensive laboratory measurements required to measure soil hydrologic properties, it is desirable to estimate the hydrologic properties of these soils using more readily obtainable data. Total porosity can be estimated by equation [1] if the bulk density and particle densities are known as shown by:

$$f = 1 - \frac{\rho_b}{\rho_p} \qquad [1]$$

where f is the total porosity, ρ_b is the bulk density, and ρ_p is the particle density of the soil. The 94.2 lb ft^{-3} (1.51 g cm^{-3}) particle density for organic matter in the natural southeastern organic soils estimated in this study can be used to determine total porosity if the bulk density of a particular soil has been determined. Using this particle density, equation [1] performed reasonably well in predicting the total porosities of 49 organic soil samples collected in the reference sites ($R^2 = 0.65$, $P < 0.0001$).

Saturated hydraulic conductivity is a soil property that is highly variable due to the effects of compaction, macropores, soil sample size, temperature, and entrapped air (Ahuja et al., 1999). In this study, Ahuja et al. reported that K_{sat} was closely related to effective porosity, which is the difference between the water content at saturation and at –130 in. (–330 cm) soil water pressure head. The relationship between K_{sat} and effective porosity is expressed using the Kozeny-Carman equation:

$$K_{sat} = B\phi_e^n \qquad [2]$$

where ϕ_e is the effective porosity, and B and n are constants.

For this study, values of B and n were estimated using in situ K_{sat} measurements for the Oe and Oa organic soil horizons of the natural southeastern organic soils. Unfortunately, there were no samples from Oi horizons for which both an in situ conductivity measurement and soil water characteristic data were measured. Values for B and n were 69 and 1.91, respectively, for the Oe horizons, and 70 and 4.30, respectively, for the Oa horizons. Measured K_{sat} values and those predicted using the Kozeny-Carman equation for samples of Oe and Oa horizons are shown in Table 3.4. This equation predicted K_{sat} very well for most of the data points, but not as well for locations TM6 at the 25-28 in (64-72 cm) depth (Oe horizon) and TM2A at the 9-12 in (23-31 cm) depth (Oa horizon). The measured K_{sat} values for these two points were different from the others measured for the same horizon type by an order of magnitude or more. The depths at which K_{sat} was measured for these points were very near the transition from the Oe horizon and the Oa horizon at each location. It is possible that the depth where these measurements were taken in the field was actually representative of the Oa horizon in the case of the TM6 location (25-28 in, 64-72 cm depth), and the Oe horizon for TM2A (9-12 in, 23-31 cm depth). Using values of B and n in equation [2] for

Oa horizons instead of those for Oe horizons at the TM6 location yields a predicted K_{sat} of 1.1 in hr^{-1} (2.9 cm hr^{-1}), much closer to the measured K_{sat} of 0.21 in hr^{-1} (0.53 cm hr^{-1}). Similarly, using values of B and n for Oe horizons to predict K_{sat} at location TM2A yields a value of 3.9 in hr^{-1} (9.9 cm hr^{-1}) compared to the measured value of 4.3 in hr^{-1} (11 cm hr^{-1}). This illustrates the importance of properly identifying the type of organic soil horizon when using this method to predict K_{sat} for a given soil, and also the potential for error at depths in the soil profile near the transition between horizon types.

CONCLUSIONS

Bulk density, total porosity, and particle density were similar among the Oi, Oe, and Oa horizons of the southeastern organic soils. However, the quantity of large pores (greater than 0.012 in (0.3 mm diam.)) and K_{sat} tended to decrease progressively from the Oi to the Oa horizon. The large pores of the Oi horizons are probably root channels since this horizon occurs at the soil surface where most roots occur. K_{sat} values measured in situ for Oi horizons were about two times greater than those measured in the laboratory on soil cores. The deeper Oe and Oa horizons had fewer pores the size of root channels. The soil pores in these horizons were apparently interconnected such that K_{sat} values measured in the laboratory and in situ were similar. The particle densities of the Oi, Oe, and Oa horizons were identical, thus the decomposition process is believed to reduce only the size of the organic particles without changing their composition, at least from a particle density perspective.

Physical properties of the organic soils at the reference sites were similar across the three sites for similar soil types. As a result, we believe that these data can be used for other natural Carolina Bay wetland sites in the southeastern U.S. with organic soils formed under forest vegetation and saturated by fresh groundwater. These results may apply to organic soils in other geographic locations, other wetland types, and/or in areas saturated with brackish/saline water. Further study would be required to confirm this possibility. Methods presented here to estimate total porosity based on bulk density and K_{sat} based on effective porosity performed reasonably well in predicting these parameters and could be used in other studies where direct measurement is not practical. The results of this study have significant importance in understanding the natural hydrology of Carolina Bay wetlands and in predicting the hydrology of wetland restoration sites.

REFERENCES

Ahuja, L.R., W.J. Rawls, D.R. Nielsen, and R.D. Williams. 1999. Determining soil hydraulic properties and their field variability from simpler measurements. p. 1207-1233. *In* R.W. Skaggs and J. van Schilfgaarde (eds.) Agricultural drainage, Agron. Monogr. 38, ASA, CSSA, and SSSA, Madison, WI.

Amatya, D.M. 1993. Hydrologic modeling of drained forested lands. Ph.D. dissertation, North Carolina State Univ., Raleigh, NC.

Amatya, D.M. and R.W. Skaggs. 2001. Hydrologic modeling of a drained pine plantation on poorly drained soils. For. Sci. 47:103-114.

Boelter, D.H. 1964. Water storage characteristics of several peats in situ. Soil Sci. Soc. Proc. 28:433-435.

Boelter, D. H. 1965. Hydraulic conductivity of peats. Soil Sci. 100:227-231.

Boelter, D. H. 1969. Physical properties of peats as related to degree of decomposition. Soil Sci. Soc. Am. Proc. 33:606-609.

Caldwell, P.V., A.A. Adams, C.P. Niewoehner, M.J. Vepraskas, and J.D. Gregory. 2005. Sampling device to extract intact cores in saturated organic soils. Soil Sci. Soc. Am. J. 69:2071-2075.

Collins, M.E., and R.J. Kuehl. 2001. Organic matter accumulation and organic soils. p. 137-162. *In* J.L. Richardson and M.J. Vepraskas, (eds.) Wetland soils: Genesis, hydrology, landscapes, and classification. Lewis Publ., Boca Raton, FL.

Ewing, J. M. 2003. Characterization of soils in a drained Carolina Bay wetland prior to restoration. Ph.D. dissertation, North Carolina State Univ., Raleigh, NC.

Ewing, J. M., M. J. Vepraskas, and C.W. Zanner. 2005. Using historical records of land use to improve wetland mitigation. Southeastern Geogr. 45(1):25-43.

Fioretto, A., C. Di Nardo, S. Papa, and A. Fuggi. 2004. Lignin and cellulose degradation and nitrogen dynamics during decomposition of three leaf litter species in a Mediterranean ecosystem. Soil Biol. and Bioch. 37: 1083-1091.

Flint, A.L. and L.E. Flint. 2002. Particle density. p. 235-239. *In* J.H. Dane and G.C. Topp (eds.) Methods of soil analysis, Part 4. SSSA Book Ser. No. 5. SSSA, Madison, WI.

Hillel, D. 2004. Introduction to environmental soil physics. Elsevier Academic Press, Amsterdam, Netherlands.

Ilnicki, P. and J. Zeitz. 2003. Irreversible loss of organic soil functions after reclamation. p. 15-32. *In* L. Parent and P. Ilnicki (eds.) Organic soils and peat materials for sustainable agriculture. CRC Press, Boca Raton, FL.

Kellogg, R.M. and F.F. Wangaard. 1969. Variation in the cell-wall density of wood. Wood and Fiber Sci. 1:180-204.

Klute, A. 1986. Water retention: laboratory methods. p. 635-662. *In* A. Klute (ed.) Methods of soil analysis, part 1. 2nd ed. Agron. Monogr. 9, ASA and SSSA, Madison, WI.

Klute, A., and C. Dirksen. 1986. Hydraulic conductivity and diffusivity: laboratory methods. p. 687-734. *In* A. Klute (ed.) Methods of soil analysis, part 1. 2nd ed. Agron. Monogr. 9, ASA and SSSA, Madison, WI.

Leab, R.J. 1990. Soil survey of Bladen County North Carolina. USDA-SCS. U.S. Gov. Print. Off. Washington, D.C.

Lees, B.P. 2004. Characterization and community analysis of three Carolina Bays in Bladen County, North Carolina. M.S. thesis, North Carolina State Univ., Raleigh, NC.

Lilly, J.P. 1981. The blackland soils of North Carolina. Their characteristics and management for agriculture. North Carolina Agric. Res. Ser. Tech. Bul. 270, Raleigh, NC.

Luthin, J.N., and D. Kirkham. 1949. A piezometer method for measuring permeability of soil in situ below a water table. Soil Sci. 68:349-358.

McCarthy, E.J., J.W. Flewelling, and R.W. Skaggs. 1992. Hydrologic model for drained forest watershed. J. Irr. Drain. Eng. 118:242-255.

McDonald, M.G. and A.W. Harbaugh. 1988. A modular three-dimensional finite difference ground water flow model. Techniques of water resources investigations of the U.S. Geol. Surv., Book 6, Chap. A1. U.S. Geological Survey, Washington, DC.

Mitsch, W.J. and J.G. Gosselink. 2000. Wetlands 3rd ed. John Wiley & Sons, New York, NY.

Nifong, T.D. 1998. An ecosystem analysis of Carolina bays in the coastal plain of the Carolinas. Ph.D. dissertation, Univ. of North Carolina, Chapel Hill.

Prouty, W.F. 1952. Carolina Bays and their origin. Geol Soc. Amer. Bull. 63:167-224.

Rycroft, D.W., D. J. A. Williams, and H. A. P. Ingram. 1975. The transmission of water through peat. II. Field experiments. J. Ecol. 63:557-568.

SAS Institute. 2002. The SAS system for Windows. Release 9.1. SAS Inst., Cary, NC.

Skaggs, R. W. 1978. A water management model for shallow water table soils. Tech. Rep. 134. Water Res. Instit., Raleigh, NC.

Soil Survey Staff. 1993. Soil survey manual. USDA-NRCS. U.S. Gov. Print. Off., Washington, D.C.

Soil Survey Staff. 2003. Keys to soil taxonomy. 9th ed. USDA-NRCS. U.S. Gov. Print. Off., Washington, D.C.

USDA. 2002. WETS table documentation. Elizabethtown lock 2, NC2732 [Online]. Available at ftp://ftp.wcc.nrcs.usda.gov/support/climate/wetlands/nc/37017.txt (verified 08 Mar. 2006).

Vepraskas, M. J., A.G. Jongmans, M.T. Hoover, and J. Bouma. 1991. Hydraulic conductivity of saprolite as determined by channels and porous groundmass. Soil Sci. Soc. Am. J. 55:932-938.

ACKNOWLEDGEMENT

This chapter was published in the Soil Science Society of America Journal (2007, 71:1051-1057). It was also used as a portion of P.V. Caldwell's Ph.D. dissertation (2005) entitled "Characterization of the hydrologic regime of four Carolina Bay plant communities" that was earned through NC State University and is available through the university's library.

Table 3.1. Profile description of a deep organic soil illustrating the morphological characteristics of major horizon types. Adapted from Ewing (2003).

Horizon	Depth	Description
	in	
Oi	0-8	Black (10YR2/1) fibric material that is part of the root mat; weak coarse platy structure from layering of plant debris; gradual boundary.
Oe	8-20	Very dark brown (10YR2/2) hemic material; massive structure with many organic bodies 0.2 to 2.5 in (0.5 to 1.0 cm) in diameter; gradual boundary.
Oa1	20-33	Black (10YR2/1) sapric material; massive structure; gradual boundary.
Oa2	33-43	Black (N 2.5/0) sapric material; massive structure; gradual boundary.
OC	43-55	Very dark brown (10YR2/2) mucky sandy loam; massive structure; gradual boundary.
C	55-67	Dark yellowish brown (10YR4/4) sandy loam; massive structure.

Table 3.2. Laboratory bulk density, particle density, and total porosity for natural organic soils across the three reference sites. Properties across horizons were not significantly different at the 0.05-level.

		Bulk Density			Particle Density			Total Porosity		
Soil Horizon	Organic Decomposition	n	mean	std. error	n	mean	std. error	n	mean	std. error
			---lb ft^{-3}---			---lb ft^{-3}---			---ft^3 ft^{-3}---	
Oi	Fibric (Peat)	6	9.4	2.50	5	100	6.86	6	0.90	0.02
Oe	Hemic (Mucky Peat)	18	10.0	1.87	15	94	3.74	18	0.89	0.01
Oa	Sapric (Muck)	25	10.6	1.25	20	94	3.12	25	0.89	0.01

Table 3.3. Laboratory measured and in situ measured saturated hydraulic conductivity for natural southeastern organic soils.

		Saturated Hydraulic Conductivity					
		Laboratory			In situ		
Soil Horizon	Organic Decomposition	n	geometric mean	geometric std. error	n	geometric mean	geometric std. error
			---in h^{-1}---			---in h^{-1}---	
Oi	Fibric (Peat)	3	$5.5^{a\dagger}$	0.79	2	18^{a}	0.32
Oe	Hemic (Mucky Peat)	11	2.7^{a}	0.38	9	2.8^{b}	0.47
Oa	Sapric (Muck)	23	0.33^{b}	0.55	4	0.59^{c}	0.71

[†] Geometric mean soil physical property values within a given column with the same letter do not differ significantly at the 0.05 level.

Table 3.4. Field measured and predicted saturated hydraulic conductivity values (K_{sat}) for the Oe and Oa horizons of natural organic soils.

Organic Horizon	Depth	Location[†]	ϕ_e	Measured K_{sat}	Predicted K_{sat}
	in		$ft^3\ ft^{-3}$	---in h^{-1}---	
Oe	6-9	TM2	0.50	7.5	7.5
	9-12	TM2	0.46	3.6	6.3
	17-20	TM3	0.38	4.3	4.3
	25-28	TM6	0.48	0.21	6.7
Oa	18-21	CW4	0.39	0.67	0.43
	9-12	TM2A	0.36	4.3	0.35
	33-36	TM4	0.46	0.94	0.94
	32-35	TM5	0.32	0.20	0.20
	31-34	TM6	0.31	0.15	0.18

[†] Location where conductivity was measured. First two characters indicate site (TM = Tatum Millpond Bay, CW = Causeway Bay). Third and optionally fourth characters indicate plot location along transect (Fig. 3.1).

Charlie Long Millpond Bay

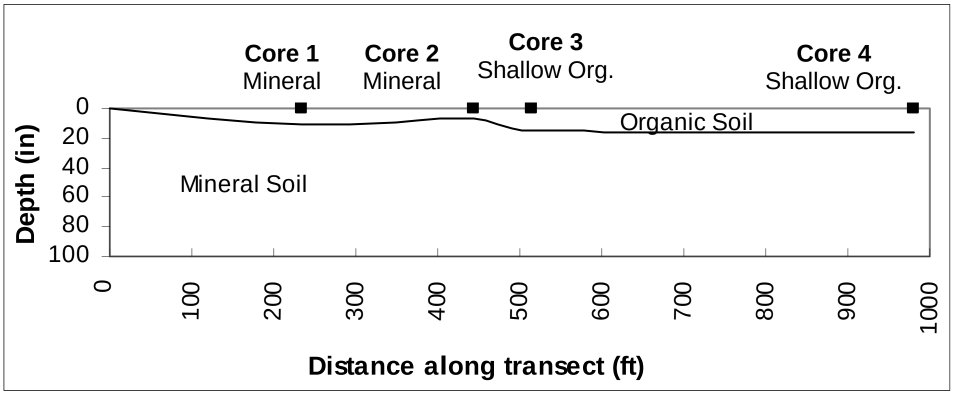

Causeway Bay

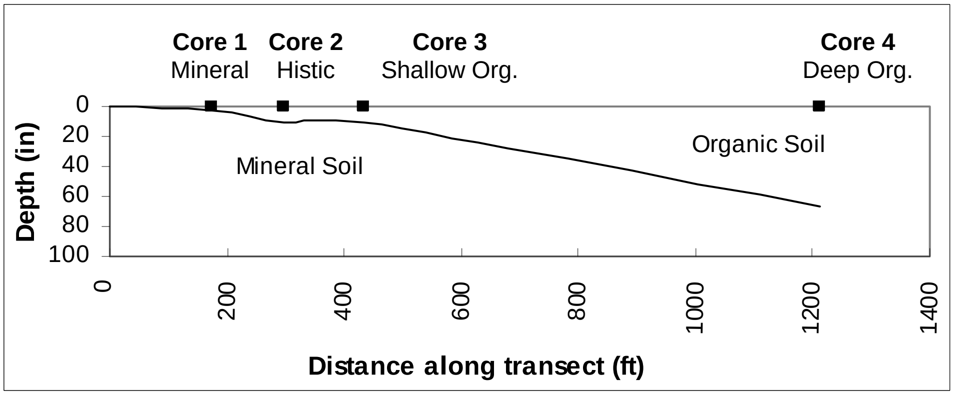

Tatum Millpond Bay

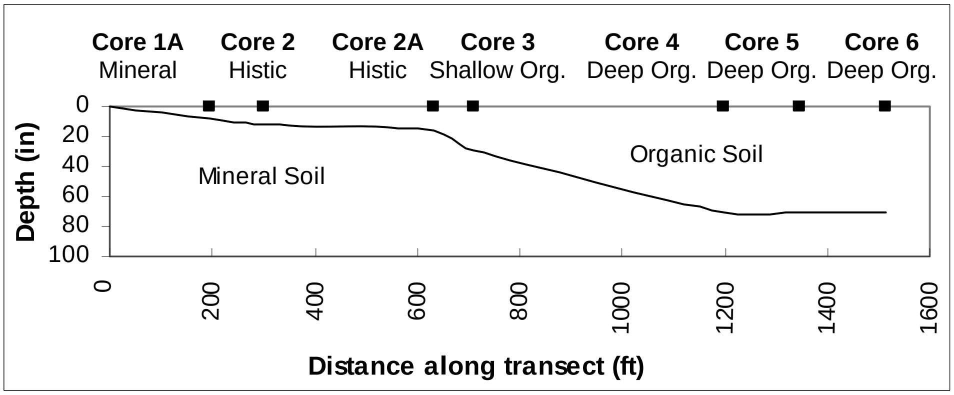

Figure 3.1. Approximate depths of organic soil layers and location of sampling plots along each bay transect. Relative surface elevations along transects are not represented.

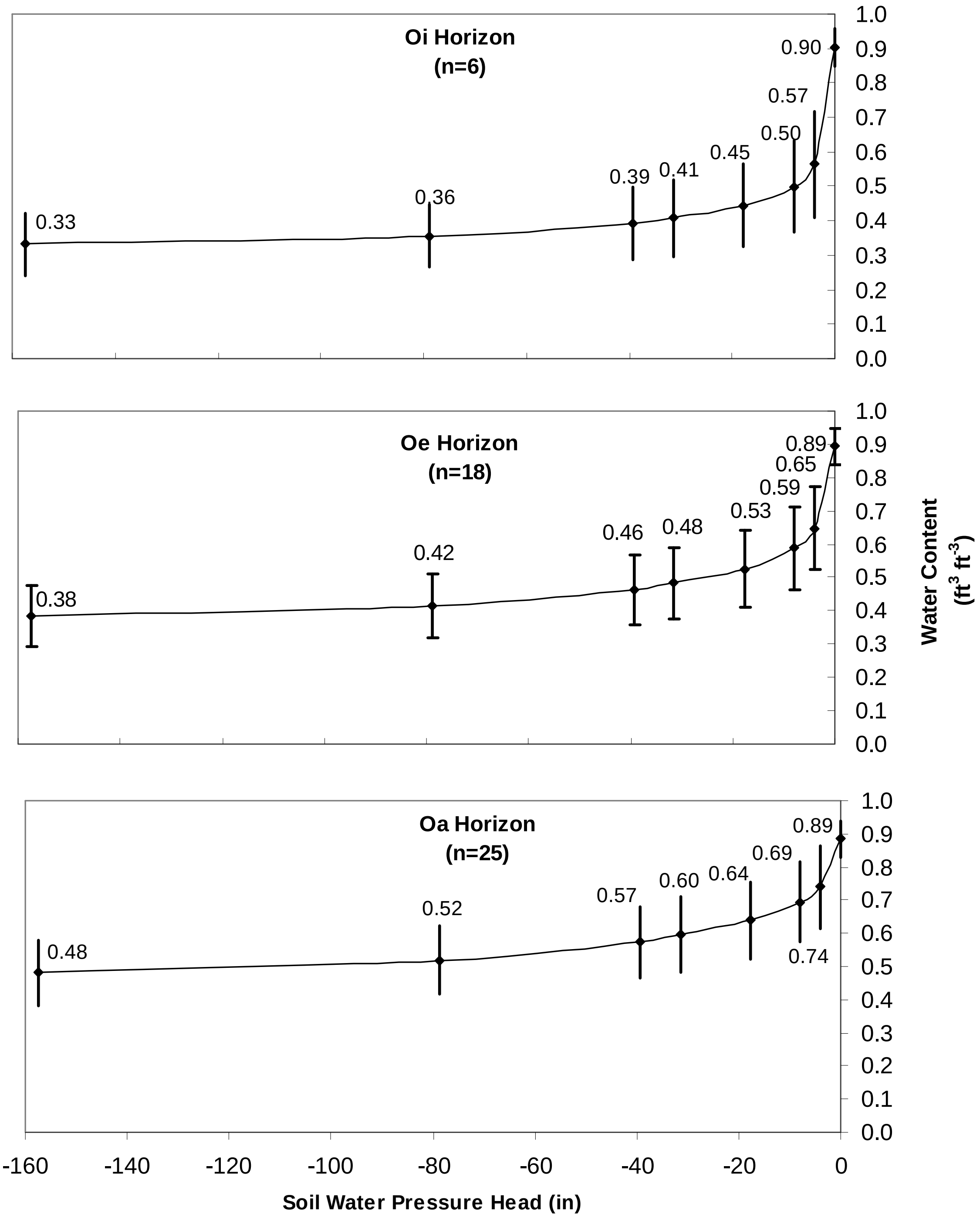

Figure 3.2. Mean soil water characteristic curves for Oi, Oe, and Oa horizons of the organic soils. Numbers are the average water contents at that soil water pressure. Error bars show one standard deviation around the mean.

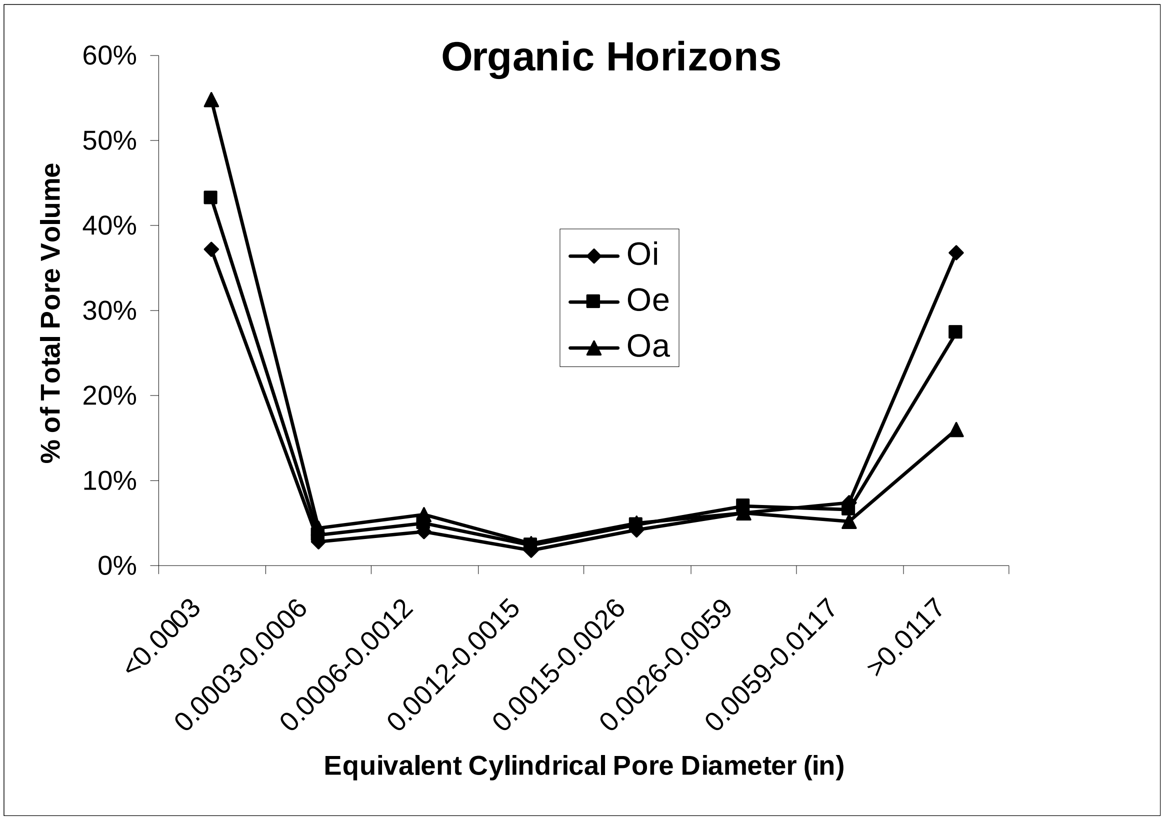

Figure 3.3. Volumes of various sizes of equivalent cylindrical pore diameters expressed as a percentage of total pore volume for organic soil horizons, averaged over the three reference sites.

Chapter 4

SIMULATING THE WATER BUDGETS OF NATURAL CAROLINA BAY WETLANDS

P.V. Caldwell, M.J. Vepraskas, R.W. Skaggs, and J.D. Gregory

INTRODUCTION

Carolina Bays are elliptical depressions oriented on the landscape such that the major axis of the bay is in the northwest-southeast direction (Prouty, 1952). They are formed in poorly drained Coastal Plain sediments all along the Atlantic seaboard of the United States. They can be found as far south as northern Florida and as far north as New Jersey, but are concentrated in the Carolinas. Carolina Bays have a rim of well-drained sandy textured soils that is generally higher in elevation on the southeastern edge (Prouty, 1952; Sharitz and Gibbons, 1982). Within the sandy rim, the bays have poorly drained and darker-colored soils that may be of mineral and/or organic composition (Daniels et al., 1999). In some cases, organic soil layers within the bays can reach 15 ft (4.5 m) thick (Ingram and Otte, 1981).

Several researchers have conducted studies describing the hydrology of Carolina Bays. Bruland et al. (2003) studied a Carolina Bay in Cumberland County, North Carolina over a 2-yr period, describing the seasonal variation in water table depth as a balance between precipitation and evapotranspiration (ET). During time periods when precipitation exceeded ET, the water table was above the surface, and when ET exceeded precipitation, the water table dropped below the surface. Schalles and Shure (1989) also found a strong relationship between precipitation and water level in a Carolina Bay in Barnwell County South Carolina over a 4-yr period, and noted that there may be surface and groundwater connections during wet periods. They asserted that these hydrologic connections must occur laterally rather than vertically due to a dense clay aquitard below the bay, and that the lateral exchange only occurs when the water table elevation is above the clay layer. Lide et al. (1995) studied the hydrology of the same Carolina Bay in South Carolina over a 4-yr period and confirmed that there was interaction between groundwater in the bay and in the area proximate to the bay. However, in their study they discovered that the interaction occurred in both the vertical and lateral directions. During periods of moderate water table depths, vertical and lateral seepage losses from the bay resulted in groundwater mounding in the bay and adjacent area. During periods of high water tables, groundwater inflow occurred in excess of seepage losses.

It is clear that the hydrology of Carolina Bays varies from site to site, can be very complex, and may involve connections with surface and groundwater outside of the bay. In general, the hydrologic role of Carolina Bays on the landscape is poorly understood. This is due in part to the inherent difficulties in measuring the water fluxes in and out of the bays (Sharitz and Gibbons, 1982). Hydrologic models provide a means to estimate these fluxes so that the water budgets of Carolina Bays can be quantified. As federal jurisdiction over "isolated" wetlands continues to be a subject of debate, it is critical that the connections of these wetland types to surrounding waters be better understood. The objective of this study was to compute water budgets for three natural Carolina Bays using calibrated DRAINMOD models.

MATERIALS AND METHODS

The three Carolina Bays evaluated in this study are located in Bladen County, North Carolina, near Bladen Lakes State Forest in the vicinity of 34°40'59" N and 78°34'54" W. The area has a high density of Carolina Bays positioned on terraces of the Cape Fear River. The average annual air temperature in this region is 62.2° F (16.8° C) and average annual rainfall is 48.4 in (123 cm) (USDA, 2002). Tatum Millpond Bay (1997 ac, 808 ha) and Charlie Long Millpond Bay (504 ac, 204 ha) have been managed by the North Carolina Division of Forest Resources since 1938, and have not been extensively logged or burned in the last 65 to 70 yr (Ewing, 2003). Causeway Bay (358 ac, 145 ha) is located on privately owned land and also has not been logged or burned in the last 65 to 70 yr. The hydrology of the study sites has not been altered by artificial drainage.

Soil types in the bays typically transition from mostly mineral composition near the bay perimeter to mostly organic composition in the center. Torhunta (coarse-loamy, siliceous, active, acid, thermic, Typic Humaquepts), Lynn Haven (sandy, siliceous, thermic, Typic Alaquods), and Leon (sandy, siliceous, thermic, Aeric Alaquods) soil series are found along the perimeter, while Pamlico (sandy or sandy-skeletal, siliceous, dysic, thermic, Terric Haplosaprists) and Croatan (loamy, siliceous, dysic, thermic, Terric Haplosaprists) soil series can be found near the centers of the bays (Leab, 1990). Typical tree species include pond pine (*Pinus serotina* L.), swamp tupelo (*Nyssa biflora* L.), loblolly bay (*Gordonia lasianthus* L.), sweetbay (*Magnolia virginiana* L.), and swamp red bay (*Persea palustris* L.). The understory consists of gallberry (*Ilex coriacea* L.), giant cane (*Arundinaria gigantean* L.), fetterbush (*Lyonia lucida* L.), coastal sweet-pepperbush (*Clethera alnifolia* L.), highbush blueberry (*Vaccinium corymbosum* L.), and green briar (*Smilax laurifolia* L.) (Lees, 2004).

One access trail (straight line transect) was cut with hand-tools through the dense natural vegetation of each bay. The trails were located roughly along the minor axes of the bays, and extended from the perimeter to the center for a distance of 1000 to 1500 ft (300 to 460 m). Along each transect, 15 to 20 plots (16 ft by 16 ft, 5 m by 5 m) were established approximately every 100 ft (30 m) for soil and vegetation classification. Water level recording wells (Remote Data Systems, Inc., Wilmington, NC) were installed to a depth of 39 in (1 m) in each of 15 plots (4 to 7 plots at each site) that were distributed along the length of each transect (Fig. 2). Water table depths were recorded on an hourly basis and the data were summarized on a daily basis over a 2-yr period from April 2003 to May 2005 for DRAINMOD model calibration. Relative surface elevations at the four wells in Charlie Long Millpond Bay were measured using a CMT Z33 survey grade, real-time kinematic GPS unit (CMT Inc., Corvallis, OR). One Davis tipping bucket rain gauge (Davis Instruments, Hayward, CA) was installed near the perimeter of each bay. The rainfall data were summarized on an hourly basis over the same 2-yr calibration period for DRAINMOD model input. Other weather data such as air temperature, relative humidity, wind speed, solar radiation, and barometric pressure used in ET estimation were obtained from the Turnbull Creek North Carolina Division of Forest Resources weather station in Bladen Lakes

State Forest (Western Regional Climate Center, 2005). The weather station is located at distances of approximately 7.5, 3.3, and 9 mi (12.0, 5.3, and 14.5 km) from Charlie Long Millpond Bay, Tatum Millpond Bay, and Causeway Bay, respectively.

Hydrologic models such as DRAINMOD (Skaggs, 1978) and MODFLOW (McDonald and Harbaugh, 1988) are powerful tools that can be used to both understand the hydrology of natural wetlands as well as to predict the hydrology of those wetlands that have been restored or created for mitigation purposes. DRAINMOD is a hydrologic modeling package originally developed to simulate agricultural drainage systems in poorly drained soils like those of the Coastal Plain of North Carolina. The model assumes a network of parallel drainage ditches or drain tiles at a given depth and spacing above a restrictive layer (Fig. 4.1). Based on these parameters, the relationship between the water table depth and the drainage rate is determined using the Hooghoudt equation (Hooghoudt, 1940). An hourly water balance on a unit area of the soil profile is computed based on inputs of weather (e.g. hourly rainfall and daily maximum and minimum temperatures used to calculate evapotranspiration losses), soil properties, and drainage rates. DRAINMOD has been used extensively for optimizing drainage systems for agricultural land uses, but it has also been used to simulate the hydrology of natural, undrained wetlands such as Carolina Bays (Chescheir et al., 1994; He et al., 2002).

DRAINMOD requires that soil water characteristic (water retention) and saturated hydraulic conductivity data input for each horizon in the portion of the soil that lies above a restrictive layer. Using this information, a utility in the model's software calculates additional soil properties as a function of the water table depth. The horizontal saturated hydraulic conductivity was measured in close proximity (approximately 6.5 ft, 2 m) to each water level recording well using the piezometer method (Luthin and Kirkham, 1949). In addition, an intact soil core was collected near each well location to a depth of 39 in (1 m) using the methods of Caldwell et al. (2005). Using this method, continuous soil samples 3 in (7.6 cm) diameter by 3 in (7.6 cm) long along the 39 in (1 m) long soil core were collected and tested in the laboratory for saturated hydraulic conductivity and soil water characteristic data. The cores were dissected and used for laboratory measurement of soil water characteristic curves using a pressure cell apparatus (Klute, 1986).

Depths to a restrictive layer were identified for each plot using a 3 in (7.6 cm) diameter bucket auger. Borings were made to a depth of 10 ft (3 m), or to the top of a layer having a sandy clay or clay texture. For the DRAINMOD model input, the depth to the restrictive layer for each site was set either at the depth that a sandy clay or clay layer was observed, or at the maximum depth reached during soil exploration if clay content did not increase with depth. It was assumed that the relationship between drainage rate and water table depth could still be estimated in the model calibration process by adjusting other drainage system parameters, despite possible errors associated with the depth to the restrictive layer.

DRAINMOD calculates potential evapotranspiration (PET) using the Thornthwaite equation (Thornthwaite, 1948), with inputs of daily maximum and minimum air temperature and site latitude data. However, PET estimates made using the Thornthwaite equation are not considered to be very accurate (Nokes, 1995), particularly for winter months. DRAINMOD partially overcomes this limitation by allowing the user to enter monthly correction factors into the model to adjust the Thornthwaite PET estimates based on PET estimates calculated from more accurate means, such as the Penman-Monteith equation (Monteith, 1965). In this study, PET was calculated as the sum of transpiration from the vegetation and evaporation from the soil. Transpiration was calculated using the Penman-Monteith equation. Evaporation from the soil was estimated using the Thornthwaite equation, taking into account the effects of canopy closure using the methods of McKenna and Nutter (1984) as described by McCarthy (1992). Stomatal resistance, which is used to calculate surface resistance in the Penman-Monteith equation, was estimated with a regression equation (Amatya, 1993) that computed stomatal resistance based on air temperature, net radiation, vapor pressure deficit, and day of year. Leaf area index, used to calculate surface resistance, was estimated on a monthly basis using data from Amatya (1993) for similar vegetation. The monthly correction factors for PET were determined by calculating the ratio between the cumulative monthly PET estimated by the methods above and that calculated using the Thornthwaite equation for each month of the 2-yr calibration period. The correction factors for each month during the 2 yrs were averaged to estimate the monthly correction factor used in DRAINMOD.

The DRAINMOD model assumes a drainage system consisting of parallel drainage ditches or drain tiles (Fig. 4.1), and calculates the drainage rate (q) as a function of water table depth (m) using the Hooghoudt equation (Hooghoudt, 1940):

$$q = \frac{8K_1 d_e m + 4K_2 m^2}{L^2} \qquad [1]$$

where K_1 is the effective lateral saturated hydraulic conductivity of the soil above the drain, K_2 is the effective lateral hydraulic conductivity of the soil below the drain, L is the lateral distance between drain tiles, and d_e is the effective depth of the restrictive layer below the drain. The d_e parameter is computed separately as a function of the drain depth (b in Fig. 4.1), measured depth to the restrictive layer (h), L, and the effective radius of the drains (r_e). No such drainage system existed at the natural Carolina Bays in this study. However, the natural relationship between water table depth and the drainage rate out of the system can be estimated using equation [1]. For this study, the parameters in equation [1] were treated as calibration parameters without specific physical definition. Adjusting these parameters essentially changes the nature of the relationship between the drainage rate and the water table depth as predicted by the Hooghoudt equation, thereby approximating the relationship that naturally exists at the wetland sites. The drain depth, b, spacing, L, and surface storage, s, were adjusted in DRAINMOD such that the difference between simulated and measured water table depths over the calibration period were minimized. This calibration process enabled the natural relationship between water table depth and drainage rate to be estimated for the study sites.

DRAINMOD also estimates the amount of deep seepage through the restrictive layer below the drains to the semi-confined aquifer below (Fig. 4.1). Depending on the difference in hydraulic heads above and below the restrictive layer, the seepage will either enter or exit the surficial aquifer system from or to the semi-confined aquifer below. Additional DRAINMOD model inputs required to simulate deep seepage include the vertical saturated hydraulic conductivity and thickness of the restrictive layer, and the pressure head at the bottom surface of the restrictive layer. The distance between the simulated water table and the top surface of the restrictive layer is used to estimate the pressure head above the restrictive layer for calculation of vertical water flux across the restrictive layer. A confined aquifer below a layer of dense sandy clay was discovered at Charlie Long Millpond Bay that had a hydraulic head greater than that above the sandy clay layer, providing a gradient for upward water movement into the bay. For models in this bay, the saturated hydraulic conductivity of the sandy clay layer (i.e. restrictive layer) was an additional variable that was adjusted during model calibration. A piezometer installed in the semi-confined aquifer provided pressure head data at these locations. The piezometer was constructed of a 12 ft (3.7 m) long, 2 in (5.1 cm) diameter PVC pipe, screened in the lower 20 in (50 cm). A Solinst model LT 3001 levelogger (Solinst Canada, Ltd., Ontario, Canada) was placed in the piezometer to record daily pressure head in the semi-confined aquifer.

The success of the models in simulating water table depths over the calibration period was assessed by computing the average absolute deviation, α, between simulated and measured daily water table depths as:

$$\alpha = \frac{\sum \left| Y_m - Y_p \right|}{n} \qquad [2]$$

where Y_m is the measured water table depth on a particular day, Y_p is the predicted water table depth as simulated using DRAINMOD, and n is the total number of days during the calibration period.

Fifteen sets of DRAINMOD model inputs were generated, each corresponding to one of the well locations in the three bays. The models were calibrated for each well location by first assuming a drain depth and surface storage depth. The drain spacing was iterated until α was minimized. This process was repeated for the other drainage system parameters, iterating the drain depth next and the surface storage depth last. For sites where groundwater inflow from the semi-confined aquifer was significant, the vertical saturated hydraulic conductivity of the restrictive layer was iterated in conjunction with each of these variables.

RESULTS AND DISCUSSION

Rainfall

Monthly rainfall recorded at Charlie Long Millpond Bay during the model calibration period is shown in Figure 4.3. Also shown are ranges in normal monthly rainfall from 1971-2000 measured at Elizabethtown Lock, Bladen County (USDA, 2002). The lower limit of normal rainfall in this case is defined such that there is a 30% chance that there will be rainfall less than this amount during a given time period, based on recorded historical precipitation (Sprecher and Warne, 2000). Similarly, the upper limit of normal rainfall is defined such that there is a 30% chance that there will be rainfall greater than this amount (i.e. 70th percentile). Rainfall during most of the study period was within or close to the normal range. Exceptions include the months of July 2003 and August 2004 where rainfall was well above the 70th percentile. December 2003 through February 2004 was a period of drier than normal conditions.

Estimating Potential Evapotranspiration

The Thornthwaite method of estimating PET used by DRAINMOD tends to underestimate PET during the winter months and overestimate during the summer months relative to the Penman-Monteith method (Amatya et al., 1995). As a result, the monthly Thornthwaite correction factors calculated for the DRAINMOD models are greater than unity during the winter months, and less than unity during the summer (Table 4.1). The monthly corrected DRAINMOD Thornthwaite PET correlated very well with monthly PET estimated by the Penman-Monteith equation over the calibration period ($R^2 = 0.97$).

Modeling the Impact of a Semi-Confined Aquifer

Near well location no. 2 in Charlie Long Millpond Bay, a 22 in (55 cm) thick, dense sandy clay layer was found underlying 67 in (170 cm) of organic and sandy-textured mineral soil materials (Fig. 2). Below this sandy clay layer, another sandy-textured soil layer was found. The hydraulic head measured with a piezometer in the semi-confined aquifer was greater than that in the overlying unconfined aquifer, providing potential for vertical water movement into the bay (Fig. 4.4). In fact, the water level in the piezometer was consistently above the land surface in the bay. Based on auger borings, the semi-confined aquifer system appeared to be continuous along the monitoring transect, but it may not be continuous across the entire bay. The recharge area for the semi-confined aquifer is not known. A linear regression analysis indicated good correlation between the change in pressure head in the semi-confined aquifer in response to rainfall and the rainfall measured at the study site ($R^2 = 0.87$). Given the high spatial variability in precipitation in this region, this suggested that the recharge area for the semi-confined aquifer was relatively close to the bay.

Figure 4.5 shows the land surface and water table elevations measured at Charlie Long Millpond Bay for 8/15/02 (prior to this study), a dry condition, 3/26/04, a wet condition, and 7/19/04, a condition of wetness between the other two. During the dry condition (8/15/02), the water table was essentially flat along the transect with very slight gradients from well no. 1 to well no. 2, and from well no. 4 to well no. 3. During the wet condition (3/26/04) these gradients increased but were still quite small. Also during the wet condition, an additional gradient was established between well no. 3 and well no. 2. These gradients indicate lateral flow from wells no. 1, no. 3, and no. 4 to well no. 2 during wet conditions. During dry conditions, the gradients along the bay transect were reduced by an order of magnitude, thus reducing the rate of groundwater movement along the transect. Given that the water table elevation near well no. 4 can be higher than the land surface near well no. 2, where the semi-confined aquifer was discovered, it is possible that the recharge area providing the pressure head in this aquifer was within the bay itself in an area where the confining clay layer is less restrictive or not present.

Hourly water table data from well locations in Charlie Long Millpond Bay revealed that indeed, groundwater was entering the bay. Distinct diurnal water table fluctuations were observed at three of the four wells in the bay such that the water table was drawn down during the day due to ET demands, and rose again at night due to an influx of groundwater. This groundwater inflow is presumed to travel from the semi-confined aquifer below the bay, moving vertically through the sandy clay layer into the unconfined surficial aquifer, but it could also move laterally from areas of higher elevation either inside or outside the bay.

Preliminary DRAINMOD simulations for the wells in Charlie Long Millpond Bay revealed the necessity of adding a deep seepage component to these models to account for this groundwater input. DRAINMOD inputs for the deep seepage component include the thickness of the restrictive layer, the vertical saturated hydraulic conductivity of the restrictive layer, and the pressure head in the semi-confined aquifer below the restrictive layer. The distance between the simulated water table in the unconfined aquifer and the top surface of the restrictive layer is used to estimate the pressure head in the unconfined aquifer above the restrictive layer. In DRAINMOD, the pressure head in the semi-confined aquifer is assumed to be constant, but it was found to be quite variable for the confined aquifer below Charlie Long Millpond Bay. To address this problem, the DRAINMOD software was modified to allow the user to input a file containing daily pressure head data for the confined aquifer. Daily field-measured pressure head data from a piezometer installed in the confined aquifer were used for model input to simulate groundwater inflow from the semi-confined aquifer.

Model Calibration

By adjusting the drain depth and spacing, surface storage, and the vertical saturated hydraulic conductivity of the restrictive layer (for those locations with an apparent groundwater inflow component to their water balance), the natural relationship between the water table depth and subsurface drainage flow rate was approximated. Figure 4.6 shows this relationship for the four well locations in Charlie Long Millpond Bay. The x-intercept in these curves is set by the drain depth parameter. The y-intercept and the shape of these curves are determined by the drain depth, spacing, and the hydraulic conductivity of the various layers in the soil profile. The drainage rates at well locations 3 and 4 were higher than those of well locations 1 and 2 for water table depths near the ground surface. This was likely because wells 3 and 4 were located at higher elevations relative to the areas surrounding these locations than wells 1 and 2 (Fig. 4.5), thus they had higher subsurface drainage rates. Well no. 1 had very low drainage rates relative to the other wells, and if the water table was greater than 2 in. below the ground surface, no drainage occurred.

To effectively calibrate the models of well locations near the perimeters of Tatum Millpond Bay and Causeway Bay (well no. 1A at Tatum Millpond Bay and no. 1 at Causeway Bay), it was necessary to also add a deep seepage component to these models (Table 4.2). These wells also exhibited diurnal water table fluctuations due to the combined effects of ET and groundwater inflow. It was assumed that the semi-confined aquifer system observed at Charlie Long Millpond Bay would adequately approximate the mechanism providing groundwater input at these well locations. In reality, however, the groundwater could enter laterally in addition to, or instead of vertically as was the case in Charlie Long Millpond Bay. The DRAINMOD drainage system parameters quantified as a result of the model calibration process for each of the well locations are shown in Table 4.2.

Average absolute deviations for the 15 DRAINMOD models of well locations in the study sites were quite low, averaging approximately 1.5 in (4 cm) (Table 4.2). These low deviations were partly due to the very shallow water table depths observed over the calibration period, which served to minimize deviations between simulated and measured data. Plots of measured and simulated water table depths for well locations near the perimeter and near the centers of the three bays are shown in Figure 4.7. Overall, the simulated water table depths correlated very well with those measured at the study sites, providing us with good confidence in the ability of the models to predict water table depths at these sites. Water tables predicted by the models in late 2003 were generally further below the land surface than those measured in situ, especially at Charlie Long Millpond Bay. This was following the above normal rainfall in July of that year. Some additional water must have entered the bays not accounted for in the models, perhaps lateral groundwater flow or surface run-on during these extreme rainfall events.

Water Balance Components

Though the DRAINMOD models were calibrated to simulate water table depths and not specific components of the hydrologic water balance, a good deal of information on the hydrology of natural Carolina Bays can be obtained by studying the simulated water balances predicted by DRAINMOD. The water balance equation is:

$$\Delta S = P - ET - RO - GO + GI \qquad [3]$$

where ΔS is the change in water storage, P is gross precipitation, ET is evapotranspiration, RO is the surface runoff, GO is the groundwater outflow, and GI is the groundwater inflow. The RO term quantifies the amount of water that was lost from the system when the surface storage depth was exceeded. The GO term is the amount of water lost in subsurface drainage. The GI term is the amount of water that entered the system either vertically through the restrictive layer from the semi-confined aquifer below or laterally from adjacent areas of higher elevation.

The water balance components over the 2-yr study period for each well location are shown in Table 4.3, and organized into two groups: wells near the perimeters of the bays and wells near the centers of the bays. Evapotranspiration was by far the largest water loss component, amounting to about 75% of rainfall. On a monthly basis, ET could be equal to or greater than precipitation, resulting in a decline in water table elevations for that month.

Surface runoff (RO) was typically low, averaging less than 10% of the total water input. Runoff was lower at well locations nearest the perimeter of the bays, a result of deeper water tables that allowed more rainfall to infiltrate the soil rather than running off when the surface storage depth was exceeded. Runoff from these types of wetlands generally occurs as sheet flow over broad stretches rather than channelized flow in streams or ditches (Ash et al., 1983). Sheet flow occurs just below the litter layer following small but relatively discrete channels. The surface layer of these organic soils, commonly called “root mat”, is a zone of dense plant roots and partially decomposed organic material that has a very high hydraulic conductivity (Caldwell et al., 2007). Runoff from one area of a bay may then provide an input in the form of surface run-on or shallow groundwater inflow to down-gradient areas in the bay. In Charlie Long Millpond Bay and Tatum Millpond Bay, surface flow outlets exist that could carry surface runoff out of the bay.

Groundwater outflow averaged roughly 15% of rainfall at the bays for locations near the centers of the bays (Table 4.3). On the other hand, groundwater inflow for locations near the perimeters of the bays averaged 16% of the total water input during the study period while groundwater outflow averaged 27% of total water input. Total water input is defined as the sum of rainfall and groundwater inflow. Locations near the centers of the bays can be considered recharge areas, meaning there was a consistent net groundwater outflow component of the water balance for these areas. Locations near the perimeters of the bays exhibited characteristics of recharge, discharge (net groundwater inflow), and flow-through (groundwater inflow equal to outflow) wetlands at various times during the study period.

These groundwater flows are illustrated in Figure 4.8 for a location near the perimeter of Tatum Millpond Bay and a location near the center of the bay. Net groundwater flow was consistently negative for the bay center location over the study period. In other words, groundwater flowed out of the center of the bay. During some periods, this groundwater flow approaches zero. These instances occurred during dry periods when the water table at this location dropped sufficiently to make the head gradient for groundwater flow negligible, thereby virtually eliminating flow. Meanwhile, it can be seen that the net groundwater flow for the location near the perimeter of the bay was either positive or negative at various times during the study period. When net groundwater flow was positive, this area near the perimeter of the bay acted as a discharge wetland and when net groundwater flow was negative, the area acted as a recharge wetland.

CONCLUSIONS

The DRAINMOD models were successful in simulating water table depths at all well locations over the 2 yr calibration period despite not having regularly spaced drains at the study sites. Groundwater inflow was detected in measured water table fluctuations for areas near the bay perimeters and this inflow was necessary to calibrate the hydrologic models for these locations. The source for this inflow is not known, but for some locations is believed to originate from a semi-confined aquifer found beneath the water table aquifer. The recharge area for the semi-confined aquifer providing the groundwater inflow is not known but it is believed to be close to the bay. Surface elevations within the bay indicate that the source area for this semi-confined aquifer could be within the bay itself, in an area of higher elevation that lacks the confining layer below. Further study will be required to fully understand the source and sink of groundwater flow in the bays.

Model simulation results revealed that locations near the perimeters of the bays act as recharge, discharge, or flow through wetlands under various conditions. Groundwater outflow exceeded inflow on an annual basis, but inflow could exceed outflow during periods of low rainfall. On the other hand, locations near the bay centers consistently acted as recharge wetlands. The elevation of the water table in these areas was controlled primarily by rainfall and evapotranspiration. During periods when evapotranspiration exceeded rainfall, the water table depth increased. When rainfall exceeded evapotranspiration, the water table depth decreased.

The calculated water budgets were fairly consistent across the three Carolina Bays in this study, and may be similar to other sites. Further investigation of this nature will be necessary to determine whether these water budgets are universally representative of these types of wetlands. The results of this study can be used to better understand the hydrology of natural Carolina Bays thereby improving the success of restoration projects of similar sites, and they provide a foundation for evaluating the hydraulic connectivity between these wetlands and other aquatic ecosystems.

REFERENCES

Amatya, D. M. 1993. Hydrologic modeling of drained forested lands. Ph.D. Dissertation. North Carolina State University, Raleigh, NC, USA.

Amatya, D. M., R. W. Skaggs, and J. D. Gregory. 1995. Comparison of methods for estimating REF-ET. Journal of Irrigation and Drainage Engineering 121:427-435.

Ash, A. N., C. B. McDonald, E. S. Kane, and C. A. Pories. 1983. Natural and modified pocosins: Literature synthesis and management options. U.S. Fish and Wildlife Service, Department of Biology, Washington, DC, USA. FWS/OBS-83/04.

Bruland, G. L., M. F. Hanchey, and C. J. Richardson. 2003. Effects of agriculture and wetland restoration on hydrology, soils, and water quality of a Carolina Bay complex. Wetlands Ecology and Management 11:141-156.

Caldwell, P. V., A. A. Adams, C. P. Niewoehner, M. J. Vepraskas, and J. D. Gregory. 2005. Sampling device to extract intact cores in saturated organic soils. Soil Science Society of America Journal 69:2071-2075.

Caldwell, P. V., M. J. Vepraskas, and J. D. Gregory. 2007. Physical properties of natural organic soils in Carolina Bays of the southeastern United States. Soil Science Society of America Journal (In Press).

Chescheir, G. M., D. M. Amatya, and R. W. Skaggs. 1994. Modeling the hydrology of a natural wetland. International Meeting of the American Society of Agricultural Engineers, St. Joseph, MI, USA. Paper number 942597.

Daniels, R. B., S. W. Buol, H. J. Kleiss, and C. A. Ditzler. 1999. Soil systems in North Carolina. North Carolina State University, Soil Science Department, Raleigh, NC, USA. Bulletin 314.

Ewing, J. M. 2003. Characterization of soils in a drained Carolina Bay wetland prior to restoration. Ph.D. Dissertation. North Carolina State University, Raleigh, NC, USA.

He, X., M. J. Vepraskas, R. W. Skaggs, D. L. Lindbo. 2002. Adapting a drainage model to simulate water table levels in coastal plain soils. Soil Science Society of America Journal 66:1722-1731.

Hooghoudt, S. B. 1940. Bijdragon tot de Kennis van Eenige Natuurkundige Groothen van den Grond, 7. Algemeene Beschouwing van het Probleem van de Detail Ontwatering en de Infiltratie door middle van Parallel Loopende Drains, Greppels, Slooten en Kanalen, Verslag. Landbouwk. Onderzoek. 46, 515–707.

Ingram, R. L. and L. J. Otte. 1981. Peat in North Carolina wetlands. p. 125-134. In C. J. Richardson (ed.) Pocosin Wetlands. Hutchinson Ross Publishing Company, Stroudsburg, PA, USA.

Klute, A. 1986. Water retention: laboratory methods. p. 635-662. In A. Klute (ed.) Methods of Soil Analysis, Part 1, second edition. Agronomy Monograph 9, American Society of Agronomy and Soil Science Society of America, Madison, WI, USA.

Leab, R. J. 1990. Soil Survey of Bladen County North Carolina. United States Department of Agriculture Soil Conservation Service, Washington, DC, USA.

Lees, B. P. 2004. Characterization and community analysis of three Carolina Bays in Bladen County, North Carolina. Masters Thesis. North Carolina State University, Raleigh, NC, USA.

Lide, R. F., V. G. Meentemeyer, J. E. Pinder, and L. M. Beatty. 1995. Hydrology of a Carolina bay located on the upper coastal plain of western South Carolina. Wetlands 15:47-57.

Luthin, J. N., and D. Kirkham. 1949. A piezometer method for measuring permeability of soil in situ below a water table. Soil Science 68:349-358.

McCarthy, E. J., J. W. Flewelling, and R. W. Skaggs. 1992. Hydrologic model for drained forest watershed. Journal of Irrigation and Drainage Engineering 118:242-255.

McDonald, M. G. and A. W. Harbaugh. 1988. A modular three-dimensional finite difference ground water flow model. Techniques of Water Resources Investigations of the U.S. Geological Survey, book 6, chapter A1. U.S. Geological Survey, Washington, DC, USA.

McKenna, R. and W. L. Nutter. 1984. Some modifications to CREAMS for forested applications. Forest Resources Research Report. School of Forest Resources, University of Georgia, Athens, GA, USA.

Monteith, J. L. 1965. Evaporation and the environment. Symposia of the Society for Experimental Biology 19:205-234.

Nokes, S. E. 1995. Evapotranspiration. p. 91-132. In A. D. Ward and W. J. Elliot (ed.) Environmental Hydrology. CRC Press, Boca Raton, FL, USA.

Prouty, W. F. 1952. Carolina Bays and their origin. Geological Society of America Bulletin 63:167-224.

Schalles, J. F. and D. J. Shure. 1989. Hydrology, community structure, and productivity patterns of a dystrophic Carolina Bay wetland. Ecological Monograph 59:365-385.

Sharitz, R. R. and J. W. Gibbons. 1982. The ecology of southeastern shrub bogs (pocosins) and Carolina Bays: A community profile. U.S. Fish and Wildlife Service, Division of Biological Services, Washington, DC, USA. FWS/OBS-82/04.

Skaggs, R. W. 1978. A water management model for shallow water table soils. Water Resources Institute, Raleigh, NC, USA. Technical Report 134.

Sprecher, S. W. and A. G. Warne. 2000. Accessing and using meteorological data to evaluate wetland hydrology. U.S. Army Engineer Research and Development Center, Vicksburg, MS, USA. Technical Report TR-WRAP-00-1.

Thornthwaite, C. W. 1948. An approach toward a rational classification of climate. Geographical Review 38:55-94.

USDA. 2002. WETS table documentation. Elizabethtown lock 2, NC2732 [Online WWW]. Available URL: ftp://ftp.wcc.nrcs.usda.gov/support/climate/wetlands/nc/37017.txt. [Accessed 08 Mar. 2006].

Western Regional Climate Center. 2005. Station data retrieval. Turnbull Creek North Carolina. [Online WWW]. Available URL: http://www.wrcc.dri.edu/cgi-bin/wea_list.pl?txNTUR. [Accessed 17 Mar 2006].

ACKNOWLEDGEMENT

This chapter was accepted for publication in the journal *Wetlands.* It was also used as a portion of P.V. Caldwell's Ph.D. dissertation (2005) entitled "Characterization of the hydrologic regime of four Carolina Bay plant communities" that was earned through NC State University and is available through the university's library.

Table 4.1. Monthly PET correction factors used in DRAINMOD simulations.

Month	Correction Factor
January	1.88
February	2.33
March	1.64
April	0.90
May	0.80
June	0.77
July	0.83
August	0.83
September	0.91
October	0.91
November	1.03
December	1.85

Table 4.2. Average absolute deviations (α) between measured and predicted water table depths for DRAINMOD models during the 2-yr calibration period and the DRAINMOD model drainage system parameters resulting from calibration process.

Site	Well Location	Distance From Bay Perimeter	α	Drain Depth	Drain Spacing	Surface Storage	Depth to Restrictive Layer	Thickness of Restrictive Layer	Conductivity of Restrictive Layer
		ft	in	in	ft	in	in	in	in hr^{-1}
Charlie Long Millpond Bay	1	235	1.6	2.0	427	1.8	66.9	22	0.00023
	2	445	1.3	34	328	0.4	66.9	22	0.00173
	3	515	1.9	37	180	0.8	72.0	44	0.00386
	4	981	2.4	26	103	0.3	66.9	22	0.00114
Causeway Bay	1	176	1.7	7.9	115	0.0	66.9	22	0.00051
	2	297	0.6	3.9	32808	1.7	66.9	ND†	ND†
	3	432	0.2	18	14436	2.9	66.9	ND†	ND†
	4	1213	0.4	16	32808	2.4	66.9	ND†	ND†
Tatum Millpond Bay	1A	197	2.2	22	295	0.0	66.9	22	0.00110
	2	302	0.1	28	10958	5.9	66.9	ND†	ND†
	2A	632	0.4	26	3510	5.5	66.9	ND†	ND†
	3	712	0.1	26	16289	6.3	66.9	ND†	ND†
	4	1199	0.3	22	4921	6.3	66.9	ND†	ND†
	5	1346	0.6	22	11647	4.7	66.9	ND†	ND†
	6	1513	0.2	22	2966	5.5	66.9	ND†	ND†

ND† Not determined. No groundwater inflow required to calibrate these models.

Table 4.3. Water balance components for the modeled well locations in the study sites during the model calibration period.

Site[†]	Well Location	Change in Storage (ΔS)	Outputs Runoff (RO)	Groundwater Outflow (GO)	Evapotranspiration (ET)	Inputs Precipitation (P)	Groundwater Inflow (GI)
		in	in	in	in	in	in
Locations near bay perimeters							
CL	1	0.0	6.6	17	71	92.09	2.7
CL	2	-1.1	16	33	71	92.09	27
CL	3	-0.83	18	37	71	92.09	33
CL	4	-1.7	5.1	37	71	92.09	19
CW	1	-1.8	5.3	20	66	86.10	2.8
TM	1A	0.43	9.1	27	65	85.71	16
Mean		-0.83 (0.4)[††]	10.0 (2.3)	29 (3.5)	69 (1.2)	90.0 (1.3)	17 (5.0)
Percent of total water input			9%	27%	65%	84%	16%
Locations near bay centers							
CW	2	0.51	18	1.7	66	86	0.0
CW	3	0.43	14	5.5	66	86	0.0
CW	4	2.1	14	3.9	66	86	0.0
TM	2	1.5	0.91	19	70	91	0.0
TM	2A	3.2	0.20	18	65	86	0.0
TM	3	2.1	0.94	18	70	91	0.0
TM	4	1.8	0.55	19	70	91	0.0
TM	5	3.4	1.8	16	65	86	0.0
TM	6	4.2	1.6	15	65	86	0.0
Mean		2.1 (0.4)	5.9 (2.5)	13 (2.3)	67 (0.83)	88 (0.91)	0.0 (0.0)
Percent of total water input			7%	15%	76%	100%	0%

[†] Location where conductivity was measured. First two characters indicate site (CL = Charlie Long Millpond Bay, TM = Tatum Millpond Bay, CW = Causeway Bay).

[††] Numbers in parentheses are the standard error of mean water balance components.

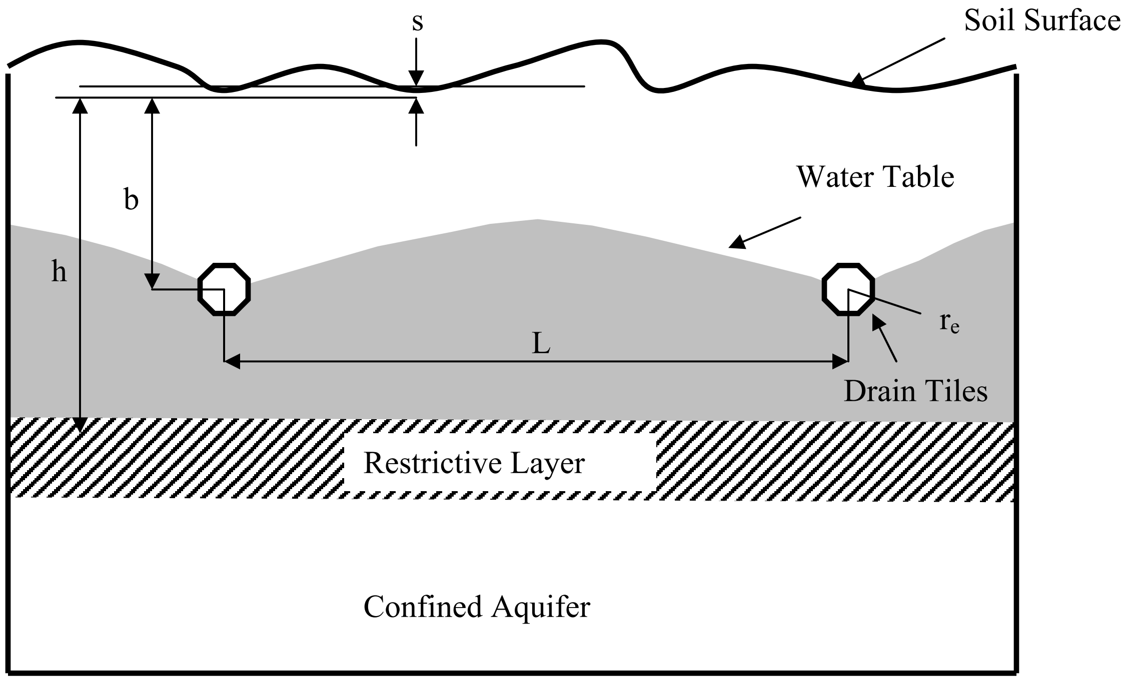

Figure 4.1. Schematic diagram of the drainage system simulated by DRAINMOD. Dimensions include the drain depth, b, drain spacing, L, depth to restrictive layer, h, effective radius of drains, r_e, and surface storage, s.

Charlie Long Millpond Bay

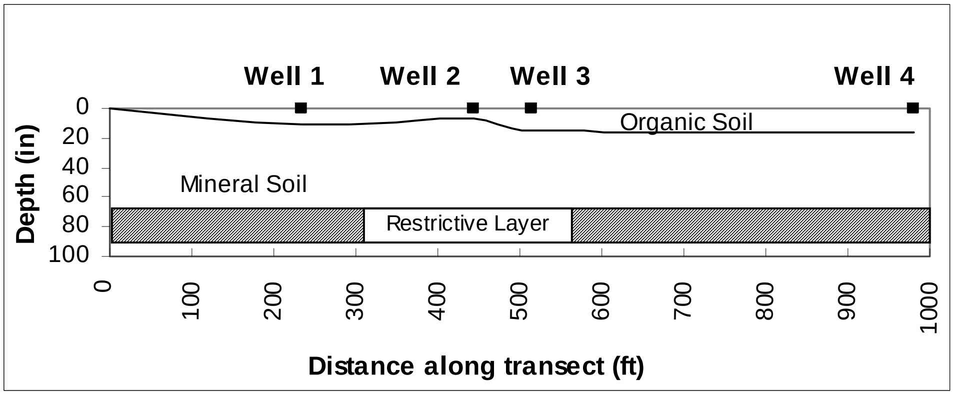

Causeway Bay

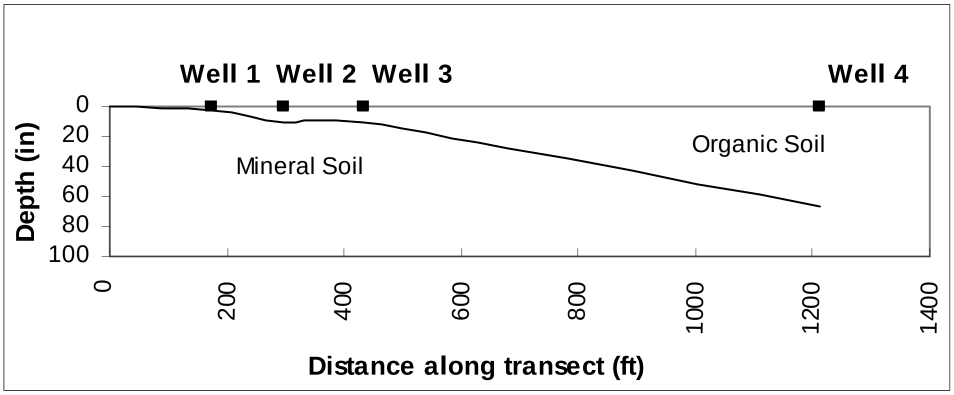

Tatum Millpond Bay

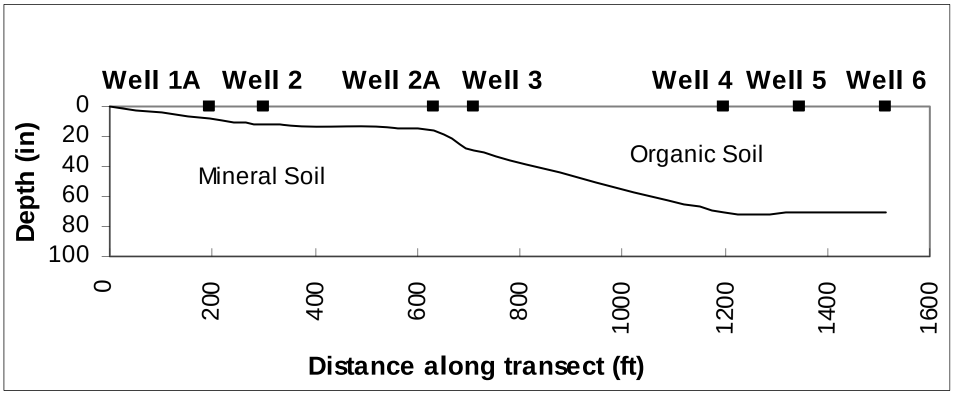

Figure 4.2. Well locations and approximate depths of organic soil layers along each transect. Relative surface elevations along transects are not represented.

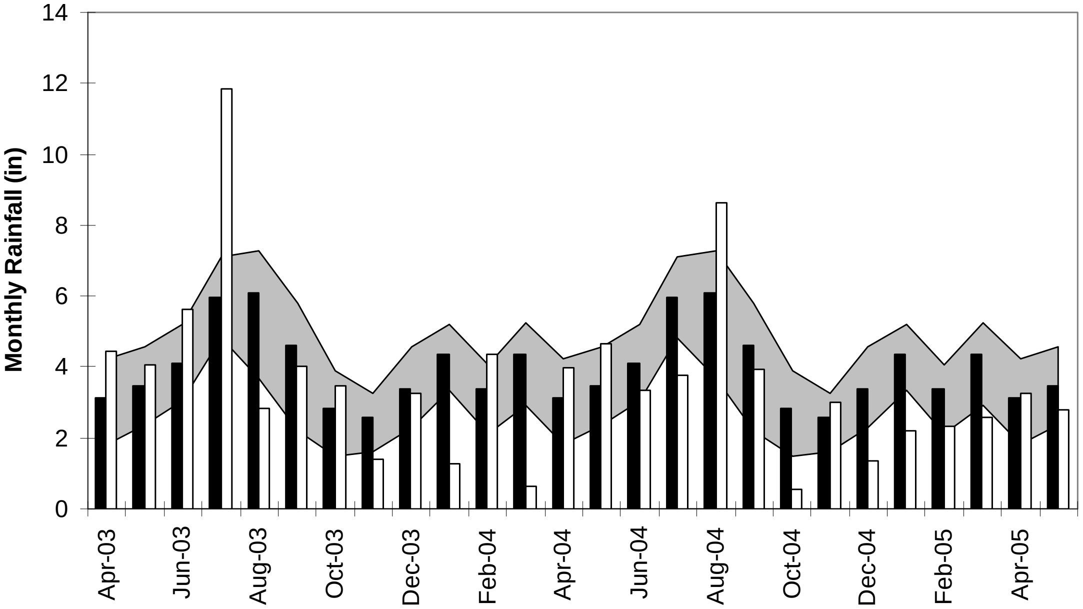

Figure 4.3. Monthly rainfall during the 2-yr calibration period. Black bars are the long-term average monthly rainfall amounts. White bars are monthly rainfall amounts measured at Charlie Long Millpond Bay. Gray area represents the range in normal rainfall amounts between the 30th and 70th percentile probability of occurrence.

Figure 4.4. Hydraulic heads above and below restrictive layer in Charlie Long Millpond Bay near well no. 2.

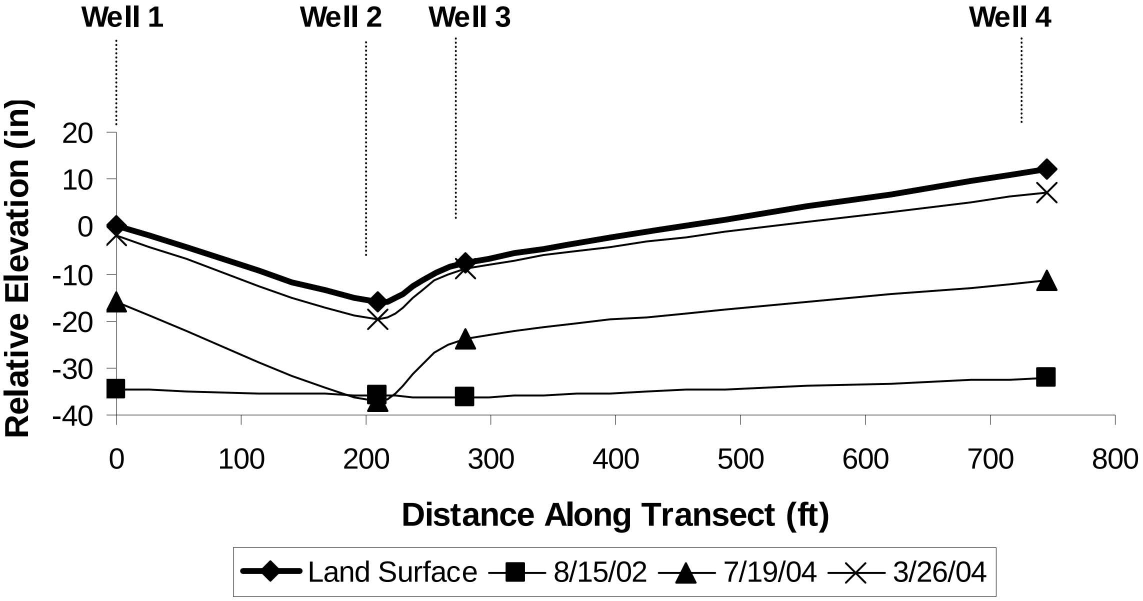

Figure 4.5. Relative land surface and water table elevations on various dates across the Charlie Long Millpond Bay transect. The 8/15/02 water table elevation data are adapted from Lees (2004).

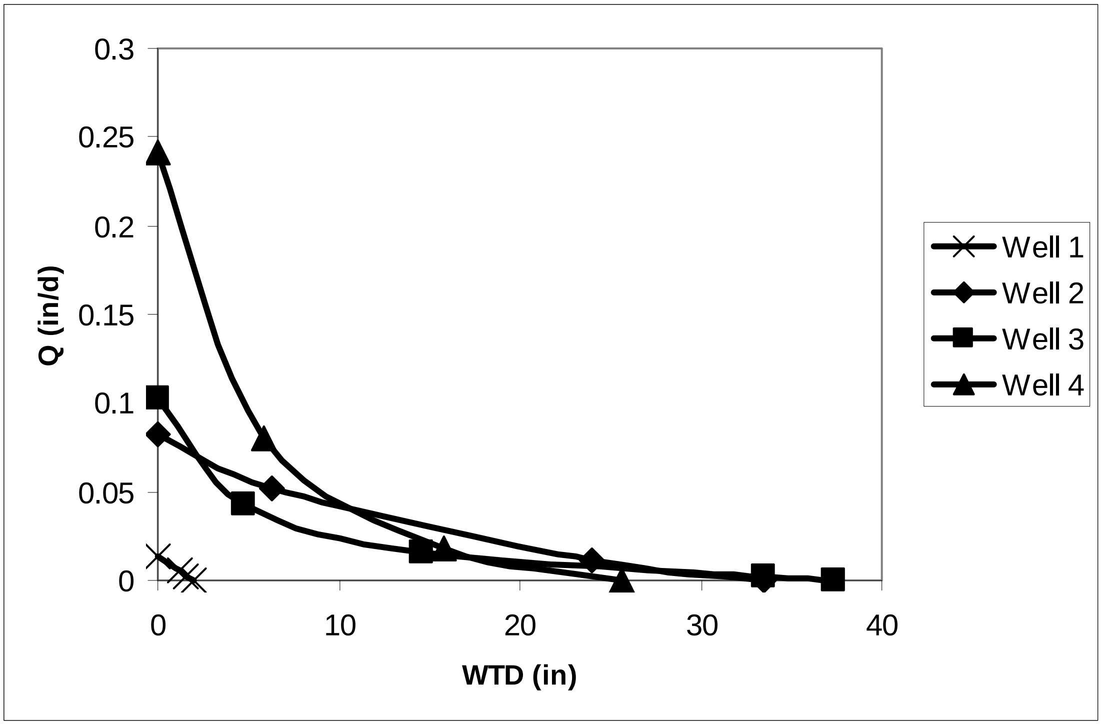

Figure 4.6. Relationship between drainage rate and water table depth for the four well locations in Charlie Long Millpond Bay as determined in the DRAINMOD model calibration process.

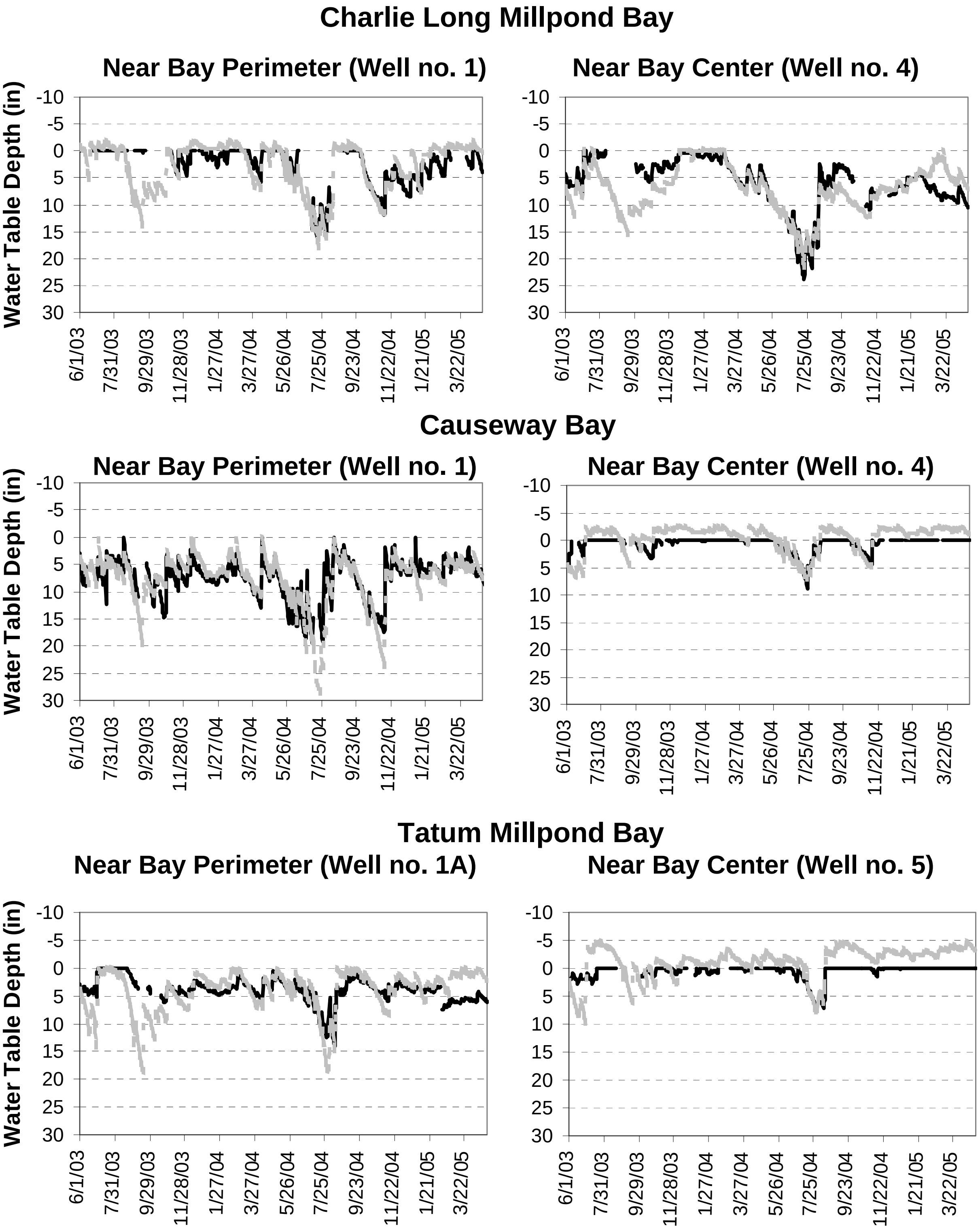

Figure 4.7. Measured (black solid line) and simulated (gray dotted line) water table depths at selected well locations in the study sites. Zero water table depth is at the land surface, positive depths below the land surface, and negative depths above the land surface. Field measured water table depths above the land surface during ponding events were not recorded and are shown as zero water table depths.

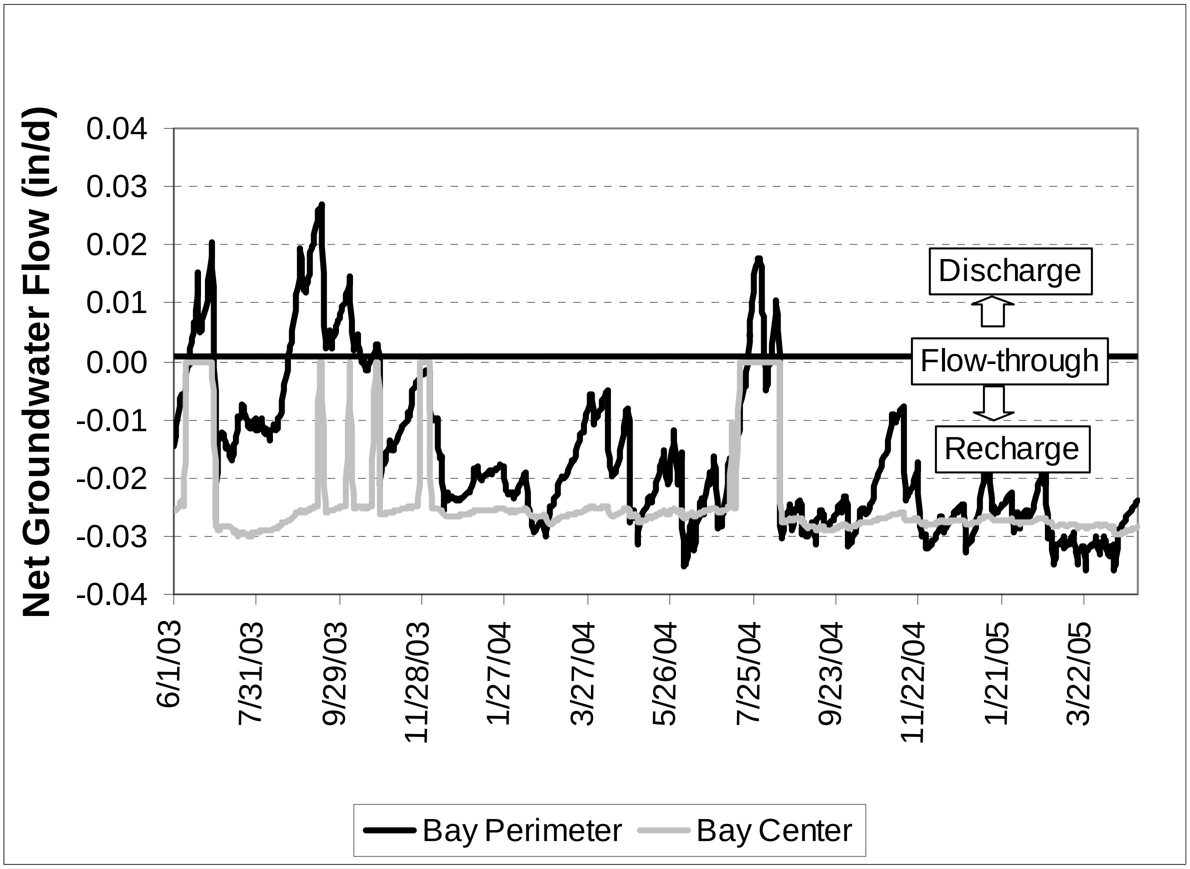

Figure 4.8. Simulated net groundwater flows for locations near the perimeter and near the center of Tatum Millpond Bay.

Chapter 5

QUANTIFYING THE HYDROLOGIC REQUIREMENTS OF WETLAND PLANT COMMUNITIES

P.V. Caldwell, M.J. Vepraskas, J.D. Gregory, R.W. Skaggs, and R.L. Huffman

INTRODUCTION

The field of restoration ecology utilizes tools that speed the process by which lands, wetlands, and waters impacted by human activities recover to their natural state (1). In the area of wetland restoration, three elements must be present for a restoration to be a success: wetland soils, hydrology, and vegetation. In most cases, a specific wetland plant community is selected as the target ecosystem, and plant species associated with that community are planted at the restoration site. Unfortunately, the hydrologic regime of restored wetlands frequently cannot adequately sustain these communities (2). This is sometimes a result of improper hydrologic design, but in many cases it is due to a lack of understanding of the hydrology required by these plant communities. To insure that at least some vegetation survives, wetland designers will frequently plant a variety of vegetation at a site with a wide range of hydrologic requirements in hopes that the hydrologic conditions of a restored wetland will be able to support some of the planted species (3). This practice, though effective in some cases, is inefficient and has no guarantee of success. Quantitative scientific data describing the hydrology of various plant communities in terms of the average depth of the water table, frequency and duration of ponding, etc. could allow much more efficient and successful establishment of wetland vegetation at a restoration site.

Most of the information found in the literature concerning the hydrologic requirements of wetland plant communities is described in qualitative terms. Expressions such as “seasonally or frequently flooded or ponded to the surface” are used to describe hydrology. Much more quantitative data describing the required hydrology of plant communities is required so that a wetland system to fulfill those requirements can be designed. Some studies did successfully quantify the hydrology of wetland plant communities, but did so during a period of only a few years, not taking into account the year-to-year variability in weather patterns that affect the long-term hydrology of a wetland ecosystem. This is partly because the field of wetland science is fairly young, so there are few wetland hydrologic data sets that go back more than a decade or so. In lieu of long-term water table measurements, the use of calibrated hydrologic computer models can generate reasonably accurate long-term data using measured historical weather data as model inputs. These weather data are readily available for at least the past 40-50 years and maybe longer for some geographical locations.

MATERIALS AND METHODS

We developed calibrated hydrologic computer models of four wetland plant communities found in three Carolina Bay wetlands located on the Coastal Plain of North

Carolina (34^{o}40’59” N and 78^{o}34’54” W), and simulated long-term water table depths in each plant community using a 40-year weather record (4). Our objectives in doing this work were two-fold. First, we wanted to determine whether differences in the hydrologic regime of these plant communities might explain their spatial establishment at the study sites. Second, we wanted to quantify these differences, if they exist, to aid in the selection of the appropriate plant species for establishment at a wetland restoration site. The sites, ranging in size from 360 ac to 2000 ac (145 ha to 808 ha), have not been disturbed in at least 65 years or modified in any way and thus represent reference conditions for these plant communities. The average air temperature in the region is 62.2 F (16.8 C), with average annual rainfall amounting to 48.4 in (123 cm) (5). Carolina Bays are elliptical depressions oriented on the landscape such that the major axis of the bay is in the northwest-to-southeast direction (6). They are formed in poorly drained Coastal Plain sediments, and occur along the Atlantic seaboard from northern Florida to New Jersey, but are concentrated in the Carolinas.

RESULTS AND DISCUSSION

The Pond Pine Woodland community (PPW) was found nearest the edges of the bays, and High Pocosin (HP) nearest the center. One of the bays also exhibited the Non-riverine Swamp Forest (NRSF) plant community as well as Bay Forest (BF) (7). Differences in dominant species, size, and density of the canopy and shrub layers serve to distinguish one plant community from another (8). Environmental factors believed to affect the establishment of these communities include peat accumulation, fire frequency and intensity, soil nutrient levels, hydrology, and disturbance history (9). Hydrology is believed to have a major impact on the relative contributions of the other factors (10, 11).

Figure 5.1 shows the percentage of the time over the 40 yr simulation that the water table was equal to or deeper than various depths relative to the soil surface in each plant community. Positive water table depths indicate times when the water table was above the ground surface while negative depths are when it was below the surface. We found that the difference in the curves for the NRSF and BF was not significant at the 0.05 level. The PPW community was significantly different from the NRSF but not different from the BF. This was due primarily to the small sample size associated with the BF ($n = 2$). We believe that a larger sample size would show differences between these two communities.

The HP community hydrology was not found to be significantly different from any of the other communities, though it was more similar to that of the NRSF and BF communities than the PPW. We found that this community tended to have a hydrologic regime similar to the communities adjacent to it along transects cut through the sites. HP communities that were near PPW communities had water table depths similar to PPW while those near NRSF or BF communities had water table depths similar to those communities. Based on this fact and that the HP canopies typically have trees of small stature and low density (Table 5.1), we believe that this community is a result of a past disturbance (fire, storm damage, logging, etc.). It has been found that HP communities could be incorrectly identified in areas damaged by fire that were originally PPW communities (8). Prior to the damage, these areas most likely resembled adjacent communities, but the vegetation is now in the process of regenerating and will one day return to the original community type.

The deepest water tables measured 61, 25, 20, and 22 in (155, 63, 51, and 55 cm) below the ground surface for the PPW, NRSF, HP, and BF communities, respectively (Fig. 5.1). The median water table depths for each community were 4.3 in (11 cm) below the surface in the PPW, and 3.1, 2.0, and 2.7 in (8, 5, and 7 cm) above the surface for the NRSF, HP, and BF communities, respectively. The water table was above the ground surface (>0 in) about 24% of the time in the PPW, but 83%, 60%, and 80% of the time in the NRSF, HP, and BF communities. When water was above the surface, it reached a maximum depth of 6.3 in (16 cm) above the surface for the HP and NRSF, 5.5 in (14 cm) for the BF, and only 1.6 in (4 cm) for the PPW. Water levels above the surface, or ponding, do not indicate that the entire area is completely flooded with water. At our study sites, the ground surface varied in elevation by 6 in (15 cm) or more on a local scale due to a large amount of microtopography in the form of natural hummocks and swales. The magnitude of this microtopography appeared to be similar among the various plant communities studied. Typically, the local high elevations were occupied by trees and were above the levels of ponded water. The water table depths we present here are measured relative to the ground surface in the local low elevations.

These times when water is above the ground surface have been shown to be an important factor in the survival and growth of wetland plant species, and thus the establishment of plant communities on the landscape (12). It has been found that ponding in extremely wet years (i.e. 90th percentile hydroperiods) has an important influence on species composition in forested riverine wetlands (13). Figure 5.2 shows the frequency of different hydroperiods in terms of total days ponded per water year for the plant communities we studied. The water year was assumed to begin in October and end in September of the following year. The median hydroperiod for the PPW, NRSF, HP, and BF communities were 91, 316, 243, and 306 days per water year, respectively. The 90th percentile hydroperiod, that which is believed to control plant community establishment, was 116, 360, 292, and 355 days for the PPW, NRSF, HP, and BF communities, respectively.

In addition to considering hydroperiod in terms of *total* days ponded per water year, we also studied hydroperiod in terms of *maximum consecutive* days ponded per water year. Our results show that the median water year of our 40 year simulation had maximum ponding durations of 51, 271, 181, and 252 consecutive days for the PPW, NRSF, HP, and BF communities, respectively. The 90th percentile water year had ponding durations of 72, 346, 249, and 339 consecutive days for these communities, durations greater than 11 consecutive months for the NRSF and BF. During times of high rainfall, some of these ponding events lasted longer than a single water year. The maximum ponding durations were 92 consecutive days in the PPW, and 913, 580, and 907 days in the NRSF, HP, and BF communities. However, a significant portion of the ponding events (18%, 12%, 9%, and 13% for the PPW, NRSF, HP, and BF communities, respectively) lasted one day or less.

It has been shown that many wetland plant species do not extend roots below the water table and that periodically flooded examples develop deeper root systems than those that are continuously flooded (12, 14). One of the explanations in the literature for the establishment of the PPW and possibly the NRSF communities is the ability of the vegetation to extend roots down into the mineral soil horizons that lie below the accumulated peat on the surface during drier periods, thereby accessing potentially higher nutrient reserves in these soil materials (8, 13, 15). Results at our study sites refuted this assertion by showing that the nutrient status of the mineral soils was not significantly greater than the overlying peat horizons (7, 16). We propose that access to mineral soil may facilitate the growth of larger trees such as those found in the PPW and NRSF communities, not because of higher fertility in the mineral soils, but rather by providing more mechanical support to resist blow-down during strong storms than communities whose roots are supported only be the weak, fragile structure of saturated organic soils.

To determine whether there were differences among the communities in terms of access to mineral soils, we studied the interaction of the water table with the mineral soil horizons in each plant community. The PPW community had water tables that extended into mineral soil every year of the 40 years simulated, averaging 73 total days (37 consecutive days) per year. The NRSF community had water tables in mineral soils in only 5 of the 40 years simulated, occurring on a 4-13 year interval. During these years, the water table was in mineral soil for an average of 21 total days (19 consecutive days) during the year. The BF community occurred only on deep organic soils (greater than 67 in (170 cm)), and given the maximum water table depth of 22 in (55 cm) in this community, the water table never reached mineral soil. The HP community (a result of past disturbance) tended to be similar to those communities surrounding it. HP communities near PPW frequently had water tables in mineral soils while those near BF communities never reached mineral soil. Based on these data, the communities with the largest trees (i.e. PPW and NRSF) had access to mineral soil on a regular basis for weeks at a time, while those with smaller trees (i.e. BF) did not. Given that there was no difference in the fertility of the mineral soil horizons, we conclude that access to mineral soil horizons in the PPW and NRSF communities may provide the mechanical support required for the establishment of large trees. The hydrologic regime of the HP community further supports this conclusion. The hydrology of this community was most similar to the BF, which occurred only on deep organic soils. This would imply that disturbance, particularly wind blow-down, is more likely to occur in the BF than in the PPW and probably the NRSF communities. A lack of soil support is a reasonable explanation for this phenomenon.

In addition to differences in water table depths, we discovered differences in the flow of ground water through the communities in this study. The NRSF and BF communities only had groundwater leaving the system while the PPW community had an inflow of groundwater that was about 15% of total water input (the sum of rainfall and groundwater inflow). Annual groundwater outflow exceeded inflow, but during dry periods inflow exceeded outflow, helping to keep water tables generally within 12 in (30 cm) of the surface even during periods of moderate drought. It has been proposed that communities with larger trees (i.e. PPW and NRSF) receive an influx of groundwater that could carry dissolved nutrients into these communities to be used by the vegetation to create biomass (8, 15). Our data indicate that this is at least physically possible for the PPW community, though soil fertility in this community was not significantly different from the BF community. Our data do not, however, prove a physical means of transporting dissolved nutrients to the NRSF to account for the large trees in this community.

CONCLUSIONS

Based on the results of this study, we propose recommendations for restoration of these plant communities for wetland mitigation sites as shown in Table 5.2. The three site factors we considered include thickness of organic soil layers, available phosphorus averaged over the upper 35 in (90 cm) of soil, and median hydroperiod (total days per water year) for the site. To use these recommendations for a wetland restoration, an initial site reconnaissance visit should be taken and the thickness of organic soil layers recorded and soil samples collected for analysis of available soil phosphorus. Rainfall and water level data should be recorded over a period of at least one year for the calibration of hydrologic models. Once the models are calibrated, they can be used to simulate the long term water levels at various locations at the site after the restoration of wetland hydrology. The models can also be used to determine exactly how to prepare the site to achieve a hydroperiod of a particular length.

If the thickness of organic soil layers is less than 16 in (40 cm) and the median hydroperiod estimated by hydrologic simulation is 45-135 days per water year, the PPW community would be a good candidate for restoration at that location, and tree species typical of that community should be planted there. This is likely to be the case regardless of the level of available soil phosphorus, though in our study the PPW community only occurred when phosphorus levels were below 18 mg dm^{-3}. For sites with organic soil layers between approximately 8 and 31 in (20 and 80 cm), phosphorus levels greater than 18 mg dm^{-3}, and a median hydroperiod of 300-320 days per water year, the NRSF community would be a good choice for restoration. For sites with similar hydroperiods, similar or greater organic layer thicknesses, and phosphorus levels below 18 mg dm^{-3}, the BF community would be recommended.

There are several combinations of organic soil layer thicknesses, available soil phosphorus levels, and hydroperiod that are not addressed in these recommendations. For instance, what if your site has organic soil layers less than 16 in (40 cm), but the estimated median hydroperiod is 300-320 days per water year rather than 45-135 days, or what if the hydroperiod is somewhere between these ranges? These gaps in our recommendations represent opportunities for further research in wetland ecosystem restoration. Studies at other sites, using the methodology presented here, could serve to fill these gaps in the environmental factors that affect the establishment of these and other plant communities.

The results of our study have several implications. First, we have determined that there are distinct differences in the hydrologic regime of the PPW community relative to the NRSF and BF that likely determine where these communities become established on the landscape. Second, we have provided evidence of differences in root access to mineral soil layers between the PPW and NRSF compared to the BF community. We believe these differences allow the growth of larger trees in the PPW and NRSF communities. Third, we have quantified the hydrologic regimes of these communities so that engineers designing wetland restoration sites can approximate these conditions and maximize the chances of successfully establishing wetland vegetation. Finally, we have validated a methodology that can be used to quantify the hydrology of other wetland plant communities in other parts of the world, helping others to restore the function of these valuable ecosystems.

REFERENCES

1. A. P. Dobson, A. D. Bradshaw, A. J. M. Baker, *Science* **277**, 515 (1997).
2. M. S. Dennison, J. A. Schmid, "Wetland mitigation: Mitigation banking and other strategies for development and compliance" (Government Institutes, Inc., Rockville, MD, 1997).
3. K. L. Morgan, T. H. Roberts, *Wetlands* **23**, 65 (2003).
4. Details regarding materials and methods are available on Science Online.
5. USDA, "WETS table documentation. Elizabethtown lock 2, NC2732" (Natural Resources Conservation Service, Water and Climate Center, Portland, OR, 2002).
6. W. F. Prouty, *Geol. Soc. Am. Bull.* **63**, 167 (1952).
7. B. P. Lees, thesis, North Carolina State University (2004).
8. M. P. Schafale, A. S. Weakley, "Classification of the natural communities of North Carolina: Third Approximation" (North Carolina Natural Heritage Program, Division of Parks and Recreation, Department of Environment, Health, and Natural Resources, Raleigh, NC, 1990).
9. R. R. Sharitz, J. W. Gibbons, "The ecology of southeastern shrub bogs (pocosins) and Carolina bays: A community profile" (U.S. Fish and Wildl. Serv., Div. Biol. Serv., Tech. Rep. FWS/OBS-82/04, U.S. Fish and Wildl. Serv., Washington, D.C., 1982).
10. D. D. Steven, M. M. Toner, *Wetlands* **24**, 23 (2004).
11. L. K. Kirkham, P. C. Goebel, L. West, M. B. Drew, B. J. Palik, *Wetlands* **20**, 373. (2000).
12. J. P. Megonigal, F. P. Day, *Ecology* **73**, 1182 (1992).
13. P. A. Townsend, *Plant Ecology* **156**, 43 (2001).
14. C. R. Schwintzer, S. A. Lancelle, *J. Ecol.* **71**, 489 (1983).
15. L. J. Otte, "Origin, development, and maintenance of the pocosin wetlands of North Carolina" (Rept. To N.C. Natural Heritage Program, 1982).
16. J. M. Ewing, thesis, North Carolina State University (2003).
17. T. F. Hall, W. T. Penfound, *Am. Mid. Nat.* **22**, 369 (1939).
18. Funding for this research was provided by the North Carolina Department of Transportation (Research Project No. HWY-2004-19) and is gratefully appreciated.

ACKNOWLEDGEMENT

This chapter used as a portion of P.V. Caldwell's Ph.D. dissertation (2005) entitled "Characterization of the hydrologic regime of four Carolina Bay plant communities" that was earned through NC State University and is available through the university's library.

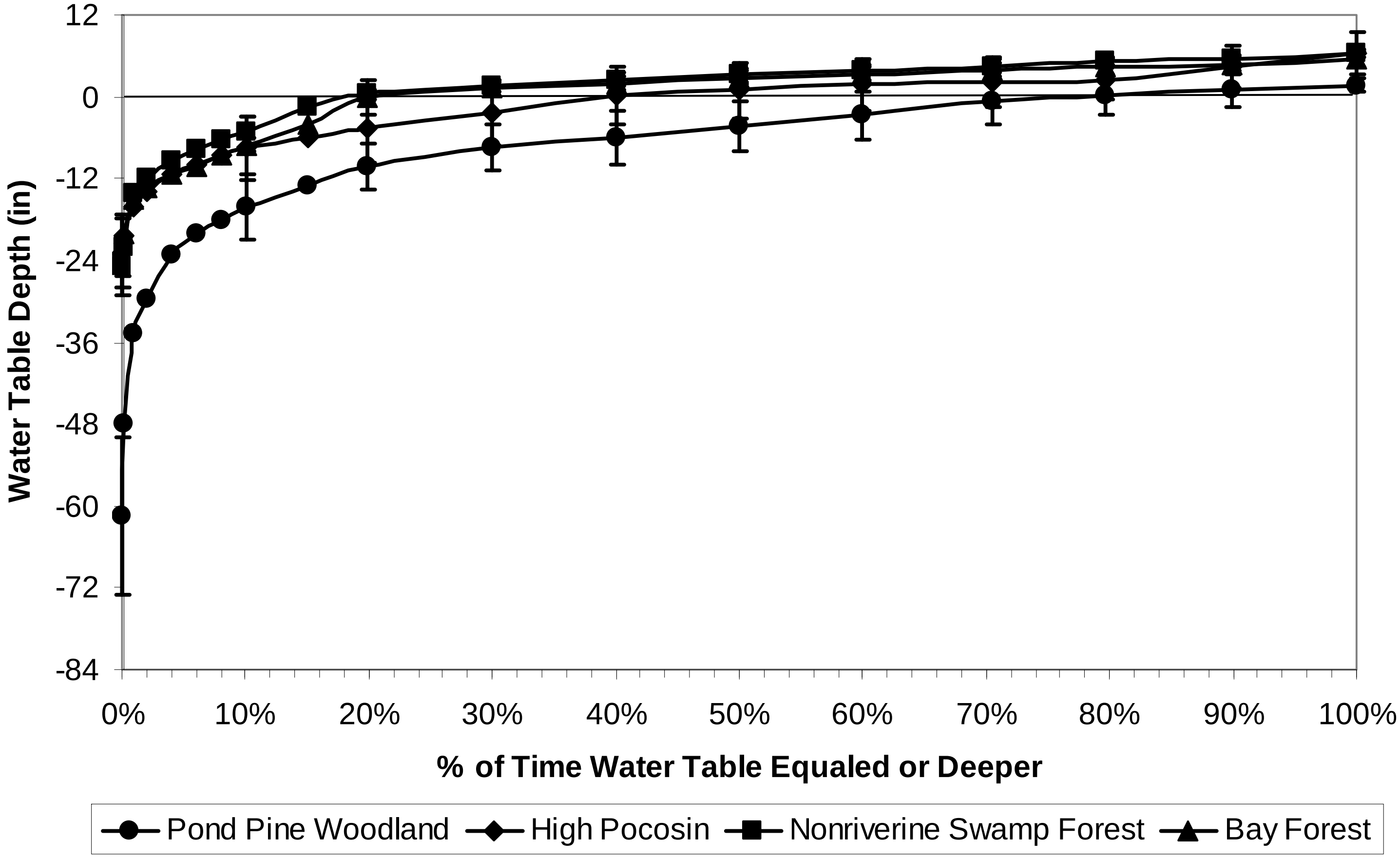

Fig. 5.1. Water table depth frequency curves for each plant community over the 40 yr simulation. Data shown for each plant community are averages among the various locations simulated. Error bars represent one standard error above and below the mean.

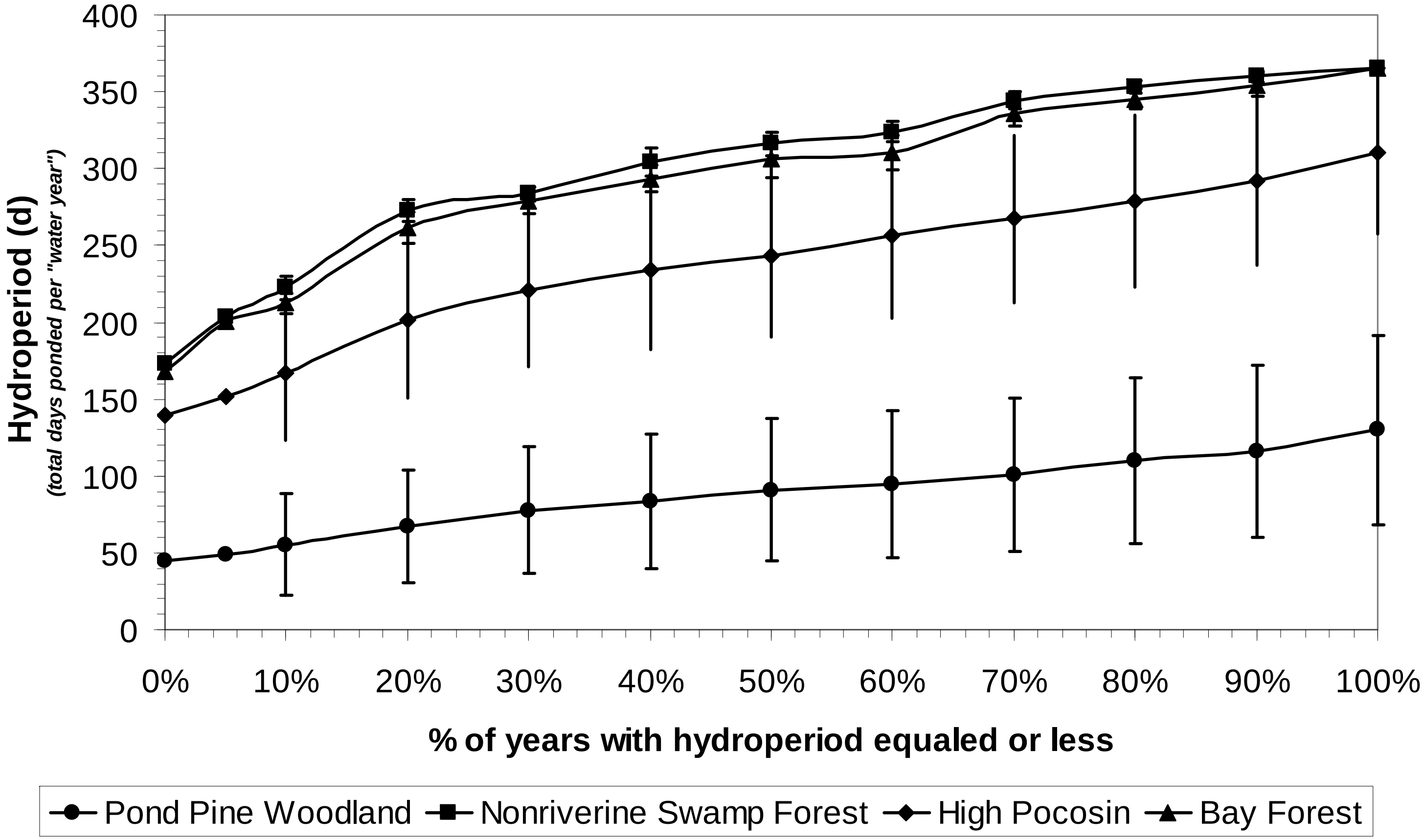

Fig. 5.2. Hydroperiod (total days ponded per water year) frequency curves for each plant community over the 40 yr simulation. Data shown for each plant community are averages among the various locations simulated. Error bars represent one standard error above and below the mean.

Table 5.1. Characteristics of the plant communities investigated in this study.

Characteristic	Refs.	Plant Community			
		Pond Pine Woodland	Nonriverine Swamp Forest	High Pocosin	Bay Forest
Dominant canopy species	(8)	*Pinus serotina* (Pond Pine)	*Taxodium distichum* (Bald Cypress) *Taxodium ascendens* (Pond Cypress) *Nyssa biflora* (Swamp Tupelo)	*Pinus serotina* (Pond Pine) *Gordonia lasianthus* (Loblolly Bay) *Persia palustris* (Red Bay) *Magnolia virginiana* (Sweet Bay)	*Gordonia lasianthus* (Loblolly Bay) *Persia palustris* (Red Bay) *Magnolia virginiana* (Sweet Bay)
Canopy height (ft)	(15, 17)	59	82	25	33
Basal area (ft^2 ac^{-1})	(7)	54.6	98.1	8.4	34.8
Available soil phosphorus (mg dm^{-3})	(7)	12.3	17.8	9.2	12.1
Thickness of surface organic soil layer (in)	(7)	<16	8-32	>32	>32

Table 5.2. Recommendations for the establishment of wetland plant communities based on site characteristics.

Site Characteristics			
Thickness of Organic Soil Layer (in)	Available Soil Phosphorus (mg dm^{-3})	Median Hydroperiod (Total days ponded per water year)	Recommended Plant Community
< 16	<> 18	45-135	Pond Pine Woodland
8 - 32	> 18	300-320	Nonriverine Swamp Forest
8 - 32	< 18	300-320	Bay Forest
> 32	< 18	300-320	Bay Forest

Chapter 6

USING SOIL APPARENT ELECTRICAL CONDUCTIVITY (EC_A) TO DETERMINE PARTICLE SIZE DISTRIBUTION OF SOILS FOR WETLAND RESTORATION

K.M. Davis, J.G. White and M.J. Vepraskas

INTRODUCTION

Carolina bays are wet, shallow, oval elliptical depressions located in eastern United States. They are common to the Coastal Plain from Delaware to Florida (Kaczorowski, 1977). Some 500,000 bays are estimated to exist with variable size (Prouty, 1952), but the actual number may be less than 100,000 (Nifong, 1998). Generally, Carolina bays are oriented in the northwest to southeast direction (Kaczorowski, 1977; Sharitz and Gibbons, 1982; Carver and Brook, 1989). The bays are ovate shaped with the large end in the northwest direction and the smaller end in the southeast direction (Sharitz and Gibbons, 1982). The cause of the formation of the Carolina bays is still unknown.

Carolina bays characteristically have organic centers and mineral rims. Sand rims surround the Carolina bays and are most visible on the southeastern edge of the bay (Kaczorowski, 1977; Johnson, 1942; Glenn, 1895; Prouty, 1952). However, the rim can encircle the entire bay, be lacking at any point, or be lacking completely (Johnson, 1942; Bliley and Pettry, 1979). The sand rims are usually of coarse sand or sandy loam that is white or buff in color (Johnson, 1942). The rims have low CEC, organic matter, and base saturation (Ewing, 2003). Bay fill is generally characterized as lacustrine sediment. Soil in drier depressions is known to be fine loam, dark gray to black in color, high organic content, and partially decayed beds of peat. Under the loam, silty to sandy clay is found, and sometimes sand and quicksand occur (Johnson, 1942).

Juniper Bay is a Carolina bay located in Robeson County, NC approximately 6.2 mi (10 km) south of Lumberton, NC. The bay is approximately 1 mi^2 (256 ha) and was drained through an extensive network of ditches starting with the northwest third of the bay in 1971, the center third in 1981 and the southeast third in 1986 (Ewing, 2003). Upon the completion of drainage, each section was placed into agriculture. In 1999, the North Carolina Department of Transportation (NCDOT) purchased the property with intention of restoration for wetland mitigation credits. Restoration efforts started June 2003 and ditch-filling began in late 2005 (Ewing, 2003). The NCDOT with the aid of USDA-NRCS personnel mapped Juniper bays soils as: Ponzer, Leon, and Pantego soil series. Ponzer mucks are loamy, mixed, dysic, thermic Terric Haplosaprists. Leon is described as a sandy, siliceous, thermic Aeric Haplaquod. Pantego is described as a fine-loamy, siliceous, thermic Umbric Paleaquult. The Ponzer series covers 60% of the Juniper bay and is the organic portion. Juniper bay has higher nutrient content than less disturbed Carolina bays due to the fact that it was fertilized and limed for so many years (Ewing, 2003).

Because of restoration, the physical and chemical properties of Juniper Bay soils are being evaluated. One major property evaluated is soil apparent electrical conductivity (EC_a), also known as the bulk soil electrical conductivity; it is the depth-weighted average of the bulk soil electrical conductivity (Cook and Walker, 1992; Greenhouse and Slaine, 1983). In other words, it is the average of the electrical conductivity integrated over different depths in the soil, these depths being dependent on the instrument used to make the measurement. The EC_a includes the conductance through the soil solution, the solid soil particles, and the exchangeable cations that are located on the soil-water interface of clay minerals (Corwin and Lesch, 2003). It can be determined by above ground measurements using an electromagnetic induction (EMI) meter (Rhoades et al., 1989). The method is non-invasive and non-destructive to the soil (Corwin and Lesch, 2003; Scanlon et. al, 1997). However, some ground-truthing is required in order to accurately assess the data collected. Salinity, soil water content, and clay content and mineralogy are the three main factors that contribute to soil EC_a (Cook et al., 1989; Nadler and Frenkel, 1980). Previous studies suggested that EC_a, was positively correlated with clay and silt, and negatively correlated with the sand fractions (McKenzie et al., 1997).

Two EMI meters used in EC_a evaluation are the EM38 (Geonics, Ltd., Missassauga, ON, Canada) and the GEM-300 (Geophysical Survey Systems, Inc., [GSSI] Salem, NH. The EM38 is a digital, hand-held, single-frequency (14.6 kHz.) electromagnetic meter. It is roughly 3.28 ft (1 m) long and resembles a carpenter's level weighing about 6.61 lbs (3 kg). The EM38 has two coils: a transmitting and a receiving coil. The transmitting coil transmits radio frequency (RF) energy, which induces a magnetic field that varies in strength with the depth of soil. The receiving coil measure primary and secondary induced RF in the soil and relates them to the soil EC (McNeill, 1980; Doolittle et al., 1994; Davis et al., 1997). The inter-coil spacing is 3.28 ft (1 m), which determines depth of observation (Nettleton et al., 1994; McNeill, 1999). The EM38 in the vertical dipole orientation is purported to measure to a depth of $\underset{\sim}{~}$4.92 ft (1.5 m) and in the horizontal dipole orientation to $\underset{\sim}{~}$2.46 ft (0.75 m) deep (McNeill, 1986; Doolittle et al., 1994; Sherlock and McDonnell, 2003; Triantafilis et al., 2001). The EM38 must be calibrated each time the instrument is turned on.

The GEM-300 is a digital, hand-held, multi-frequency electromagnetic sensor weighing about 8.82 lbs (4 kg) (Geophex, 2005). The GEM-300 has three coils: transmitter, receiver, and bucking (Won et. al, 1996). The transmitter coil induces the eddy-circular current. The receiving coil intercepts the secondary electromagnetic field. The receiver and transmitter coils are separated by 4.27 ft (1.3 m). The bucking coil removes the primary field from the receiver coil. The GEM-300 is a multi-frequency instrument that can record up to 16 frequency readings at one time. The frequency is inversely proportional to the skin depth or depth of exploration (Won et. al, 1996; McNeill and Bosnar, 1999). This instrument also can be used in the vertical and horizontal dipole orientations. The GEM-300 is initially calibrated by the manufacturer.

The purpose of the project was to determine whether EC_a measured via EMI can be used to characterize soils for wetland restoration. For this specific study, the objective was to determine whether EC_a was related to the particle size distribution of Juniper Bay soils. The hypothesis was that soil EC_a would be a function of the particle distribution of Juniper Bay soils, and therefore, models could be created in order to estimate clay content from EC_a readings.

MATERIALS AND METHODS

Study Site and Sampling

The study site was Juniper Bay, a 1-mi^2 (256-ha) Carolina bay located approximately 6.2 mi (10 km) south of Lumberton, NC in Robeson County, NC. The bay was drained through an extensive network of ditches starting with the northwest third of the bay in 1971, the center third in 1981 and the southeast third in 1986 (Ewing, 2003). The drainage ditches subdivided the bay into "fieldlets," defined as areas of the bay enclosed by ditches on all sides (Fig. 6.1). Upon the completion of drainage, each section was placed into agriculture. In 1999, the North Carolina Department of Transportation (NCDOT) purchased the property with intention of restoration for wetland mitigation credits. Restoration efforts started June 2003 and ditch-filling began in late 2005.

There are three main soil map units at Juniper Bay: Pantego fine sandy loam (fine-loamy siliceous, thermic Umbric Paleaquults), Ponzer muck (loamy, siliceous, dysic, thermic Terric Medisaprist), and Leon fine sand (sandy, siliceous, thermic Aeric Haplaquods) (McCachren, 1978). The initial investigation of soil stratigraphy was performed in 2000. A hydraulic drilling machine with an overshot wireline split-barrel sampler for continuous coring with a hollow stem auger was used to drill 29 cores in and around Juniper Bay to 20- or 50-ft (6.1- or 15.2-m) depth. The 17 core locations within the bay were determined by an equilateral triangle grid placed in an attempt to adequately represent each soil type (Fig. 6.2). The cores were sampled at every naturally delineated horizon. To compare analytical data among cores, depth-weighted average analytical values were calculated for each 1-ft (0.31-m) increment. All samples were textured in the field using the feel method. Naturally delineated horizon samples from nine cores were dried and sent to the University of Georgia, Soil Analysis Lab in Athens, GA. for particle size analysis. Particle size analysis of 0.02 lbs (10 g) samples was performed by the pipette method; sand size fractionation was determined by sieving. In addition to soil sampling, 18 wells were used to monitor water table depths.

Soil Apparent Electrical Conductivity via Electromagnetic Induction

Electromagnetic induction (EMI) is a non-contact method of measuring soil apparent electrical conductivity (EC_a). The initial overall bay-wide survey was performed December 4 - 7, 2000. Two instruments were used in this study: The EM38 (Geonics Ltd., Mississauga, ON, Canada) and the GEM-300 (Geophysical Survey Systems, Inc., Salem, NH). The EM38 was calibrated at Juniper Bay each morning of the survey using the methods described in the "EM38 Ground Conductivity Meter Operating Manual" (Geonics Ltd., 1999). The survey was performed in the quadrature phase and with the sensitivity scale set to 100 milliSiemens per meter (mS m^{-1}). The EM38 was attached to a nonmetal cart pulled by an all-terrain vehicle (ATV). The survey was performed in continuous mode with

EC_a readings recorded every second in the vertical dipole orientation only. A Satloc SLX (Satloc, Scottsdale, AZ) differential global positioning system (DGPS) identified the locations of the readings with a 10-ft (3.1-m) off-set to the back, with data recorded simultaneously from the EM38 and GPS using SensorTrack (StarPal, Fort Collins, CO) data acquisition software. The survey was performed along transects of the centerline and one ditch edge of the fieldlets containing Cores 1 through 17 (Fig. 6.3). Readings were also collected perpendicular to the centerline and edge lines close to the core locations.

The GEM-300 was operated in station mode and measurements were taken with the sensor held 3.28 ft (1 m) above the ground surface in both the horizontal and vertical dipole orientations. The GEM-300 survey was on a point by point basis. Survey flags were inserted into the ground at intervals of approximately 98.43 ft (30 m) along the centerline and edge of the fieldlets. A line perpendicular to the centerline and edge lines was surveyed near each core location. The survey flags served as observation points. The measurements were obtained at frequencies of 3.03, 6.09, 9.81, and 14.79 kHz in the inphase and quadrature phases. The locations of the survey flags were obtained using a Precision Lightweight Global Positioning System Receiver (PLGR) (Rockwell Collins, Cedar Rapids, IA). The GEM-300 measurements were loaded into the WinGEM v.3 software program (Geophex Ltd., Raleigh NC) and converted to mS m^{-1}. The EM38 measurements were also converted to mS m^{-1} from parts per million (ppm). The converted EC_a readings were loaded into ArcGIS 9.1 as tables. Shapefiles were created from the tables of measurements. The geographical coordinates were projected to the North Carolina State Plane coordinate system in meters using the North American Datum of 1983 (NAD83). The EC_a readings were kriged using parameters identified by GS^+ Version 5. In the Geostatistical Analyst Extension of ArcGIS 9.1, the Geostatistical Wizard was used with kriging as the method of interpolation to produce an ordinary kriging prediction map, and indicating the model, major range, partial sill, nugget, lag size, and number of lags determined by GS^+. The circular search neighborhood included at least 5 neighbors at a 79 degree angle, the approximate orthogonal to the transect lines.

Analysis

Once the prediction maps were created, the sampling tool was used to sample the rasters under the core and pit locations. The raster samples were joined to the soil sample layers and exported. The particle size analyses were then added to the spreadsheets at the corresponding soil core and pit locations. SAS version 9.1 was used to determine if there was correlation of the EC_a of each frequency with any of the soil properties analyzed. Henceforth, all correlations discussed were significant ($p \leq 0.05$).We also defined weak correlations as having a correlation coefficient (r) < 0.4, moderate correlation as $0.4 \leq r < 0.7$, and strong correlations as $r \geq 0.7$.

Using Apparent Electrical Conductivity to Predict Clay Content

Clay content of the original cores that had been analyzed for particle size distribution was relatively strongly correlated with EC_a, so we determined equations to predict clay content from EC_a. We attempted to validate these equations using clay contents estimated by the texture-by-feel method for the unanalyzed cores. To estimate the potential accuracy of the "texture-by-feel" results for the analyzed cores, we compared the "texture-by-feel" results with the particle size analysis of the nine analyzed cores. The mean clay content was estimated as the mean of the textural class identified by texture-by-feel method. The mean clay contents of texture-by-feel of the analyzed cores were graphed versus the actual clay content by depth increments. Excel produced a regression line and equation for each 1-ft (0.31-m) depth increment. The nine analyzed core clay contents were graphed against the kriged EC_a value beneath the core. Regression lines and clay content prediction equations were determined at each frequency and depth. Using the five strongest prediction equations, the kriged EC_a beneath the unanalyzed cores was used to estimate the clay content of the unanalyzed cores. The estimated clay contents of the unanalyzed cores were graphed against the texture-by-feel mean clay contents. The SAS PROC CORR procedure was used to determine if there was a correlation between estimated clay content using EC_a values and clay content determined by feel.

RESULTS AND DISCUSSION

Apparent Electrical Conductivity

Electrical conductivity measurements tended to vary throughout all surveys. Conductivity readings from the horizontal dipole frequency tended to be lower than those of the vertical dipole orientation of the same frequency for both the EM38 and the GEM-300. When the EC_a values were kriged, the EM38 vertical dipole orientation kriged EC_a had a much narrower range than those of the GEM-300. Figures 6.4 and 6.5 show the kriged initial overall December 2000 EM38 vertical dipole orientation EC_a and the GEM-300 3.03 kHz horizontal dipole EC_a. Note that the EC_a readings are on two different scales. The GEM-300 kriged maps differed depending on dipole orientation (Figs. 6.5 and 6.6). The horizontal dipole orientation maps had lower EC_a in the upper northwest corner of Juniper Bay and had a high EC_a in a fieldlet parallel to Fieldlet 3 that crossed both Ponzer and Leon soil map units. Vertical dipole orientation kriged EC_a maps had higher EC_a in the eastern part of Juniper Bay and had low EC_a in the northwest corner as well. In general the deeper the sensing depth of the frequency (i.e., the lower the frequency), the greater the EC_a readings.

Cores

The particle size analysis of the nine soil cores resulted in a mean total clay content of 21%, total sand content of 61%, and a mean total silt content of 18%. Medium and fine sand were the majority of the sand fraction. Average total clay content increased with depth as average total sand decreased with depth. Total sand percentage was greatest from 2 ft (0.61 m) to 4 ft (1.22 m) with total clay percentage greatest from 10 ft (3.05 m) to 12 ft (3.66 m).

Preliminary evaluations of initial overall December 2000 EC_a and core clay contents suggested that clay content and EC_a were correlated at some depths and frequencies (Table 1). By 1-ft (0.31-m) increments, it appeared that correlations were prominent in the vertical dipole orientation at each frequency, dropped off after 4 ft (1.22 m) and then picked up at 9 ft (2.74 m).

Core clay content was strongly correlated (*r* > 0.7, p < 0.05) with EC_a values of most frequencies recorded in December 2000, but significance was lacking with other particle size distribution parameters (Table 6.1). The EC_a values were weakly correlated with overall mean medium sand, fine sand, very fine sand, total sand, total silt, and total clay content of the cores at most frequencies. The correlations of EC_a with medium, fine, and total sand were generally negative, while those with silt and clay were positive. In the north-central United States, Sudduth et al. (2005) reported that clay content was strongly correlated with EC_a and persistent across several fields and EC data types. Similarly, total clay content of the cores from 2 ft (0.61 m) to 4 ft (1.22 m) and from 9 ft (2.74 m) to 13 ft (3.96 m) at Juniper Bay proved to have consistent significant and strong, positive correlations for the vertical dipole orientation of most frequencies. From these results, you could infer that the dark red areas of Figures 6.4-6 are those of high clay content and the light areas are those of low clay content. Figure 7 shows the Pearson correlation coefficients of the initial overall December 2000 GEM-300 9.81 kHz vertical frequency EC_a with core clay content for each depth increment. These correlations had the strongest Pearson correlation coefficients of all frequencies and dipole orientations. Mean total clay contents within the 2- to 4-ft (0.61- to 1.22-m) depth range were strongly and positively correlated with the mean total clay contents within the 9- to 13-ft (2.74- to 3.96-m) depth range (Table 6.2). Fig. 6.8 shows the mean clay content of the cores for each depth increment. Comparing Fig. 6.7 with Fig. 6.8 the depths of the strong correlations of EC_a with clay corresponded to the depths of minimum and maximum mean total clay contents of all cores. From these results, it appears that clay content at 0.61 to 1.22 m and from 9- to 13-ft (2.74 to 3.69-m) depths in Juniper Bay can be detected using vertical dipole orientation EMI. Similarly, Triantafilis and Lesch (2005) found that depth weighted averaged percent clay generally reflects the known surface clay content and provides information of the variability of subsurface clay. However, we do not know whether EC_a was responding to clay differences at one or both of the depths where there were strong correlations. We hypothesized that the stronger correlations of EC_a with clay at certain depths might have been due to greater ranges in clay content at those depths. However, there was no evidence of the extent of clay range effecting the strength of correlation between EC_a and clay content (Fig. 6.8).

We hypothesized that relationships between EC_a and particle size distribution may vary among soil types. However, the initial overall December 2000 EC_a by soil type showed little correlation between core particle size distributions and EC_a within each of the two available soil map units for most frequencies and particle sizes (Table 6.3). Pantego loam soil map unit was not represented by the cores. However, positive, weak significant correlations occurred between EC_a and total clay content as well as negative correlations with EC_a and total sand content of the Leon sand soil map unit. There were no significant correlations within the Ponzer muck soil map unit. These results suggest that it is difficult to determine clay content from EMI within a soil type.

Can Apparent Electrical Conductivity Estimate Clay Content?

The purpose of this section was to determine whether EC_a readings collected in the field via EMI instruments can be used to accurately estimate clay content of soil at certain depths within the soil profile. This exercise was to aid restoration efforts by determining if aquitard layers of the soil had been punctured with the creation of ditches. Aquitard layers are important because they promote the appropriate hydrology for the production of a wetland.

The model developed to predict clay content from EC_a readings was clay = m (EC_a) + b where ‘m’ is a slope coefficient and ‘b’ is an intercept. The five models chosen to predict clay content were those derived from the strong correlations between EC_a and clay content of analyzed cores: 6.09 kHz at 2-3-ft (0.61-0.91-m) depth, 3.03 kHz at 3-4-ft (0.91-1.22-m) depth, 9.81 kHz at the 11-12-ft (3.33-3.66-m) and 12-13 ft (3.66-3.96-m) depths, and 14.79 kHz at 12-13 ft (3.66-3.96-m) depth, all in the vertical dipole orientation (Fig. 6.9). These models were validated by predicting clay content of unanalyzed cores within Juniper Bay. When correlating predicted clay content of unanalyzed cores to the estimated clay content using the texture-by-feel method, there were no significant correlations between the prediction equation estimates of the clay content of the unanalyzed cores and the clay content determined by the texture-by-feel method within each horizon (Table 6.4).

It was important to determine whether the texture-by-feel method of clay estimation of unanalyzed cores was appropriate for use in comparing with the predicted clay content from the models. The results from texture-by-feel clay content versus the actual clay content of the nine analyzed cores indicated that mean clay content of a texture was an appropriate estimation of the actual clay content. When averaged over all depths, the texture-by-feel clay content was strongly correlated with the actual clay content of analyzed cores. Texture-by-feel clay content versus actual clay content of soil cores had moderate to strong correlations when separated into the 0.31-m depth increments. The strongest correlations between actual clay content and clay content from texture-by-feel of the analyzed cores occurred at 3 ft (0.91 m) ($r = 0.95$) (Fig. 10) and 9 ft (2.74 m) ($r = 0.96$) (Fig. 6.11). Therefore, texture-by-feel clay content estimations of the unanalyzed cores were used to determine whether the predicted clay content from the models was accurate.

At this point, it was difficult to determine whether the prediction equations did not accurately predict the unanalyzed cores’ clay content, if the texture determined by texture-by-feel method was not accurate, or both. To determine this, particle size analyses needs to be performed on the unanalyzed cores. The strong EC-clay correlations at some depths and instrument frequencies indicate that it may be possible to estimate the clay content using the initial overall EC_a readings only at certain frequencies and depths within Juniper Bay. Our results indicate that it will not be possible to develop an EC-based model or models that estimate clay content at every depth and frequency.

CONCLUSIONS

Initial overall December 2000 EC_a was more strongly correlated with core clay content than was EC_a from any other survey date. Among the 0.31-m depth increments, the initial overall December 2000 EC_a was positively and strongly correlated with core clay content at depths of 2 to 4 ft (0.61 to 1.22-m) and 9 to 13 ft (2.74 to 3.96-m) at most frequencies in the vertical dipole orientation.

We developed models to estimate clay content at the five core depths that had the strongest EC_a-clay relationships. To validate these models, we estimated the clay content of eight unanalyzed cores based on texture-by-feel estimates. We tested this approach via the analyzed cores and found that texture-by-feel clay content of the analyzed cores was correlated to the actual clay content of the analyzed cores over all depths, indicating that this approach was reasonable. However, there were no significant correlations between the clay content of the unanalyzed cores estimated from the five prediction models and the texture-by-feel clay content of the unanalyzed cores. At this point we do not know whether this was because of inaccuracies in the prediction models or in the texture-by-feel clay estimates, or both. To resolve this, we are determining the particle size analysis of the unanalyzed cores.

Variations in EC_a could be due to the instruments used. Both the EM38 and GEM-300 are sensitive to temperature and moisture. Changes in these two factors throughout the survey period could have altered the readings. It appears from my research and others that EMI is useful in less complex situations. Wetlands incorporate many factors that contribute to EC_a such as moisture, water table, and fine particle-sized soils. A less complex soil-environment system would give more plausible EC_a results. An appropriate environment for which EMI could be used effectively would contain only one of the major EC_a contributors: salts, moisture, or clay content. For example, Doolittle et al. (1994) identified depth to claypans in soils in Missouri on an eroded backslope. There were few salts and the water table was deeper than the sounding depth of the instruments used. However, if salts or water table was present, then the EC_a readings would not have been as reliable for estimating clay content. The Juniper Bay wetland system was that of varying water table depth and moisture, and contained fine-textured soils. It is possible to conclude that EMI cannot be used in wetland systems due to the complexity of the environment.

From this study, it appears that clay content at some depths within Juniper Bay does affect EC_a readings via EMI. At this point, we cannot explain why the December 2000 EC_a and core clay content correlations occurred only at certain depths and within the vertical dipole orientation of the frequencies. Further studies of relationships of EC_a with soil particle size distribution in wetland settings are needed. There are many factors that contribute to EC_a in a wetland and a better understanding of those factors could promote more accurate predictions of soil particle size distribution via EMI.

REFERENCES

Bliley, D.J., and D.E. Pettry. 1979. Carolina bays on the eastern shore of Virginia. Soil Sci. Soc. Am. J. 43:558-564.

Carver, R.E., and G.A. Brook. 1989. Late Pleistocene paleowind directions, Atlantic coastal plain, USA. Palaeogeogr. Palaeoclimatol. Palaeoecol. 74:205-216.

Cook, P.G. and G.R. Walker. 1992. Depth profiles of electrical conductivity from linear combinations of electromagnetic induction measurements. Soil Sci. Soc. Am. J. 56:1015-1022.

Corwin, D.L., and S.M. Lesch. 2003. Application of soil electrical conductivity to precision agriculture: theory, principles, and guidelines. Agron. J. 95(3):455-471.

Davis, J.G., N.R. Kitchen, K.A. Sudduth, and S.T. Drummond. 1997. Using electromagnetic induction to characterize soils. *In* Applications of Electromagnetic Methods: Agriculture. Geonics Ltd. Mississauga, ON.

Doolittle, J.A., K.A. Sudduth, N.R. Kitchen, and S.J. Indorante. 1994. Estimating depths to claypans using electromagnetic induction methods. J. Soil Water Conserv. 49:572-575.

Ewing, J.M. 2003. Characterization of soils in a drained Carolina bay wetland prior to restoration. Ph.D. Dissertation. North Carolina State Univ., Raleigh.

Geonics Ltd.. 1999. EM38 ground conductivity meter operating manual. Geonics Limited, Mississauga, ON.

Geophex. 2005. How does the GEM-2 work? [Online] Available at http://www.geophex.com/Product_page/GEM2/How%20it%20works/howitworks.htm (accessed 24 May; verified 17 June 2005). Geophex, Ltd., Raleigh, NC.

Glenn, L.C. 1895. Some notes on Darlington, South Carolina bays. Science. 2:472-475.

Greenhouse, J.P., and D.D. Slaine. 1983. The use of reconnaissance electromagnetic methods to map contaminant migration. Ground Water Monit. Rev. 3:47-59.

Johnson, D.W. 1942. The origin of the Carolina bays. Columbia Univ. Press, New York.

Kaczorowski, R.T. 1977. The Carolina bays: a comparison with modern oriented lakes. Technical Report 13-CRD, Coastal Research Division Dept. Geo. Univ. South Carolina.

McCachren, C.M. 1978. Soil Survey of Robeson County North Carolina. USDA-SCS. Washington, D.C.

McKenzie, R.C., R.J. George, S.A. Woods, M.E. Cannon, and D.L. Bennett. 1997. Use of the electromagnetic-induction meter (EM38) as a tool in managing salinization. Hydrogeol. J. 5(1):37-50.

McNeill, J.D. 1980. Electrical conductivity of soils and rocks: Technical Note TN-5, Geonics Ltd. Mississauga, ON.

McNeill, J.D. 1986. Geonics EM38 ground conductivity meter operating instructions and survey interpretation techniques: Technical Note TN-21, Geonics Ltd., Mississauga, ON.

McNeill, J.D. 1999. The application of electromagnetic techniques to environmental geophysical surveys. *In* Ground Conductivity Meters For Environmental Site Evaluation. Geonics, Ltd., Mississauga, ON.

McNeill, J.D., and M. Bosnar. 1999. Application of “dipole-dipole” electromagnetic systems for geological depth sounding: Technical Note TN-31. Geonics Ltd., Mississauga, ON.

Nadler, A., and H. Frenkel. 1980. Determination of soil solution electrical conductivity from bulk soil electrical conductivity measurements by the four-electrode method. Soil Sci. Soc. Am. J. 44:1216-1221.

Nettleton, W.D., L. Bushue, J.A. Doolittle, T.J. Endres, and S.J. Indorante. 1994. Sodium-affected soil identification in south-central Illinois by electromagnetic induction. Soil Sci. Soc. Am. J. 58:1190-1193.

Nifong, T.D. 1998. An ecosystem of Carolina bays in the coastal plain of the Carolinas. Ph.D. Dissertation. Univ. of North Carolina, Chapel Hill.

Prouty, W.F., 1952. Carolina bays and their origin. Geol. Soc. Am. Bull. 63:167-224.

Rhoades, J.D., S.M. Lesch, P.J. Shouse, and W.J. Alves. 1989. New calibrations for determining soil electrical conductivity-depth relations from electromagnetic measurements. Soil Sci. Soc. Am. J. 53:74-79.

Scanlon, B.R., R.S. Goldsmith, and J.G. Paine. 1997. Analysis of focused unsaturated flow beneath fissures in the Chihuahuan Desert, Texas, USA. J. Hydrol. 203:58-78.

Sharitz, R.R., and J.W. Gibbons. 1982. The ecology of southeastern shrub bogs (pocosins) and Carolina bays: a community profile. FWS/OBS-82/04. US Fish and Wildlife Service, Division of Biological Services. Washington, DC.

Sherlock, M.D., and J.J. McDonnell. 2003. A new tool for hillslope hydrologists: spatially distributed groundwater level and soilwater content measured using electromagnetic induction. Hydrol. Process. 17:1965-1977.

Sudduth, K.A., H.L. Palm, D.E. Clay, R.T. Schuler, F.J. Pierce, D.G. Bullock, W.J. Wiebold, N.R. Kitchen, G.A. Bollero, and W.D. Batchelor. 2005. Relating apparent electrical conductivity to soil properties across the north-central USA. Comput. Electron. Agric. 46(1-3):263-283.

Triantafilis, J., and S.M. Lesch. 2005. Mapping clay content variation using electromagnetic induction techniques. Computers and electronics in agriculture. 46(1-3):203-237.

Triantafilis, J., A.I. Huckel, and I.O.A. Odeh. 2001. Comparison of statistical prediction methods for estimating field-scale clay content using different combinations of ancillary variables. Soil Sci. 166(6):415-427.

Won, I.J., D.A. Keiswetter, G.R.A. Fields, and L.C. Sutton. 1996. GEM-2: a new multifrequency electromagnetic sensor. J. Environ. Eng. Geophysics. 1:129-137.

ACKNOWLEDGEMENT

This chapter was as a portion of K.M. Davis's M.S. Thesis entitled "Using Apparent Electrical Conductivity (Ec_a) via Electromagnetic Induction (EMI) to Characterize Soils and the Stratigraphy for Wetland Restoration" that was earned through NC State University and is available through the university's library.

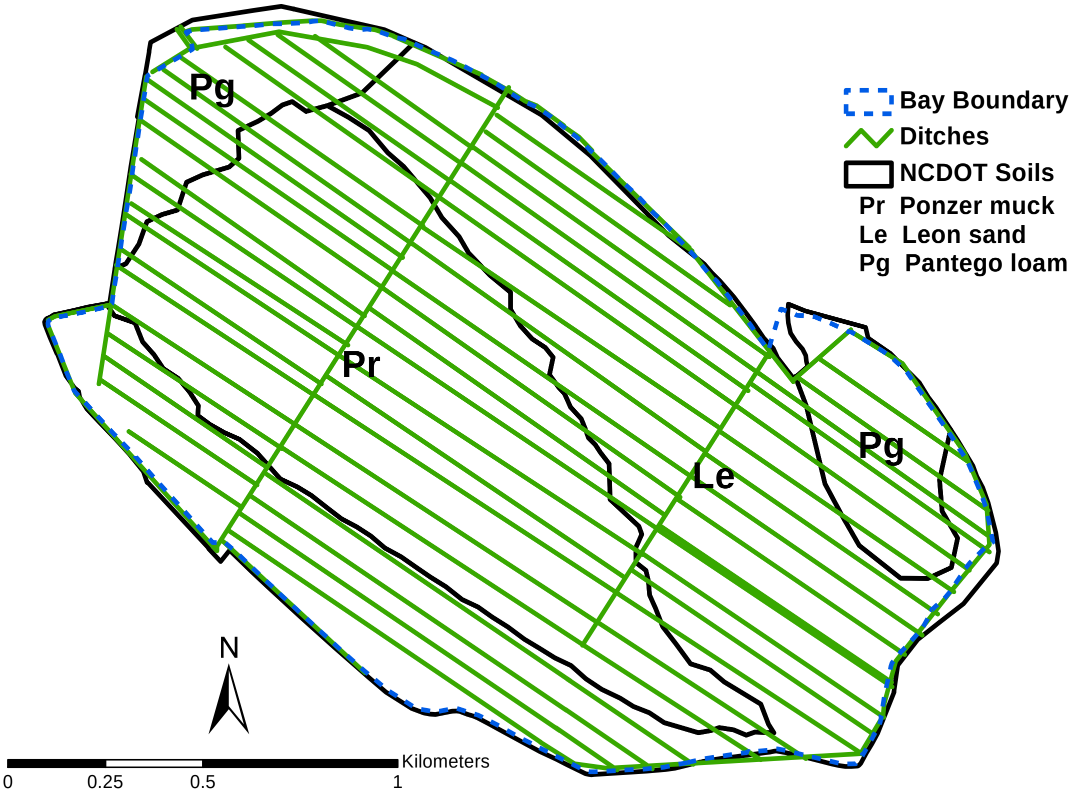

Fig. 6.1. Juniper Bay soil map units and fieldlets. Dashed line indicates bay boundary. Dark line indicates soil map units. Soil map units are as follows: Ponzer muck (Pr), Leon sand (Le), and Pantego loam (Pg). One km equals 0.62 mi.

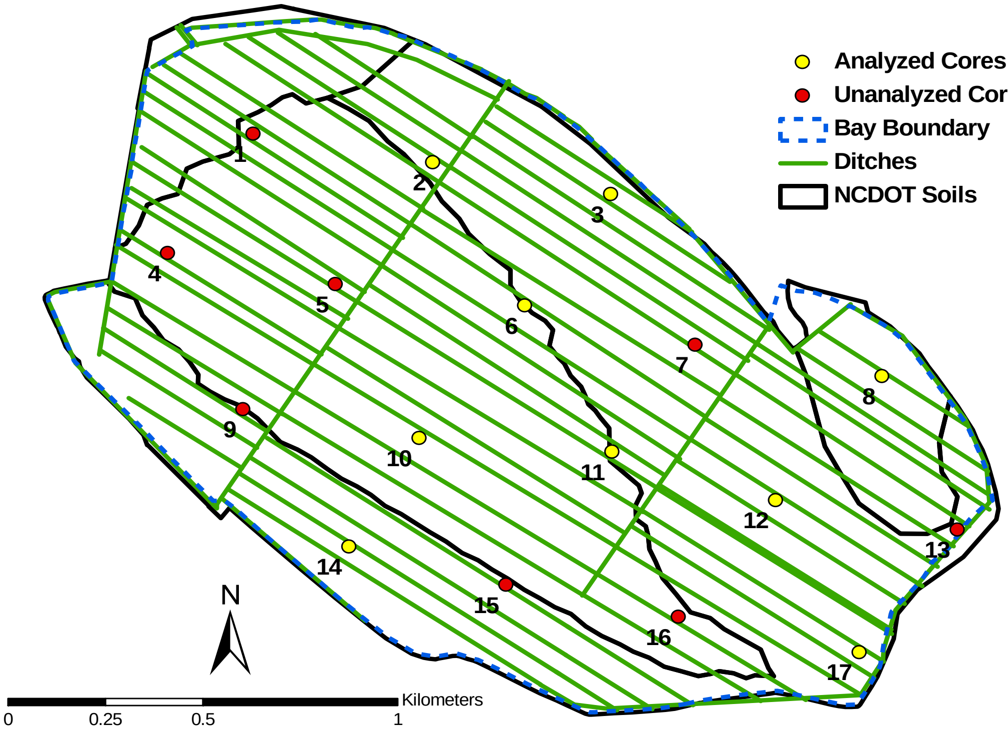

Fig. 6.2. Juniper Bay deep core locations. There were 9 particle-size analyzed core locations and 8 unanalyzed (texture-by-feel only) core locations. One km equals 0.62 mi.

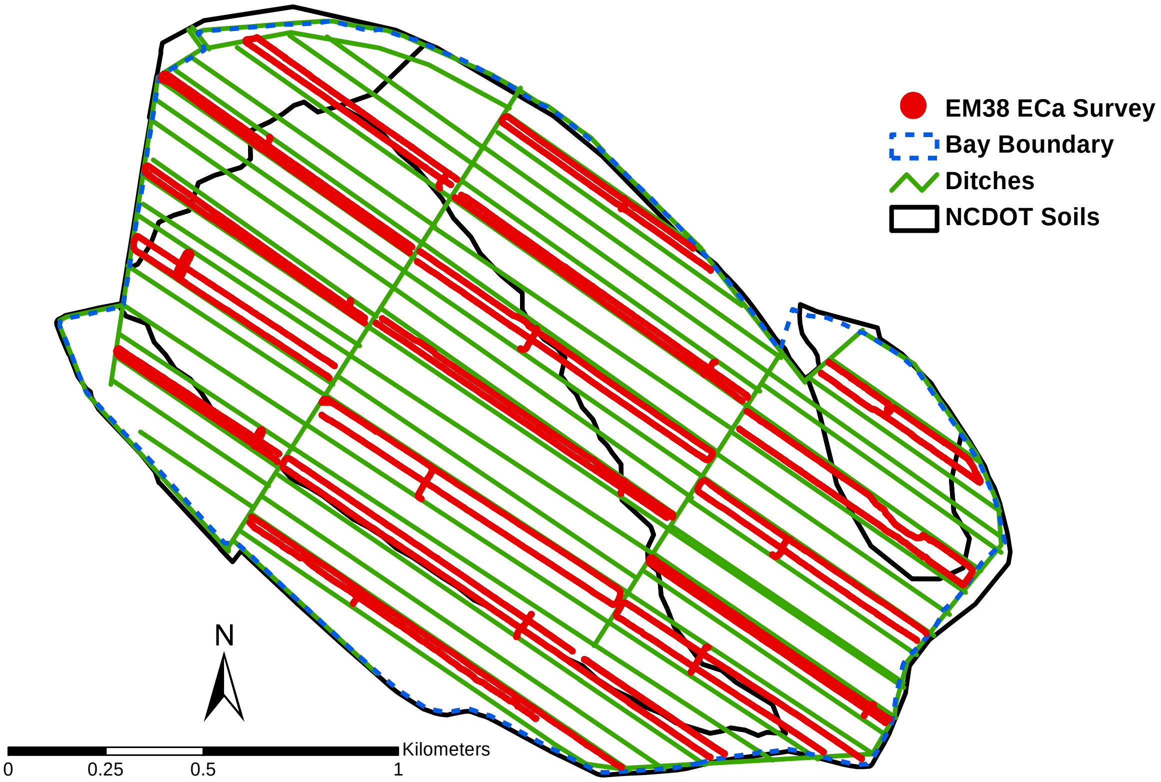

Fig. 6.3. Overall initial December 2000 EM38 EC$_a$ survey at Juniper Bay. The measurements were recorded on a continuous basis (1-s intervals). There were approximately 23,000 measurement locations. Overall initial December 2000 GEM-300 EC$_a$ survey at Juniper Bay was along the same transect lines. The measurements were recorded on a point basis. There were approximately 1,200 measurement locations. One km equals 0.62 mi.

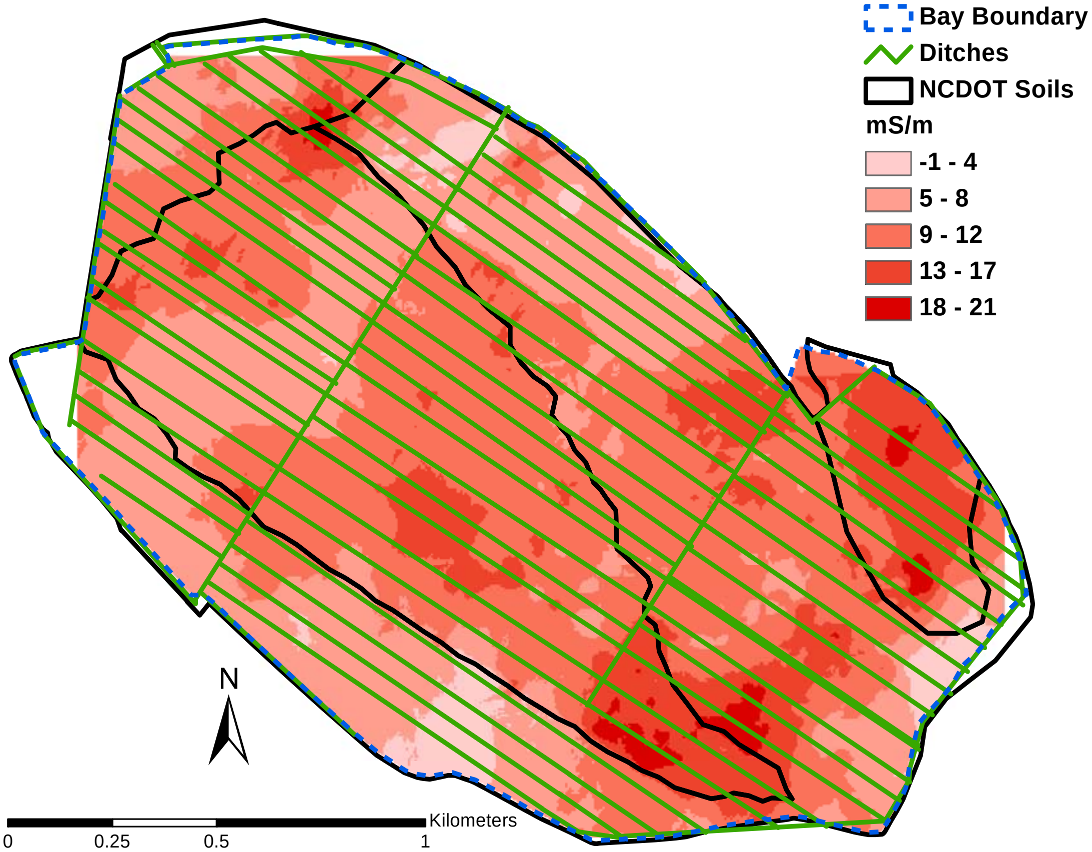

Fig. 6.4. Kriged December 2000 EM38 vertical dipole orientation EC_a. One km equals 0.62 mi.

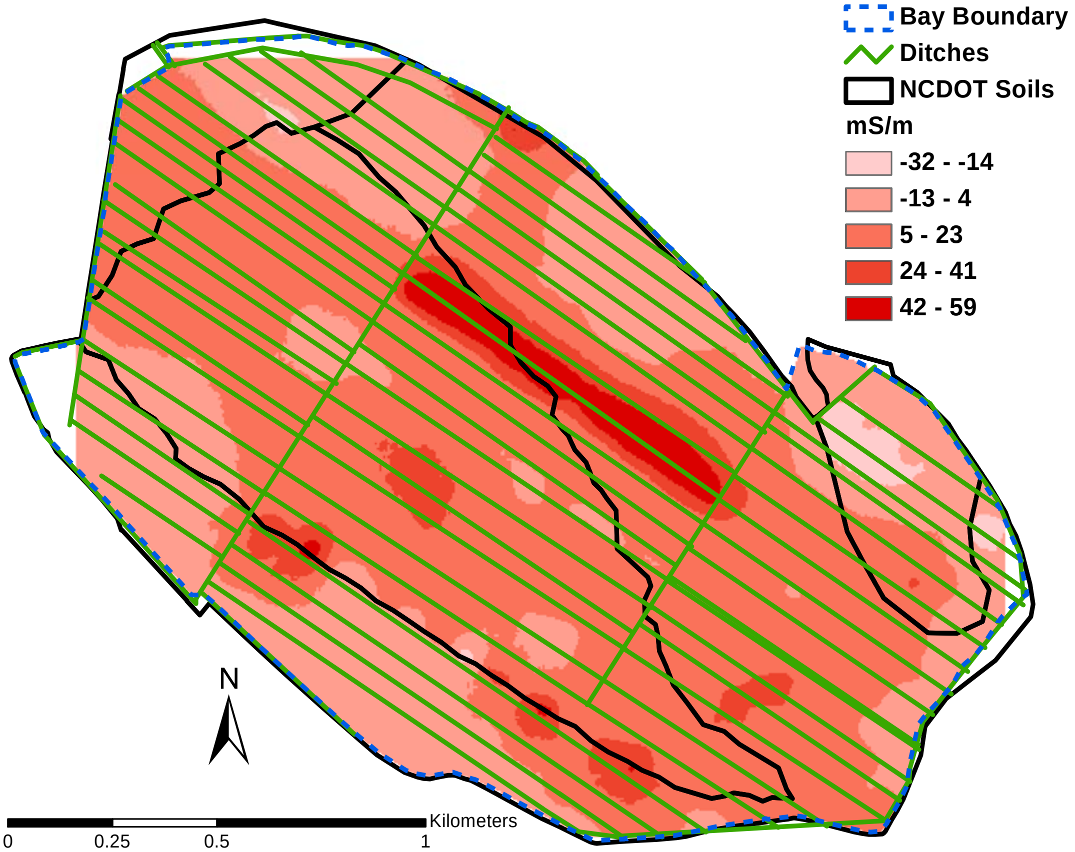

Fig. 6.5. Kriged December 2000 GEM-300 3.03 kHz. horizontal dipole orientation EC_a. One km equals 0.62 mi.

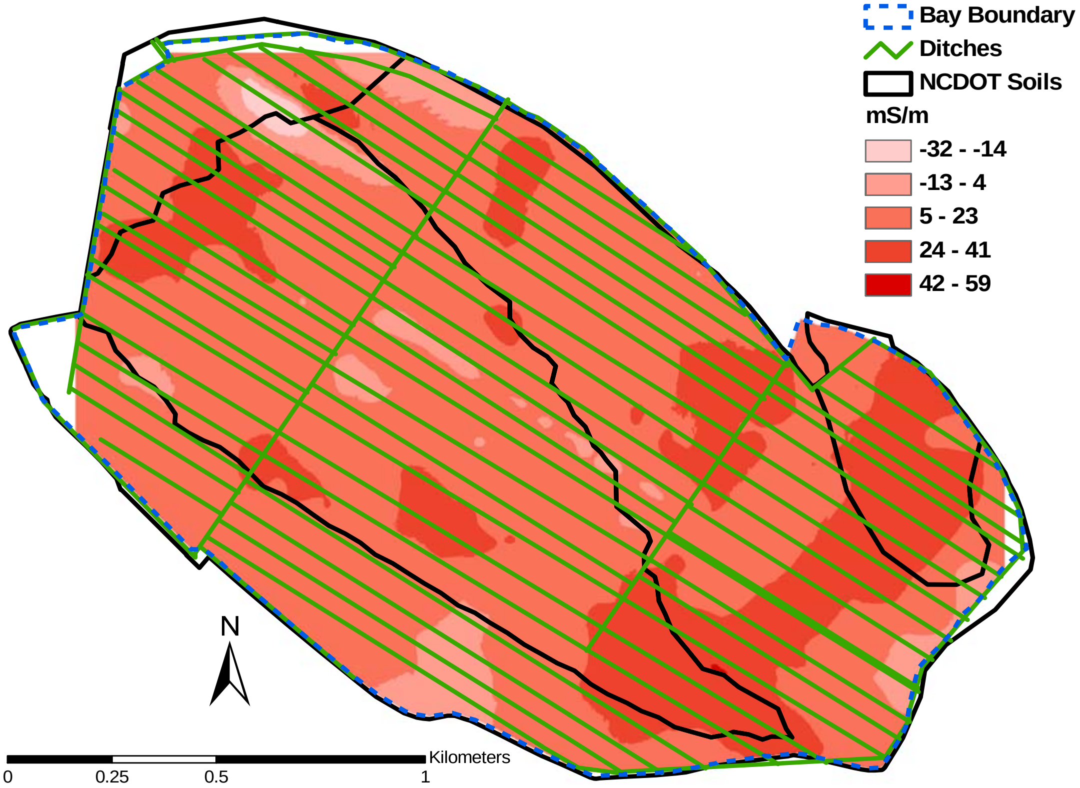

Fig. 6.6. Kriged December 2000 GEM-300 9.81 kHz. vertical dipole orientation EC_a. One km equals 0.62 mi.

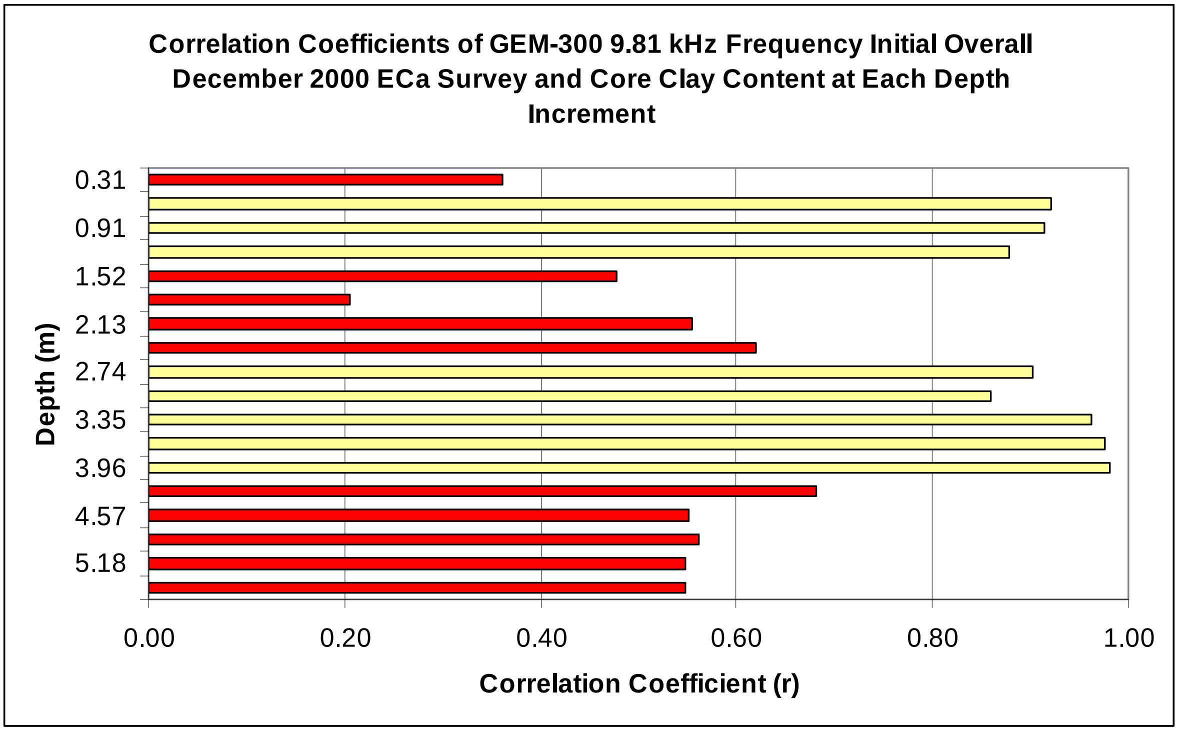

Fig. 6.7. Correlations (Pearson correlation coefficient, r) between soil apparent conductivity (EC_a) from GEM-300 9.81 kHz vertical frequency from the initial overall December 2000 EC_a survey and core clay content displayed at each depth increment. The labels of the depth increments are the bottom of the profile increments. The light bars indicate significant correlations ($p \leq 0.05$) and dark bars indicate those that were not significant.

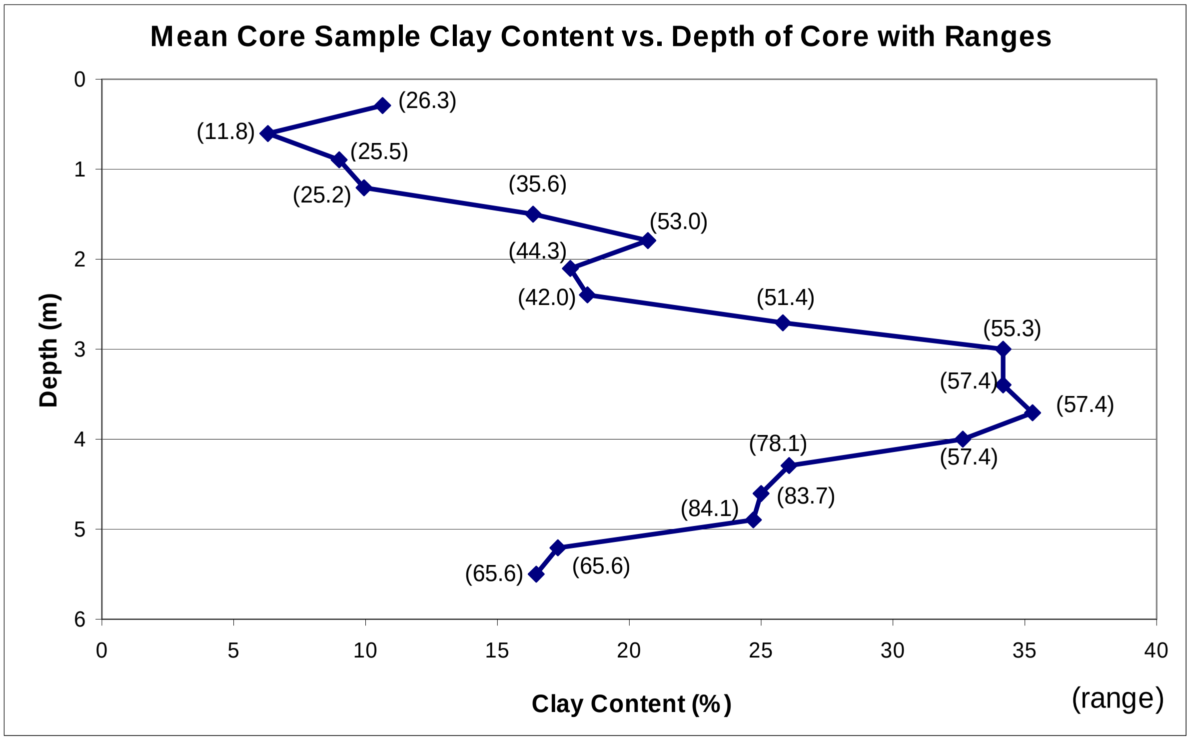

Fig. 6.8. Mean core clay content at each depth increment for the analyzed cores with ranges of clay content for each depth. One meter is 3.28 ft.

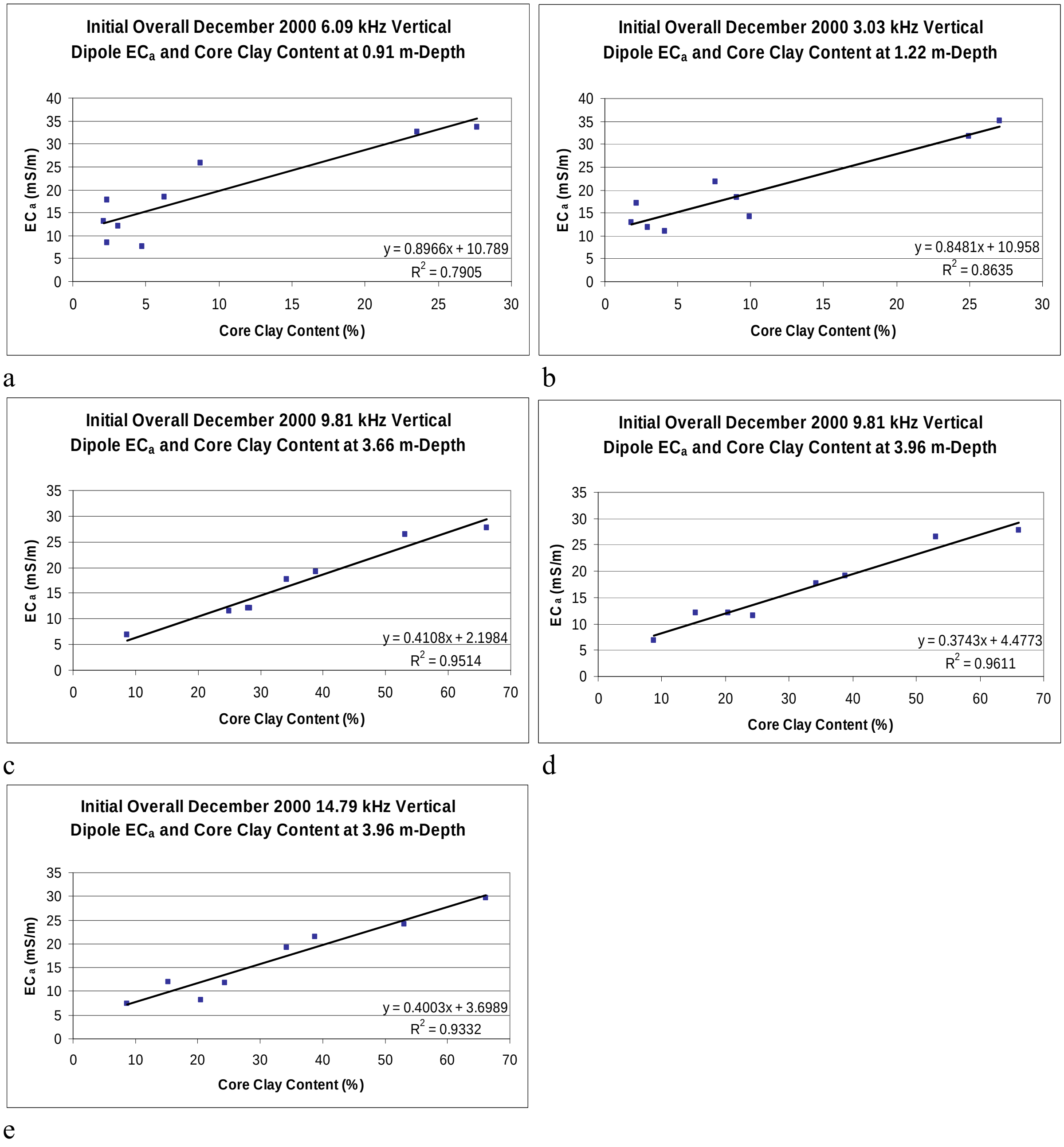

Fig. 6.9. Initial overall December 2000 EC_a data versus analyzed core clay content at specific depths. Illustrated are models of frequencies and depths at which correlations were strong: a) 6.09 kHz at 2- to 3-ft (0.61- to 0.91-m) depth, b) 3.03 kHz at 3- to 4-ft (0.91- to 1.22-m) depth, c) 9.81 kHz at 11- to 12-ft (3.33- to 3.66-m) and 12- to 13-ft (3.66- to 3.96-m) depths, and d) 14.79 kHz at 12- to 13-ft (3.66- to 3.96-m) depth, all in the vertical dipole orientation.

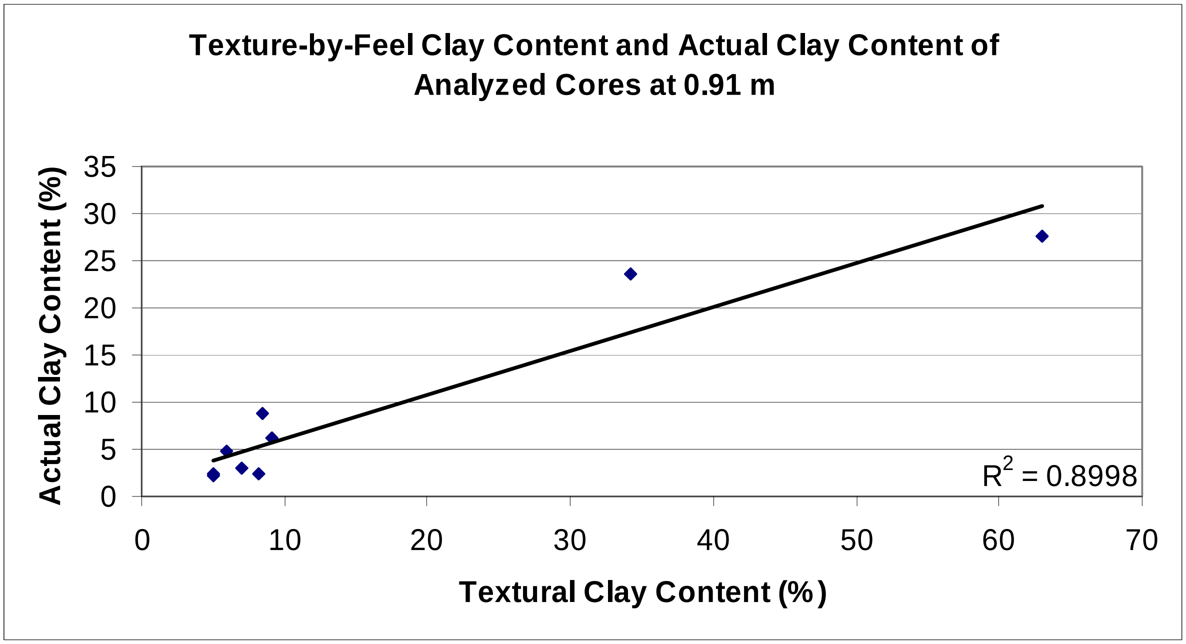

Fig. 6.10. Comparison of core clay content from the particle size analyses versus that estimated by the texture-by-feel method for the 3-ft (0.91-m) depth increment. The 3-ft (0.91-m) increment was chosen because there was a strong relationship between measured clay content and the texture-by-feel clay content of the analyzed cores. Clay content for the texture-by-feel method was estimated as the mean clay content of each textural class.

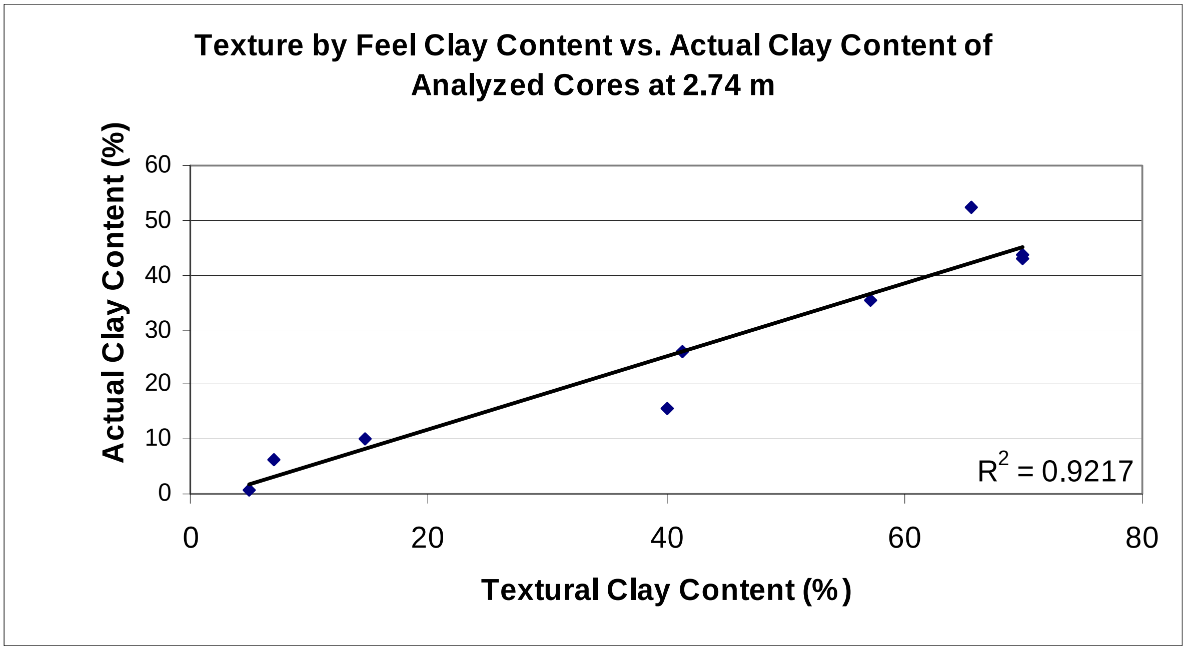

Fig. 6.11. Comparison of core clay content from the particle size analyses versus that estimated by the texture-by-feel method for the 9-ft (2.74-m) depth increment. The 9-ft (2.74-m) increment was chosen because there was a strong relationship between measured clay content and the textural clay content of the analyzed cores. Clay content for the texture-by-feel method was estimated as the mean clay content of each textural class.

Table 1 (continued).

Table 6.1. Correlations (Pearson correlation coefficient, r) of apparent soil electrical conductivity (EC_a) from the initial overall December 2000 EC_a survey with core particle size distribution. Depth increment “All” used particle size distribution averaged over all depths sampled. Particle size distribution for the other depth increments was the depth-weighted average of the naturally delineated horizons sampled within that increment. Frequency is designated EM38v for the EM38 frequency in the vertical dipole orientation; otherwise, frequencies are from the GEM-300, v for vertical dipole orientation and h for horizontal dipole orientation. Every 0.31 m equals 1 ft.

Depth increment	**EMI frequency**	**Number of observations**	**Very coarse sand**	**Coarse sand**	**Medium sand**	**Fine sand**	**Very fine sand**	**Total sand**	**Total silt**	**Total clay**
m	**kHz**	**n**	---*r*---							
All	EM38v	9	-0.04	0.04	-0.25*	-0.40*	0.14	-0.49*	0.19*	0.52*
All	3.030v	9	-0.09	0.01	-0.14	-0.29*	0.15*	-0.33*	0.05	0.41*
All	3.030h	9	0.05	0.02	-0.24*	-0.20*	0.19*	-0.31*	0.40*	0.12
All	6.090v	9	-0.11	-0.03	-0.25*	-0.34*	0.22*	-0.45*	0.17*	0.49*
All	6.090h	9	0.02	-0.03	-0.27*	-0.25*	0.20*	-0.38*	0.39*	0.23*
All	9.810v	9	-0.13	-0.08	-0.25*	-0.40*	0.22*	-0.51*	0.16*	0.57*
All	9.810h	9	-0.01	-0.06	-0.25*	-0.27*	0.19*	-0.39*	0.34*	0.28*
All	14.790v	9	-0.14	-0.09	-0.32*	-0.37*	0.23*	-0.54*	0.19*	0.60*
All	14.790h	9	-0.02	-0.04	-0.28*	-0.28*	0.22	-0.42*	0.35*	0.31*
0-0.31	EM38v	9	0.07	0.63	-0.63	-0.41	0.63	-0.82	0.85*	0.43
0-0.31	3.030v	9	-0.28	0.43	-0.35	-0.21	0.73*	-0.46*	0.62	-0.08
0-0.31	3.030h	9	0.90*	0.66	-0.20	-0.42	0.15	-0.44	0.17	0.84*
0-0.31	6.090v	9	-0.02	0.62	-0.35	-0.38	0.66	-0.61	0.68*	0.21
0-0.31	6.090h	9	0.90*	0.69*	-0.24	-0.50	0.11	-0.55	0.29	0.90*
0-0.31	9.810v	9	0.17	0.71*	-0.35	-0.47	0.56	-0.67*	0.69*	0.36
0-0.31	9.810h	9	0.93*	0.70*	-0.19	-0.53	0.04	-0.55	0.29	0.92*

Table 1 (continued).

Depth increment	EMI frequency	Number of observations	Very coarse sand	Coarse sand	Medium sand	Fine sand	Very fine sand	Total sand	Total silt	Total clay
m	**kHz**	**n**	---*r*--							
0-0.31	14.790v	9	0.22	0.72*	-0.24	-0.58	0.40	-0.72*	0.71*	0.46
0-0.31	14.790h	9	0.82*	0.76*	-0.17	-0.62	0.06	-0.64	0.39	0.94*
0.31-0.61	EM38v	9	0.57	0.07	-0.18	-0.52	0.63	-0.71*	0.65	0.77*
0.31-0.61	3.030v	9	0.65	0.09	0.00	-0.64	0.21	-0.65	0.60	0.69*
0.31-0.61	3.030h	9	0.41	-0.21	-0.46	-0.04	0.42	-0.53	0.47	0.59
0.31-0.61	6.090v	9	0.65	0.02	-0.09	-0.61	0.38	-0.73*	0.64	0.86*
0.31-0.61	6.090h	9	0.34	-0.19	-0.37	-0.10	0.55	-0.50	0.42	0.67*
0.31-0.61	9.810v	9	0.57	0.13	0.03	-0.67*	0.56	-0.66	0.55	0.92*
0.31-0.61	9.810h	9	0.26	-0.10	-0.25	-0.14	0.63	-0.41	0.32	0.67*
0.31-0.61	14.790v	9	0.42	0.10	-0.03	-0.52	0.62	-0.57	0.44	0.91*
0.31-0.61	14.790h	9	0.26	-0.13	-0.26	-0.17	0.61	-0.47	0.37	0.72*
0.61-.91	EM38v	9	0.58	0.26	-0.25	-0.52	0.40	-0.69*	0.49	0.89*
0.61-.91	3.030v	9	0.46*	0.33	-0.19	-0.45	0.46	-0.56*	0.36	0.78*
0.61-.91	3.030h	9	0.42	0.25	-0.29	-0.24	0.26	-0.48	0.33	0.63
0.61-.91	6.090v	9	0.57*	0.27	-0.30	-0.44	0.48	-0.66*	0.45	0.89*
0.61-.91	6.090h	9	0.39	0.22	-0.23	-0.25	0.19	-0.44	0.27	0.63
0.61-.91	9.810v	9	0.59	0.38	-0.24	-0.47	0.49	-0.62*	0.38	0.91*
0.61-.91	9.810h	9	0.31	0.34	-0.12	-0.24	0.15	-0.32	0.12	0.59
0.61-.91	14.790v	9	0.54	0.35	-0.28	-0.42	0.42	-0.61	0.36	0.91*
0.61-.91	14.790h	9	0.26	0.42	-0.09	-0.28	0.14	-0.32	0.09	0.64
0.91-1.22	EM38v	9	0.49	0.08	-0.39	-0.39	0.61	-0.75*	0.54	0.85*
0.91-1.22	3.030v	9	0.51	0.19	-0.49	-0.41	0.74*	-0.85*	0.64	0.93*

Table 1 (continued).

Depth increment	**EMI frequency**	**Number of observations**	**Very coarse sand**	**Coarse sand**	**Medium sand**	**Fine sand**	**Very fine sand**	**Total sand**	**Total silt**	**Total clay**
m	**kHz**	**n**	**---------------------------*r*---------------------------**							
0.91-1.22	3.030h	9	-0.17	-0.46	0.02	-0.27	0.22	-0.25	0.35	0.07
0.91-1.22	6.090v	9	0.39	0.05	-0.45	-0.41	0.68*	-0.83*	0.65	0.88*
0.91-1.22	6.090h	9	-0.08	-0.40	0.07	-0.33	0.16	-0.24	0.28	0.14
0.91-1.22	9.810v	9	0.50	0.16	-0.33	-0.49	0.60	-0.75*	0.53	0.88*
0.91-1.22	9.810h	9	0.00	-0.28	0.13	-0.33	0.09	-0.18	0.18	0.13
0.91-1.22	14.790v	9	0.41	0.12	-0.28	-0.39	0.43	-0.62	0.41	0.76*
0.91-1.22	14.790h	9	-0.10	-0.34	0.04	-0.27	0.09	-0.22	0.24	0.15
1.22-1.52	EM38v	9	0.72*	0.01	-0.46	-0.32	0.70*	-0.73*	0.72*	0.30
1.22-1.52	3.030v	9	0.78*	0.12	-0.33	-0.52	0.76	-0.73*	0.60	0.42
1.22-1.52	3.030h	9	0.13	-0.51	-0.12	0.11	0.22	-0.04	0.35	-0.29
1.22-1.52	6.090v	9	0.71*	-0.07	-0.37	-0.48	0.72*	-0.76*	0.66	0.41
1.22-1.52	6.090h	9	0.19	-0.46	-0.11	0.03	0.19	-0.10	0.34	-0.20
1.22-1.52	9.810v	9	0.73*	0.04	-0.28	-0.54	0.58	-0.72*	0.53	0.48
1.22-1.52	9.810h	9	0.17	-0.36	-0.06	-0.02	0.08	-0.10	0.23	-0.10
1.22-1.52	14.790v	9	0.53	-0.11	-0.34	-0.38	0.45	-0.70*	0.48	0.49
1.22-1.52	14.790h	9	0.09	-0.45	-0.14	-0.02	0.11	-0.20	0.32	-0.03
1.52-1.83	EM38v	9	-0.26	0.21	-0.42	-0.29	0.67*	-0.39	0.55	0.11
1.52-1.83	3.030v	9	-0.05	-0.05	-0.38	-0.20	0.79*	-0.29	0.16	0.23
1.52-1.83	3.030h	9	-0.37	0.37	0.25	0.10	0.06	0.25	0.31	-0.44
1.52-1.83	6.090v	9	-0.24	0.05	-0.25	-0.17	0.68*	-0.20	0.24	0.08
1.52-1.83	6.090h	9	-0.37	0.46	0.24	-0.01	0.03	0.14	0.33	-0.35
1.52-1.83	9.810v	9	-0.19	0.29	-0.23	-0.30	0.56	-0.31	0.23	0.21

Table 1 (continued).

Depth increment	**EMI frequency**	**Number of observations**	**Very coarse sand**	**Coarse sand**	**Medium sand**	**Fine sand**	**Very fine sand**	**Total sand**	**Total silt**	**Total clay**
m	**kHz**	**n**	----------------------------***r***----------------------------							
1.52-1.83	9.810h	9	-0.34	0.56	0.24	-0.08	-0.06	0.07	0.29	-0.24
1.52-1.83	14.790v	9	-0.39	0.24	-0.15	-0.17	0.37	-0.18	0.22	0.07
1.52-1.83	14.790h	9	-0.46	0.42	0.25	-0.04	-0.06	0.11	0.33	-0.31
1.83-2.13	EM38v	9	-0.23	0.54	-0.12	-0.22	0.45	-0.38	0.10	0.44
1.83-2.13	3.030v	9	-0.04	0.16	0.16	-0.27	0.25	-0.19	-0.20	0.39
1.83-2.13	3.030h	9	-0.35	0.42	-0.33	0.37	0.38	0.24	-0.13	-0.22
1.83-2.13	6.090v	9	-0.23	0.31	0.07	-0.27	0.29	-0.27	-0.11	0.45
1.83-2.13	6.090h	9	-0.35	0.55	-0.27	0.22	0.31	0.08	-0.07	-0.06
1.83-2.13	9.810v	9	-0.16	0.52	0.11	-0.35	0.18	-0.34	-0.14	0.55
1.83-2.13	9.810h	9	-0.31	0.63	-0.22	0.13	0.20	0.00	-0.07	0.06
1.83-2.13	14.790v	9	-0.36	0.53	0.01	-0.34	0.12	-0.45	-0.05	0.64
1.83-2.13	14.790h	9	-0.44	0.58	-0.22	0.02	0.24	-0.16	0.08	0.16
2.13-2.44	EM38v	9	0.12	0.11	-0.25	-0.15	0.63	-0.29	-0.15	0.44
2.13-2.44	3.030v	9	-0.35	-0.34	-0.13	-0.06	0.56	-0.17	-0.17	0.31
2.13-2.44	3.030h	9	0.87*	0.80*	-0.20	-0.12	0.27	-0.11	-0.05	0.17
2.13-2.44	6.090v	9	-0.05	-0.08	-0.23	-0.15	0.59	-0.31	-0.14	0.46
2.13-2.44	6.090h	9	0.89*	0.82*	-0.20	-0.22	0.24	-0.26	-0.01	0.31
2.13-2.44	9.810v	9	0.11	0.08	-0.20	-0.30	0.44	-0.49	-0.08	0.62
2.13-2.44	9.810h	9	0.90*	0.83*	-0.19	-0.30	0.13	-0.37	0.02	0.42
2.13-2.44	14.790v	9	0.20	0.13	-0.35	-0.24	0.39	-0.53	-0.16	0.72*
2.13-2.44	14.790h	9	0.87*	0.80*	-0.24	-0.30	0.25	-0.41	0.02	0.45
2.44-2.74	EM38v	9	0.06	-0.06	-0.35	-0.35	0.19	-0.56	0.06	0.70*

Table 1 (continued).

Depth increment	EMI frequency	Number of observations	Very coarse sand	Coarse sand	Medium sand	Fine sand	Very fine sand	Total sand	Total silt	Total clay
m	kHz	n	----------*r*----------							
2.44-2.74	3.030v	9	-0.49	-0.57	-0.28	-0.30	-0.12	-0.56	0.09	0.68*
2.44-2.74	3.030h	9	0.54	0.36	-0.43	-0.26	-0.04	-0.47	0.24	0.48
2.44-2.74	6.090v	9	-0.25	-0.38	-0.46	-0.40	0.03	-0.74*	0.19	0.85*
2.44-2.74	6.090h	9	0.57	0.39	-0.42	-0.34	0.04	-0.54	0.26	0.55
2.44-2.74	9.810v	9	-0.14	-0.26	-0.41	-0.49	-0.06	-0.78*	0.22	0.90*
2.44-2.74	9.810h	9	0.58	0.43	-0.39	-0.37	0.00	-0.55	0.25	0.57
2.44-2.74	14.790v	9	-0.01	-0.16	-0.56	-0.40	0.13	-0.75*	0.14	0.91*
2.44-2.74	14.790h	9	0.66	0.49	-0.50	-0.41	0.23	-0.63	0.30	0.65
2.74-3.05	EM38v	9	0.01	-0.03	-0.49	-0.47	0.17	-0.61	0.38	0.66
2.74-3.05	3.030v	9	-0.36	-0.43	-0.52	-0.25	0.03	-0.53	0.31	0.57
2.74-3.05	3.030h	9	-0.06	-0.02	-0.46	-0.41	-0.13	-0.56	0.52	0.50
2.74-3.05	6.090v	9	-0.27	-0.34	-0.66	-0.47	0.13	-0.75*	0.56	0.75*
2.74-3.05	6.090h	9	-0.03	0.02	-0.51	-0.49	0.00	-0.64	0.56	0.58
2.74-3.05	9.810v	9	-0.30	-0.34	-0.62	-0.55	0.08	-0.81*	0.53	0.86*
2.74-3.05	9.810h	9	-0.03	0.02	-0.46	-0.53	-0.02	-0.65	0.52	0.63
2.74-3.05	14.790v	9	-0.19	-0.24	-0.64	-0.61	0.21	-0.84*	0.59	0.87*
2.74-3.05	14.790h	9	0.16	0.18	-0.50	-0.66	0.14	-0.74*	0.67	0.67*
3.05-3.35	EM38v	9	-0.12	-0.19	-0.60	-0.54	0.07	-0.68*	0.28	0.78*
3.05-3.35	3.030v	9	-0.43	-0.47	-0.53	-0.17	0.20	-0.64	0.22	0.77*
3.05-3.35	3.030h	9	-0.15	-0.20	-0.54	-0.52	0.21	-0.64	0.79*	0.42
3.05-3.35	6.090v	9	-0.39	-0.46	-0.71*	-0.35	0.30	-0.81*	0.42	0.89*
3.05-3.35	6.090h	9	-0.16	-0.21	-0.62	-0.57	0.29	-0.71*	0.77*	0.52

Table 1 (continued).

Depth increment	EMI frequency	Number of observations	Very coarse sand	Coarse sand	Medium sand	Fine sand	Very fine sand	Total sand	Total silt	Total clay
m	kHz	n	------------------------------*r*------------------------------							
3.05-3.35	9.810v	9	-0.47	-0.54	-0.82*	-0.30	0.47	-0.88*	0.46	0.96*
3.05-3.35	9.810h	9	-0.19	-0.25	-0.66	-0.49	0.39	-0.71*	0.74*	0.55
3.05-3.35	14.790v	9	-0.34	-0.43	-0.84*	-0.41	0.47	-0.88*	0.50	0.93*
3.05-3.35	14.790h	9	-0.02	-0.10	-0.71*	-0.59	0.35	-0.69*	0.70*	0.54
3.35-3.66	EM38v	8	-0.36	-0.48	-0.60	-0.64	-0.12	-0.82*	0.34	0.91*
3.35-3.66	3.030v	8	-0.32	-0.37	-0.47	-0.42	-0.17	-0.60	0.05	0.84*
3.35-3.66	3.030h	8	-0.15	-0.32	-0.55	-0.58	0.17	-0.69	0.93*	0.18
3.35-3.66	6.090v	8	-0.44	-0.56	-0.68	-0.51	-0.01	-0.81*	0.30	0.92*
3.35-3.66	6.090h	8	-0.25	-0.42	-0.63	-0.60	0.26	-0.77*	0.91*	0.33
3.35-3.66	9.810v	8	-0.54	-0.65	-0.81*	-0.50	0.18	-0.89*	0.38	0.98*
3.35-3.66	9.810h	8	-0.30	-0.46	-0.68	-0.53	0.37	-0.77*	0.87*	0.35
3.35-3.66	14.790v	8	-0.49	-0.66	-0.83*	-0.47	0.24	-0.88*	0.41	0.94*
3.35-3.66	14.790h	8	-0.36	-0.55	-0.77*	-0.51	0.39	-0.83*	0.85*	0.45
3.66-3.96	EM38v	8	-0.32	-0.38	-0.65	-0.66	-0.15	-0.81*	0.36	0.92*
3.66-3.96	3.030v	8	-0.30	-0.34	-0.53	-0.40	-0.19	-0.60	0.08	0.84*
3.66-3.96	3.030h	8	-0.10	-0.16	-0.58	-0.65	0.14	-0.70	0.93*	0.27
3.66-3.96	6.090v	8	-0.40	-0.45	-0.74*	-0.55	-0.04	-0.81*	0.33	0.95*
3.66-3.96	6.090h	8	-0.20	-0.26	-0.67	-0.67	0.23	-0.78*	0.90*	0.41
3.66-3.96	9.810v	8	-0.50	-0.55	-0.83*	-0.52	0.15	-0.86*	0.39	0.98*
3.66-3.96	9.810h	8	-0.26	-0.31	-0.69	-0.59	0.35	-0.75*	0.86*	0.42
3.66-3.96	14.790v	8	-0.44	-0.49	-0.84*	-0.56	0.21	-0.87*	0.42	0.97*
3.66-3.96	14.790h	8	-0.30	-0.36	-0.77*	-0.61	0.37	-0.82*	0.84*	0.53

Table 1 (continued).

Depth increment	EMI frequency	Number of observations	Very coarse sand	Coarse sand	Medium sand	Fine sand	Very fine sand	Total sand	Total silt	Total clay
m	kHz	n	---------------------------*r*---------------------------							
3.96-4.27	EM38v	8	0.01	0.14	-0.22	-0.53	-0.46	-0.46	-0.14	0.65
3.96-4.27	3.030v	8	0.09	0.25	-0.02	-0.22	-0.45	-0.12	-0.47	0.44
3.96-4.27	3.030h	8	0.09	0.14	-0.28	-0.54	0.11	-0.46	0.77*	0.09
3.96-4.27	6.090v	8	-0.01	0.14	-0.25	-0.38	-0.33	-0.36	-0.19	0.56
3.96-4.27	6.090h	8	-0.03	0.01	-0.44	-0.59	0.13	-0.60	0.76*	0.27
3.96-4.27	9.810v	8	-0.17	-0.03	-0.38	-0.46	-0.16	-0.52	-0.07	0.68
3.96-4.27	9.810h	8	-0.14	-0.11	-0.50	-0.60	0.23	-0.67	0.77*	0.35
3.96-4.27	14.790v	8	-0.19	-0.10	-0.53	-0.56	-0.13	-0.67	0.07	0.78*
3.96-4.27	14.790h	8	-0.16	-0.12	-0.56	-0.61	0.21	-0.71*	0.72*	0.43
4.27-4.57	EM38v	8	-0.09	0.19	-0.13	-0.58	-0.28	-0.39	-0.38	0.59
4.27-4.57	3.030v	8	-0.01	0.30	0.08	-0.26	-0.24	-0.03	-0.61	0.27
4.27-4.57	3.030h	8	0.02	0.14	-0.28	-0.23	0.28	-0.25	0.33	0.15
4.27-4.57	6.090v	8	-0.12	0.20	-0.16	-0.27	-0.02	-0.21	-0.44	0.41
4.27-4.57	6.090h	8	-0.11	0.01	-0.42	-0.27	0.32	-0.40	0.32	0.33
4.27-4.57	9.810v	8	-0.28	0.03	-0.29	-0.26	0.06	-0.34	-0.43	0.55
4.27-4.57	9.810h	8	-0.21	-0.11	-0.49	-0.23	0.37	-0.46	0.30	0.41
4.27-4.57	14.790v	8	-0.28	-0.06	-0.48	-0.30	0.19	-0.51	-0.24	0.66
4.27-4.57	14.790h	8	-0.23	-0.11	-0.56	-0.19	0.45	-0.48	0.25	0.44
4.57-4.88	EM38v	8	-0.14	0.16	-0.07	-0.61	-0.31	-0.40	-0.36	0.59
4.57-4.88	3.030v	8	-0.07	0.27	0.12	-0.30	-0.26	-0.05	-0.58	0.28
4.57-4.88	3.030h	8	-0.01	0.12	-0.21	-0.27	0.26	-0.25	0.33	0.15
4.57-4.88	6.090v	8	-0.18	0.16	-0.09	-0.32	-0.04	-0.23	-0.41	0.42

Table 1 (continued).

Depth increment	**EMI frequency**	**Number of observations**	**Very coarse sand**	**Coarse sand**	**Medium sand**	**Fine sand**	**Very fine sand**	**Total sand**	**Total silt**	**Total clay**
m	**kHz**	**n**	---*r*---							
4.57-4.88	6.090h	8	-0.14	-0.02	-0.34	-0.31	0.29	-0.41	0.32	0.34
4.57-4.88	9.810v	8	-0.33	0.01	-0.17	-0.36	0.00	-0.35	-0.41	0.56
4.57-4.88	9.810h	8	-0.23	-0.13	-0.38	-0.30	0.32	-0.47	0.29	0.41
4.57-4.88	14.790v	8	-0.33	-0.08	-0.37	-0.39	0.14	-0.51	-0.22	0.67
4.57-4.88	14.790h	8	-0.26	-0.12	-0.44	-0.27	0.40	-0.48	0.25	0.45
4.88-5.18	EM38v	8	-0.09	0.25	-0.05	-0.44	-0.15	-0.31	-0.20	0.60
4.88-5.18	3.030v	8	-0.28	0.33	0.14	-0.07	-0.28	0.10	-0.59	0.44
4.88-5.18	3.030h	8	0.35	0.03	-0.27	-0.39	0.49	-0.41	0.72*	-0.17
4.88-5.18	6.090v	8	-0.26	0.21	-0.10	-0.10	0.00	-0.11	-0.32	0.46
4.88-5.18	6.090h	8	0.24	-0.08	-0.39	-0.40	0.55	-0.54	0.72*	0.01
4.88-5.18	9.810v	8	-0.31	0.07	-0.17	-0.21	0.13	-0.27	-0.19	0.55
4.88-5.18	9.810h	8	0.17	-0.17	-0.43	-0.41	0.60	-0.60	0.72*	0.08
4.88-5.18	14.790v	8	-0.25	-0.01	-0.36	-0.21	0.27	-0.44	-0.05	0.62
4.88-5.18	14.790h	8	0.10	-0.16	-0.48	-0.33	0.65	-0.59	0.64	0.14
5.18-5.49	EM38v	8	0.47	0.46	0.05	-0.31	-0.33	-0.07	-0.47	0.59
5.18-5.49	3.030v	8	0.32	0.52	0.18	-0.29	-0.23	0.09	-0.54	0.47
5.18-5.49	3.030h	8	0.38	0.08	-0.15	0.36	0.11	0.17	0.02	-0.24
5.18-5.49	6.090v	8	0.34	0.45	0.01	-0.08	-0.07	0.08	-0.53	0.47
5.18-5.49	6.090h	8	0.32	0.02	-0.23	0.37	0.13	0.09	-0.05	-0.06
5.18-5.49	9.810v	8	0.36	0.37	0.01	-0.02	-0.05	0.10	-0.63	0.55
5.18-5.49	9.810h	8	0.30	-0.04	-0.23	0.38	0.17	0.09	-0.12	0.02
5.18-5.49	14.790v	8	0.28	0.24	-0.20	0.04	0.11	-0.06	-0.50	0.61

Table 1 (continued).

Depth increment	**EMI frequency**	**Number of observations**	**Very coarse sand**	**Coarse sand**	**Medium sand**	**Fine sand**	**Very fine sand**	**Total sand**	**Total silt**	**Total clay**
m	**kHz**	**n**	----------------	----------------	----------------	--------*r*	--------	----------------	----------------	----------------
5.18-5.49	14.790h	8	0.29	0.00	-0.29	0.42	0.26	0.08	-0.17	0.08

* Significant at the 0.05 probability level.

Table 2 (continued).

Table 6.2. Correlations (Pearson correlation coefficient, r) between core clay contents at all depth increments for the nine analyzed cores. Every 0.31 m equals 1 ft.

Depth increment							
	m						
	0-0.31	**0.31-0.61**	**0.61-0.91**	**0.91-1.22**	**1.22-1.52**	**1.52-1.83**	**1.83-2.13**
m	***r***						
0-0.31	1.00*						
0.31-0.61	0.59	1.00*					
0.61-0.91	0.18	0.80*	1.00*				
0.91-1.22	0.10	0.70*	0.96*	1.00*			
1.22-1.52	-0.13	0.23	0.35	0.54	1.00*		
1.52-1.83	-0.18	0.05	0.18	0.34	0.46	1.00*	
1.83-2.13	0.10	0.36	0.37	0.48	0.87*	0.49	1.00*
2.13-2.44	0.36	0.50	0.34	0.45	0.81*	0.31	0.90*
2.44-2.74	0.46	0.91*	0.75*	0.72*	0.53	0.00	0.52
2.74-3.05	0.52	0.84*	0.65	0.68*	0.62	0.14	0.60
3.05-3.35	0.38	0.88*	0.81*	0.78*	0.48	0.19	0.56
3.35-3.66	0.39	0.84*	0.88*	0.87*	0.57	0.34	0.70
3.66-3.96	0.44	0.88*	0.89*	0.82*	0.40	0.17	0.60
3.96-4.27	0.43	0.58	0.51	0.49	0.47	0.32	0.81*
4.27-4.57	0.48	0.45	0.36	0.34	0.35	0.27	0.72*
4.57-4.88	0.49	0.47	0.37	0.35	0.35	0.28	0.72*
4.88-5.18	0.18	0.35	0.46	0.48	0.49	0.40	0.80*
5.18-5.49	0.12	0.33	0.48	0.51	0.53	0.44	0.82*

Table 2 (continued).

Depth increment							
	m						
	2.13-2.44	2.44-2.74	2.74-3.05	3.05-3.35	3.35-3.66	3.66-3.96	3.96-4.27
m	*r*						
2.13-2.44	**1.00***						
2.44-2.74	**0.67***	**1.00***					
2.74-3.05	**0.79***	**0.96***	**1.00***				
3.05-3.35	**0.70***	**0.87***	**0.87***	**1.00***			
3.35-3.66	**0.67**	**0.84***	**0.82***	**0.96***	**1.00***		
3.66-3.96	**0.59**	**0.83***	**0.77***	**0.97***	**0.97***	**1.00***	
3.96-4.27	**0.79***	**0.52**	**0.54**	**0.74***	**0.75***	**0.77***	**1.00***
4.27-4.57	**0.74***	**0.36**	**0.43**	**0.65**	**0.64**	**0.66**	**0.96***
4.57-4.88	**0.74***	**0.37**	**0.44**	**0.66**	**0.64**	**0.67**	**0.96***
4.88-5.18	**0.69**	**0.30**	**0.34**	**0.58**	**0.66**	**0.66**	**0.94***
5.18-5.49	**0.68**	**0.29**	**0.32**	**0.57**	**0.67**	**0.65**	**0.93***

Depth increment				
	m			
	4.27-4.57	4.57-4.88	4.88-5.18	5.18-5.49
m	*r*			
4.27-4.57	**1.00***			
4.57-4.88	**1.00***	**1.00***		
4.88-5.18	**0.93***	**0.93***	**1.00***	
5.18-5.49	**0.90***	**0.90***	**1.00***	**1.00***

Table 2 (continued).

* Significant at the 0.05 probability level.

Table 6.3. Correlations (Pearson correlation coefficient, r) of apparent soil electrical conductivity (EC_a) from the initial overall December 2000 EC_a survey with core particle size distribution by soil map unit. Depth increment "All" used particle size distribution averaged over all depths sampled. Particle size distribution for the other depth increments was the depth-weighted average of the horizons sampled within that increment. Frequency is designated EM38v for the EM38 frequency in the vertical dipole orientation; otherwise, frequencies are from the GEM-300, v for vertical dipole orientation and h for horizontal dipole orientation.

Depth increment	**Soil type**	**EMI frequency**	**Number of observations**	**Very coarse sand**	**Coarse sand**	**Medium sand**	**Fine sand**	**Very fine sand**	**Total sand**	**Total silt**	**Total clay**
m	**map unit**	**kHz**	**n**					***r***			
All	Ponzer	EM38v	2	0.05	0.29	-0.05	-0.02	0.11	0.03	-0.03	-0.03
All	Ponzer	3.030v	2	0.06	0.28	-0.10	-0.06	0.13	-0.02	0.02	0.01
All	Ponzer	3.030h	2	-0.03	-0.27	-0.02	-0.04	-0.07	-0.09	0.08	0.08
All	Ponzer	6.090v	2	0.06	0.28	-0.10	-0.07	0.13	-0.02	0.02	0.01
All	Ponzer	6.090h	2	-0.04	-0.28	0.00	-0.02	-0.08	-0.08	0.07	0.06
All	Ponzer	9.810v	2	0.06	0.28	-0.10	-0.06	0.13	-0.02	0.02	0.01
All	Ponzer	9.810h	2	-0.04	-0.28	0.02	-0.01	-0.09	-0.06	0.05	0.05
All	Ponzer	14.790v	2	0.07	0.27	-0.14	-0.10	0.14	-0.06	0.07	0.04
All	Ponzer	14.790h	2	-0.04	-0.28	0.02	-0.01	-0.09	-0.06	0.05	0.05
All	Leon	EM38v	6	-0.03	-0.03	-0.08	-0.10	0.14	-0.20	0.27*	0.07
All	Leon	3.030v	6	-0.23*	-0.36*	0.07	-0.11	0.22*	-0.19	-0.05	0.33*
All	Leon	3.030h	6	0.02	0.11	-0.44*	0.19	0.12	-0.17	0.28*	0.02
All	Leon	6.090v	6	-0.24*	-0.32*	-0.13	-0.08	0.32*	-0.34*	0.12	0.40*
All	Leon	6.090h	6	-0.05	0.00	-0.41*	0.10	0.23*	-0.29*	0.34*	0.14
All	Leon	9.810v	6	-0.27*	-0.33*	-0.07	-0.13	0.31*	-0.34*	0.02	0.49*
All	Leon	9.810h	6	-0.12	-0.04	-0.37*	0.03	0.28*	-0.35*	0.23*	0.33*
All	Leon	14.790v	6	-0.23*	-0.24*	-0.22*	-0.07	0.33*	-0.39*	0.15	0.45*

Depth increment	Soil type	EMI frequency	Number of observations	Very coarse sand	Coarse sand	Medium sand	Fine sand	Very fine sand	Total sand	Total silt	Total clay
m	**map unit**	**kHz**	**n**	-- ***r*** --							
All	Leon	14.790h	6	-0.07	-0.01	-0.32*	-0.05	0.29*	-0.37	0.31*	0.29*

* Significant at the 0.05 probability level.

Table 6.4. Correlations (Pearson correlation coefficient, r) of clay content of unanalyzed cores determined by texture-by-feel method and the clay content estimated from the five strongest prediction equations of initial overall December 2000 EC_a and actual clay content of the analyzed cores. Depth and frequency refer to those at which the models were derived and the estimations made. Every 0.31 m equals 1 ft.

Depth Increment	**EMI Frequency**	**Estimated Clay**
m	**kHz**	***r***
0.61-0.91	6.09v	-0.63
0.91-1.22	3.03v	-0.45
3.55-3.66	9.81v	0.57
3.66-3.96	9.81v	0.54
3.66-3.96	14.79v	0.62

* Significant at the 0.05 probability level.

Chapter 7

STORM EFFECTS ON NUTRIENT CONCENTRATIONS IN THE VADOSE ZONE, SHALLOW GROUNDWATER, AND DRAINAGE DITCHES PRIOR TO WETLAND RESTORATION OF A CAROLINA BAY

S. Abit, A. Amoozegar, and M.J. Vepraskas

INTRODUCTION

Plant nutrients, mainly phosphorus and nitrogen, are among the principal factors that may adversely affect surface water quality. Of the 700,000 miles of rivers and streams assessed for water quality status in the U.S. in 2000, 8% or 55,398 miles of rivers and streams were impaired by excess nutrients (USEPA, 2000). In addition, excessively high nutrient load is the primary reason for the impairment of 22% of the 3.8 million acres (equal to 1.52 M ha) of lakes that had been assessed (USEPA, 2000). Excess nutrients adversely affect humans and domestic animals, as well as causing damage on aquatic life (Dodds and Welch 2000). Excess nitrogen and phosphorus are also known chemicals that lead to eutrophication that can cause proliferation of algal masses leading to degradation of water quality (Correll, 1998).

On a watershed scale, dissolved nutrients are transported with water as water moves towards the streams via overland flow (i.e., runoff), subsurface stormflow (or interflow) and ground water flow (Freeze and Cherry, 1979). Overland flow or runoff takes place when rainfall rates exceed infiltration capacity of the soil at certain portions of the watershed. In runoff, rainwater that cannot infiltrate the soil will dissolve nutrients near or at the soil surface and also transport the suspended soil particles (including the sorbed nutrients ions) as it moves laterally along the land surface gradient. Subsurface stormflow resulting from storm events is comprised of the lateral inflow to streams that takes place in a shallow horizon with high permeability underlain by a slowly permeable soil layer (Freeze, 1972). Ground water flow is characterized by the movement of water below the water table along streamlines response to the subsurface hydraulic gradient. In addition to the water moving into withdrawal wells, this process is responsible for the regular supply of water to streams and other surface bodies of water (Hillel, 1998). The same processes could also be assumed to contribute to the transport of dissolved nutrients to drainage ditches at field scales.

Significant changes in nutrient discharges from an area (e.g., drainage basin and wetlands) had been reported following storm events. It is reported for a karst terrain in northwest Arkansas that as much as 26% of the nitrate-nitrogen that exits the drainage basin in a year are due to rapid recharge associated with a few storm pulses (Peterson et al., 2002). Davis et al. (2000) reported that elevated nitrate nitrogen (NO_3-N) concentration (16.7 mg L^{-1}) in selected springs in northwest Arkansas was observed during storm events as compared to base flow (13.0 mg L^{-1}). A wetland treating water from an agricultural and forest watershed was also found to export significantly higher soluble reactive phosphorus and total phosphorus during precipitation events as compared to dry-weather conditions (Fink and Mitsch, 2004). The increased rainfall intensity in storm events causes an increase in the extent of transfer of ions into runoff water due to the increased degree of turbulent mixing and dispersion of the soil resulting from a greater raindrop impact (Ahuja, 1986).

Rainfall intensity has been reported to influence significant changes in nutrient levels in drainage ditches. In a year-long monitoring of nutrient concentration at the main ditch exit in Juniper Bay, a Carolina Bay in Robeson County, North Carolina, two rain events which exceeded 5 cm d^{-1} accounted for 74% of the phosphates and almost all of the nitrates exported out of the bay (Kreiser, 2003). It also accounted for 62, 66, and 61 % of the total organic carbon, calcium and magnesium exported out of the Bay in the drainage water for the year, respectively. This increase in nutrient load in the drainage water was attributed to surface runoff contributions to the ditch which may have occurred when the heavy rain intensity during storm events exceeded the infiltration rate.

In addition to inducing surface runoff, we hypothesized that the major storm events (e.g., 2 in. d^{-1}) cause significant changes in the nutrient concentrations in the soil solution in the subsurface, and that subsurface flow of soil water and dissolved nutrients contribute to the elevated nutrient load in the ditches. The objective of this study was to evaluate the impact of storm events on the nutrient concentrations of the soil solution in the vadose zone, groundwater and ditch water in Juniper Bay.

METHODOLOGY

The study was conducted at Juniper Bay, a 740-acre (300-hectare) Carolina Bay located 6.2 mi (10 km) southeast of Lumberton, in Robeson County, North Carolina ($34^o30'30"$N $79^o01'30"$E). The site was drained by a number of lateral ditches connected to a main ditch that traversed the entire width of the Bay. Two relatively small areas, one containing a mineral soil located at the NE end, and the other with an organic soil near the center of the Bay, were chosen for nutrient monitoring (Fig. 7.1). These locations were chosen because they were typical of mineral and organic soils in Juniper Bay and for their close proximity to lateral ditches that drained into the main ditch.

Soil Profile Characterization, Soil Sampling and Soil Analysis

Soil profile pits were dug near the study locations at both the mineral and organic soil sites. At each site, the soil profile was characterized and bulk soil samples were collect from the pit-walls at 0.5 ft (15 cm) depth intervals from the surface to the bottom of the unsaturated zone of the profile at the time of sampling. Intact cylindrical soil samples [diameter and length of 0.25 ft (7.6 cm)] were also collected, in a vertical orientation, at 0.5-ft depth intervals. The bulk soil samples from both mineral and organic sites were air-dried and passed through a 0.08-in (2-mm) sieve before analysis.

Extractable P, K, Ca, Na and Mg were determined by running Mehlich III extracts (Mehlich, 1984) through an inductively coupled plasma (ICP) emission spectrograph. Cation exchange capacity (CEC) was calculated by adding the exchangeable basic cations determined using Mehlich III extracts (Mehlich, 1984) and the exchangeable acidity (Mehlich et. al, 1976). The pH was determined using a 1:1 soil to water ratio. Organic carbon and total nitrogen were determined through dry combustion with a Perkin-Elmer PE2400 CHN Elemental Analyzer (Culmo, 1988).

Using the bulk samples, particle size distribution was determined by the hydrometer method (Gee and Or, 2002) where soil samples were pre-treated with 30 percent hydrogen peroxide (H_2O_2) to oxidize the organic matter prior to the dispersion and sedimentation. Saturated hydraulic conductivity (K_{sat}) of the intact core samples was measured by the constant head procedure (Amoozegar and Wilson, 1999). Soil water retention of the intact cores between 0 and 15 bar pressure was also measured (Dane and Hopmans, 2002). Bulk density at different depth intervals was determined by the core method (Grossman and Reinsch, 2002) and particle density was determined by the air pycnometer (gas displacement) technique (Flint and Flint, 2002).

Installation of Tension Lysimeters, Piezometers and Wells

At the mineral site, eight tension lysimeters (soil solution samplers) with their porous cups at 0.5, 1.0, 1.5, 2.0, 2.5, 3.0, 3.5 and 4.0 ft depths were installed on equally spaced spots on the arc of a 60-cm diameter circle at a distance of five meters from the side of the soil profile characterization pit and seven meters from the side ditch. Seven observation/sampling wells (hereafter referred to as piezometers), each with 0.5-ft long perforation at the bottom, were installed at equally spaced spots on the arc of a 4.0-ft (120-cm) diameter circle inscribing the tension lysimeters. The perforated sections of these piezometers were located at 1.25 to 1.75, 1.75 to 2.25, 2.25 to 2.75, 2.75 to 3.25, 3.25 to 3.75, 3.75 to 4.25 and 4.25 to 4.75 ft depths. Three fully perforated wells (hereafter referred to as wells) were also installed on the vertices of a triangle enclosing the two concentric circles. The distance between wells was 11.8 ft (3.6 m). Figure 2 presents a photograph of the monitoring set-up showing the locations of the lysimeters, piezometers and wells. Tension lysimeters, piezometers and wells were also installed at a distance of five meters to the side of the soil profile characterization pit at the organic soil site using the same pattern as in the mineral soil site. The only difference was that the depth of the tension lysimeters ranged from 1.0 to 6.0 ft.

The depths at which tension lysimeters, piezometers and wells were installed were based on three years of water fluctuation data that were collected prior to the initiation of this study (Vepraskas et al., 2003). These depths were selected to assure that both soil solution samples from the vadose zone and ground water samples from different depth intervals below the water table could be collected during the course of the study. Subsurface hydraulic gradient at both sites was determined using the three-point technique (Sanders, 1998) using the water table depths measured in the three wells that were arranged in a triangle at each site.

Monitoring Instrumentation

A tipping bucket rain gauge was set up halfway between the mineral and organic soil sites [roughly 980 ft (300 m) from either site]. Volumetric soil water content (VWC) at different depths in the monitoring sites were measured by Time Domain Reflectometer (TDR) using two five-segmented Moisture Point TDR probes (Gable Corp, Victoria, Canada) installed just outside the circle of piezometers (see Figure 2 for location of probes). One probe measured VWC at zero (surface) to 0.5, 0.5 to 1.0, 1.0 to 1.5, 1.5 to 2.0 and 2.0 to 3.0 ft depth intervals. The other probe measured VWC at zero to 0.5, 0.5 to 1.0, 1.0 to 2.0, 2.0 to 3.0 and 3.0 to 4.0 ft depth intervals. Time domain reflectometry measurements were taken every time soil water samples were collected from the monitoring sites. These were then compared to the soil water characteristic data at the corresponding 0.5 ft depth intervals in the soil to determine the degree of saturation of each given layer. Tensiometers were also installed at 0.5 ft depth intervals from 1.0 to 5.0 ft depths to measure matric potential at different depths (see Figure 7.2 for location of tensiometers).

Water Sample Collection and On-site Measurements

Soil water samples were collected from both mineral and organic sites at least monthly, with more frequent sampling during the summer months. Samples were also collected within 36 hours after major rain events. During a scheduled sampling date, water table depths in the three wells and the depth to the water level in the piezometers were first measured using a dipper (Herron Instruments Dipper T).

A vacuum trap was attached to each tension lysimeter in both saturated and unsaturated zones for collecting soil water samples (see Hendrickx et al., 2002). Using a hand pump, each sampler was initially purged (i.e., emptied) by applying vacuum to the trap. After emptying the trap and reattaching it to the sampler, the air from the trap was evacuated to create approximately 0.8 bar of tension (equivalent to –800 cm of pressure) inside the sampling cup. The vacuum inside the trap was maintained for thirty minutes to two hours to draw soil solution into the porous cup and then into the sample bottle in the trap. Up to 60 mL of soil solution samples was collected by this procedure.

Using plastic hand bailers, the wells were bailed slowly three times. Then each well was allowed to fill with ground water to the static level before 60 mL of groundwater sample was collected. The same procedure was used with the piezometers to collect ground water samples from different depth intervals below the water table.

Water samples from the lateral ditch directly across each monitoring location and from the main ditch immediately below and above the point of discharge of the lateral ditch into the main ditch at both organic and mineral soil sites were collected every time soil solution and ground water samples were collected. In addition, one sample from the main ditch exit (where all the water in the ditches exits the Bay) was collected for analysis. For relative locations of surface water sampling points see Figure 7.1. After collecting ground water samples, matric potential and VWC at various depths were measured using a digital pressure transducer known as Tensimeter (Soil Moisture Measurement System, Arizona) and the Moisture Point TDR System, respectively.

Chemical Analysis of Water Samples

Prior to chemical analysis, soil water samples were filtered using a Whatman # 40 filter paper (Whatman Int. Ltd, Maidstone, England). Two drops of concentrated sulfuric acid (H_2SO_4) were then added to each 60 mL of filtered sample reducing the pH to around 1 to eliminate microbial activity in the sample. Nutrient analyses were performed on bulk precipitation, ditch water, soil solution and ground water samples. Water samples were tested for NH_4^+-N, NO_3^--N, PO_4^{3-}, total organic carbon (TOC), Ca^{2+}, K^+, Mg^{2+}, Cl^- and Na^+. Phosphate, TOC, NH_4^+-N, and NO_3^--N were measured using Lachat Quickechem 8000 slow injection auto analyzer. Calcium, K^+, Mg^{2+} and Na^+ were measured using ICP. Chloride concentration was analyzed using ion chromatography. Methods used in the analysis are outlined in Greenberg et al. (1992).

RESULTS AND DISCUSSION

Soil and Site Characteristics

As described earlier, two sites were chosen to represent each of the mineral soil and the organic soil areas of Juniper Bay. The mineral soil site had textural classes of either loamy sand or sandy loam with sand content ranging from 78 to 87% from the surface down to a depth of 4.0 ft. Saturated hydraulic conductivity ranged from 3.0 to 18 ft d^{-1} (0.92 to 5.65 m d^{-1}) without any indication of a restricting layer. Bulk density increased and porosity decreased from the surface down to 3.5 ft depth. Extractable K, Ca and Mg contents were observed to be considerably higher in the upper 1.5 ft with highest concentrations of 31, 698, and 97 ppm (mg L^{-1}), respectively. Concentrations of these cations in layers below 1.5 ft were considerably lower. Total nitrogen and percent organic carbon (OC) were also observed to be considerably higher in the upper 1.5 ft. Organic carbon ranged from 3.4 to 3.7% while total N ranged from 1,053 to 2,360 ppm. High levels of Mehlich-extractable phosphorus (P) were also observed closer to the surface with concentrations of 96 to 142 ppm in the upper 1.0 ft and <17 ppm below the 1.0 ft depth. Soil pH was acidic with values ranging from 4.0 to 4.8 from the surface down to 4.0 ft depth.

The organic site had organic soil material in the upper 2.0 ft. Mineral soils were observed below 2.0 ft with clay contents ranging from 23 to 45%. The surface layer (top 15 cm) had an OC content of 12% and the mucky layers (0.5 to 2.0 ft depth) had OC content ranging from 40 to 45%. As in the mineral soil site, higher concentrations of K, Ca, Mg, total N and P were observed closer to the surface. Details on soil properties were reported by Abit (2005).

Hydrologic Observations

Rain data are presented in Figure 7.3. During the monitoring period, a total of 37 in (94 cm) of rain was recorded wherein two major rain events took place. Rain events that exceeded 2 in d^{-1} were considered major rain events. Major rain events were recorded on August 29-30 and November 23, 2004. Water table data at both mineral and organic sites taken during days when water samples were collected are presented in Figure 7.4. For both sites, deepest WT measurements were observed on July 16 and November 3. High demand for water by shrubs and weeds growing on site should have contributed to the deep WT in July when weed growth was observed to be very extensive. The absence of rain in the days prior to November 3 may have caused the deep WT. Shallow water tables were observed during days with rain events or during days immediately following significant rain events. For example, the water table that was relatively shallow on August 31 was largely due to the increased recharge resulting from the 2.6 in-rain event that took place on August 29 and 30.

Figure 7.5-A shows that in the organic site, during the days that the WT was observed to be shallow (Aug. 31 and Sept. 14), the general direction of the subsurface gradient tended to be more perpendicular to the ditch. In contrast, when the WT was deep (July 16 and Nov. 2), the flow was going away from the ditch. The same trend was observed at the mineral site (Fig. 7.5-B). Water table depths also had an effect on the magnitude of the subsurface hydraulic gradient. Shown in Figure 4 are the WT data together with the computed magnitude of the subsurface hydraulic gradient along an axis perpendicular to the lateral ditch. Here, a positive value indicates that the flow is towards the ditch and away from the ditch if it is negative. The plot shows that the magnitude of the gradient increased when the WT was closer to the surface. Conversely, it was also observed to decrease when the WT was deeper.

Due to their influence on the WT elevation and water level in the ditch, rain and evapotranspiration should largely affect the changes in hydraulic gradient in the area. Assuming no runoff or subsurface recharge to the ditches, we expect the increase in water level in the ditches to be equivalent to the amount of rain. For example, a 1-inch rain would lead to a 1-inch rise in water level in the ditch. Due to the fact that water that enters the soil can only fill the air-filled pore volume, 1-inch of rain percolating in the soil at the monitored site would translate into a rise in WT far in excess of 1 inch. In addition, the capillary fringe above the WT, being already close to saturation, could lead to a rapid rise in WT elevation even with minimal percolation (Gilliam, 1984). These factors make the WT significantly higher relative to the surface of the water in the ditch leading to an increase in hydraulic gradient towards the ditch (i.e., recharging the ditches). During dry days, continuous evapotranspiration by plants growing near the monitored site and lateral drainage into the ditch may result in accelerated removal of groundwater. When this happens, the water table could recede at a much higher rate than the decrease in water level at the ditch. This could result in a decrease in the magnitude of the hydraulic gradient towards the ditch, or in some cases, would lead in the shift of the gradient to a direction away from the ditch causing water discharge from the ditches back into the groundwater.

Solute Concentration in the Water Samples from Ditch and Wells

Soil water samples collected were classified as one of the following:
storm samples are those collected following the rain events that exceeded 2 inch d^{-1}

base flow samples are those collected at least 2 days since the last rain event (not a storm event) regular rain samples are those collected within two days after a rain event not classified as a storm event.

Average concentration of phosphate (PO_4-P), TOC, Ca and Mg in the water that exits the Bay through the main exit were observed to be higher in storm samples as compared to base flow and regular rain samples (Fig. 7.6). This was consistent with the results of the nutrient budget experiment of Kreiser (2003) in Juniper Bay. The same trend was observed at the lateral ditches except for Mg at the mineral site which was higher in base flow samples.

Well water samples were collected to evaluate the impact of the rain events on the concentrations of solutes in the groundwater. No significant spikes in the solute concentration in well samples were observed following storm events (data not shown). For additional information, see Abit (2005).

Solute Changes with Depth (Rain Effect)

To evaluate the effect of the storm event on the changes in solute concentration in the soil solution in the profile, the samples collected on August 12 and 31 were chosen to represent baseflow and storm samples, respectively. Figure 7.7 shows that at the mineral site there was a marked increase in TOC and phosphate concentrations at depths closer to the surface following a storm event. It should be noted that higher organic carbon and extractable P contents were also determined to be limited to soil layers closer to the surface. Calcium and Mg concentrations in soil solution, on the other hand, were observed to be highest in storm samples in most depths until 105 cm from the surface.

At the organic site, a general increase in TOC concentration in the soil solution was observed at depths closer to the surface (Fig. 7.8). This is particularly true from 2 ft to 3.5 ft depth. An increase in soil solution Ca concentrations following a major storm event was also observed at 2.0 ft, 2.5 ft and 3.5 ft depths. Changes in Mg and PO_4-P concentrations following storm events were observed to be relatively minimal.

Relatively high amounts of organic carbon were limited to layers close to the surface. It was then expected that during rain events, organic carbon near the surface could be dissolved and an increased TOC concentration in the soil solution would be most obvious closer to the surface. Extractable levels of Ca, Mg and PO_4-P were also relatively higher at certain depths close to the soil surface. During a major storm event, significant amounts of rainwater, with minimal Ca, Mg and PO_4-P content, may have immediately percolated to deeper depths. To achieve equilibrium conditions, some of the Ca, Mg and PO_4-P sorbed in the soil could have come into solution, thereby increasing the soil solution concentration of Ca, Mg and PO_4-P at depths where relatively higher extractable quantities of these soil nutrients are found.

We evaluated the fluctuation in chloride (Cl^-) concentration as a representative ion for those that were observed to have lower concentrations at the main ditch exit in storm samples compared to base flow (see Figure 7.6). It is interesting to note that following the storm event, Cl^- concentrations were markedly decreased in all depths in both the organic and mineral soil sites (Fig. 7.9). Chloride ions, being negatively charged, could not be sorbed in large quantities at the predominantly negatively charged exchange sites. Hence, in the event that rainwater (that is low in Cl^-) enters the pores, very limited amount of Cl^- could go into solution and the native concentration of the Cl in the soil is further diluted.

SUMMARY AND CONCLUSIONS

This study was conducted in Juniper Bay, a 740–acre (300-hectare) Carolina Bay in Robeson, County, North Carolina. The Bay was originally a forested wetland on an inter-stream divide that had been drained and devoted to agricultural production. The objective of this study was to evaluate the impact of storm events on the soil solution nutrient concentrations in the vadose zone, groundwater and ditch water at this Bay by evaluating the changes in nutrient concentrations in the ditch, groundwater and vadose zone at representative mineral and organic sites. Possible relationships between variation in nutrient loads (in ditch water, groundwater and soil solution) and changes in subsurface hydrology were also evaluated.

Our results show that the sample taken from the main ditch exit following a storm event had higher concentrations of total organic carbon (TOC), phosphates (PO_4-P), calcium (Ca) and magnesium (Mg) compared to the average of those gathered during baseflow conditions. The same general trend was observed at the lateral ditches close to the mineral and organic monitoring sites. Analysis of well water samples revealed no immediate response in nutrient concentration to the storm event indicating that the increase in nutrient concentration in the ditches was not due to groundwater flow. On the other hand, changes in nutrient concentrations in the soil solution at specific depths in the vadose zone and immediately below the water table were observed following the storm event. At the mineral site, TOC, PO_4-P, Ca and Mg concentrations in soil solution following the storm event were higher at depths closer to the surface. At the organic site, increases in TOC and Ca in soil solution were observed closer to the surface but no considerable increase in PO_4-P and Mg were observed following major rain events. Chloride concentration was observed to decrease in the ditches following a storm event. Its concentration at various depths in the profile was also observed to be lower after storm.

Percent organic carbon as well as extractable P, Ca and Mg were higher at depths closer to the surface. During major storm events, more organic carbon near the surface could be dissolved and an increased TOC concentration in the soil solution would be most obvious closer to the surface. Significant amounts of rainwater, which had very minimal Ca, Mg and PO_4-P content, may have percolated to deeper depths during and immediately after the storm event. In response, some of the Ca, Mg and PO_4-P sorbed in the soil could have come into solution, thereby increasing the soil solution concentration of Ca, Mg and PO_4-P at depths where relatively higher extractable quantities of these soil nutrients are found. In contrast, chloride ion, being negatively charged, could not be sorbed in large quantities at the predominantly negatively charged exchange sites. Hence, in the event that rainwater (that is low in Cl^-) enters the pores, very limited amount of Cl^- could go into solution and the native concentration of the Cl^- in the soil solution could be further diluted.

The increase in concentration of some nutrients in the ditches and upper layers of the soil profile coincided with observed increase in the magnitude of the subsurface hydraulic gradient. In addition, it was observed that immediately following the storm event, the direction of the subsurface lateral hydraulic gradient tended to become more perpendicular to the nearby lateral ditch suggesting that the route taken by the water as it moves in the subsurface towards the ditch is shortened. We believe that the increase in concentration of PO_4-P, Ca, Mg and TOC in the soil solution at certain depths in the soil profile, coupled by its more effective movement in the subsurface towards the ditch following the storm event, should have contributed to the increase in concentration of such nutrients in the ditches.

We cannot separate the contributions of surface runoff and subsurface flow to the increased concentration of some solutes in the ditches. However, because the soil at the site had high infiltration rate and there was no evidence of extensive runoff, we believe that contributions of subsurface flow to an increase in nutrient concentration is significant.

REFERENCES

Abit, S.M. 2005. Evaluation of subsurface solute transport and its contribution to nutrient load in the drainage ditches prior to restoration of a Carolina Bay. Electronic M.Sc. thesis copy at **http://www.lib.ncsu.edu/theses/available/etd-11152005-183644/unrestricted/etd.pdf**

Ahuja, L.R. 1986. Characterization and modeling of chemical transfer to runoff. Adv. Soil Sci. 4:149–188.

Amoozegar, A. and G. V. Wilson. 1999. Methods for Measuring Hydraulic Conductivity and Drainable Porosity. In: R.W. Skaggs and J. van Schilfgaarde (eds). Agricultural Drainage. Agronomy Monograph no. 38. SSSA, Madison, Wisconsin.

Correll, D. 1998. The role of phosphorus in the eutrophication of receiving waters: A review. J. Environ. Qual. 27:261–266.

Culmo, F.C. 1988. Principle of Operation – The Perkin-Elmer PE 2400 CHN Elemental Analyzer. Perkin Elmer Corp, Norwalk, CT.

Dane, J.H. and J.W. Hopmans. 2002. Water Retention and Storage. In: J.H. Dane and G.C. Topp (eds). Methods of Soil Analysis Part 4: Physical Methods. No. 5 in SSSA Book Series. SSSA, Madison, Wisconsin.

Davis, R.K., J.V. Brahana and J.S. Johnston. 2000. Groundwater in NW Arkansas: Minimizing nutrient contamination from non-point sources in karts terrane. Final Report for Tasks 94-300 and 95-300 to Arkansas Soil and Water Commission for USEPA Projects Number C9996103-02 and C9996102-03. AR Soil Water Conservation Commission, Little Rock, AR.

Dodds, W. K., and E. B. Welch, 2000, Establishing nutrient criteria in streams, J.N. Am. Benthol. Soc., Vol 19(1):186-196.

Fink, D.F. and W.J. Mitsch. 2004. Seasonal and storm event nutrient removal by a created wetland in an agricultural watershed. Ecological Engineering 23: 313-325.

Flint, A.L. and L.E. Flint. 2002. Particle Density. In: J.H. Dane and G.C. Topp (eds). Methods of Soil Analysis Part 4: Physical Methods. No. 5 in SSSA Book Series. SSSA, Madison, Wisconsin.

Freeze, R. A. and J. A. Cherry. 1979. Groundwater. Prentice Hall, Inglewood Cliffs, NJ.

Freeze, R.A. 1972. Role of subsurface flow in generating runoff: 1. Upstream source areas. Water Resources Research. 8:1272-1283.

Gee, G.W. and D. Or. 2002. Particle-Size Analysis. In: J.H. Dane and G.C. Topp (eds). Methods of Soil Analysis Part 4: Physical Methods. No. 5 in SSSA Book Series. SSSA, Madison, Wisconsin.

Greenberg , A.E., L.S. Clesceri and A.D. Eaton. 1992. Standard methods for examination of water and waste water. 18th Ed. APHA. Washington D.C.

Grossman, R.B. and T.G. Reinsch. 2002. Bulk Density. *In:* J.H. Dane and G.C. Topp (eds). Methods of Soil Analysis Part 4: Physical Methods. No. 5 in SSSA Book Series. SSSA, Madison, Wisconsin.

Hendrickx, J. M., J. M. Wraith, D. L. Corwin, and R. G. Kachanoski. 2002. Miscible Solute Transport. *In:* J. H. Dane, and G. C. Topp (eds). Methods of Soil Analysis Part 4: Physical Methods. No. 5 in Soil Sci. Soc. Am. Book Series. Soil Sc. Soc. Am., Madison, WI.

Hillel, D. 1998. Environmental Soil Physics. Academic Press. San Diego, CA.

Kreiser, G.S. 2003. Nutrient analysis of drainage waters from Juniper Bay. MSc Thesis, Department of Soil Science. North Carolina State University. At: http://www.lib.ncsu.edu/theses/available/etd-07022003-105052/unrestricted/etd.pdf

Mehlich, A., S.S. Bowling and A.L. Hatfield. 1976. Buffer pH acidity in relation to nature of soil acidity and expression of lime requirement. Commun Soil Sci Plant Anal 7(3):253-63.

Mehlich, A. 1984. Mehlich-3 soil test extractant: a modification of Mehlich-2 extractant. Commun Soil Sci Plant Anal 15(12): 1409-16.

Peterson, E.W., R.K. Davis, Brahana, J.V. and H.A. Orndorff. 2002. Movement of nitrate through regolith covered karst terrain, northwest Arkansas. Journal of Hydrology. 256:35-47.

Sanders, L. L. 1998. A manual of field hydrogeology. Prentice Hall, Upper Saddle River, N.J.

USEPA. 2000. National Water Quality Report. Available at: http://www.epa.gov/305b/2000report/

Vepraskas, M.J. J.G White, R.L Huffman, G.P Fernandez, R.W. Skaggs, C.W. Zanner, J.M. Stucky, J.D. Gregory, S.W. Broome, J.M. Ewing, B. Lees, S. Luginbuhl, G.S. Kreiser and R.P. Szuch. 2003. Methods to assess soil, hydrologic, and site parameters that affect wetland restoration. Project report to NCDOT, NCSU, NC.

ACKNOWLEDGEMENT

This chapter was as a portion of S. Abit's M.S. Thesis entitled "Evaluation of Subsurface Solute Transport and its Contribution to Nutrient Load in the Drainage Ditches Prior to Restoration of a Carolina Bay" that was earned through NC State University and is available through the university's library.

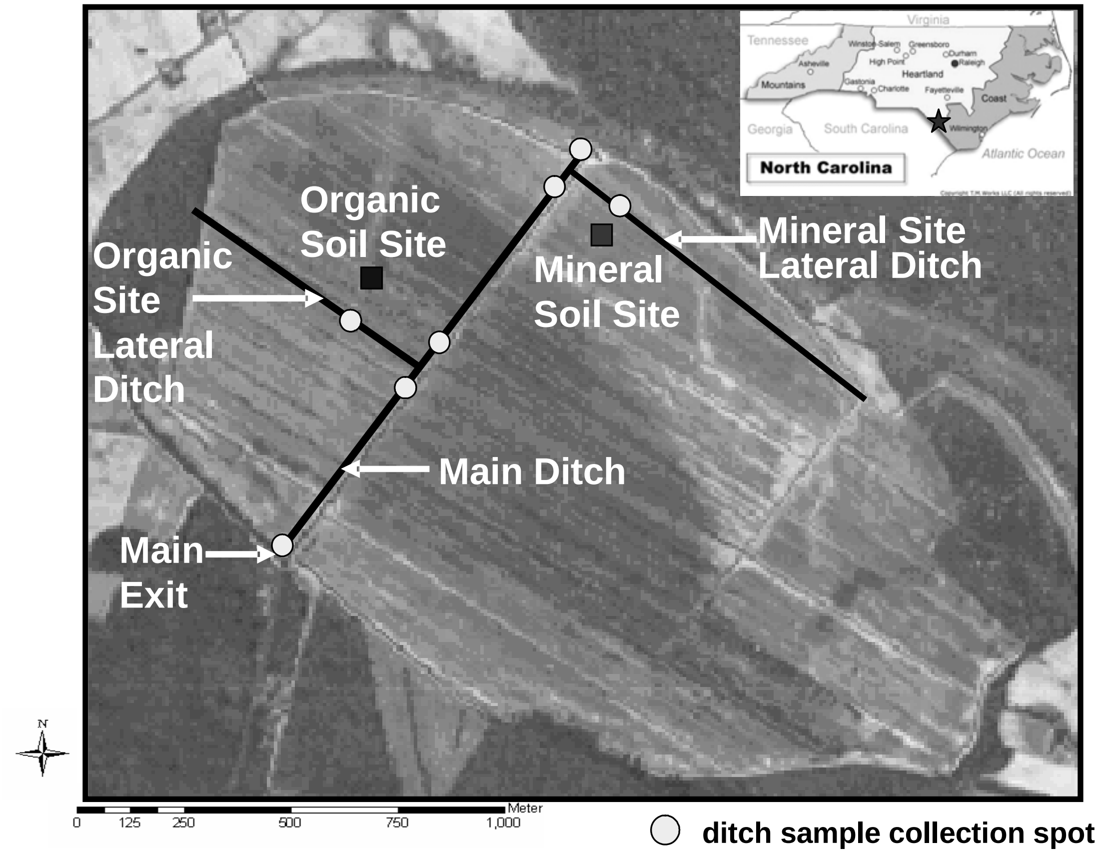

Figure 7.1. Aerial photograph of Juniper Bay with marked location of the organic and mineral soil sites, the main and side ditches, the main ditch exit and the ditch sample collection spots. In the inset, the location of Juniper Bay in the SE part of North Carolina is shown by the star.

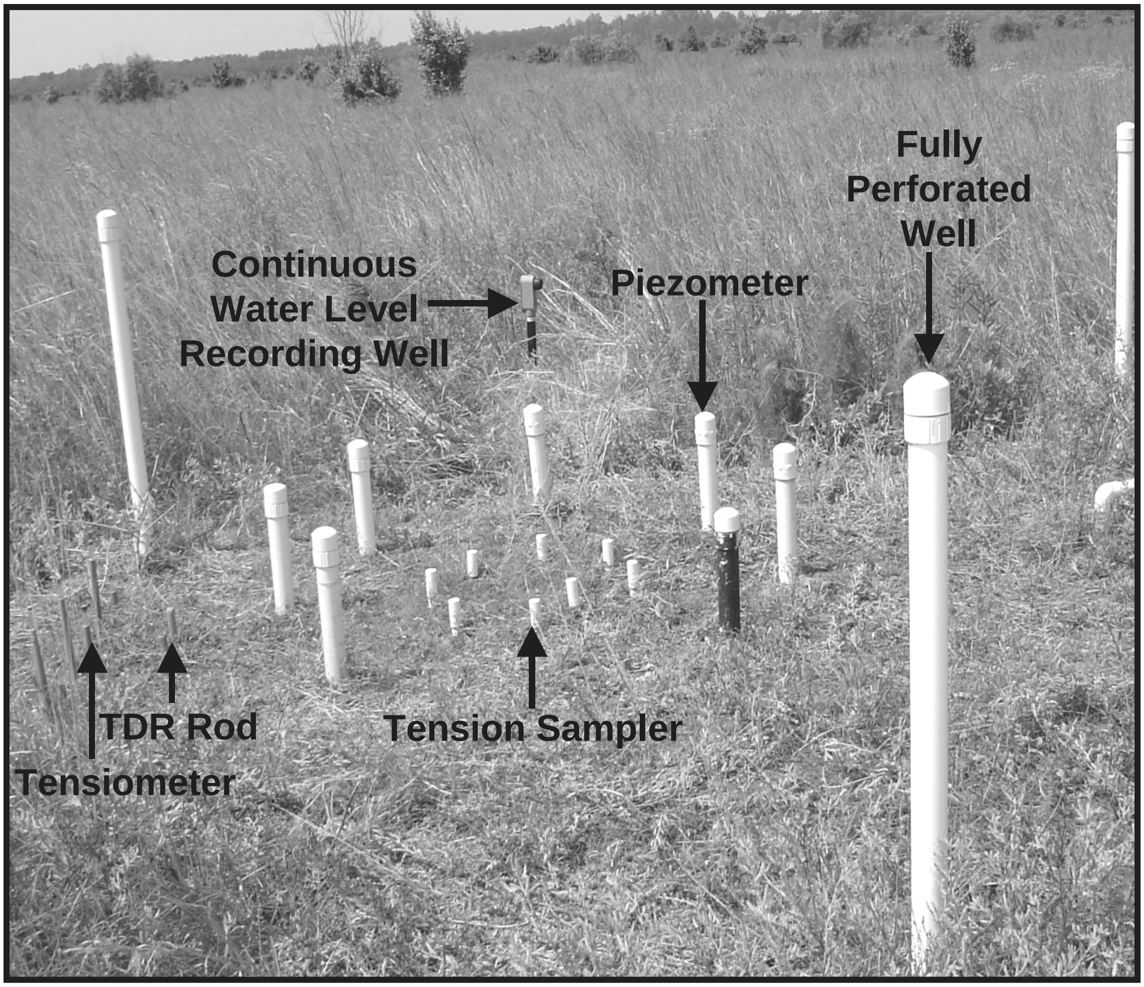

Figure 7.2. Photograph of the monitoring set-up.

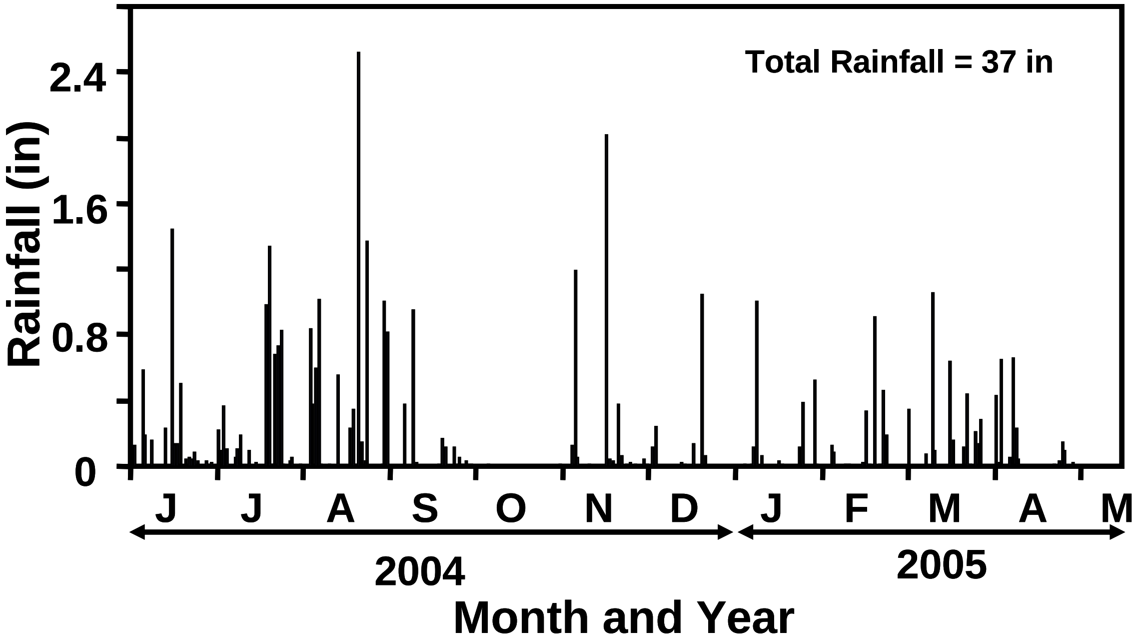

Figure 7.3. Rainfall data at Juniper Bay for the duration of the experiment.

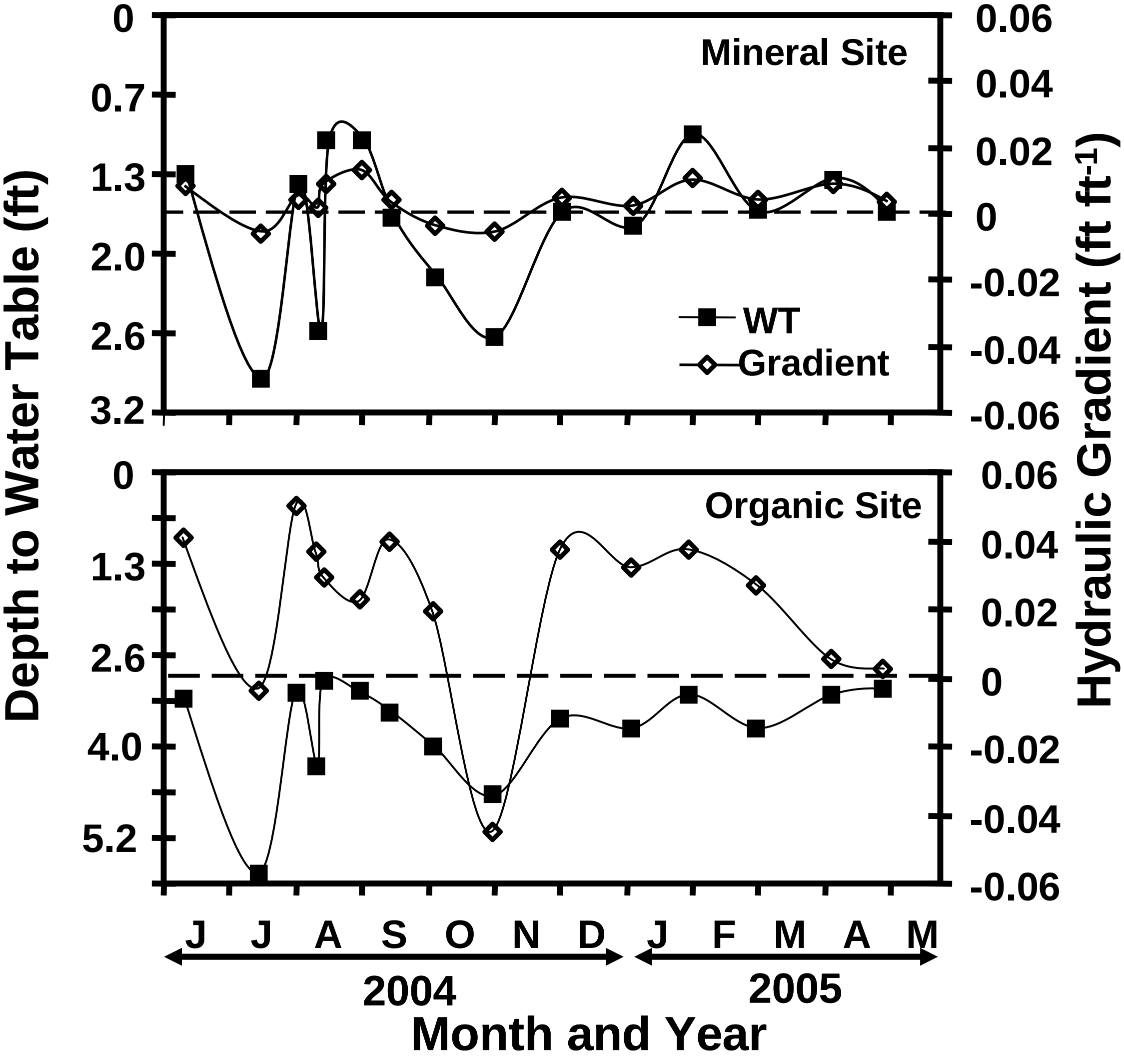

Figure 7.4. Depth to the water table and the subsurface hydraulic gradient computed for the axis that is perpendicular to the ditch. By convention, a positive hydraulic gradient value means that gradient is towards the ditch and a negative value indicates that it is going away from the ditch.

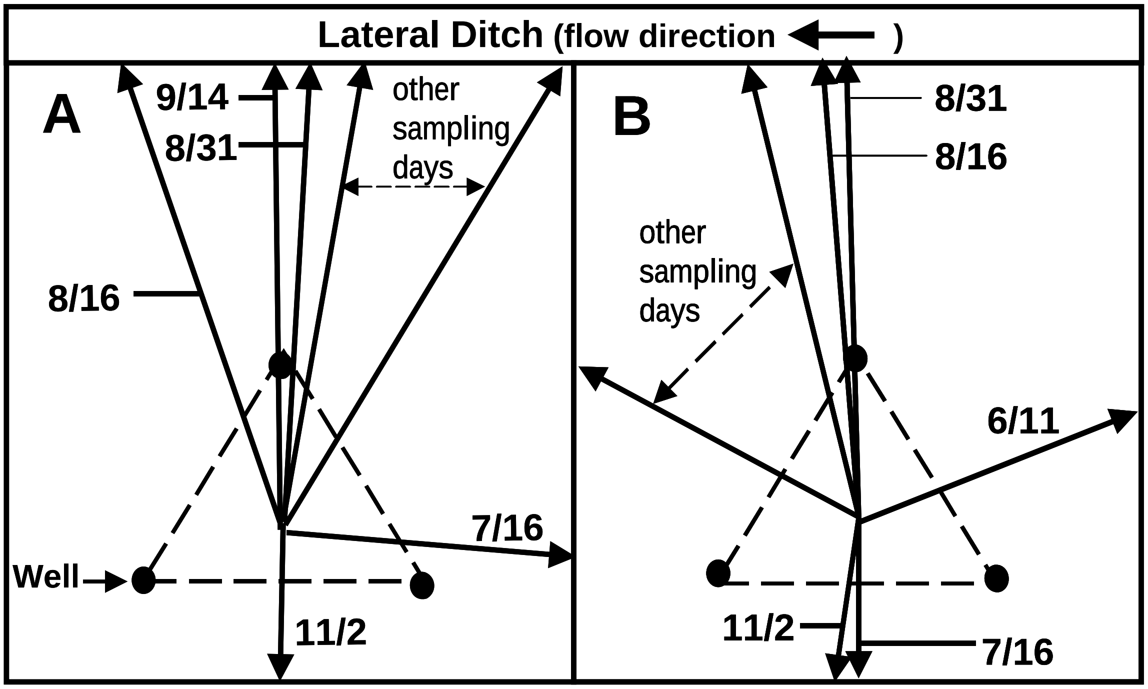

Figure 7.5. Relative direction of the subsurface lateral hydraulic gradient at the organic (A) and mineral (B) soil sites determined using the three-point technique.

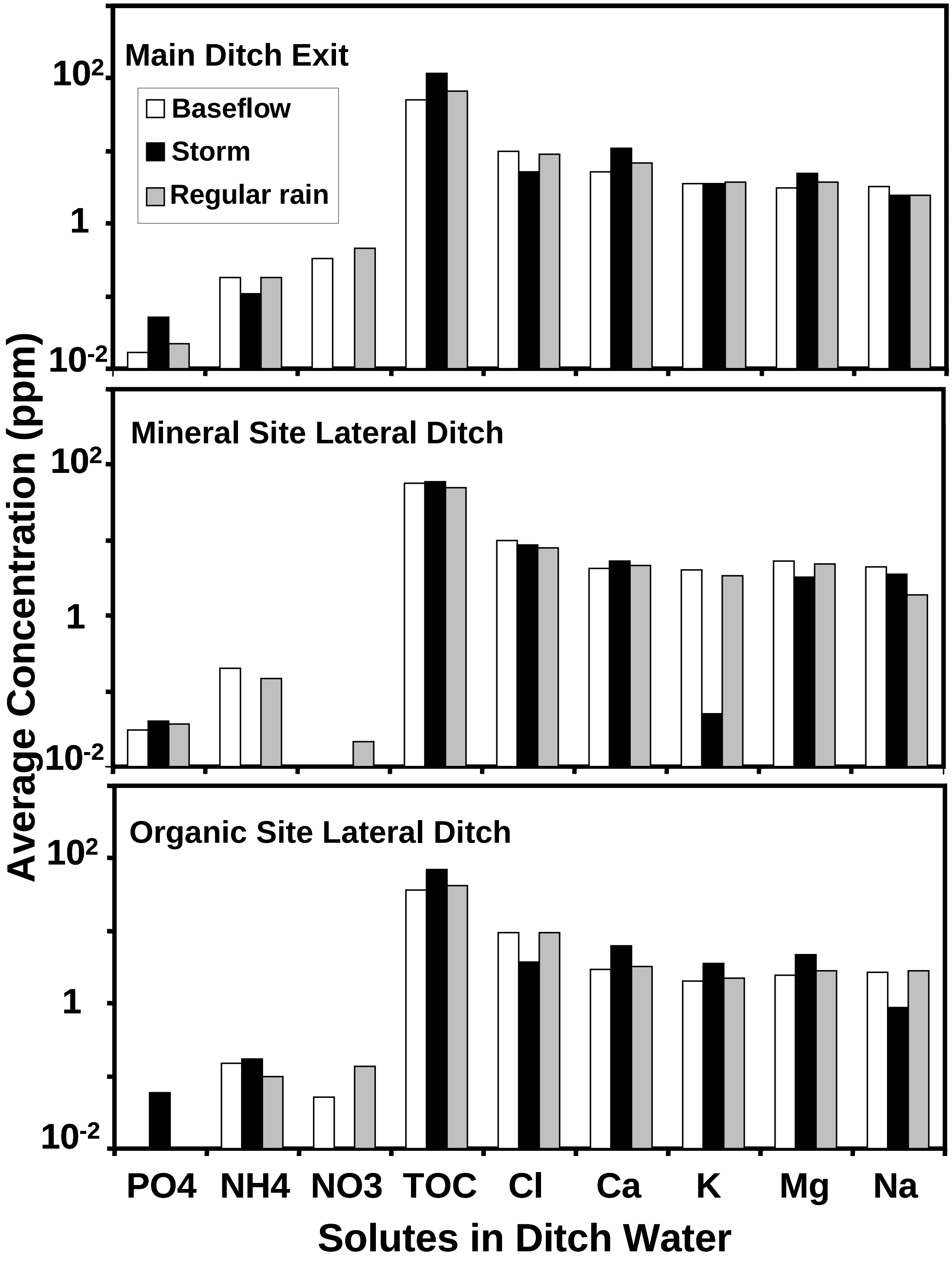

Figure 7.6. Average concentrations of different solutes monitored at the main ditch exit, side ditch at the mineral site, and side ditch at the organic site for base flow condition, days following a regular rain event, and days following a major storm event.

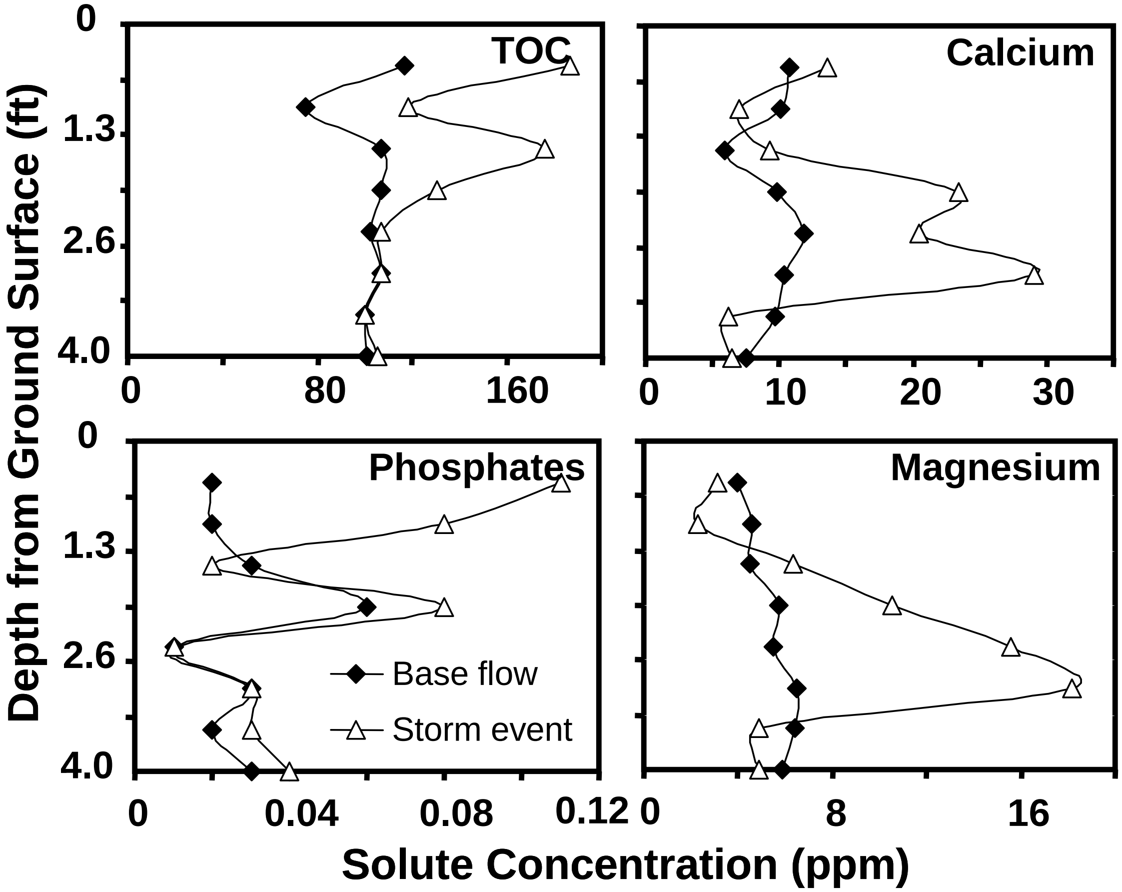

Figure 7.7. Soil solution nutrient profile for sampling dates that represented base flow conditions and the day following the storm event at the mineral soil site.

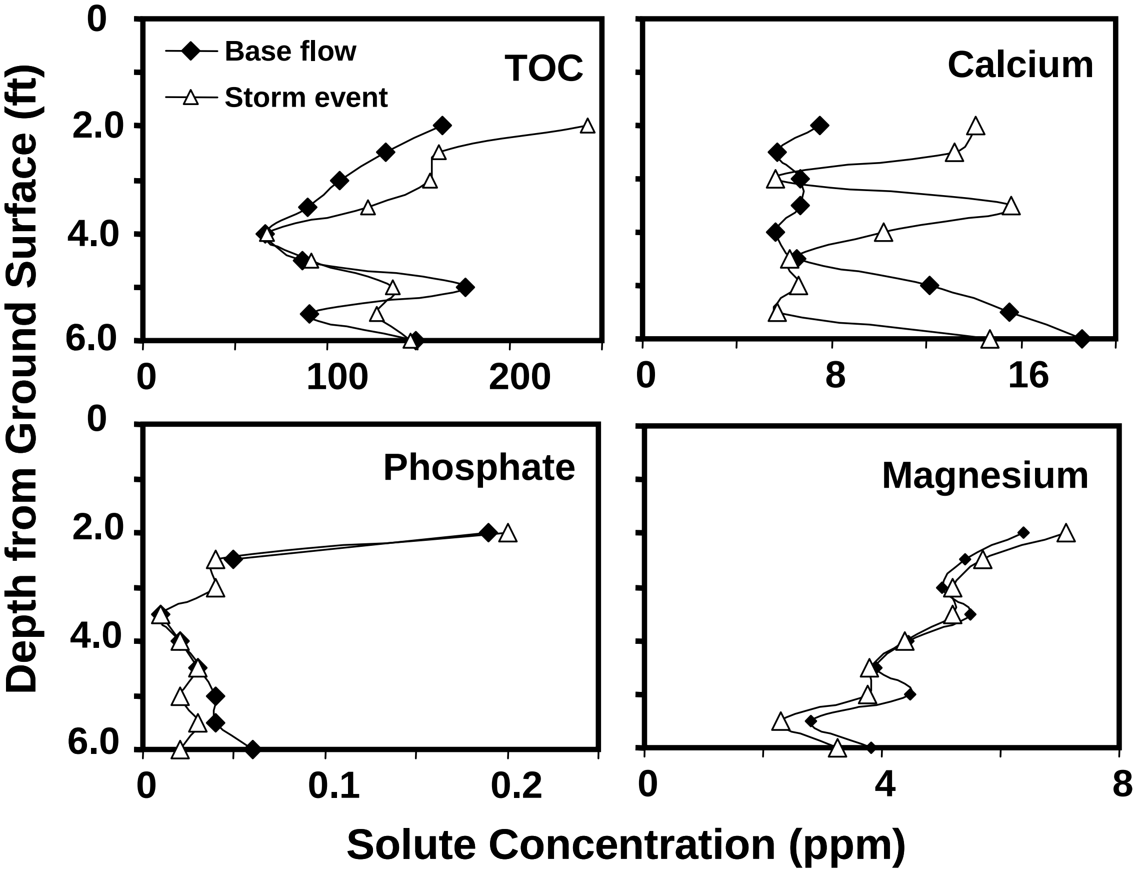

Figure 7.8. Soil solution nutrient profile for sampling dates that represented base flow conditions and the day following the storm event at the organic soil site.

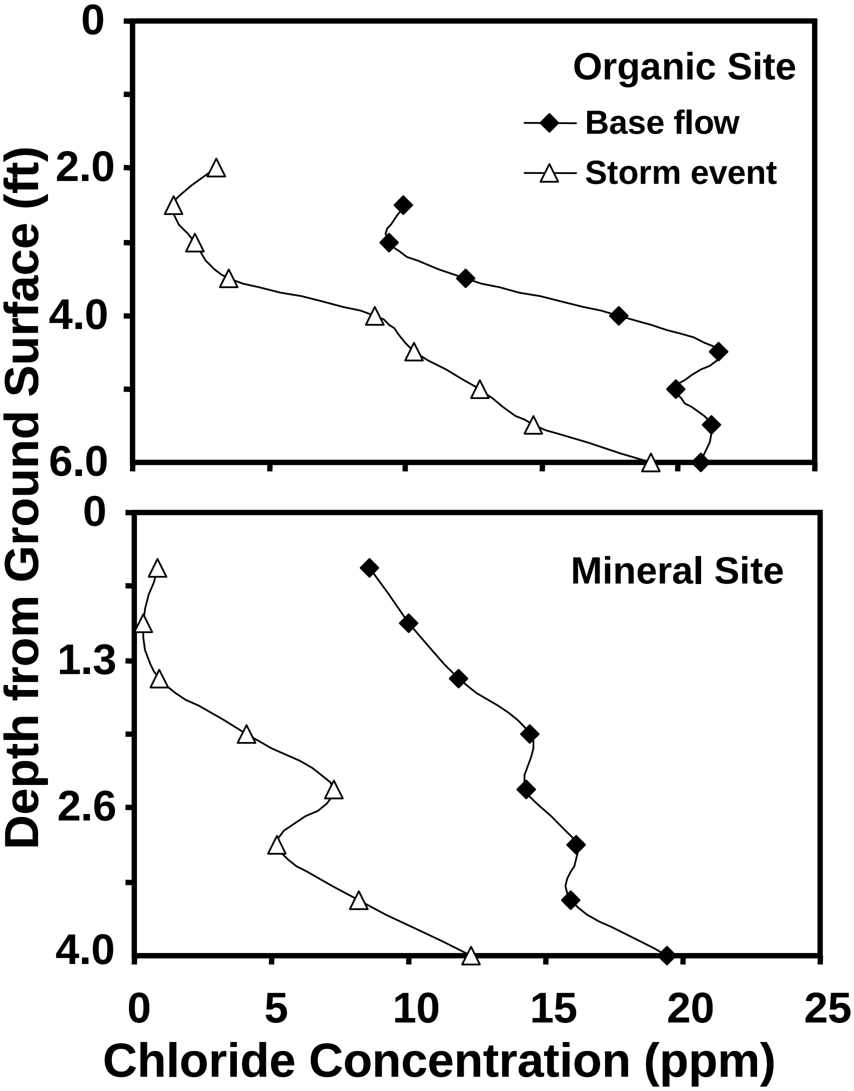

Figure 7.9. Soil solution chloride profile for sampling dates that represented base flow conditions and the day following the storm event at the organic and mineral soil sites.

Chapter 8

FATES OF NITRATE IN THE CAPILLARY FRINGE AND SHALLOW GROUNDWATER IN A DRAINED SANDY SOIL

S. Abit, A. Amoozegar, and M.J. Vepraskas

INTRODUCTION

According to the U.S. Environmental Protection Agency (USEPA, 2002), 104 million people, or 37% of the U.S. population, rely on groundwater as a source of drinking water. Concentrations of NO_3^--N above 10 mg L^{-1} in drinking water (including groundwater) has been linked to infantile methaemoglobinemia or blue-baby syndrome (USEPA, 2005a). Although blue-baby syndrome is relatively rare in industrialized nations, it is a risk in developing countries, especially where drinking water comes from shallow wells in heavily fertilized farming areas (WHO, 2005). In addition, NO_3^- from drinking water could be converted by stomach enzymes in the gastrointestinal tract into carcinogenic compounds (Cogger, 1988; Gerba, 1996). Nitrate concentrations above 100 mg L^{-1} are also considered unfit for livestock (Freitas and Burr, 1996). Excessively high NO_3^- concentrations in groundwater discharged to surface water bodies can also cause eutrophication (Correll, 1998) that leads to a decrease in dissolved O_2, ultimately impacting aquatic animal life negatively.

Plants can take up nitrogen as ammonium (NH_4^+) and NO_3^-. To assure that sufficient nitrogen is available to crops, NO_3^- is often applied to soils in the form of nitrogen-containing fertilizers. Hallberg (1989) reported that the application of these fertilizers to irrigated crops has been the most extensive human cause of NO_3^- pollution in groundwater systems. In the U.S. alone, the amount of inorganic NO_3^- that had been released to land and water bodies from 1991 through 1993 was more than 50 million kg, of which approximately 22.8 million kg were from nitrogenous fertilizer inputs (USEPA, 2005b). In addition to nitrogen fertilizers [worldwide is estimated to be 100 tons yr^{-1} (Food and Agriculture Organization Database, 1996)], significant NO_3^- contributions to soil are derived from animal manure (Griffin and Honeycutt, 2000; Eghball, 2000) and surface-applied wastewater (Reddy and Dunn, 1984). Other sources of NO_3^- in the soil are atmospheric deposition (Rubio et al., 2002; Cerón et al., 2002) as well as in situ decomposition of organic matter in well-aerated soils.

Because NO_3^- is soluble and negatively charged, it is not strongly adsorbed to soil colloids and moves with moving water at about the same rate (Artiola et al., 1996; Fuller and Warrick, 1984; Jenkinson and Smith, 1998). As a result, excess NO_3^- in areas with abundant rainfall is subject to leaching loss (Gilliam, 1988). The primary mechanisms that can reduce NO_3^- concentrations in soil are uptake by plants and microbial denitrification (Korom, 1992; van der Ploeg et al., 1997). Essential conditions favoring denitrification include: (1) presence of denitrifying bacteria, (2) presence of organic materials as electron donors, (3) anaerobic conditions or restricted oxygen availability, and (4) presence of NO_3^- as a terminal electron acceptor (Firestone, 1982; Vepraskas and Richardson, 2000).

Wells or piezometers installed below the water table (WT) are generally used in monitoring subsurface movement of NO_3^- in agricultural watersheds (Tomer and Burkart, 2003; Thurnburn et al., 2003), high density animal farming operations (Rodvang et al., 2004), septic systems (Kampbell et al., 2003), and even in evaluating the efficacy of certain riparian buffer systems for improving subsurface water quality (Bedard-Haughn et al., 2004; Young and Briggs, 2005). The main rationale for using wells and piezometers for monitoring is that it is assumed that NO_3^- is only transported horizontally in the saturated zone below the WT. Results from a limited number of laboratory studies, however, have demonstrated that horizontal water flow and solute transport can take place in the capillary fringe (CF), which is the tension-saturated zone above the WT where the water content is close to saturation (Freeze and Cherry, 1979; Soil Science Society of America, 2006). Up to 100% of solutes entering the CF from the unsaturated zone can move horizontally as shown in flow-cell experiments (Silliman et al., 2002; Amoozegar et al., 2006). The fact that the CF can be more than a meter thick above the WT (Ronen et al., 2000) increases the likelihood that wells and piezometers may not detect a horizontally moving plume.

While nitrate can be denitrified in an anoxic environment below a WT, the CF, due to its “partially saturated” nature and presence of air, may not allow denitrification. Therefore, it is likely that NO_3^- that enters into the CF would retain its chemical integrity, and like other highly soluble and non-reactive (with soil) pollutants, could be transported horizontally into water wells or nearby streams or drainage systems. If the retention and horizontal transport of NO_3^- in the CF hold true under field conditions, it could pose serious doubt about the efficacy of collecting and analyzing only groundwater samples for monitoring horizontal subsurface NO_3^- movement. The objective of this study was to evaluate the fate of NO_3^- in the CF and shallow groundwater in a sandy field site drained by ditches.

MATERIALS AND METHODS

A field solute transport experiment was conducted in a flat area at the northeastern end of Juniper Bay in Robeson County, NC (34°30’30”N 79°01’30”E). At the time of the study, this bay (previously a forested wetland) had been drained by a series of lateral ditches connected to a main ditch that traversed the bay in the NE to SW direction. The soils in the general area of the study were mapped as Leon series (sandy, siliceous, thermic, Aeric Alaquod) (Vepraskas et al., 2003). This experiment was conducted at a location 23 ft (7 m) from a lateral ditch and 66 ft (20 m) from the bay’s main drainage ditch. A pit was dug to 3.4 ft (105 cm) depth to describe the soil profile and collect soil samples. The pit was dug 33 ft (10 m) from the experiment area, and 23 ft from the lateral ditch. Bulk soil samples were collected from the pit wall at 0.5 ft (15 cm) depth intervals to a depth of 3.4 ft. Intact core samples [3 in (7.6 cm) diameter and 3 in long] in vertical orientation were also collected in triplicate from the same depth intervals.

Saturated hydraulic conductivity (K_{sat}) was measured below the water table by a slug test (Amoozegar, 2004; Bouwer and Rice, 1976) with computations done with the Bouwer and Rice Parameter Estimation method using the Super Slug Version 3.1.8 (Starpoint Software Inc., Cincinnati, Ohio). Saturated hydraulic conductivity of the unsaturated zone was measured in situ by the constant-head well permeameter technique (Amoozegar and Wilson, 1999). Soil water retention of the intact cores between 0 and 1.5 MPa pressure was measured by the pressure cell procedure (Dane and Hopmans, 2002). Bulk density of soil at different depth intervals was determined by the core method (Grossman and Reinsch, 2002), and particle density was determined by the air pycnometer (gas displacement) technique (Flint and Flint, 2002). Particle size distribution was determined by the hydrometer method (Gee and Or, 2002). For this analysis, soil bulk samples were pre-treated with 30-percent hydrogen peroxide (H_2O_2) to oxidize the organic matter prior to the dispersion and sedimentation. Total organic carbon was determined by dry combustion with a Perkin-Elmer PE2400 CHN Elemental Analyzer (Culmo, 1988).

Installation of Tension Samplers and Wells

In a preliminary study (Abit, 2005), Br^- was applied to an auger hole above the WT and eight nests of tension samplers (also referred to as tension lysimeters or lysimeters) were installed on equally spaced spots on the perimeter of a 2-ft (60-cm) radius circle around the application spot to catch the moving plume (1st set in Fig. 8.1). Each nest of tension lysimeters included five lysimeters with their porous cups at 0.5-ft depth intervals from 18 to 42 in (45 to 105 cm) (Fig. 1- inset). Based on the direction of the groundwater movement, as determined by the water table gradient and movement of the Br^- plume, three additional sets of tension samplers (each containing five nests of lysimeters) were installed at radial distances of 4 ft (120 cm), 7.3 ft (220 cm) and 10.7 ft (320 cm) from the Br^- solution application spot along the general direction of the groundwater flow (2nd, 3rd and 4th sets in Fig. 8.1). A total of 23 nests were installed in an arrangement shown in Figure 1. Finally, five lysimeters (referred to as nest 0), with their porous cups at similar depths as the other nests of lysimeters, were installed on the arc of a 0.7-ft (20-cm) radius semi-circle near the application spot.

Each tension lysimeter was made from a porous ceramic cup (air-entry pressure = 0.101 MPa) attached to a section of ¾-inch schedule 80 polyvinyl chloride (PVC) pipe. The length of the PVC pipe connected to each porous cup was based on the desired depth to which the porous cup was installed. The other end of the pipe was plugged by a rubber stopper with tight access holes for two plastic tubes: one extending to the bottom of the inside chamber of the lysimeter while the other served as a vent. Similar to the system described by Corwin (2002), each tension lysimeter was attached to a dedicated trap for collecting soil solution samples.

The tension lysimeters were used to collect samples of soil solution in the vadose zone (above the WT) and shallow groundwater (below the WT). To collect soil solution or a groundwater sample, a vacuum trap was attached to each tension lysimeter. The lysimeter was initially emptied by applying vacuum to the trap using a hand pump. After emptying the trap and placing the sample bottle in it, the air in the trap was removed to create approximately 0. 8 bar of tension (equivalent to -800 cm water of pressure head) inside the sampling cup. After maintaining vacuum inside the trap for 10 to 30 minutes, the air vent cover on the tension lysimeter was removed, thereby drawing the remaining solution in the lysimeter cup into the sample bottle in the trap. Up to 30 mL sample of soil solution or groundwater was collected each time by this procedure.

Three fully perforated wells (hereafter referred to as wells) were installed at the vertices of a triangle near the nests of lysimeters for determination of the depth to the WT. The distance between wells was 9.8 ft (3 m). The location of the CF was determined based on the depth to WT. The same set of wells was used to estimate the general direction and magnitude of the groundwater horizontal hydraulic gradient via the triangulation or three-point technique (Sanders, 1998). Water table depths in the three wells were measured using a dipper (Herron Instruments Dipper T, Ontario, Canada) every time water samples were collected.

A five-segmented Moisture Point time domain reflectometer (TDR) probe (Gable Corp, Victoria, Canada) was installed outside the first set of lysimeters (circle of nests-Fig. 1). The probe measured volumetric water content (VWC) at 0 to 0.5, 0.5 to 1.0, 1.0 to 1.5, 1.5 to 2.0 and 2.0 to 3.0 ft depth intervals. Water content was taken every time soil water samples were collected from the lysimeters.

Monitoring of Solute Transport

The spot in the center of the circle of lysimeters was selected for the application of a solution containing potassium bromide (KBr) and magnesium nitrate $Mg(NO_3)_2$. Prior to the application of the tracer solution, background soil solution and groundwater samples were collected from all the tension samplers and analyzed for $Br^-$and NO_3^-content using a Lachat Quickechem 8000 slow injection auto analyzer (Greenberg et. al., 1992).

Fourteen days after the collection of background soil solution and groundwater samples, an auger hole was dug to the 1.0 ft (30 cm) depth at the center of the 1st layer of nests (i.e., circle of nests) and 10 L of a solution containing 9,120 ppm (9.12 g L^{-1}) KBr and 2,660 ppm (2.66 g L^{-1}) $Mg(NO_3)_2$ were applied to the bottom of the hole (see Fig. 1 for location of application spot). A modified Compact Constant Head Permeameter (Amoozegar, 1989) was used to control the rate of application of the solution into the hole. At the time of tracer application, the water table was 2.0 ft (60 cm) from the surface and the upper boundary of the CF was projected to be at the 1.3 ft (40 cm) depth (CF thickness discussed under Soil and site characteristics). In effect, the solution containing the Br^- and NO_3^- tracers was applied into an unsaturated region of the soil about 0.3 ft (10 cm) above the CF. The auger hole was back filled after the solution infiltrated the soil. An hour after the solution had completely infiltrated, soil solution samples were collected from the lysimeters at nest 0 [0.7 ft (20 cm) from application spot] to determine the initial depth reached by Br^- and NO_3^-. Soil water samples were then collected from nest 0 and all nests in the 1st and 2nd set of lysimeters 3 and 6 days after solution application. In addition to these, samples were collected from the 3rd set of lysimeters (at 7.3 ft or 220 cm from the application spot) on days 10 and 17. Judging by the rate of advance of the plume, the nests at the 4th set (10.7 ft or 320 cm from the application spot) were included among the nests sampled on days 20 and 28. On day 28, both solutes were already below the detection limit at nest 0 and were only detected at nests 1 and 2 in the 1st set. Based on our analysis of samples, samples were collected only from nest 1 and 2 (in 1st set) and all nests in the 2nd, 3rd and 4th sets on days 30 and 38. Concentration of each of the two solutes at the 1st set was already below the detection limit on day 38, therefore, for days 42, 49, 59 and 84, samples were collected only from nests in the 2nd, 3rd and 4th sets.

Detected concentrations of $Br^-$and NO_3^- (in mg L^{-1}) were converted to normalized concentrations by dividing the detected solute concentration in each soil water sample by the concentration of the corresponding solute in the applied solution. This allowed the comparison of the relative degree of persistence of the applied Br^- and NO_3^-as they moved through the CF and shallow groundwater.

RESULTS AND DISCUSSION

Soil and Site Characteristics

The slope of the land surface in the bay was generally less than 2% and the soil at the location where the solute transport study was conducted had textural classes of either loamy sand or sandy loam with sand content ranging from 78 to 87% from the surface to a depth of 3.5 ft (105 cm) (Table 8.1). Saturated hydraulic conductivity in the upper 105 cm ranged from 1.35 to 6.46 ft d^{-1} without any indication of a restricting layer. Bulk density increased from 73.04 lb ft^{-3} (1.17 g cm^{-3}) at the surface layer to 100.51 lb ft^{-3} (1.61 g cm^{-3}) at 3.5 ft. Porosity was observed to decrease from 0.53 ft^3 ft^{-3} at the surface layer to only 0.37 ft^3 ft^{-3} at the 3.5 ft depth.

Results from the analysis of background soil solution and shallow groundwater samples revealed that detectable NO_3^- concentrations were observed only at the 1.5 and 2.0 ft depths in most nests. The highest background NO_3^- concentration detected was 1.6 ppm at the 1.5 ft depth at nest 3. No background sample yielded Br^- above the detection limit.

Soil water characteristic curves of samples collected from the 1.5 to 2.0 ft (45 to 60 cm) depth interval, which was immediately above the water table for most of the study period, indicated that the soil at that depth remained nearly-saturated after application of 7.8 in (20 cm water) of tension (Fig. 8.2-A). This indicated that the CF above the water table was at least 7.8 in (20 cm) thick. Because of the relatively uniform soil texture at depths where the WT fluctuated, it was expected that the thickness of the CF would remain close to 7.8 in for the duration of the study. The time domain reflectometry (TDR) measurements taken after each sampling showed that the minimum thickness of the near-saturated zone above the water table was approximately 7.8 in (Fig. 8.2-B). These results agree with the data from a laboratory study by Amoozegar et al. (2006), which demonstrated that in a coarse-textured soil the CF could be as thick as 7.8 in above the

WT. Based on these, it was conservatively assumed that soil solution samples collected within 7.8 in above the water table were from the CF.

Subsurface Transport of NO_3^- Relative to the Water Table

The applied solution contained both NO_3^- and Br^-. This paper focuses on NO_3^- transport, but comparisons will be made with the Br^- movement in the CF and SGW. More detailed Br^- transport data are reported by Abit (2005).

On the day that the tracer solution was applied (t = 0), NO_3^- was detected only at the 1.5-ft depth (within the CF) at nest 0 located 0.7 (20 cm) from the application spot (Fig. 3-A). Three days after tracer solution application, the WT was below 2 ft depth and NO_3^- was found only in the 1.5 and 2.0 ft depths in this nest (see WT data in Fig. 8.3-B). There was no rain during the first three days after tracer solution application, but a 0.35 in (0.9 cm) rain occurred on day 4 (Fig. 3B). The samples collected on day 6 reveal that NO_3^- was present below the WT at the 2.5 ft (75 cm) depth. This suggests that the rain event resulted in a partial vertical leaching of the NO_3^-. In addition, between days 3 and 6, there was a marked decrease in NO_3^- concentration at the 1.5 ft depth that was coupled by an increase in NO_3^- concentration at 2 ft from the surface. Nitrate concentrations at all three depths at nest 0 were decreasing on day 10 suggesting that the bulk of the plume had moved towards nests 1 and 2 (see Fig. 8.1 for nest locations).

Nitrate was detected at nest 1 (2 ft from the application spot) on day 6 (Fig. 8.4-A) where the NO_3^- was only present at the 1.5 and 2.5 ft depths (in the CF). When the peak of the moving plume arrived at nest 1 on day 10 (highest nitrate concentration of 338 ppm), there was evidence of partial leaching below the WT as shown by the detection of NO_3^- at 2.5 ft depth. After a major rain event (1.1 in) on day 12, the WT rose to as shallow as 1.5 ft on day 17 (see Fig. 3– B). However, we detected no upward movement of the solute plume. By day 17, NO_3^- concentration had decreased at the 1.5 and 2.0 ft depths in nest 1. These reductions were accompanied by the detection of NO_3^- at 3 ft (90 cm) (13.3 ppm was observed). No NO_3^- was ever detected at the 3.5 ft depth. The decrease in NO_3^- concentration at the 1.5 ft depth in nest 1, coupled with the marked increase at 2.0 ft on day 17 at nest 2 (Fig. 8.4-B), also showed that limited leaching occurred when the WT dropped following the major rain event on day 12.

Nitrate was detected both in the CF and SGW at a distance of 4 ft from the application spot (nests 3, 4 and 5) on day 17 (Fig. 8.5). Among the samples collected from these nests, the highest NO_3^- concentration (139 ppm) was detected on day 17 at the 2 ft depth of nest 4 (Fig. 8.5-B). Unlike nests 0, 1 and 2, where NO_3^- concentrations were higher at the 1.5 ft depth when initially detected, for nests 3 and 4, higher solute concentrations were initially detected at the 2 ft depth. However, an appreciable amount of NO_3^- (15.6 ppm) was still present at the 1.5 ft depth in nest 4. In addition, NO_3^- was detected at the 2.5 ft depth. It appears that the plume had moved downward within the CF, and partially below the WT as a result of the major rain event that occurred on day 12.

Among the nests installed 7.3 ft from the application spot, the highest NO_3^- concentration was detected at nest 7 (Fig. 8.6-A). At this nest, NO_3^- was first detected on day 17 at the 1.5 ft depth (in the CF), which showed that NO_3^- had traveled at least 7.3 ft horizontally in the CF in 17 days. However, no NO_3^- was detected at the 3.0 ft depth until day 28 (11 days after initial detection and following approximately 1.6 in of rain) when 1.72 ppm of NO_3^- was found.

Among those nests installed 10.7 ft from the application spot, nest 12 had the highest NO_3^- concentrations indicating that this nest was in the center of the moving plume. As high as 24 ppm nitrate in the soil solution was detected at the 45 cm depth at nest 12 (Fig. 8.6-B). This indicated that some NO_3^- had traveled in the CF through a horizontal distance of at least 10.7 ft in less than 30 days. This observation is supported by the detection of considerable amounts of nitrate at the 1.5 ft depths at nests 10, 11 and 13 (data not shown) (see Fig. 8.1 for nest locations).

Persistence of Nitrate in the CF and SGW

Unlike NO_3^-, Br^- is a conservative non-reactive ion that is neither preferentially taken-up by plants nor utilized by microorganisms in the soil. Bromide also does not participate in redox reactions, is not sorbed onto soil particles surfaces, and does not form insoluble precipitates (Fetter, 1999). Because of these properties, we used it as a reference tracer and applied it jointly with NO_3^- to the unsaturated soil above the CF to evaluate the degree of persistence of the biologically essential and reducible NO_3^- as both moved horizontally in the subsurface.

Initially, Br^- was detected on the same day at nest locations where NO_3^- was detected, suggesting that they were transported horizontally at the same rate (data not shown; refer to Abit, 2005). It should be noted, however, that when transported vertically below the WT, the two solutes differed in their degree of persistence. Using normalized NO_3^- and Br^- concentrations (concentration in soil solution/concentration in applied solution), there was an observed consistent reduction in the concentration of NO_3^- as compared to the Br^- concentrations in samples collected from below the WT. We believe this indicates loss of NO_3^- potentially due to denitrification.

The ensuing discussion on the persistence of NO_3^- as it moved away from the application spot focuses on the transect defined by nests 0, 4, 7 and 12. These nests were in the middle of the moving plume (Fig. 8.1) and should provide the best information on the flow process. It should also be noted that the experimental area was devoid of surface vegetation indicating the absence of NO_3^- removal by plant roots.

Three days after application of the tracer solution, Br^- and NO_3^- were both detected at the 1.5 and 2.0 ft depths in nest 0 (Fig. 8.7 –A). Through the first three days of the experiment, both sampling depths remained above the WT and the normalized concentrations of both solutes at both depths were comparable (see Fig. 8.3-B for WT depths). On day 17, the advancing tracers were detected at nest 4 (120 cm from the application spot), and the plume was at the 1.5, 2.0 and 2.5 ft depths (Fig. 8.7-B). The

2.5 ft depth had always been below the WT, and at such depth, the normalized concentration of NO_3^- was noticeably lower than that of Br^- giving an indication of NO_3^- transformation or removal below the WT. On day 28, the plume had already reached nest 7 (7.3 ft from the application spot) and both solutes were detected at the 3.0 ft depth (Fig. 8.7-C). It was noted that at a deeper depth of 3.0 ft, the difference in the normalized concentrations of NO_3^- and Br^- had widened (compared to their difference at the 2.5 ft depth), suggesting that NO_3^- transformation, most likely due to denitrification, as it is favored in deeper depths. This was made even more obvious on day 58 at nest 12 (10.7 ft from the application spot) (Fig. 8.7-D). Through the first 58 days, the 3.0 and 3.5 ft depths had always been below the WT, and at each of those depths, appreciable amounts of Br^- was detected while no NO_3^- was observed to be above the detection limit. These findings confirm our observation of NO_3^-loss in nests closer to the initial source.

In contrast, for all sampling locations within the transect and at all sampling times, the normalized concentration of $NO_3^-$and Br^- had remained comparable at the 45 cm depth (Fig. 8.7). Since the 1.5 ft depth was within the CF for most of the study period, and the results confirm that there is very little if any NO_3^- transformation within the CF. The limited transformation of NO_3^- in the CF allows it to persist longer at such location than it would below the WT. Moreover, the presence of appreciable amount of NO_3^- at the 1.5 ft depth, and its absence at 3.0 and 3.5 ft some 10.7 ft (horizontal distance) from the application spot 58 days after tracer solution application, show that nitrate persists longer in the CF and allows it to be transported to greater distances in the CF than it would below the WT.

The requirements for denitrification namely; presence of organic matter, active microorganisms and anoxic environment (Vepraskas and Richardson, 2000); may have been met below the WT allowing NO_3^- to be converted and removed from the soil as N_2. We believe the CF, because of its “partially saturated” property, has some unsaturated pores that allow the regular re-supply of oxygen. This may have inhibited the development of anoxic conditions, and thus preventing denitrification of nitrates.

SUMMARY AND CONCLUSIONS

This study evaluated the fate of nitrate (NO_3^-) in the capillary fringe (CF) and shallow groundwater in a sandy field site drained by ditches. Results showed that NO_3^- was transported horizontally in the CF under field conditions. The results also showed that the NO_3^- plume that entered into the CF from the unsaturated zone stayed and moved horizontally in it until it was partially carried below the WT by rain events. Also, nitrate was found to persist longer in the CF, allowing a greater fraction of it to be transported to greater horizontal distances in the CF than in the shallow groundwater. We believe that conditions favoring denitrification were not totally met in the CF largely due to its “nearly saturated” nature that allows room for re-supply of oxygen and inhibiting development of anoxic conditions.

Although this study monitored the horizontal transport of NO_3^- through a distance of only 10.7 ft from the application spot in a sandy soil with shallow groundwater, we believe the results provide sufficient evidence to suggest that monitoring of subsurface horizontal flow of NO_3^- should include efforts to collect samples in the CF. It appears that solely relying on groundwater samples may result in underestimation of the amount of NO_3^- that can travel horizontally through the subsurface from a source. Failure to account for NO_3^- or other pollutants in the CF may have serious implications. We recommend further studies to examine the lateral transport of solutes in the CF as well as on the development (or non-development) of a reduced state in the CF under various conditions in different soils.

REFERENCES

Abit, S.M. 2005. Evaluation of subsurface solute transport and its contribution to nutrient load in the drainage ditches prior to restoration of a Carolina Bay. Electronic M.Sc. thesis copy at http://www.lib.ncsu.edu/theses/available/etd-11152005-183644/unrestricted/etd.pdf.

Amoozegar, A. 1989. A compact constant-head permeameter for measuring saturated hydraulic conductivity of the vadose zone. Soil Sci. Soc. Am. J. 53:1356-1361.

Amoozegar, A. and G. V. Wilson. 1999. Methods for Measuring Hydraulic Conductivity and Drainable Porosity. *In:* R.W. Skaggs and J. van Schilfgaarde (eds). Agricultural Drainage. Agronomy Monograph no. 38. SSSA, Madison, Wisconsin.

Amoozegar, A. 2004. Soil permeability and dispersion analysis. p. 625-677. *In* R. D. Down and J. H. Lehr (ed.). Environmental instrumentation and analysis handbook. John Wiley and Sons, Inc. Hoboken, New Jersey.

Amoozegar, A., C. P. Niewoehner, and D. L. Lindbo. 2006. Lateral movement of water in the capillary fringe under drainfields. *In* the Proc. of the 2006 Technical Education Conference. National Onsite Wastewater Recycling Association (NOWRA).

Artiola, J.F, M. L Brusseau, A.D. Matthias, and S.A. Musil. 1996. Environmental monitoring in pollution science. P. 115-134. *In* I.L. Pepper, CP. Gerba and M. L. Brusseau (ed). Pollution Science. Academic Press, San Diego, Ca.

Bedard-Haughn, A. K. W. Tate and C. van Kessel. 2004. Using nitrogen-15 to quantify vegetative buffer effectiveness for sequestering nitrogen in runoff. J. Environ. Qual. 33: 2252-2262.

Bouwer, H. and R. C. Rice. 1976. A slug test for determining hydraulic conductivity of unconfined aquifers with completely or partially penetrating wells. Water Resour. Res., 12: 423-428.

Cerón, R. M. B., H. G. Padilla, R. D. Belmont, M. C. B. Torres, R. M. García and A. P. Báez. 2002. Rainwater chemical composition at the end of the mid-summer drought in the Caribbean shore of the Yucatan Peninsula. Atmos. Environ. 36(14): 2367-2374 .

Cogger, C.G. 1988. On-site septic systems: the risk of groundwater contamination. J. Environ. Health 51:12-16.

Correll, D. 1998. The role of phosphorus in the eutrophication of receiving waters: A review. J. Environ. Qual. 27:261–266.

Corwin, D. L. 2002. Measurement of solute concentration using soil water extraction. p. 1261-1275. *In:* J.H. Dane and G.C. Topp (eds). Methods of Soil Analysis Part 4: Physical Methods. No. 5 in SSSA Book Series. SSSA, Madison, Wisconsin.

Culmo, F.C. 1988. Principle of Operation – The Perkin-Elmer PE 2400 CHN Elemental Analyzer. Perkin Elmer Corp, Norwalk, CT.

Dane, J.H. and J.W. Hopmans. 2002. Water retention and storage. *In:* J.H. Dane and G.C. Topp (eds). Methods of Soil Analysis Part 4: Physical Methods. No. 5 in SSSA Book Series. SSSA, Madison, Wisconsin.

Eghball, B. 2000. Nitrogen Mineralization from Field-Applied Beef Cattle Feedlot Manure or Compost .Soil Sci. Soc. Am. J. 64: 2024-2030.

Fetter, C.W. 1999. Contaminant Hydrology. 2nd Edition. Prentice-Hall. Upper Sadle River, NJ.

Firestone, B.K. 1982. Biological denitrification. *In* F.J. Stevenson (ed) Nitrogen in Agriculture Soils. American Society of Agronomy, Madison, WI.

Flint, A.L. and L.E. Flint. 2002. Particle Density. *In:* J.H. Dane and G.C. Topp (eds). Methods of Soil Analysis Part 4: Physical Methods. No. 5 in SSSA Book Series. SSSA, Madison, Wisconsin.

Food and Agriculture Organization Database, 1996. Agricultural data. Available at: http://faostat.fao.org/faostat/form?collection=Fertilizers&Domain=Means&servlet=1&hasbulk=&version=ext&language=EN

Freeze, R. A. and J. A. Cherry. 1979. Groundwater. Prentice Hall, Englewood Cliffs, NJ.

Freitas, R. J. and M.D. Burr. 1996. Animal Waste. pp 237-251. *In* I.L. Pepper, CP. Gerba and M. L. Brusseau (ed). Pollution Science. Academic Press, San Diego, CA.

Fuller, W.H. and A.W. Warrick. 1984. Soils in Waste Treatment and Utilization: Vol. 1 Land Treatment._CRC Press Inc., Boca Raton, Florida.

Gee, G.W. and D. Or. 2002. Particle-Size Analysis. *In:* J.H. Dane and G.C. Topp (eds). Methods of Soil Analysis Part 4: Physical Methods. No. 5 in SSSA Book Series. SSSA, Madison, Wisconsin.

Gerba, C. P. 1996. Principles of Toxicology. pp. 323-343. *In* I.L. Pepper, CP. Gerba and M. L. Brusseau (ed). Pollution Science. Academic Press, San Diego, Ca.

Gilliam, J. W. 1988. Nitrate in North Carolina groundwater. Proc. NC Soil Science Society. 31:70-78.

Greenberg , A.E., L.S. Clesceri and A.D. Eaton. 1992. Standard methods for examination of water and waste water. 18th Ed. APHA. Washington D.C.

Griffin, T.S. and C.W. Honeycutt. 2000. Using Growing Degree Days to Predict Nitrogen Availability from Livestock Manures Soil Sci. Soc. of Am. J. 64:1876-1882.

Grossman, R.B. and T.G. Reinsch. 2002. Bulk Density. *In:* J.H. Dane and G.C. Topp (eds). Methods of Soil Analysis Part 4: Physical Methods. No. 5 in SSSA Book Series. SSSA, Madison, Wisconsin.

Halberg, G.B. 1989. Nitrate in groundwater in the United States. *In:* Follet, R. F. (Ed) Nitrogen Management and Groundwater Protection, Developments in Agricultural and Managed-Forest Ecology. 21: 35-74. Elsevier, NY.

Jenkinson, D.S. and K.A. Smith (ed). 1998. Nitrogen Efficiency in Agricultural Soils. Elsevier, London.

Kampbell, D.H, Y. An, K. P. Jewell and J.R. Masoner. 2003. Groundwater quality surrounding Lake Texoma during short-term drought conditions. Environ. Pollut. 125(2): 183-191.

Korom, S.F. 1992. Natural denitrification in the saturated zone: A review. Water Resour. Res. 28:1657-1668.

Reddy, M. R. and S. J. Dunn. 1984. Effect of domestic effluents on groundwater quality: A case study. Sci. Total Environ. 40(1):115-124.

Rodvang, S.J. D.M. Mikalson and M.C. Ryan. 2004. Changes in groundwater quality in an irrigated area of Southern Alberta. J. Environ. Qual. 33: 476-487.

Ronen, D., H. Scher, M. Blunt. 2000. Field observation of the capillary fringe before and after a rainy season. J. Contam. Hydrol. 44:103-118.

Rubio,M. A., E. Lissi and G. Villena. 2002. Nitrite in rain and dew in Santiago City, Chile. Its possible impact on the early morning start of the photochemical smog. Atmos. Environ. 36(2):293-297.

Sanders, L. L. 1998. A manual of field hydrogeology. Prentice Hall, Upper Saddle River, N.J.

Silliman, S.E. , B. Berkowitz, J. Simunek and M. Th. Van Genuchten. 2002. Fluid flow and solute migration within the capillary fringe. Groundwater. 40(1):76-84.

Soil Science Society of America. 2006. Internet Glossary of Soil Science Terms. At: http://www.soils.org/sssagloss/.

Thurnburn, P.J., J. S. Biggs, K. L. Weier and B. A. Keating. 2003 Nitrate in groundwaters of intensive agricultural areas in coastal Northeastern Australia. Agric. Ecosyst. Environ. 94(1):49-58.

Tomer, M.D. and M. R. Burkart. 2003. Long-term effects of nitrogen fertilizer use on groundwater nitrate in two small watersheds. J. Environ. Qual. 32:2158-2171.

USEPA.2002. Public Water Drinking Water Systems: Facts and Figures. http://www.epa.gov/safewater/pws/factoids.html

USEPA. 2005a. List of Drinking Water Contaminants and Maximum Contaminant Levels http://www.epa.gov/safwater/mcl.html#inorganic

USEPA. 2005b.Consumer Factsheet: Nitrates/Nitrites http://www.epa.gov/safwater/dwh/c-ioc/nitrates.html

van der Ploeg, R., H. Ringe, G. Machella and D. Hermsmeyer. 1997. Postwar nitrogen use efficiency in West German agriculture and groundwater quality. J. Environ. Qual. 26: 1203-1212.

Vepraskas, M.J and J.L. Richardson. 2000. Wetland Soils: Genesis, Hydrology, Landscapes and Classification. CRC Press, Boca Raton, Florida.

Vepraskas, M.J. J.G White, R.L Huffman, G.P Fernandez, R.W. Skaggs, C.W. Zanner, J.M. Stucky, J.D. Gregory, S.W. Broome, J.M. Ewing, B. Lees, S. Luginbuhl, G.S. Kreiser and R.P. Szuch. 2003. Methods to assess soil, hydrologic, and site parameters that affect wetland restoration. Project report to NCDOT, NCSU, NC.

WHO. 2005. Water-related diseases: Methaemoglobinemia http://www.who.int/water_sanitation_health/diseases/methaemoglob/en/

Young, E. and R. Briggs. 2005. Shallow groundwater nitrate-N and ammonium-N in cropland and riparian buffers. Agriculture, Ecosystems & Environment, Volume 109, Issues 3-4 (297-309).

ACKNOWLEDGEMENT

This chapter was as a portion of S. Abit's M.S. Thesis entitled "Evaluation of Subsurface Solute Transport and its Contribution to Nutrient Load in the Drainage Ditches Prior to Restoration of a Carolina Bay" that was earned through NC State University and is available through the university's library.

Table 8.1. Selected properties of the soil in the experimental area.

Depth Interval		Sand	Clay	Soil Texture	K_{sat}	Bulk Density	Porosity	Organic Carbon
ft	(cm)	- - - - - % - - - -			ft d^{-1} (m d^{-1})	lb ft^{-3} (Mg m^{-3})	in^3 in^{-3}	%
0 to 0.5	(0 to 15)	87	13	LS	ND	73.04 (1.17)	0.53	3.70
0.5 to 1.0	(15 to 30)	84	13	LS	ND	77.41 (1.24)	0.49	3.39
1.0 to 1.5	(30 to 45)	87	13	LS	1.35 (0.41)	87.40 (1.40)	0.44	3.74
1.5 to 2.0	(45 to 60)	87	13	LS	1.90 (0.58)	94.50 (1.52)	0.42	0.21
2.0 to 2.5	(60 to 75)	79	19	SL	2.53 (0.77)	94.50 (1.52)	0.41	1.00
2.5 to 3.0	(75 to 90)	85	14	LS	2.62 (0.80)	94.30 (1.51)	0.42	0.56
3.0 to 3.5	(90 to 105)	78	20	SL	6.46 (1.97)	100.51 (1.61)	0.37	1.16

ND- Not Determined

LS = loamy sand, SL = sandy loam

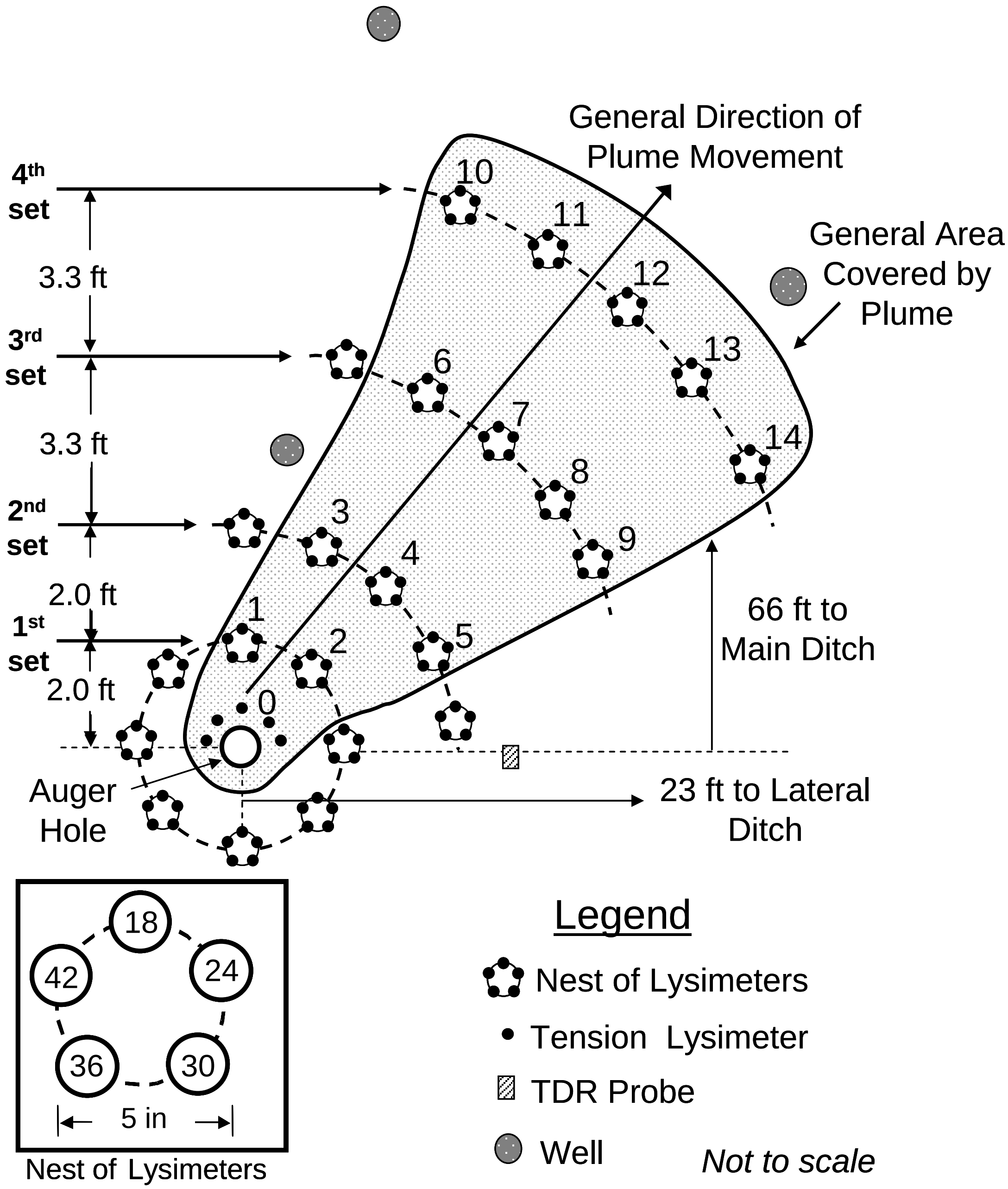

Figure 8.1. Schematic diagram of the plan view of the locations of the lysimeter nests, wells, and time domain reflectometry (TDR) probe in the experimental area. The inset shows the position of the tension lysimeters in a nest with porous cups at 1.5, 2.0, 2.5, 3.0 and 3.5 ft from the surface.

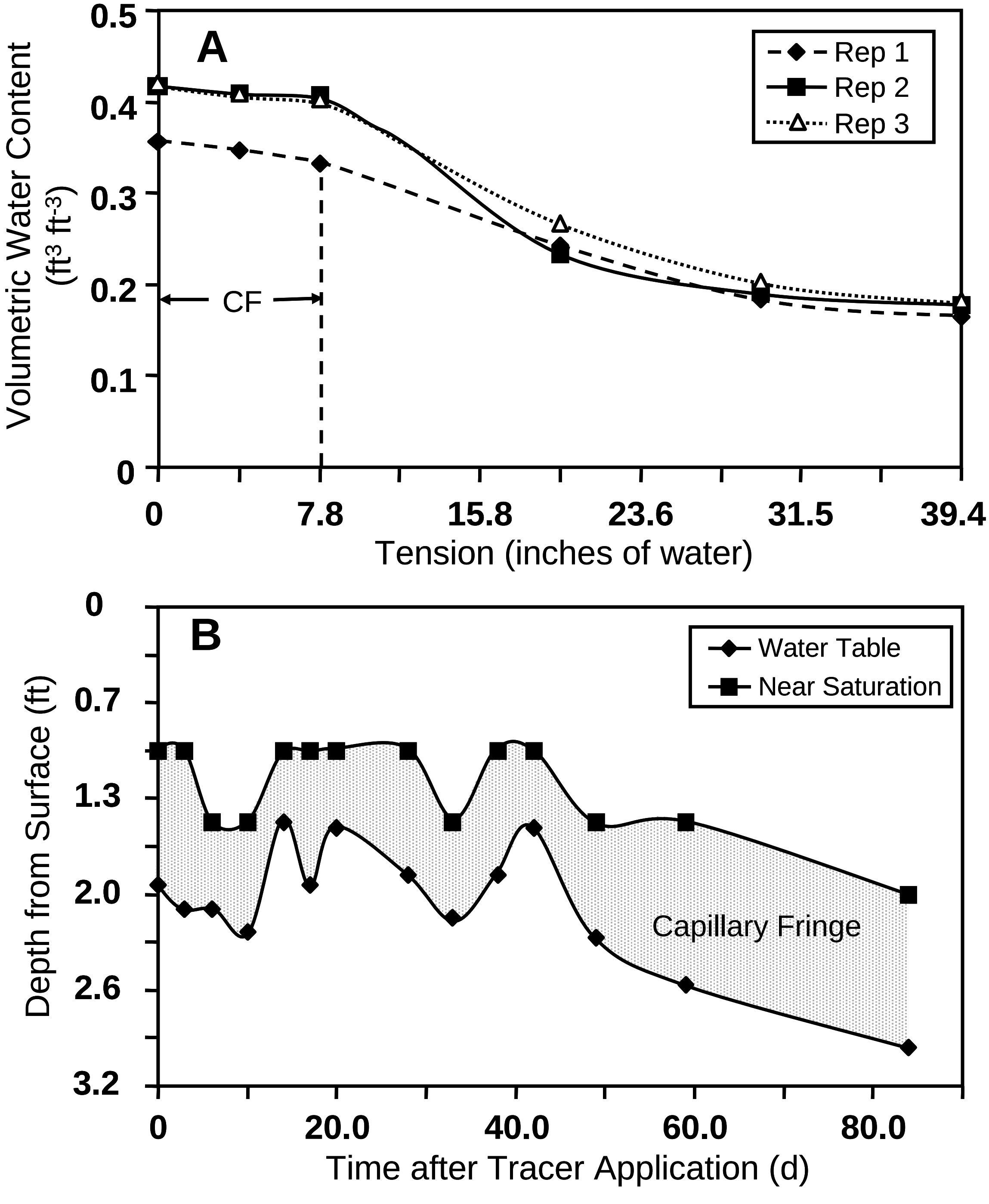

Figure 8.2. Soil water characteristic curves for three intact soil cores from the 1.5 to 2.0 ft layer (A), and depth to water table and the upper boundary of the near-saturated zone (measured using TDR) during the study (B). The 1.5 to 2.0 ft depth interval was mainly in the CF for most of the study period.

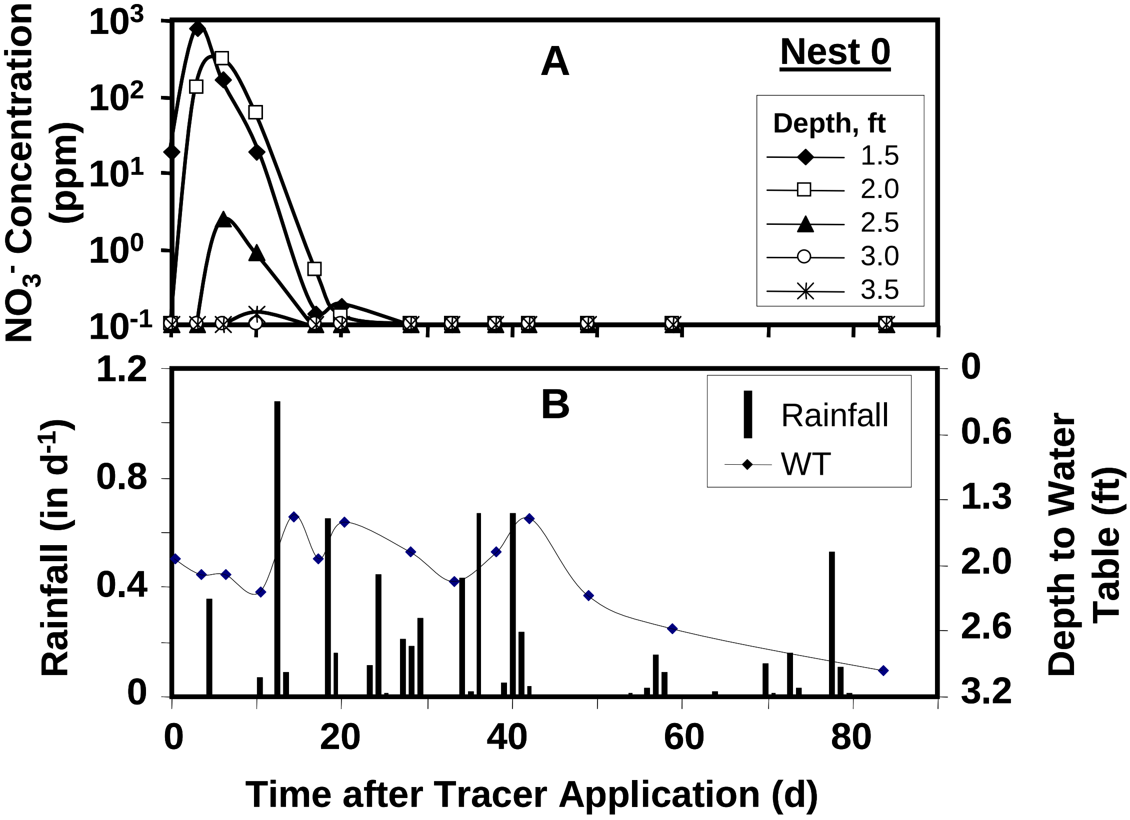

Figure 8.3. The nitrate concentrations detected at various depths at 0.7 ft (20 cm) horizontal distance from the tracer application spot in nest 0 (A), and rainfall data and measured water table during the study (B).

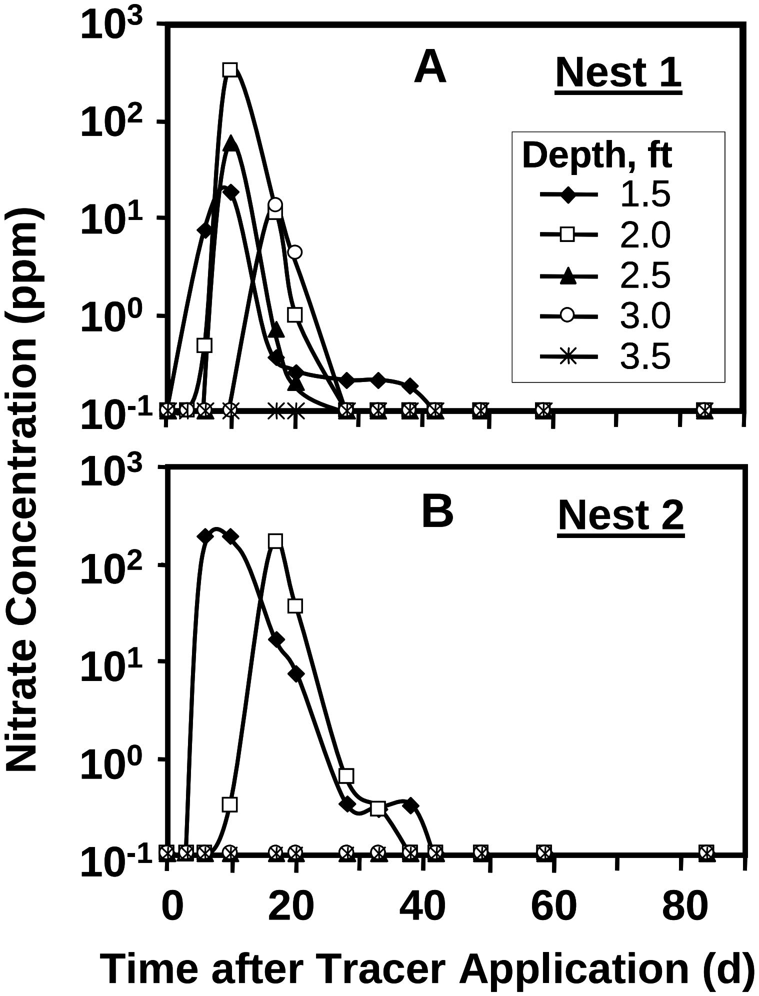

Figure 8.4. The nitrate concentrations detected at various depths at 2 ft (60 cm) horizontal distance from the tracer application spot in nests 1 (A) and 2 (B) during the study.

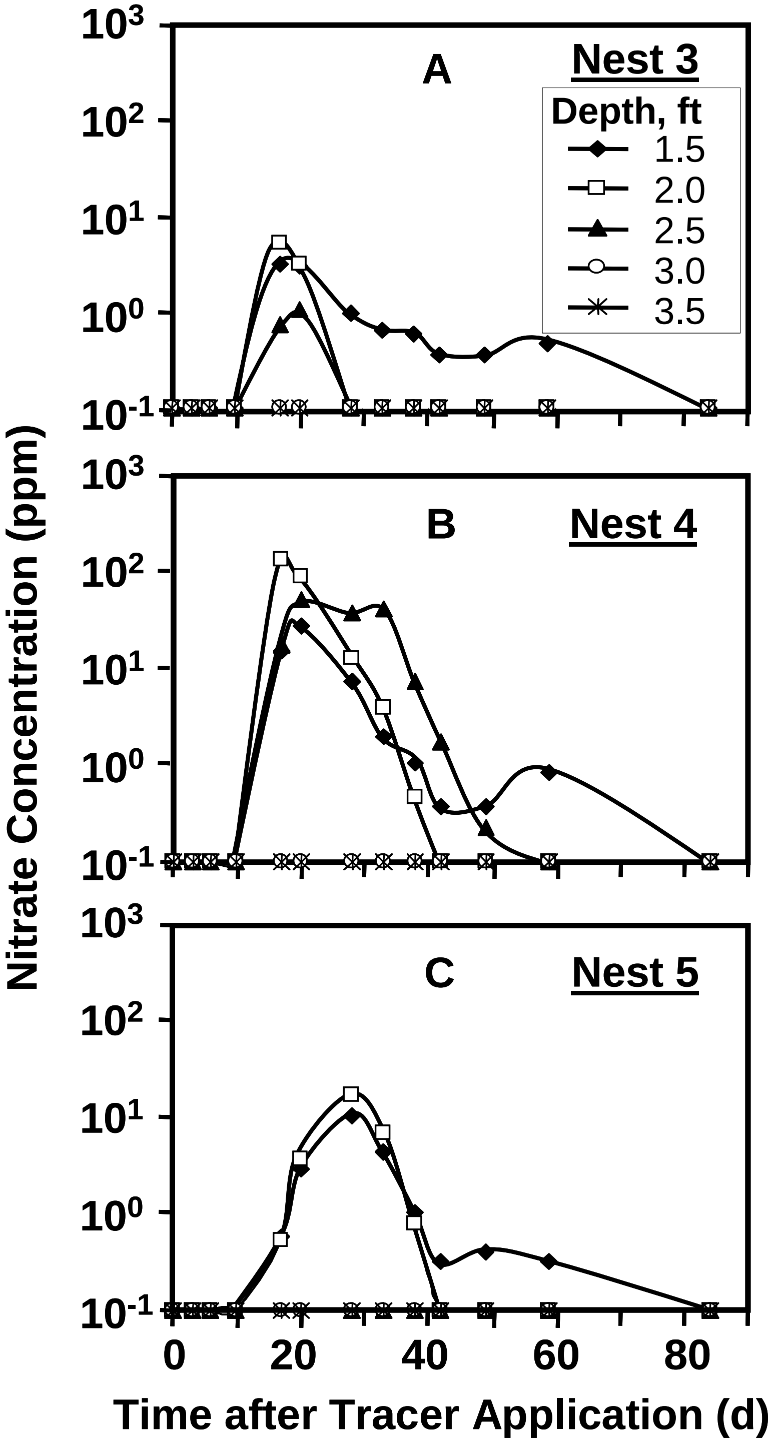

Figure 8.5. The nitrate concentrations detected at various depths at 4 ft (120 cm) horizontal distance from the tracer application spot in nests 3 (A), 4 (B) and 5 (C) during the study.

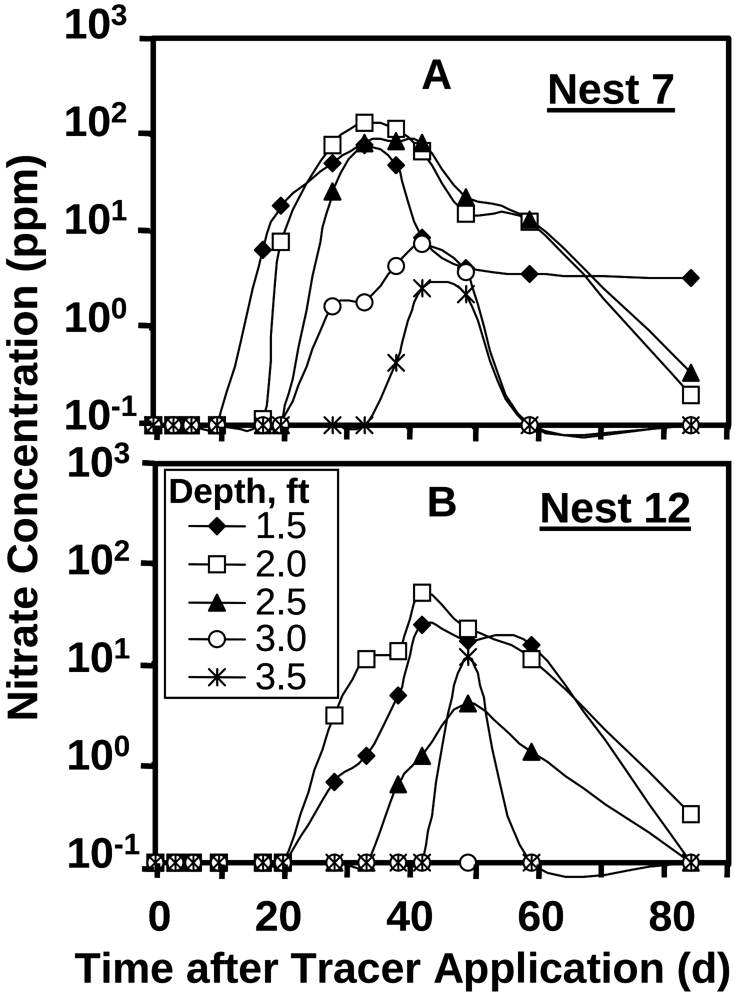

Figure 8.6. The nitrate concentrations detected during the study at various depths at nest 7 (A) and nest 12 (B). Nests 7 and 12 are located 7.3 ft (220 cm) and 10.7 ft (320 cm) from the tracer application spot, respectively.

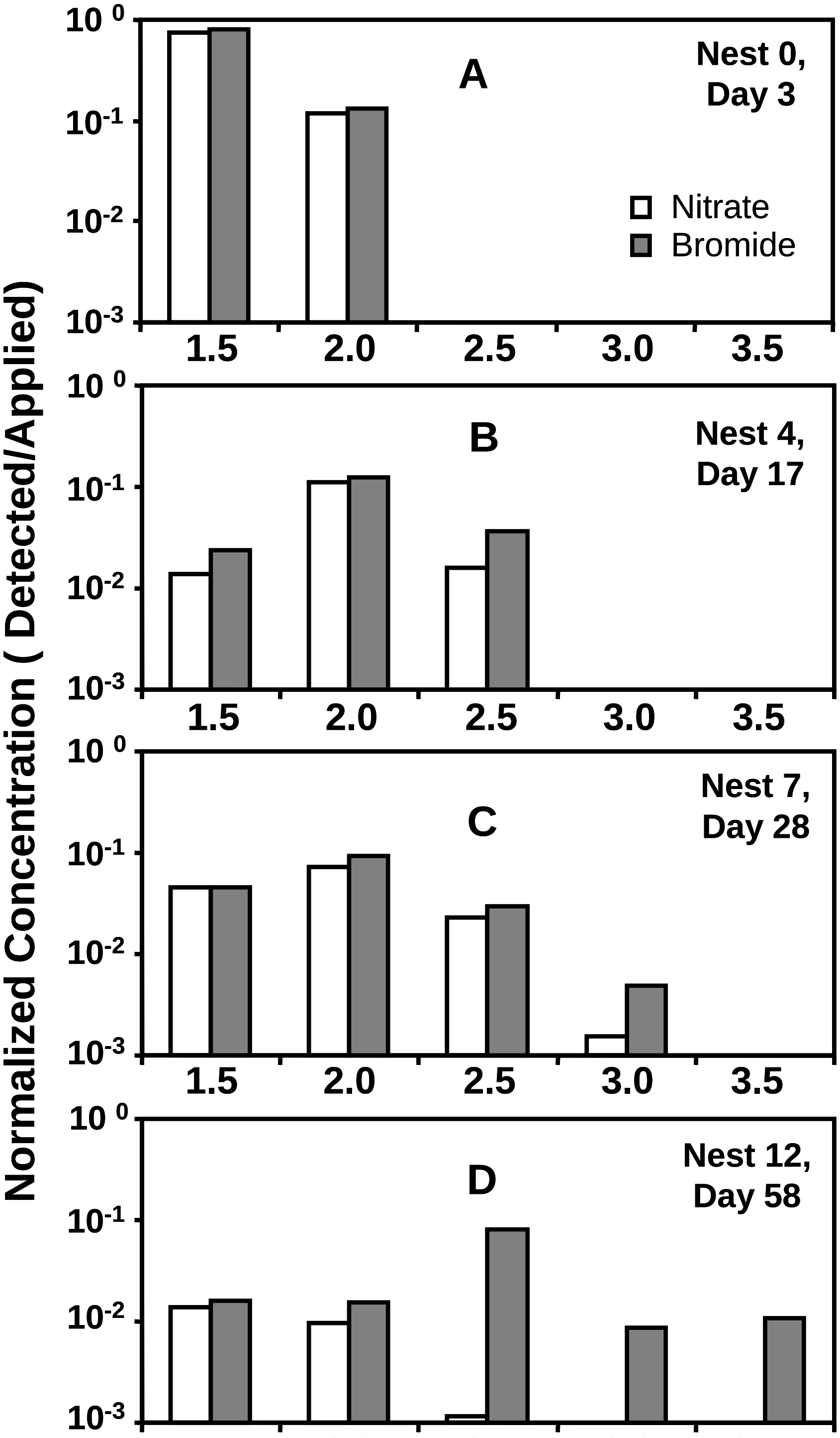

Figure 8.7. Normalized concentration of nitrate and bromide detected at various depths as the tracer plume moved through nest 0, 4, 7 and 12 located 0.67, 4.0, 7.3 and 10.7 ft, respectively, from the tracer application.

Chapter 9

DEVELOPMENT OF REDUCING CONDITIONS AS A FUNCTION OF SATURATION, ORGANIC CARBON, AND TEMPERATURE UNDER FIELD CONDITIONS

H.C. Smith, M.J. Vepraskas, and W.H. Hudnall

INTRODUCTION

Jurisdictional wetlands must have hydric soils, hydrophytic vegetation, and wetland hydrology (Environmental Laboratory 1987). Hydric soils, by definition, formed under conditions of saturation, flooding, or ponding long enough during the growing season to develop anaerobic conditions in the upper part (USDA, Soil Conservation Service 1987). These soils are identified in the field using soil color patterns that only develop under anaerobic conditions (USDA, NRCS 2002). Hydrophytic plants are those adapted to live in water, or saturated soils that are periodically anaerobic soils (Cronk and Fennessey 2001). Wetland hydrology requires that soils be saturated within 12 in. the surface for 5% or more of the growing season Environmental Laboratory, 1987; U.S. Army Corps of Engineers, 2005).

Hydrologic models are available that compute water table depth from climatic and soil data (Skaggs 1978). Such models have been used to compute 40 years of daily water table levels to determine if a site meets wetland hydrology (Vepraskas et al. 2004). The models can also be used to relate soil color patterns to wetland hydrology (He et al. 2003). It should be possible to use these long-term hydrologic simulations to evaluate the hydrologic and soil requirements for specific plant species and plant communities. To do this, the models must be able to compute durations of anaerobic conditions, because these conditions strongly influence plant development (Cronk and Fennessey 2001).

Anaerobic conditions occur when O_2 levels in the soil fall to the point that organisms respiring in the soils must use electron acceptors other than O_2 to oxidize organic matter (Sylvia et al. 2005). Aerated soils become anaerobic when: 1) soils are saturated such that atmospheric O_2 cannot diffuse quickly into the soil, and 2) bacteria that are decomposing organic tissues deplete the soil and water of dissolved oxygen (Ponnamperuma 1972). The soil is anaerobic when virtually all the oxygen has been depleted in the soil water. Microbial respiration continues under anaerobic conditions, but the microbes must use other substances as electron acceptors in the sequence of: NO_3^-, oxidized forms of Mn and Fe, SO_4^{2-} and CO_2 (Patrick and Jugsujinda 1992). Denitrification, hydrogen sulfide production, and methane production occur under anaerobic conditions when electron acceptors other than O_2 are used for microbial respiration.

When a soil becomes saturated through rainfall, the soil water usually contains dissolved oxygen that keeps the soil redox potential in the aerobic zone (Vepraskas and Faulkner 2001). The time required to develop anaerobic conditions in saturated soils is variable and can range between a few hours to months depending on soil conditions (Ponnamperuma 1972). The rate at which a saturated soil becomes anaerobic depends on a number of factors including: duration of saturation, amounts of organic C, the size and activity of the microbial population, and the rate that water moves through the soil (Meek et al. 1968; Anderson and Domsch 1980; Christenson et al. 1990; Pezeshki 1994).

Temperature also affects development of anaerobic conditions, because microbial activity increases as temperature increases. Nishio et al. (1988) found that denitrification began within 3 to 4 d after saturation at 12 $^{\circ}$C and the lag time decreased to 1 to 2 d at 20 $^{\circ}$C. Megonial et al. (1996) showed that in the southeastern United States the soil temperature at 50 cm remained above 5 $^{\circ}$C throughout the year. They suggested that the soil may produce anaerobic conditions as quickly in the winter as in the summer.

The redox potential (Eh) of a soil can be measured with a Pt microelectrode to estimate when a soil is anaerobic. Anaerobic conditions form at different redox potentials in soils depending on the pH of the soil solution (Figure 9.1. The Eh values at which a soil becomes anaerobic differ between the theoretical values determined by thermodynamic calculations and experimental results. Experiments have shown that the Eh at which O_2 is reduced to water occurs from approximately 100 to 500 mV lower than that predicted by thermodynamics (Ponnamperuma 1972; McBride 1994; Patrick and Jugsujinda 1994). According to McBride (1994) this is because the O_2-H_2O redox couple is slow to react at the Pt surface.

Hydric soils can be identified in the field by using measurements of saturation and redox potential as set forth in the Technical Standard of the National Technical Committee for Hydric Soils (NTCHS 2004). This standard uses the following equation to evaluate when a soil is anaerobic:

$$\text{Eh (mV)} = 595 - 60(\text{pH}) \qquad (1)$$

The relationship of this equation to theoretical and experimental values is shown in Figure 1. If the Eh is $\leq$175 mV at a pH of 7, then the soil is assumed to be anaerobic. The 175 mV value is the point at which some Fe^{2+} has been detected in soil solutions. When the Eh value is below the Technical Standard line shown in Figure 9.1, the soil should be anaerobic because Fe^{2+} cannot exist in this reduced form when O_2 is present in the solution.

Relatively few field studies have been conducted to document the effects of organic C and temperature on the rate of development of anaerobic or reduced soil conditions. He et al. (2003) found that in four Rains sandy-loam soils (Typic Paleaquults) the lag time for iron reducing conditions to begin ranged from 4 to 48 d. Lag time increased as soil organic carbon decreased from 2.5 to 0.2% C from the soil surface to a depth of 24 in. Such data were used with hydrologic models to compute relationships between saturation duration and soil color (Vepraskas et al. 2004), and may be used to evaluate the current criteria for wetland hydrology (R.W. Skaggs, personal communication). Similar work is needed for additional soils with a broader range of organic C levels. The objectives of this study were: 1) to determine the rate that anaerobic conditions develop following saturation under field conditions for both organic and mineral soils, and 2) to assess the effects of temperature and carbon on anaerobic condition development.

MATERIALS AND METHODS

Juniper Bay is a 750 acre drained Carolina Bay located in Robeson County, NC (Figure 9.2). The Bay was logged, drained, and put into agricultural production in 1971. Farming stopped in 2000 and the fields were left in fallow. Experiments for this research began in 2002 when the soil surface was covered with weeds. Organic soils occupied the central portion of the bay with mineral soils around the perimeter (Figure 9.2). The organic soils were members of the Ponzer series (loamy, mixed, dysic, thermic Terric Haplosaprists) and had organic layers ranging in thickness from 16 to 51 in. Most mineral soils were members of the Leon series (sandy, siliceous, thermic Aeric Alaquods). At the boundary between the organic and mineral soils, mineral soils contained a histic epipedon composed of organic soil material between 8 to 16 in. thick. These soils were members of the Rutlege series (Histic Humaquepts). The land slope across all plots was <1%.

Seven soil plots were monitored at the points shown in Figure 9.2. All plots were placed equidistant between ditches, in fields where soils had been sampled for an earlier and more extensive study (Ewing 2003). For the latter work, the plot positions were chosen by randomly placing an equilateral triangle grid over a map of Juniper Bay. Four plots were placed in the organic soils, and three plots were placed in mineral soils to evaluate both soils groups. The points were found in the field using global positioning equipment.

For each plot, a pit (5 ft. deep) was dug to describe the soil profile and collect bulk samples to determine soil chemical and physical properties. Uhland cores (3 in. in diameter by 3 in. in height) were taken from each horizon to determine bulk density (Blake and Hartge, 1986). Particle size distribution was determined by the pipette method and sieving of sands (Gee and Bauder 1986). Samples were prepared for particle size analysis by first oxidizing the organic matter with concentrated (30%) hydrogen peroxide. Bulk samples were air-dried and ground with an electric grinder to pass through a 2-mm mesh (0.08 in.) sieve. Concentrations of K, Ca, Na, and Mg in Mehlich III extracts were measured with inductively coupled plasma emission spectrograph (Mehlich 1984). Cation exchange capacity and sum of basic cations were also determined (Mehlich 1976). Soil pH was measured electrometrically using a 1:1 soil to water ratio (McLean, 1982). Organic carbon was determined through dry combustion with a Perkin-Elmer PE2400 CHN Elemental Analyzer (Culmo 1988).

Redox Potential Measurements

Soil redox potentials were measured using seven automated stations that used data loggers to record redox potentials in the soil plots shown in Figure 9.2. The systems were installed in early July 2002 and placed 12 ft. away from pits used for soil characterization. Five platinum electrodes were placed at each of two depths, 10 to 24 in., for a total of 10 electrodes in each plot. Electrodes were constructed following the procedure of Hayes (1998).

The electrodes were installed by inserting them into 1 in.-diam. holes that were filled with a slurry made from soil extracted from the holes. The Pt tip was cleaned by scraping with a knife, and then the electrode was pushed through the slurry into the undisturbed soil below. One thermocouple was constructed and installed at a depth of 20 in. following the procedures of He et al. (2003).

The redox electrodes were connected to an automated system using a multiplexer (models 16/32 and AM 416, Campbell Scientific, Inc., Logan, UT), solar panel, battery and a data logger (Campbell Scientific model CR10X). A watertight, metal box was secured to a metal pole with a battery, multiplexer, and data logger inside. The solar panel was and connected to the battery to provide constant power. Color-coded wire was used to connect each redox electrode to the multiplexer. A calomel reference electrode was attached to the data logger and placed into the salt bridge (Pickering and Veneman 1984). The thermocouple and an air temperature probe were directly attached to the data logger.

The soil redox potential measurements were recorded every 10 min. for each electrode. The 10-min. readings were averaged hourly and the hourly readings were averaged daily. The readings were automatically corrected by adding 244 mV to convert the field voltage to that which would be measured using a standard hydrogen electrode. The mean annual soil temperature and the air temperature were measured at the same intervals. Redox potential and temperature were downloaded monthly to a laptop computer. Measurements were made during a 2-year period.

Water Table

Water table depths were measured hourly using automatic monitoring wells (Remote Data Systems, Inc., Wilmington, NC) at each of the seven plots. The wells were installed using a 4-inch diameter auger to bore a hole to a depth of 80 in. The well was inserted and the hole was backfilled with sand to cover the slots in the well screen. A 1 in. thick layer of bentonite pellets was placed on top of the sand. Soil was placed above the bentonite and formed into a conical shape to shed water. The water table was measured every hour. The water table was manually averaged over the day to give the average water table depth for that day at each of the seven sites.

Anaerobic Lag Time and Extended Anaerobic Condition

The Eh required for anaerobic conditions was calculated for each site and depth using Eq. (1). Soil pH was measured in the field electrometrically on a 1:1 soil to water slurry (McLean, 1982). The pH was measured twice each year (winter and summer) at both the 25 and 61 cm depths. Mean daily soil redox potentials were compared with the daily water table depth at each depth in each plot (Figure 9.3). The duration of saturation for the site shown in Figure 3 was 40 d. Anaerobic lag time (Lag) was the time required for a saturated soil to become anaerobic as shown by Eh measurements and Eq. (1). Lag times were computed as shown in Figure 9.3 where the lag time was estimated to be 18 d in this example. After the water table fell below the depth of the electrodes the soil remained anaerobic for a period called the *extended anaerobic condition (Ea).* The Ea was estimated as shown in Figure 3 from the water table and Eh data, and was 10 d in this example.

Lag times and Ea values were determined over a 2-yr period throughout the year. For each depth, mean daily Eh values were computed. Lag times and Ea values were determined each time the soil saturated and drained at the depth of the redox electrodes. Mean values of Lag and Ea were compared during and outside the growing season, for mineral and organic soil groups separately, using a t-test. Mean Relationships between Lag times and soil properties were evaluated using the PROC GLM (SAS, 2000).

RESULTS AND DISCUSSION

Soil Properties and Temperature

Table 9.1 shows selected chemical and physical properties for the three types of soils at Juniper Bay. As organic C quantities increased across the soils, the bulk densities decreased, cation exchange capacity increased, and base saturation decreased. Soil pH values tended to be lower in organic than mineral soils. The soil pH values shown are typical for those used for agriculture in a Carolina Bay in eastern NC (Bruland et al. 2003).

Mean monthly soil temperatures are shown for an organic and mineral soil in Figure 9.4. Soil temperature was measured at a depth of 20 in. because the temperature is constant throughout the day and is equal to the average daily soil temperature. Soil temperatures were similar between the two soil groups and were above 5 °C throughout the year. This indicated that the microbial population was able to remain active year-round (Megonigal et al. 1996). The growing season in Robeson Co., NC begins on 14 March and ends on 14 November (McCachren, 1978). As shown in Figure 9.4, mean daily soil temperatures ranged from 55 to 77 °F during the growing season, while outside the growing season mean daily temperatures ranged from 45 to 54 °F.

Typical Eh changes following saturation events at 10 in. are shown in Figure 9.5 for an organic soil during the summer months. Data for all other plots were similar. The Eh that developed between saturation events was approximately 500 mV in aerobic soil and dropped quickly when the soil horizon saturated. For example, on 23 May the soil became saturated at a depth of 10 in. and anaerobic conditions began on 24 May producing a Lag value of 1 d (Figure 9.5). After the water table fell below 10 in. on 22 June, the Eh rose quickly into the aerobic zone on 24 June for an Ea (extended anaerobic condition) of 2 d. The lag time (Lag) for the soil to become anaerobic was between 1 to 2 d for the multiple saturation events shown in this example. The lowest Eh values measured were approximately 50 to 100 mV when anaerobic conditions were maintained for at least 2 days. During the winter and spring months, the Eh values continued to fall quickly once the soil saturated to produce Lag values that were similar to those in the summer months (Figure 9.6).

Mean Lag and Ea values are shown for mineral and organic soils groups in Table 9.2. Values were computed both during the growing and outside the growing season to evaluate temperature effects. Mean Lag values were consistently less than 3 d in both organic and minerals soils at both 10 to 24 in. (Table 9.2). The Lag value increased slightly at 24 in. in an organic soil during the non-growing season, and the difference was statistically significant ($p=0.018$). The Ea values were, on average, longer in the mineral soils at both depths than the organic soils (Table 9.2). The recovery times (Ea) were longer (<10 d) than the Lag values in both soil groups, and Ea values were slightly higher in the mineral soils than in organic soils (Table 9.2).

Diurnal Fluctuations

Diurnal fluctuations in Eh were observed in only one plot in Juniper Bay (Figure 9.7). Vegetation surrounding the redox electrodes consisted of a mixture of *Urochloa platyphylia* (L.), *Polygonum pensylvanicum* (L.), *Conyza Canadensis* (L.), and *Juncus* (L.). This mineral soil was saturated for the longest period of all the plots. The Eh was highest during the afternoon and the lowest Eh occurred at night (Figure 9.7). The maximum diurnal change in Eh was approximately 200 mV and the lowest was approximately 50 mV. The diurnal fluctuations were only observed when the soils were saturated and anaerobic. These fluctuations were observed only during the growing season—they began in March and ended in late October to early November.

The timing and periodicity of the diurnal Eh changes may have been caused by hydrophytic vegetation transporting oxygen to their roots. During the day, O_2 moves into open stomates on leaves, is transported through the stem to the roots along arenchema, and is expelled out of the root into the soil to oxygenate the rhizosphere (Kludze et al. 1994). This process of radial oxygen loss out of the root causes the soil Eh to rise (Armstrong 1978). Oxygen can be transported to plant roots by several processes, and some processes depend on temperature differences between leaves and soil (Cronk and Fennessy 2001). At night, the stomates close and O_2 is no longer transported to the roots; the Eh decreases in the soil around the roots as soil microbes use the O_2 as their electron acceptor. Grosse (1996) found that such radial oxygen loss exhibits a diurnal variation, with the greatest oxygen loss to the soil occurring during the day.

Tiarks et al. (1995) found similar diurnal Eh changes in long-term pine plantation studies. Maximum Eh values occurred at approximately 2 PM and minimum redox values occurred at approximately 2 AM. These diurnal values also were noted only during the growing season, which was defined by the onset of pollen initiation in the spring, and ended with the first major frost in the Fall.

Factors Affecting Lag Values

The relationship between average daily soil temperatures and Lag values is shown in Figure 9.8 for both mineral and organic soil horizons at depths of 10 and 24 in. The average daily soil temperature, measured at 20 in., had no significant relationship ($p > 0.5$) with Lag values in these soils. The interaction of soil temperature and soil organic carbon was also not significant ($p > 0.5$). Soil temperatures were probably not low enough to slow microbial activity sufficiently to increase the amount of time needed for the organisms to remove oxygen from the water. The soil temperature in the Coastal Plain of North Carolina does not generally fall below 41 $^{\circ}$F, which has been taken as "biological zero" or the temperature below which microbial activity virtually stops. However, it is possible that larger Lag values would be found at temperatures below 41 $^{\circ}$F.

The soil organic carbon at Juniper Bay ranged from less than 1% in the mineral soils to 31% in the organic soils evaluated (Table 9.1). The relationship between soil organic carbon and Lag values is shown in Figure 9.9, along with data from two prior studies in mineral Coastal Plain soils with lower levels of organic C than found in the current study (He et al. 2003, and Hayes and Vepraskas 2000). There was a significant ($p = 0.009$) relationship between soil organic carbon and Lag values, and soil organic C^2 was also significantly ($p = 0.004$) related to Lag values. Lag values were consistently small (<5d) when the soil organic C was >0.03 g/g, but increased abruptly where the soil organic C was <3%. The majority of Lag values with soil organic C <3% were $\geq$15d. Exceptions to this are circled on Figure 9.9 where horizons with low soil organic C had small Lag values, because overlying horizons had higher amounts (approximately 3% C) of soil organic C. Soluble organic C can be translocated downward through the soil during rain events allowing for short La values.

The relationship shown in Figure 9.9 probably relates to the size of the microbial population. We hypothesize that the soil horizons with high amounts of soil organic C had large microbial populations. The large microbial population was able to use the dissolved O_2 in the soil water as its major electron acceptor during respiration. This allowed anaerobic conditions to form in 1 to 2 d following the onset of saturation. The soil horizons with lower soil organic C probably had smaller microbial populations that were unable to reduce the O_2 throughout the soil as quickly and produce anaerobic conditions.

We also tried to identify soil properties that were related to Ea values using physical property data of Ewing (2003) that were determined for the soil plots. While soil pore size distribution and texture were considered in our evaluation, neither had a significant relationship with Ea values. It seems likely that Ea will increase as the number of macropores in the soil decreases, because oxygen should be able to enter the soil quickly along macropores after the water table falls.

The Lag and Ea values were determined to allow the duration of anaerobic conditions to be estimated from a record of water table levels. An equation for computing duration of anaerobic conditions from the duration of saturation is:

$$\text{Da (days)} = \text{Ds} - \text{Lag} + \text{Ea} \tag{2}$$

where: Da is duration of anaerobic conditions, Ds is duration of saturation, with the other variables as defined previously. Hydrologic simulation models have been used to compute 40 years of daily water table data (Vepraskas et al. 2004). Equation (2) can be used to take those simulation results and compute periods of anaerobic conditions over the 40-year period. Such data may be useful in determining the hydrology needed for dominance of specific plant species, as well as to better define the conditions needed to produce hydric soil field indicators.

CONCLUSIONS

The results of this study showed that the time for anaerobic conditions to develop after saturation begins (Lag) was related to soil organic C but not to average daily temperature when soils temperatures at a depth of 20 in. were between 45 and 77 °F. When soil organic carbon was <3% the Lag values ranged from 3 to 48 d. The soils containing higher soil organic carbon concentrations had Lag values that ranged from 1 to 12 days, with most being 5 d or less. In soils that have low soil organic carbon (<3%) the Lag value will be more variable than soils with higher amounts of C. The time of extended anaerobic conditions after saturation ends (Ea) ranged from 1 to 7 days in the organic soils and the mineral soils ranged from 2 to 10 d. The Ea value was probably related to soil permeability (and macropores), with shorter Ea values occurring in soils with higher permeabilities that drain quickly, but a significant relationship was not found.

Diurnal Fluctuations in Eh were observed at only one location where a hydrophytic plant was near the platinum electrodes. Diurnal Eh fluctuations ranged from 50 to 150 mV during the growing season, and were not large enough to switch the soil from anaerobic to aerobic. The fluctuations did not occur during the non-growing season.

REFERENCES

Anderson, J. P. E., and K. H. Domsch. 1980. Quantities of plant nutrients in the microbial biomass of selected soils. Soil Science 130:211-216.

Armstrong, W. 1978. Root aeration in the wetland condition. p. 269-297. *In* D. D. Hook and R. M. M. Crawford (eds.) Plant Life in Anaerobic Environments. Ann Arbor Science Publishers, Ann Arbor, MI, USA.

Blake, G.R. and K.H. Hartge. 1986. Bulk density. p. 363-375. *In* A. Klute (ed.) Methods of soil analysis. Part 1. 2nd ed. American Society of Agronomy and Soil Science Society of America, Madison, WI, USA.

Bruland, G. L., M. F. Hanchey and C.J. Richardson. 2003. Effects of agriculture and wetland restoration on hydrology, soils, and water quality of a Carolina bay complex. Wetlands Ecology and Management 11:141-156.

Christensen, S., S. Simkins, J. M. Tiedje. 1990. Temporal patterns of soil denitrification: Their stability and causes. Soil Science Society of America Journal 54:1614-1618.

Cronk, J. K., M. S. Fennessy. 2001. Wetland Plants: Biology and Ecology. Lewis Publishers, CRC Press, Boca Raton, FL, USA.

Culmo, R. F. 1988. Principle of Operation – The Perkin-Elmer PE 2400 CHN Elemental Analyzer. Perkin Elmer Corp. Norwalk, CT, USA.

Environmental Laboratory. 1987. Corps of Engineers wetlands delineation manual. Technical Report Y-87-1. U.S. Army Engineers Waterways Experiment Station, Vicksburg, MS, USA.

Ewing, J. M. 2003. Characterization of soils in a drained Carolina Bay wetland prior to restoration. Ph.D. Dissertation. North Carolina State Univ., Raleigh, NC, USA.
.

Gee, G. W. and J. W. Bauder. 1986. Particle-size analysis. p. 383-411. *In* A. Klute (ed.) Methods of soil analysis. Part 1. 2nd ed. American Society of Agronomy and Soil Science Society of America, Madison, WI, USA.

Grosse, W. 1996. Pressurized ventilation in floating-leaved aquatic macrophytes. Aquatic Botany 54:137-150.

Hayes, W. A., Jr. 1998. Effect of ditching on soil morphology, saturation, and reduction in a catena of Coastal Plain soil. M.S. thesis, North Carolina State University, Raleigh, NC, USA.

Hayes, W. A., and M. J. Vepraskas. 2000. Morphological changes in soils produced when hydrology is altered by ditching. Soil Science Society America Journal 64:1893-1904.

He, X., M. J. Vepraskas, D. L. Lindbo, and R. W. Skaggs. 2003. A method to predict soil saturation frequency and duration from soil color. Soil Science Society of America Journal 67:961-969.

Kludze, H. K., and R. D. DeLaune. 1994. Methane emissions and growth of *Spartina patens* in response to soil redox intensity. Soil Science Society of America Journal 57:386-391.

McBride, M. B. 1994. Environmental chemistry of soils. Oxford Univ. Press, New York, NY, USA.

McCachren, C. M. 1978. Soil Survey of Robeson County North Carolina. USDA-SCS. Washington, DC, USA.

McLean, E. O. 1982. Soil pH and lime requirement. p. 199-224. *In* A. L. Page, R. H. Miller, and D. R. Keeney (ed). Methods of Soil Analysis: Part 2- Chemical and Microbiological Properties. ASA and SSSA, Madison, WI USA.

Megonigal, J. P., S. P. Faulkner, and W. H. Patrick, Jr. 1996. The microbial activity season in southeastern hydric soils. Soil Science Society of America Journal 60:1263-1266.

Meek, B.D., A.J. McKenzie, and L.B. Grass. 1968. Effects of organic matter, flooding time, and temperature on the dissolution of iron and manganese from soil in situ. Soil Science Society of America Proceedings 32:634-638.

Mehlich, A. 1976. New buffer method for rapid estimation of exchangeable acidity and lime requirement. Communications in Soil Science and Plant Analysis 7:637-652.

Mehlich, A. 1984. Mehlich 3 soil test extractant: a modification of Mehlich 2 extractant. Communications in Soil Science and Plant Analysis 15(12):1409–16.

NTCHS (National Technical Committee for Hydric Soils). 2004. Technical standards for hydric soils. Technical Note no. 11 (ftp://ftp-fc.sc.egov.usda.gov/NSSC/Hydric_Soils/note11.pdf).

Nishio, T., T. Kanamori, and T. Fujimoto. 1988. Effects of organic matter, moisture content and other environmental factors on denitrification in topsoils of an upland field. Soil Science and Plant Nutrition 34:91-105.

Patrick, W. H., Jr. and A. Jugsujinda. 1992. Sequential reduction and oxidation of inorganic nitrogen, manganese, and iron in flooded soil. Soil Science Society of America Journal 56:1071-1073.

Pezeshki, S. R. 1994. Plant response to flooding. p. 289-321. *In* R. E. Wilkinson (ed.) Plant-Environment Interactions. Marcel Dekker, Inc., New York, NY, USA.

Pickering, E. W. and P. L. M. Veneman. 1984. Moisture regimes and morphological characteristics in a hydrosequence in Central Massachusetts. Soil Science Society of America Journal 48:113-118.

Ponnamperuma, F. N. 1972. The chemistry of submerged soils. Advances in Agronomy 24:29-96.

SAS Institute Inc. 2000. The SAS system for Windows. Release 8.2. SAS Inst., Cary, NC, USA.

Skaggs, R. W. 1978. A water management model for shallow water table soils. Tech. Rep. 134. Water Resources Research Institute, Raleigh, NC, USA.

Sylvia, D. M., J. J. Fuhrmann, P. G. Hartel, D. A. Zuberer. 2005. Principles and applications of soil microbiology. 2nd ed. Pearson Education, Inc., Upper Saddle River, NJ, USA.

Tiarks, A.E., W.H. Hudnall, J.F. Ragus and W.B. Patterson. 1995. Effect of pine plantation harvesting and soil compaction on soil water and temperature regimes in a semitropical environment. 3:66-78. *In* A. Schulte and D. Ruhiyat (eds.) Proceedings of the International Congress on Soil of Tropical Forest Ecosystems Mulawarman University Press, Samarinda, Indonesia.

U.S. Army Corps of Engineers. 2005. Technical standard for water-table monitoring of potential wetland sites. WRAP Technical Notes Collection, ERDC TN WRAP-05-2, U.S. Army Engineer Research and Development Center, Vicksburg, MS.

USDA, NRCS. 2002. Field indicators of hydric soils in the United States, Version 5.0. G.W. Hurt, P.M. Whited, and R.F. Pringle (eds.). USDA, NRCS in cooperation with the National Technical Committee for Hydric Soils, Fort Worth, TX, USA.

USDA Soil Conservation Service. 1987. Hydric Soils of the United States. In Cooperation with the National Technical Committee for Hydric Soils. Washington, DC, USA.

Vepraskas, M. .J. and S. P. Faulkner. 2001. Redox chemistry of hydric soils. p. 85-105. *In* J.L. Richardson and M.J. Vepraskas (ed.) Wetland Soils: Genesis, Hydrology, Landscapes, and Classification. Lewis Publishers, CRC Press, Boca Raton, FL, USA.

Vepraskas, M. J., X. He, D. L. Lindbo, and R. W. Skaggs. 2004. Calibrating hydric soil field indicators to long-term wetland hydrology. Soil Science Society of America Journal 68:1461-1469.

ACKNOWLEDGEMENT

This chapter was as a portion of H.C. Smith's M.S. Thesis entitled "Time Required for Anaerobic Conditions to Develop in Saturated Soils" that was earned through NC State University and is available through the university's library.

Table 9.1. Mean values for selected soil physical and chemical properties for soil horizons containing redox electrodes.

Soil group	Depth	Soil material	Bulk density	pH	Cation exchange capacity	Base saturation	Soil organic carbon
	iIn.		1b ft^{-3}		cmol$_c$ kg^{-1}	%	%
Mineral	10	Sand	86.7	5.47	54	71	2
“	24	Sand	99.2	4.37	38	40	1
Histic	10	Sapric	56.2	4.60	217	66	37
“	24	Loamy sand	84.9	3.90	49	23	3
Organic	10	Sapric	35.6	4.5	260	46	31
“	24	“	25.0	3.65	196	19	31

Table 9.2. Mean Lag and Ea values for mineral and organic soils groups both during and outside the growing season. Soils with Histic epipedons were split between organic and mineral groups, with the Histic epipedon being placed in the organic group and subsoil placed in the mineral group.

		Lag Period (Lag)		Extended Anaerobic Period (Ea)	
Soil group	Depth	Growing season[†]	Non-growing season	Growing season	Non-growing season
	in.	days			
Organic	10	1± 0.3	1 ± 0	2± 2	5 ± 3
(no. events)		(21)	(3)	(18)	(3)
Organic	24	1± 0	3.6 ± 2.3*	1± 0	2 ± 1
(no. events)		(6)	(3)	(4)	(2)
Mineral	10	2± 0.4	ND[††]	4 ± 1.3	ND
(no. events)		(5)		(4)	
Mineral	24	2± 1	ND	6 ± 4	ND
(no. events)		(6)		(5)	

[†] The growing season began on 14 March and ended on 14 November.

[††] ND indicates no data were obtained because soils did not saturate.

*Indicates means values were significantly different ($p<0.05$) between growing and non-growing season. No other significant differences were found among other means.

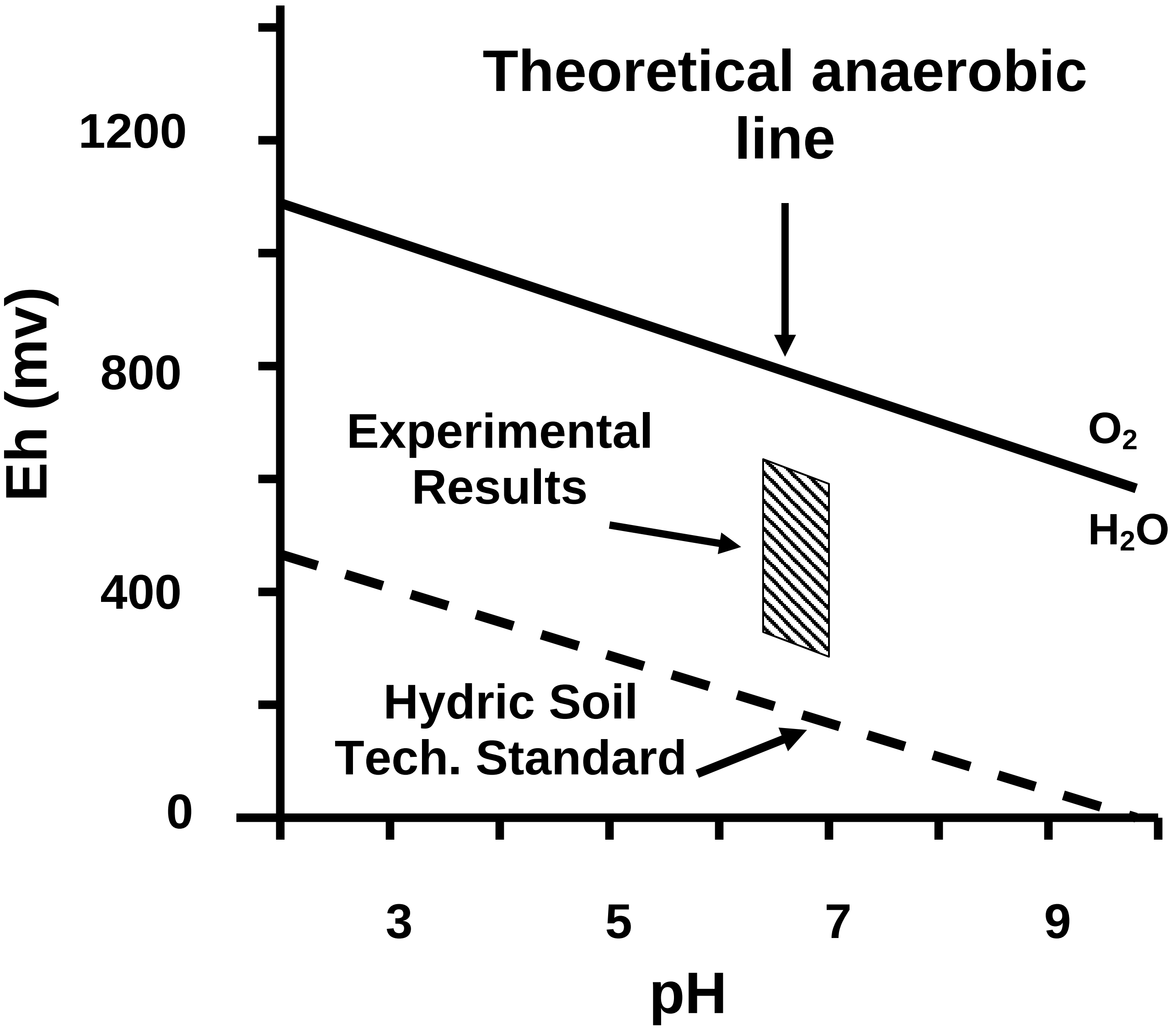

Figure 9.1. An Eh-pH diagram that shows how redox potential measurements can be used to assess when a soil has become anaerobic. The critical Eh for anaerobic conditions varies with pH. Experimental results show that O_2 is reduced to water at a lower Eh than predicted by thermodynamics (McBride 1994). The National Committee for Hydric Soils proposed the dashed line be used to interpret redox potential data to determine when anaerobic conditions occur.

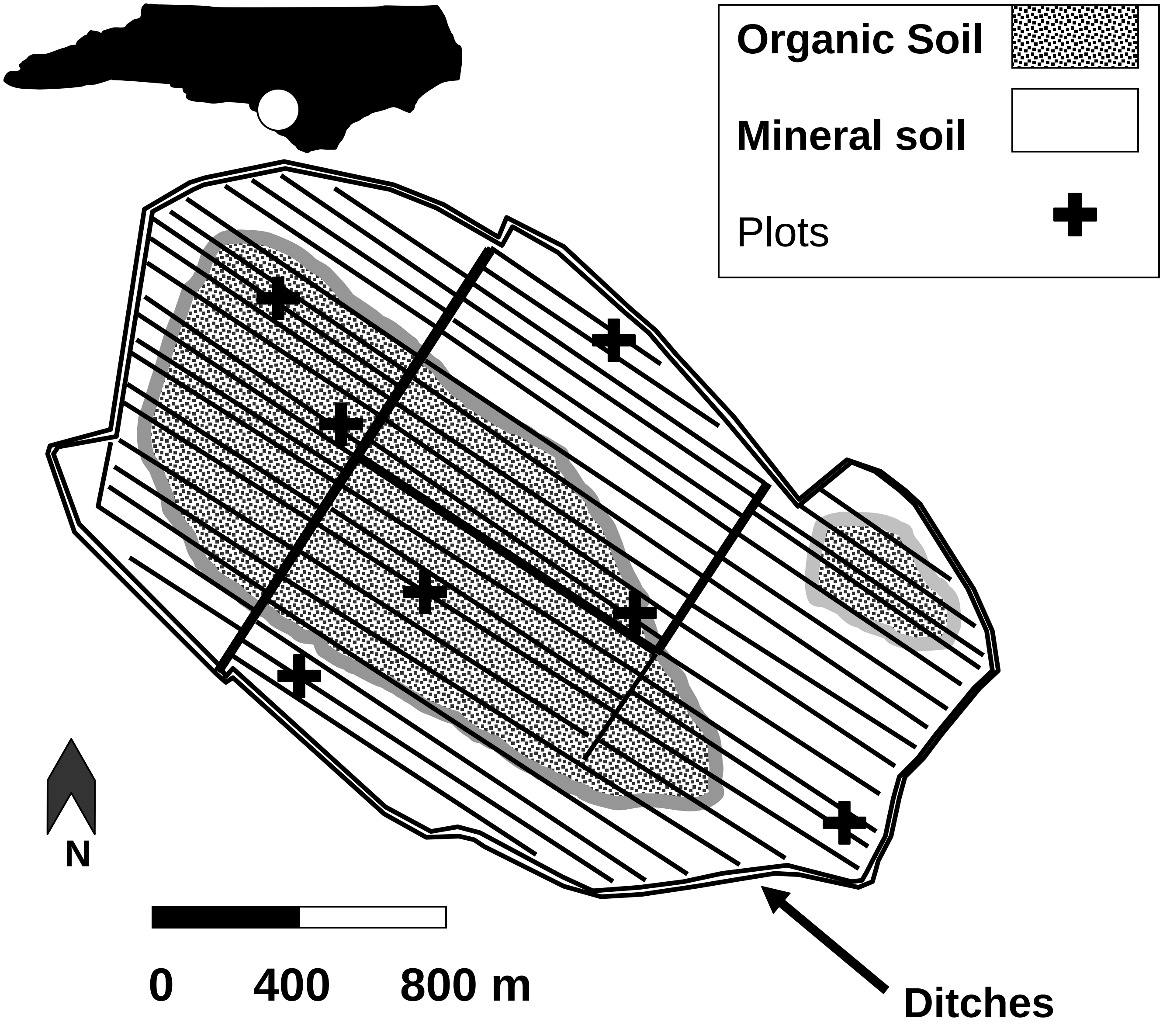

Figure 9.2. Location of study plots in Juniper Bay. Three plots were in mineral soil, three were in organic soils, and one was in a mineral soil with a Histic (organic material) epipedon.

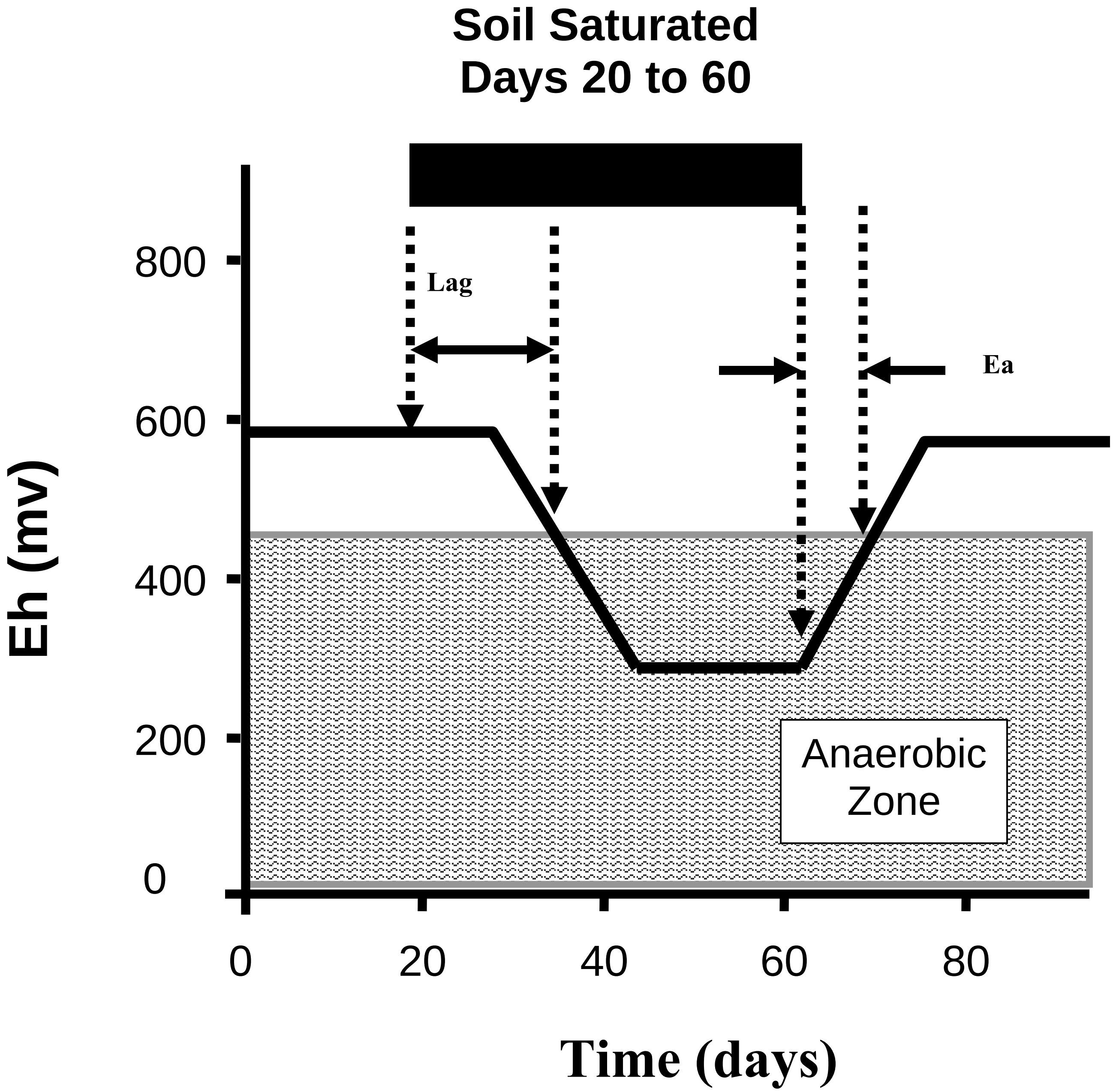

Figure 9.3. Illustration of how lag times (Lag) and extended anaerobic conditions were determined for Eh data from one depth in a soil plot. The Lag period was the time from the start of saturation to the beginning of anaerobic conditions as determined using Eq. 1. In this example, saturation began on day 20 and the Eh showed anaerobic conditions had developed on day 38, giving a Lag period of 18 days. Saturation ended on day 60 but the soil remained anaerobic until day 70, giving an extended anaerobic condition (Ea) of 10 days.

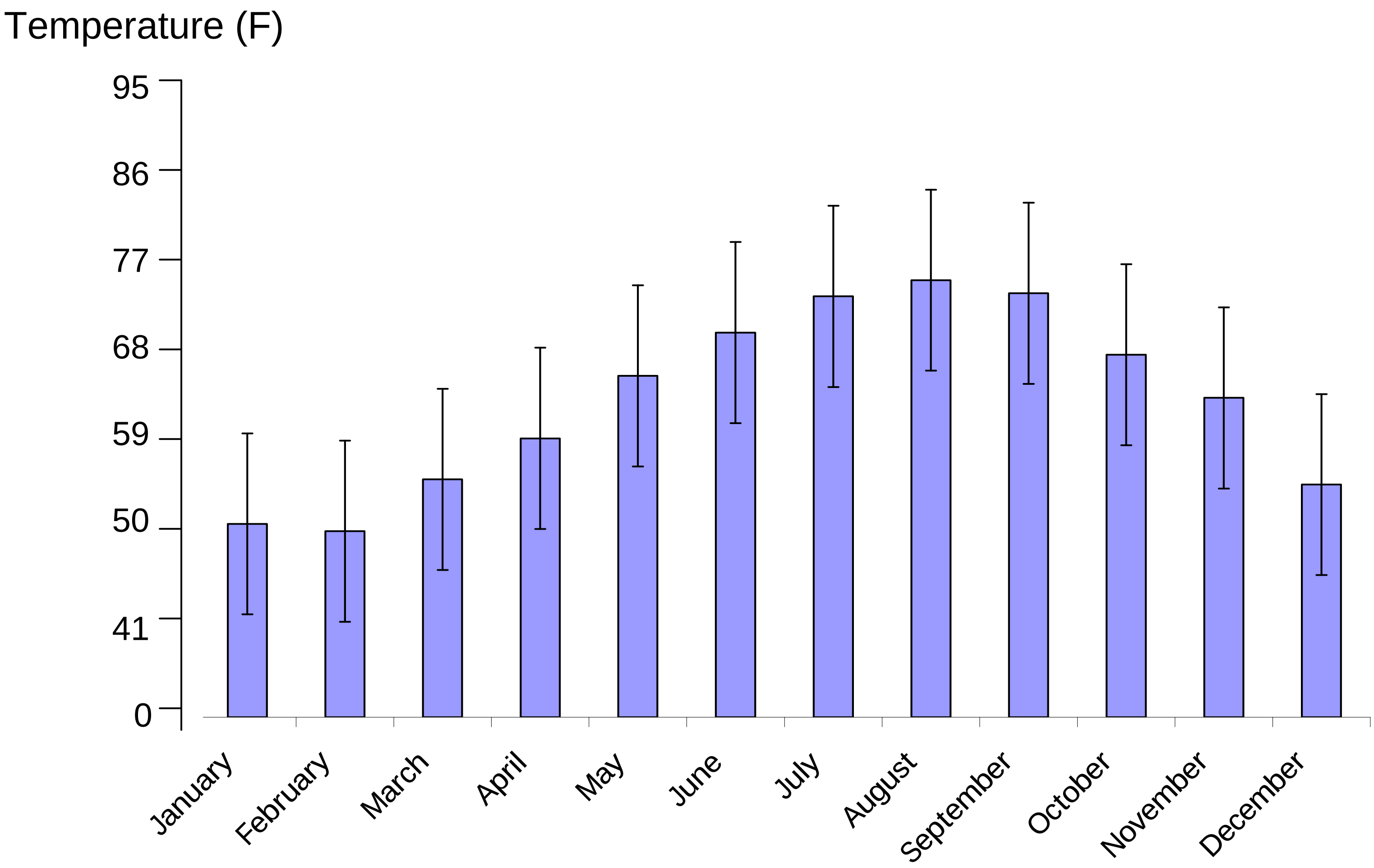

Figure 9.4. Monthly soil temperatures for 2003 as determined by computing means of daily values measured at a depth of 20 in. Soil temperatures were above 41 °F (5 °C) throughout the year, and this suggested that microbial activity should continue year round. Bars are standard deviations. The growing season occurs from 14 March through 14 October.

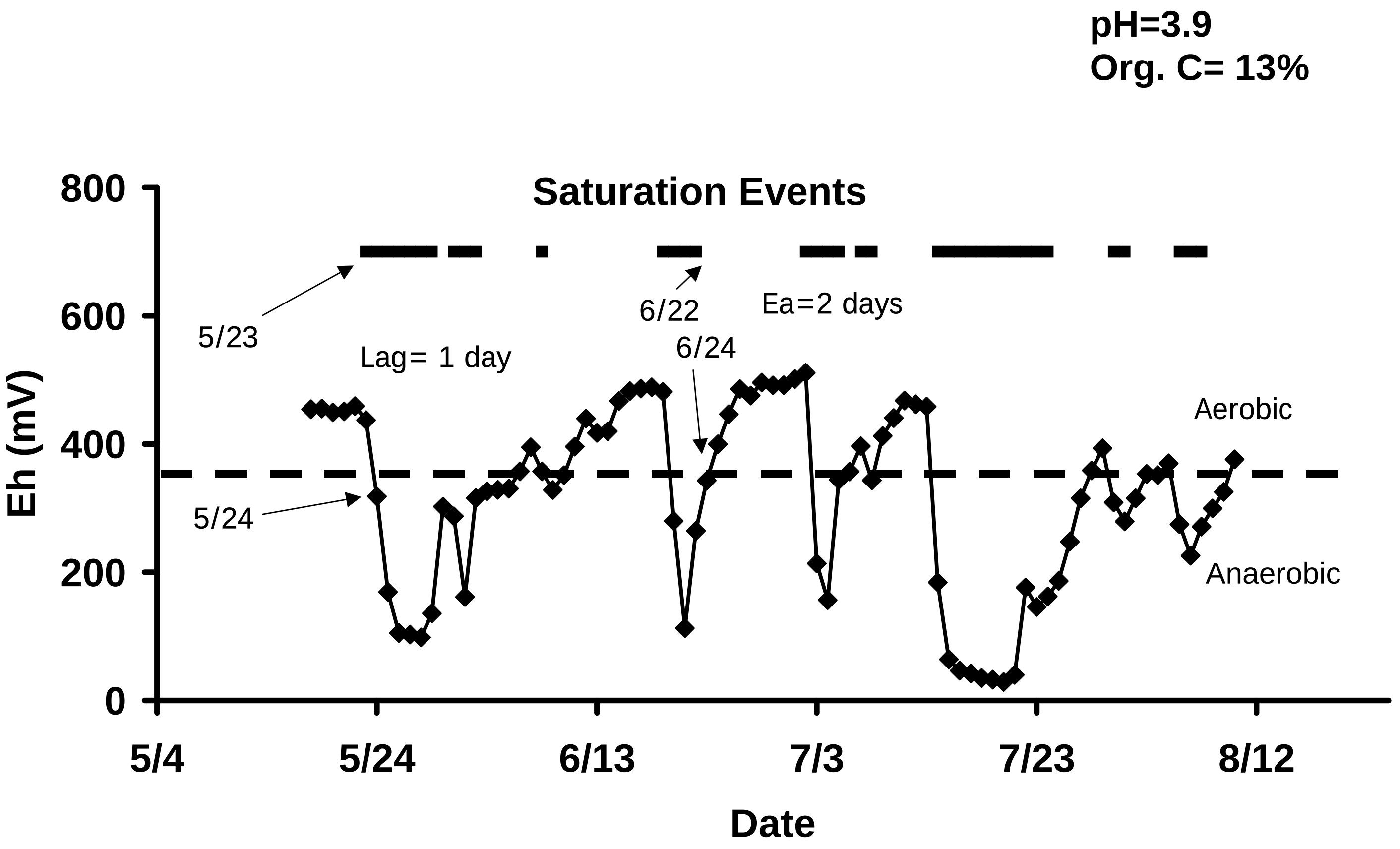

Figure 9.5. Typical Eh changes in an organic soil following saturation events at 10 in. during the summer months. The lag time (Lag) for the soil to become anaerobic was between 1 to 2d. For example, on 5/23/03 the soil saturated and anaerobic conditions began on 5/24/03, producing a La value of 1d. After the water table fell below 10 in. the Eh rose quickly requiring only 2 d for aerobic conditions to return. This occurred for example on 6/22/03 and aerobic conditions returned on 6/24/03, producing an Ea (extended anaerobic conditions) of 2d.

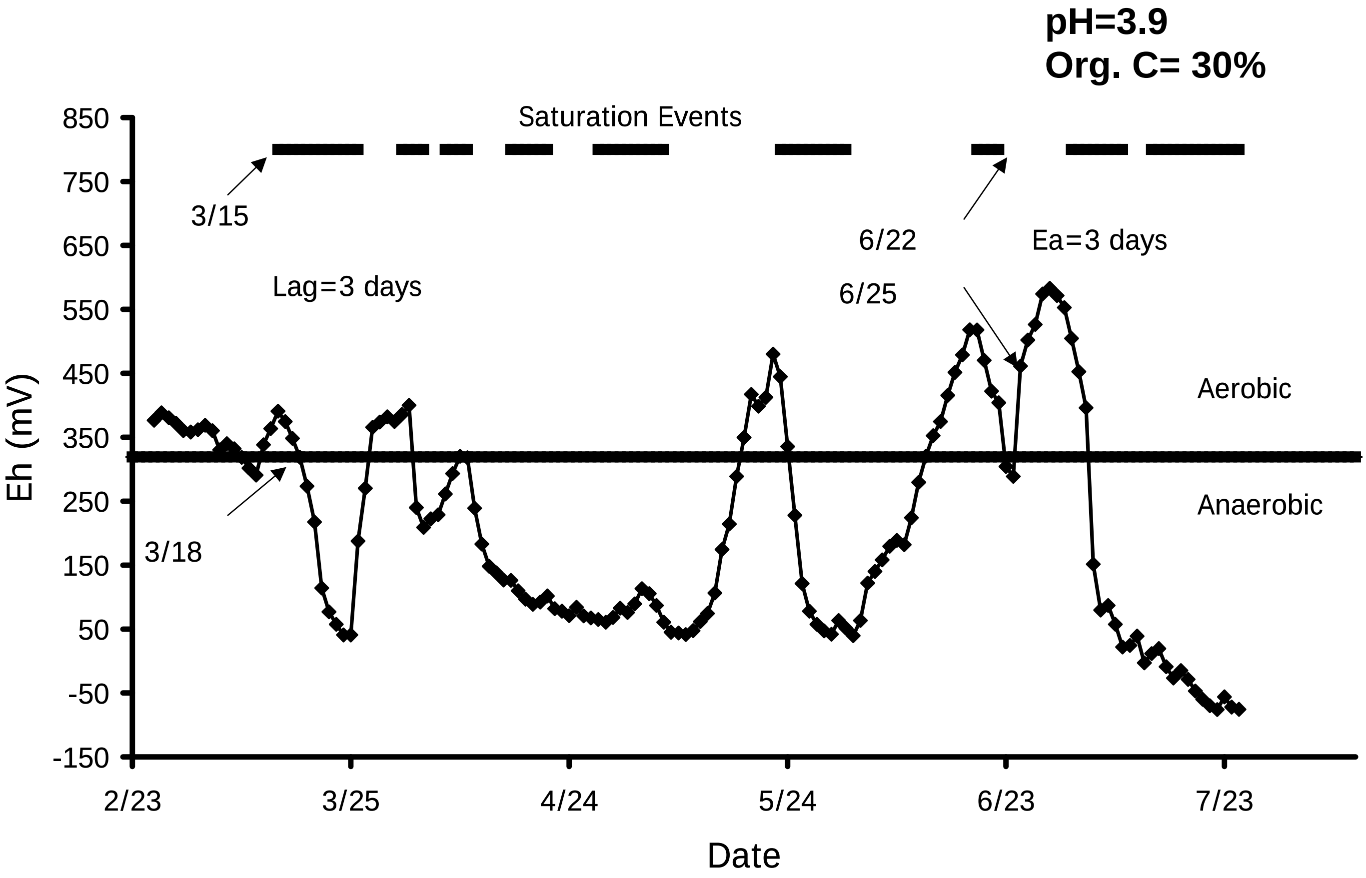

Figure 9.6. Example of Lag and Ea values at 24 in. an organic soil during winter, spring and summer months. Data points represent daily averages. The horizon saturated on 3/15/03 and anaerobic conditions began on 3/18/03, producing a Lag value of 3 days. After seven more saturation events the water table fell below 61cm on 6/22/03 and aerobic conditions returned on 6/25/03 producing and Ea value of 1d.

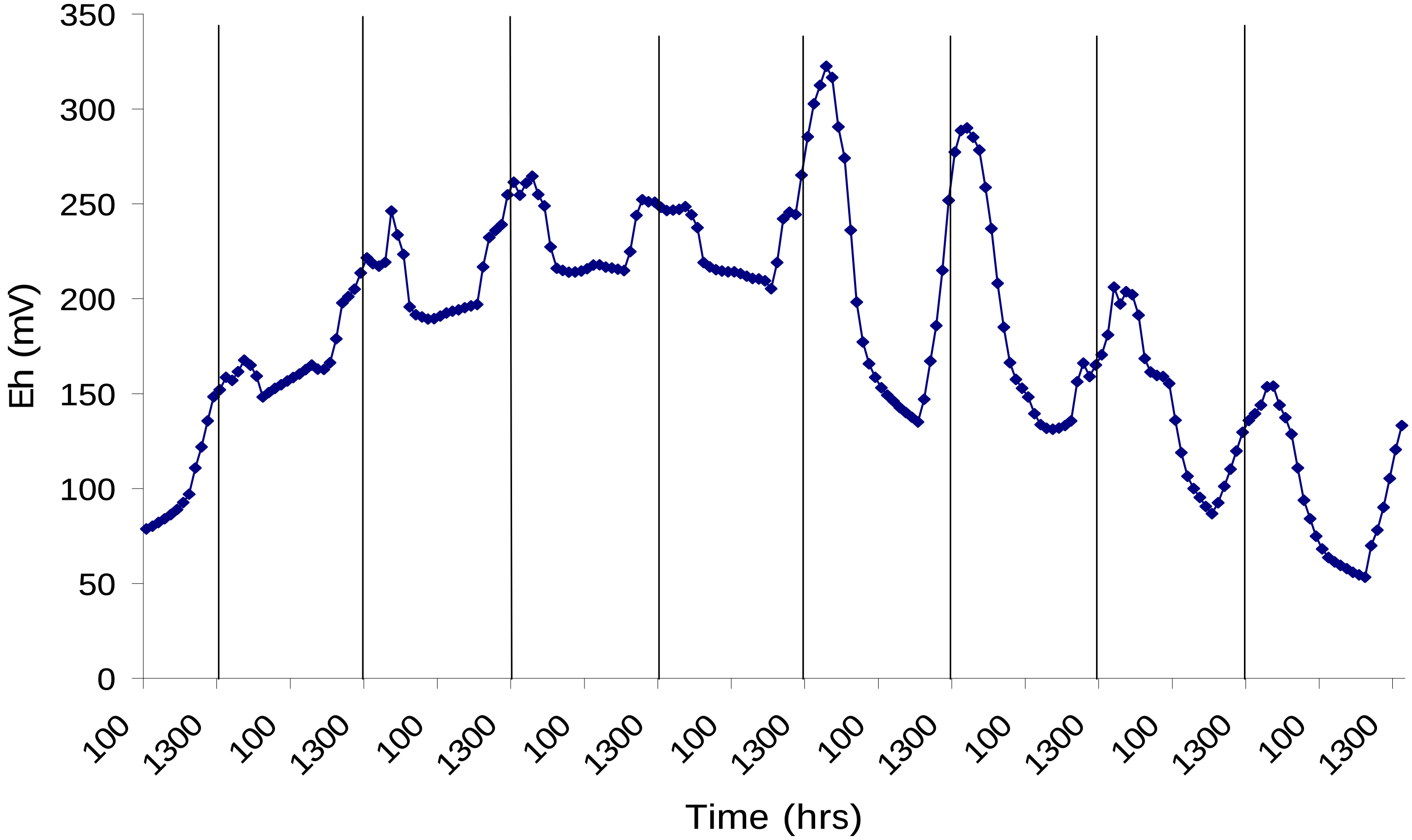

Figure 9.7. Example of diurnal fluctuations in Eh (10 in. depth) at one site with mineral soil in Juniper Bay during a time the soil was saturated. Measurements were made at 10-minute intervals between 8 to 16 October, 2003 during the growing season. A time of 100 is 1 AM and 1300 is 1 PM. The variations in Eh were observed in only one plot, and may be related to the respiration of a hydrophytic plant that is able to transmit oxygen to its roots.

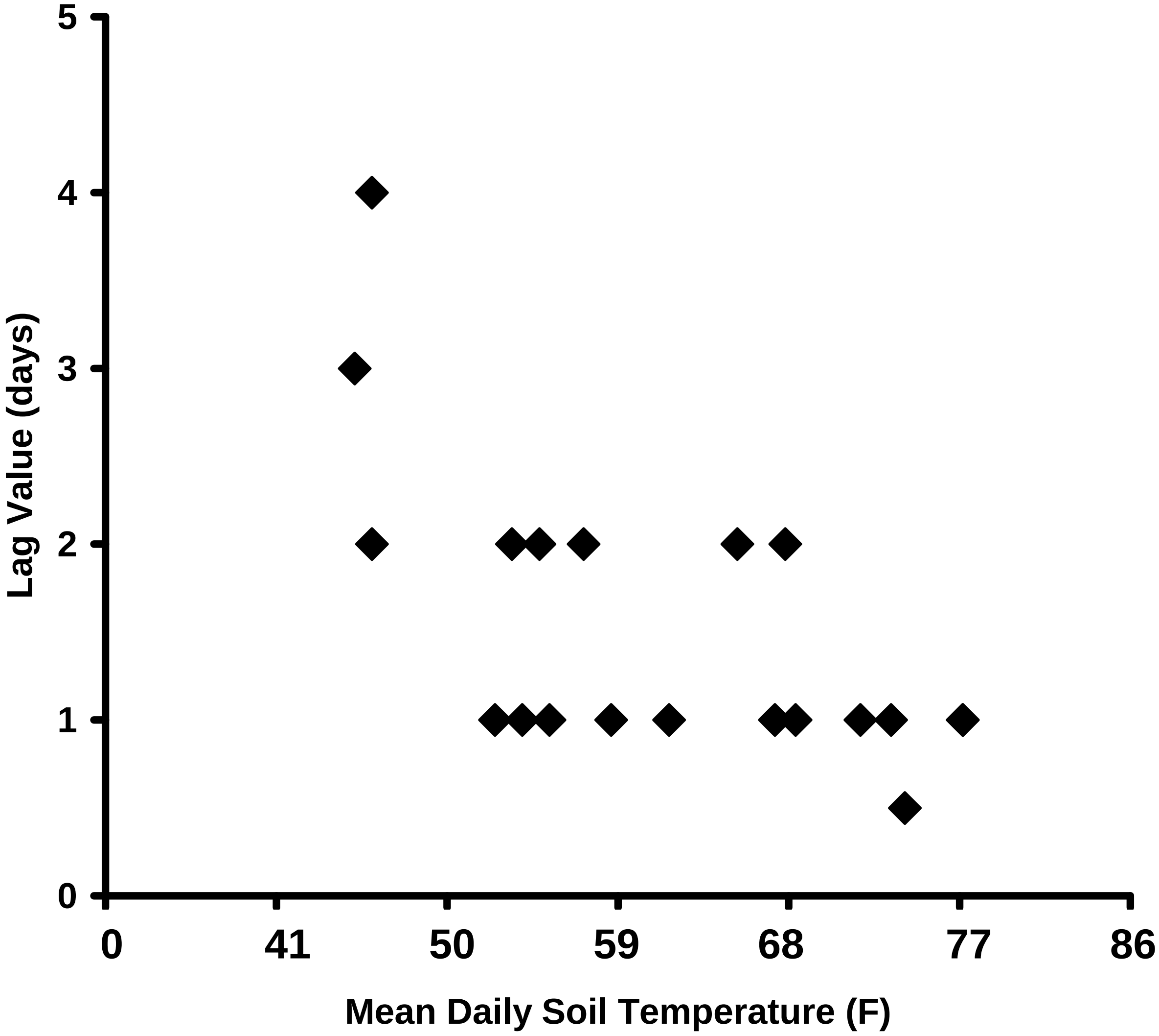

Figure 9.8. Relationship of mean daily soil temperature to Lag values in both mineral and organic soils at 10 and 24 in. Although lag time tended to increase as temperature decreased, temperatures were probably not low enough to slow microbial activity significantly. Soil temperature had virtually no significant relationship ($p > 0.5$) with Lag time, when measured at 24 in., in these soils. The interaction of soil temperature and soil organic carbon was also not significant ($p > 0.5$).

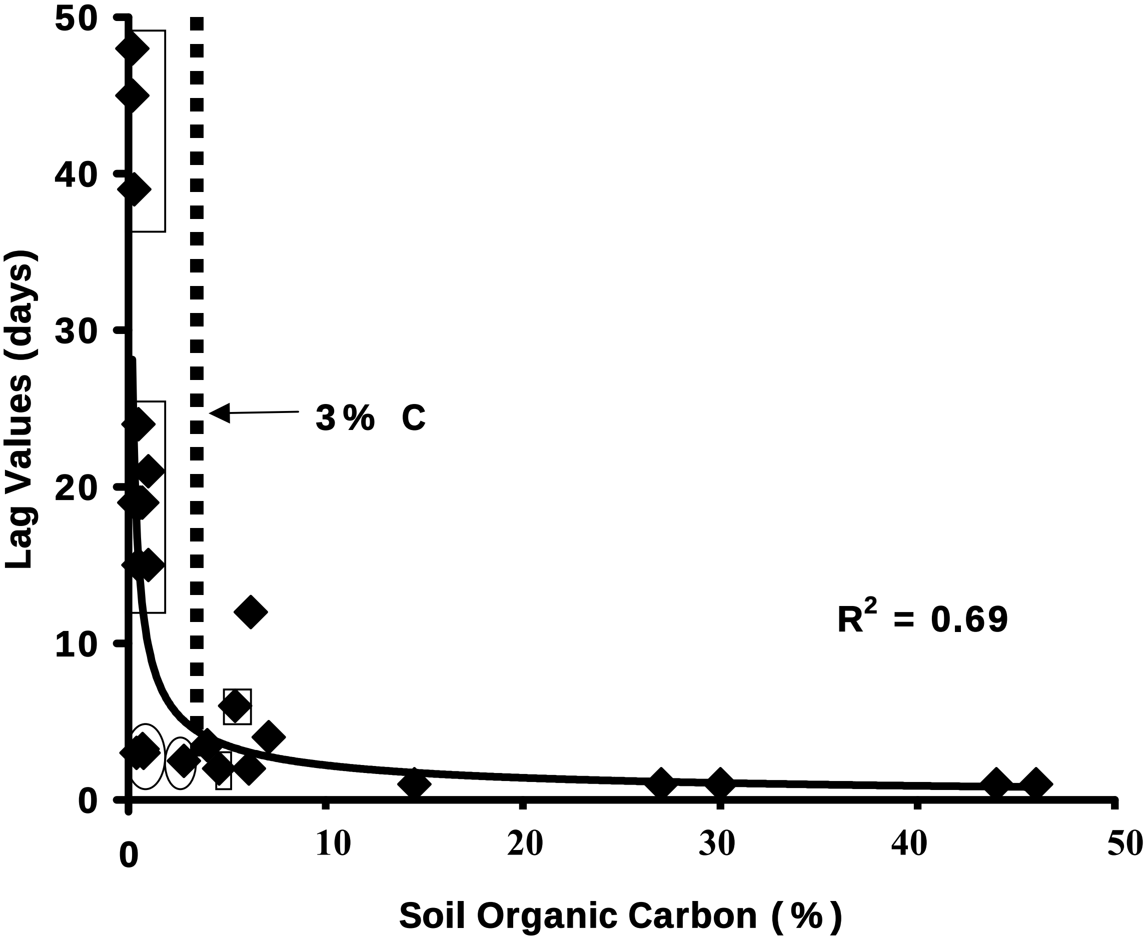

Figure 9.9. Relationship between soil organic C and Lag values. The line at 3% organic C was drawn by eye to separate plots with low lag values (1 to 5 days) from those with higher Lag values. Circled data points are for soil horizons that were overlain by horizons with higher organic C values. Data in boxes came from the study of He et al. (2003) which were added to see the influence of low C levels on Lag values.

Chapter 10

SOIL REDCUTION RATES UNDER WATER SATURATED CONDITIONS IN RELATION TO SOIL PROPERTIES IN CONTROLLED LABORATORY EXPERIMENTS

A.J. Zelasko, D.L. Hesterberg, and M.J. Vepraskas

INTRODUCTION

More than half of the original wetlands in the United States have been destroyed or otherwise lost (Dahl, 1990). Wetlands are valuable sources, sinks, and transformers of a multitude of chemical, biological and genetic materials (Mitcsh and Gosselink, 2000), and therefore must be managed as an environmental resource. Wetland restoration has become an important issue for maintaining the current land area of wetlands under the U.S. Wetland Reserve Program. According to the U.S. Army Corps of Engineers Wetland Delineation Manual (1987), if an area meets the criteria of hydrology, hydric soils, and hydrophytic vegetation; it is considered a wetland. Hydric soils are defined as soils that remain under conditions of saturation, flooding, or ponding long enough during the growing season to develop anaerobic conditions in the upper part (USDA, Soil Conservation Service, 1987). Oxygen, as O_2, is the main electron acceptor for heterotrophic microbial metabolism of organic carbon in aerobic soils. When soils are water saturated for extended periods, anaerobic conditions develop as O_2 becomes depleted during organic matter oxidation, and alternative electron acceptors such as NO_3, Mn(IV), Fe(III), and SO_4 are used. The length of time required for soils to become anaerobic varies, but the controlling factors are poorly understood. Accordingly, soil properties that are expected to affect redox reactions include water content, organic matter quantity and quality, and abundance of electron acceptors. Microbial ecology and temperature can also affect reduction rates given that they are microbially mediated processes.

Soil organic matter serves as the main energy source for microbial respiration. Research has shown that the length of time required for a soil to become anaerobic can depend on soil organic matter contents. Christensen et al. (1990) observed that a lag period of five days preceded increased denitrification rates in saturated soil cores after injection of particulate organic matter. Smith (2004) found that soils having total organic carbon (TOC) < 3% (30 g kg^{-1}) took more time to become anaerobic than soils with TOC > 3% (30 g kg^{-1}). He et al. (2003) showed that the time required to significantly reduce Fe(III) after saturation in the field varied from 2 to 48 d. Ponnamperuma (1972) indicated that soils with low organic matter concentration [(< 1.5 % (< 15 g kg^{-1})] or high Mn concentration [> 19.86 g kg^{-1} (> 390 mmol kg^{-1} soil)] could maintain redox potentials > 0 mV for 6 months or more following saturation.

With regard to carbon sources, dissolved organic carbon (DOC) is one component that serves as a source of energy for microbial respiration (Johnson and Ward, 1996;

Mann and Wetzel, 1996). In three limesink wetlands and one riparian wetland, an increase in the amount of DOC and a decrease in the proportion of aromatic carbon was noted during water inundation (Opsahl, 2005). Evidence from Hill et al. (2000) suggested that oxidized forms of N were depleted in reducing environments with high concentrations of DOC. Anaerobic conditions have been observed across a riparian zone in conjunction with DOC concentrations of 5 mg L^{-1} or higher (Vidon and Hill, 2004). Methane emissions were found to correlate to DOC concentrations in rice paddies (Lu et al., 2000). Despite correlations between DOC and soil reduction processes, Opsahl (2005) found that DOC was not a quantitative indicator of bioavailability of organic matter in all wetlands. Decreases in DOC with increasing bacterial abundances and biomass indicate that DOC stimulates microbial production (Johnson and Ward, 1996).

D'Angelo and Reddy (1999) found that microbial biomass carbon (MBC) correlated with TOC concentration in soils, and that inorganic N and MBC were the most reliable indicators of heterotrophic activity in all wetland soils studied. Lower amounts of MBC < 0.025 g kg^{-1} (< 25 μg g^{-1}) led to longer lag times for methane production in those soils.

The reduction of Fe(III) has been termed the most important chemical change that takes place in the development of anaerobic soils (Ponnamperuma, 1972). Iron is responsible for the typical red and yellow colors of soils. When Fe(III) is reduced to Fe(II), it becomes soluble and moves through the soil, altering its color. This process ultimately produces discrete features of contrasting coloration called redoximorphic features, which are used to identify hydric soils.

The course, rate, and magnitude of decreasing Eh in saturated soils also depends on the nature and content of electron acceptors (Ponnamperuma, 1972). Thermodynamics shows that more soluble Fe-oxides such as ferrihydrite provide more energy upon reduction than crystalline Fe-oxides (Lindsay, 1979). Lowe et al. (2000) suggested that poorly crystalline Fe(III) oxyhydroxides were the main terminal electron acceptors for microbial Fe(III) reduction in a salt marsh. Lovley (1991) found that hydroxylamine-extractable Fe was strongly correlated to microbial Fe(III) reduction in soils. The hydroxylamine-extractable Fe presumably contains organically-bound Fe and some poorly crystalline Fe-oxides, indicating that these forms are the primary source of reducible Fe(III) (Lovley, 1991). Roden (2003) found that the surface area of synthetic Fe(III) oxides dictated which types of Fe were more reducible, with rates of reduction being greater for ferrihydrite than goethite.

The reduction of submerged soils proceeds following a sequence of electron acceptors predicted by thermodynamics. Typically, O_2 is the first component to be reduced, followed by NO_3, Mn(IV)-oxides, Fe(III)-oxides, SO_4, and finally CO_2 (Ponnamperuma, 1972). Therefore, the amounts of reducible Mn and NO_3 in soil can have a significant affect on the rate of Fe(III) reduction under anaerobic conditions (Lovley and Phillips, 1998). According to Lovley (1991) net Fe(III) reduction does not occur in the presence of Mn(IV) and NO_3. The net suppression of Fe(III) reduction by Mn(IV) has been attributed to rapid oxidation of Fe(II) by Mn(IV), and a lower concentration of electron donors like organic matter in the presence of Mn(IV) (Lovley & Phillips, 1998). Native or added Mn(IV) poises Eh of flooded soils and suppresses the buildup of aqueous Fe(II) and other reduction products (Ponnamperuma, 1972). Soils with very elevated concentrations of nitrate 275 mg L^{-1} have also been shown to maintain higher soil Eh values for longer time periods than soils with less nitrate (Ponnamperuma, 1972).

Soil carbon to nitrogen (C/N) ratio has also been related to soil reduction rates. Gaunt et al. (1997) concluded that the C/N ratio of organically-enriched soil fractions controlled the rate of reduction upon flooding, with greater rates corresponding to lower C/N ratios. Wetland plants typically have a C/N ratio > 50, and as plant matter decays in the soil, CO_2 is evolved while N is retained. In this case, C/N ratio decreases to a stabile level of 15 to 25 instead of increasing with age (Nair et al., 2001).

In essence, the rate at which soils become reduced following water saturation depends on the availability of degradable organic carbon sources, and on the concentrations and chemical or mineralized forms of various electron acceptors ($O_{2,}$ $NO_{3,}$ Fe(III), $SO_{4,}$ CO_2). The objectives of this study were to (i) measure rates of soil reduction under water-saturated conditions for samples collected from different topographic settings and varying in redox-related properties, and (ii) determine whether reduction rate is related to soil properties, including concentrations and forms of organic matter, C/N ratio, MBC, and concentrations and forms of electron acceptors ($O_{2,}$ $NO_{3,}$ Fe(II), SO_4).

MATERIALS AND METHODS

Soil Sample Collection

Soil samples were collected from two different wetland sites, a Carolina bay named Juniper Bay located in Robeson County North Carolina and a topographic wetland Catena in Pitt county North Carolina. At Juniper Bay, soil samples were taken at two depths, 8 to 12 in. and 22 to 26 in. from three locations representing two soil series - Ponzer (a loamy, mixed, dysic, thermic, Terric Haplosaprists) and Leon (a sandy, siliceous, thermic, Aeric Alaquod). Soil profile descriptions for soils from Juniper Bay are given in Smith (2004). The wetland catena site was located approximately 5.1 km southwest of Greenville near Highway 13/264A at the Frog Level crossroads, 35° 34’ 10” latitude and 77° 26’ 26” longitude (Hayes and Vepraskas, 1998). Four sampling sites representing four different soil series were sampled: a moderately well-drained Goldsoboro soil (fine-loamy, siliceous, subactive, thermic, Aquic Paleudult), a somewhat poorly drained Lynchburg soil (fine-loamy, siliceous, semiactive, thermic, Aeric Paleaquult), a poorly-drained Rains soil (fine-loamy, siliceous, semiactive, thermic Typic Paleaquult), and a very poorly drained Pantego soil (fine-loamy, siliceous, semiactive, thermic, Umbric Paleaquult). Different soil horizons were sampled at each location down to a maximum depth of 12 in. Soil profile descriptions were conducted while sampling.

Soil Characterization

Moist soil samples were sieved through a 0.08 in. (2 mm) sieve and stored moist in 2 mil polyethylene bags at 39.2 ^oF (4 ^oC) to maintain partially aerobic conditions (Bartlett and James, 1993). The initial pH of the samples was taken within two weeks of sampling using a 1 to 1 soil to deionized-water ratio (Thomas, 1996).

Moist soil samples were analyzed for Fe and Al using citrate-bicarbonate-dithionite (CBD), sodium-pyrophosphate, and oxalate (dark) extractions. CBD and oxalate extractions were performed as described by Jackson et al. (1987). Sodium pyrophosphate extraction was performed as described by Loeppert and Inskeep (1996). All extracts were filtered through 7.9×10^{-6} in. (0.2 µm) Isopore polycarbonate filter membranes (Millipore Corp., Bedford, MA). Iron and Al in the CBD and oxalate extractions and Fe in the Na-pyrophosphate extractions were measured using flame atomic absorption spectrometry (FAAS) and reported on an oven dried [230 ^oF (110 ^oC)] basis.

Amounts of total organic carbon (TOC) and nitrogen were determined using a Perkin Elmer model PE 2400 CHNS elemental analyzer. Soil samples were oven dried at 230 ^oF (110 ºC) for 24 h, ground, and passed through a 0.08 in (2 mm) sieve prior to analysis. The C/N ratios ($g\ C - g^{-1}\ N$) were calculated from these measurements.

Fractionation of humic substances was carried out according to Swift (1996), using 10 to 20 g of moist soil. The humic acid and soil plus humin fractions were freeze dried and weighed to determine the total concentrations of humic acid and fulvic acid (by difference). Sample microbial biomass carbon (MBC) concentrations were measured using 15 g moist soil just prior to setting up the reduction incubation experiment (described below), and immediately following the experiment using the chloroform extraction method described by Vance et al. (1987).

Redox Incubation Design

Incubation experiments were performed to monitor soil reduction and re-oxidation during saturation and drainage, and soil porewater chemistry after saturation. Incubation systems consisted of 600 mL Buchner funnels with fritted glass plates and handmade polycarbonate lids (Fig. 1). A reference electrode (Ag/AgCl) and 2 handmade Pt tip electrodes (Wafer et al., 2004) were inserted into each column and connected to a Campbell Scientific CRX-10 data logger. The data logger measured Eh every 0.167 h, and averaged the six readings taken every hour. Eh measurements from both Pt tip electrodes in each column were averaged together for data analysis. Pore water samples were taken only under saturated conditions using 1.97 in. (5 cm) Rhizon Flex Pore water samplers. Samplers were buried in the columns 0.59 in. (1.5 cm) to 2.6 in. (6.5 cm) from the column rim (Item # 19.21.26, Rhizosphere Research Products, Dolderstraat 62 , NL 6706JG Wageningen. The Netherlands), and sampled water was replaced with distilled, deoxygentated H_2O.

The Pt tip electrodes were constructed as described by Wafer et al. (2004), using 5.0 in. (12.7 cm) of steel brazing rod. At the start of the incubation experiment Pt electrodes and reference electrodes were cleaned with steel wool and rinsed with DI water before testing with pH buffered quinhydrone solutions (pH 4 and 7) (Patrick et al., 1996), and a standard ferrous-ferric solution (Light, 1973). All electrodes produced Eh readings within 20 mV of the expected value. Pt tip electrodes were inserted 1.4 in. (3.5 cm) into the soil after packing and lid placement.

Salt bridges were constructed using 100 MPa round bottom straight wall ceramic cups purchased from Soil Moisture Equipment (#0652XO7-B01M1). Salt bridges were prepared by combining 20 mL of saturated KCl solution with 0.6 g of granular laboratory grade agar while continuously stirring and heating. After boiling, the hot agar mixture was transferred into the porous cups. The salt bridge was allowed to cool before inserting into the soil column. An Ag-Ag/Cl reference electrode was placed into each salt bridge after placing the lids securely onto the columns.

Following construction of the salt bridge, field moist soils were packed around the pore water samplers in the columns to a specified bulk density, 0.5 g cm^{-3} (Ponzer Oa-1, Oa-2 and Oa2-2), 0.9 g cm^{-3} (Pantego A), 1.2 g cm^{-3} (Goldsboro A, B, E, Rains A, E, Ponzer Oa2-1, Leon A/E, Bhir) and 1.5 g cm^{-3} (Lynchburg E, B, Pantego B, Rains B), depending on soil texture and assumed particle density of 1.3 g cm^{-3} for organic (Caldwell et al., 2007), and 2.65 g cm^{-1} for mineral soils.

Several precautions were taken in order to seal columns. Rubber gaskets were placed between funnel lids and the funnel and rubber stoppers were placed around Pt electrodes and pore water sampler. Silicon gel was placed around all devices on column lids to ensure lids were impervious to gas.

Incubation of Soil Samples

To aerate soil columns at the beginning of the experiment or following reduction cycles, a vacuum was placed on the bottom of the Buchner funnel and laboratory grade air (National Welders, Charlotte NC) was flushed across the headspace above the soil surface. Initial aeration was not applied to the first set of eight samples, but all results were similar so data was integrated. When Eh was $\geq$ 500 mV, anaerobic conditions were initiated by saturating with water. Saturation of columns was achieved by placing a vacuum in the headspace of each column while a constant head reservoir supplied water through the bottom of the funnel (Fig. 10.1). After soils were saturated, N_2 (g) was flushed across water ponded in the headspace of the columns. Two replications of soils underwent saturation and drainage three times for five or more days each cycle. During the last saturation phase, columns remained saturated until all samples became reduced. Soil columns were drained before removing soil for final storage and analysis, and an aerated state was maintained during storage.

Water samples were collected on days 1, 2, 3 and 5 of each 5-day reduction cycle. Samples were collected using 50 mL evacuated serum bottles with rubber stoppers that connected to the embedded pore water samplers through a lure lock valve and syringe needle. Vacuum bottles were weighed prior to and following water sampling to obtain sample masses. Sampled water was replaced with the same amount of de-oxygenated water to maintain a constant water volume in the soil columns.

The pH and concentrations of Fe(II) in water samples were analyzed immediately in most cases, and no longer than 48 h after sampling. Colorimetric determination of Fe(II) was conducted by adding 0.1 mL of concentrated HCl, 1 mL of 0.1% 1,10-phenanthroline, 0.5 mL of ammonium acetate, and 1 mL of deionized water (Clesceri et al., 1989; Olson and Ellis, 1982). Dissolved Al, Fe, SO_4, and NO_3 were measured using optical emission spectrometry and ion chromatography analysis. At the conclusion of the incubation experiment, soils were stored as described earlier (Bartlett and James, 1993), and final MBC was measured within two weeks.

Statistical Analysis

Three replications were performed for all initial soil analysis. The incubations, measurement of MBC, and Fe(II) were performed in duplicate. To quantify the rate at which soils reduced, zero order rate coefficients calculated from the slope between points within the most linear portion of each reduction phase were used. Analysis of variance and Fishers protected least significant difference tests were used to determine if groups of data were significantly different. Multiple linear regression analysis estimated relationships between reduction rate and all initial soil properties measured on both mineral and organic soils.

RESULTS AND DISSCUSION

Soil Properties

Selected soil properties for all soil samples are shown in Table 10.1. Initial pH of soil samples ranged from 3.7 to 5.4 while final pH ranged from 3.7 to 5.5. Total organic carbon ranged from 0.27% (2.7 g kg^{-1}) in mineral soils to 56% (560 g kg^{-1}) in organic soils, and C/N ratio ranged from 28 g g^{-1} to 60 g g^{-1} or greater. Extractable Fe varied among soil types, ranging from 0.30 g kg^{-1} (5.3 mmol kg^{-1}) to 10.2 g kg^{-1} (182 mmol kg^{-1}) for CBD extractable Fe, from 0.02 g kg^{-1} (0.4 mmol kg^{-1}) to 2.3 g kg^{-1} (41.4 mmol kg^{-1}) for oxalate extractable Fe, and from 0.03 g kg^{-1} (0.6 mmol kg^{-1}) to 2.6 g kg^{-1} (47 mmol kg^{-1}) for pyrophosphate extractable Fe. CBD extractable Fe was always greater than oxalate and sodium-pyrophosphate extractable Fe. CBD-extractable Al varied from 0.30 g kg^{-1} (5.3 mmol kg^{-1}) to 11.2 g kg^{-1} (200.1 mmol kg^{-1}). The temperature in the room used for soil incubation ranged from 75.2° F (24° C) to 80.6 ° F (27° C) with a mean of 78.26 ± 3.14° F (25.7 ± 1.03° C) (n = 22).

Incubation Experiment

Thirteen of the 16 soil samples were successfully incubated in duplicate. The Eh began to decrease in most incubation systems, as predicted by thermodynamics, within 12 h of water saturation. The rate of decreasing Eh was dependent on soil type and pH (Figure 10.2). Reduction rates, calculated over the linear portion or each reduction cycle as denoted by "X" in Figure 10.2, were consistently slower than oxidation rates. As illustrated in Figure 10.2, reduction rates varied between consecutive cycles, and Eh typically stabilized at different values (Figure 10.2). One mineral soil did not drain well and remained reduced following flushing with air. None of the organic soils could be re-oxidized after initial saturation, although two organic soil incubations did show increases and decreases up to ± 300 mV in Eh with imposed aeration and saturation.

The averaged reduction rates for each soil sample and cycle are shown in Figure 10.3. Reduction rates from the upland soils from the Greenville site (Goldsboro and Lynchburg) showed reduction rates that tended to decrease with consecutive reduction cycles, while lowland soils (Rains and Pantego) showed reduction rates that tended to increase with consecutive reduction cycles. Juniper Bay soils showed no consistent trends between consecutive reduction cycles. Variance between replications was high for many soils especially during the first reduction cycle. Reduction rates were also calculated using a polynomial model. Although trends in data were similar, significance or results was much lower than when using the linear method.

Manual Eh readings typically followed the same trend and were within ± 20 mV from the data logger Eh readings (data not shown), although discrepancies can occur between Eh readings taken using a data logger (Bochove et al., 2002). In the first and third replications of the experiment data logger readings were significantly different (> 20 mV) from manual readings for the third reduction cycle only. When data logger readings were continuously different than manual readings, reduction rates were calculated from manual readings. Differences between the data logger and manual readings were most likely due to drift when the redox stability of the systems was low (Bochove et al., 2002). The mean of all three reduction cycles for each sample were used to relate reduction rate to soil properties. Comparisons between measured soil properties and reduction rates were performed using mineral soils only due to problems with re-oxidizing organic soils. Eleven soil samples were compared in duplicate, yielding 22 different experimental average reduction rates.

Table 10.2 shows correlation results between reduction rate and selected soil properties, and summarizes the best fit multiple linear regression models when using all three reduction cycles to determine reduction rate. Soil properties significantly correlated to reduction rate included TOC, average DOC, and dissolved Fe(II). The strongest correlation found was between reduction rate and TOC using a linear plateau model ($r = 0.82$; Figure 10.4). It was evident that the first reduction cycle in each incubation differed from the second two (Figure 10.3). For this reason, reduction rate was also calculated using only the second two reduction cycles. Correlations were very similar and generally less significant than when using all three reduction cycles to calculate reduction rates (Zelasko, 2007).

Figure 10.4, displaying TOC in relation to reduction rate, shows that reduction rate in soils with TOC < 2.7 % (TOC < 27 g kg^{-1}) increased with increasing TOC, while reduction rate in soils with TOC ≥ 2.7 % (TOC ≥ 27 g kg^{-1}) was not dependent on TOC. When only the second and third reduction cycles were used the linear plateau model increased up to TOC = 1.66 % (TOC = 16.6 g kg^{-1}) and stabilized at TOC = 1.66 % (TOC = 16.6 g kg^{-1}) (Zelasko, 2007). Further analysis showed that soils with TOC ≥ 2.7 % (TOC ≥ 27 g kg^{-1}) had nearly three times the reduction rate (mV h^{-1}) than soils with TOC

< 2.7 % (TOC < 27 g kg^{-1}) supporting this observation (Table 3). Soils with TOC ≥ 2.7 % (TOC ≥ 27 g kg^{-1}) included the Ponzer horizons, the Leon A/E horizon, the Goldsboro A horizon, the Rains A horizon, and the Pantego A horizon. Soils with TOC < 2.7 % (TOC < 27 g kg^{-1}) included the Goldsboro E and B horizons, the Lynchburg E and B horizons, the Rains E and B horizons the Pantego B horizon, and the Leon Bhir horizon (Table 10.1). These findings are somewhat consistent with field measurements of Smith (2004) which indicated that time to reduction was slower in soils with TOC < 3.0 % (TOC < 30 g kg^{-1}) than those with TOC > 3.0 % (TOC > 30 g kg^{-1}).

When combined with TOC in a multiple linear regression model, pH was a significant variable correlated with soil reduction rates (Table 10.2). The increase in solution pH during the first saturation cycle was nearly three times larger (p-value = 0.16) for soils that released high amounts of Fe(II) than in soils that released very little to no Fe(II) during saturation, corresponding with previous research that the increase in pH of acid soils is largely due to the reduction of iron (Ponnamperuma, 1972). Initial and final pHs in redox incubation experiments were not significantly different (Table 10.3), although findings have shown that when an aerobic soil is submerged, its pH decreases during the first few days, reaches a minimum, and then increases asymptotically to a fairly stable value (Ponnamperuma, 1972).

Our measurements of DOC showed an increase from day 0 to day 1 and 2 for all soils likely due to anaerobic microbial activity (Johnson and Ward, 1996; Mann and Wetzel, 1996; Hill et al., 2000; Vidon and Hill, 2004). DOC was correlated with reduction rate ($r = 0.47$; $p = 0.02$; Table 2.2) although DOC was not significantly different between soils with TOC ≥ 2.7 % (TOC ≥ 27 g kg^{-1}) and soils with TOC < 2.7 % (TOC < 27 g kg^{-1}) (Table 10.3). Previous research indicated that DOC can indicate the bioavailability of organic matter in some wetlands, but not all (Opsahl, 2005).

Dissolved Fe(II) typically increased with decreasing Eh Figure 10.5 and was significantly correlated with reduction rate ($r = 0.45$), as predicted by thermodynamics. Three groups of soils were distinguishable when comparing dissolved Fe(II) relative to Eh (Figure 10.5). One group showed a high increase in dissolved Fe(II) with decreasing Eh (up to 23 Fe(II) mg L^{-1}), and included the Pantego A and B horizons, the Goldsboro A horizon and the Rains A horizon. The second group showed a moderate increase in dissolved Fe(II) with decreasing Eh (up to 6 Fe(II) mg L^{-1}), and included the Rains B horizon, and the Lynchburg E horizon. The remaining soil samples showed little to no increase in dissolved Fe(II) with decreasing Eh. The amount of Fe(II) dissolved decreased between consecutive reduction cycles (Zelasko, 2007).

When grouped, soils with TOC ≥ 2.7 % (TOC ≥ 27 g kg^{-1}) had nearly three times the oxalate to CBD Fe ratio as soils with TOC < 2.7 % (TOC < 27 g kg^{-1}) ($p < 0.05$) (Table 10.3), supporting previous findings that less crystalline Fe minerals are more soluble than more crystalline Fe minerals. The rate of bacterial Fe(III) reduction has been shown to depend on the surface area of Fe minerals (Roden, 2003). Our results are consistent with previous findings showing that soils with high amounts of poorly crystalline Fe-oxides reduce more quickly than soils with low amounts of poorly crystalline Fe-oxides (Lovely, 1991; Roden, 2003).

The C/N ratio was higher for organic soils collected from Juniper Bay than for mineral soils collected from the wetland catena, and was correlated to reduction rate ($r = 0.41$, p-value < 0.10). It was logical that the C/N ratio would be different between wetland sites because Juniper Bay had been in agriculture production and fertilized for several years, while the catena site had been forested. The C/N ratio was not significantly different between soils with TOC ≥ 2.7 % (TOC ≥ 27 g kg^{-1}) and soils with TOC < 2.7 % (TOC < 27 g kg^{-1}) (Table 10.3).

Initial MBC varied from 74.6 to 13200 mg kg^{-1} over all samples, while final MBC varied from 117 to 1410 mg kg^{-1} (Zelasko, 2007). The initial MBC measurements taken in this experiment were very high and often exceeded 3% of the TOC. The high measurements indicate a possible error in laboratory technique. Final MBC measurements were much lower and closer to expected values. In this research TOC was correlated to final MBC ($r = 0.76$, $p <0.0001$) as predicted by previous research (D'Angelo and Reddy, 1999).

Application of Results

Multiple soil properties appeared to affect soil reduction rates (Table 10.2) so a multiple linear regression was conducted to develop an equation that could be used to predict soil reduction rates. Of all soil properties evaluated, the best two variable model for mineral soils included pH and TOC ($R^2 = 0.49$, $p < 0.05$) (Table 2). Three or more variables could not be used due to inter-correlations between TOC and other soil properties such as MBC and C/N ratio. The regression model, listed in Table 2 could be used along with hydrologic data to predict reduction rates prior to water saturation.

As further refinement of regression analysis, soils were divided into two groups of TOC < 2.7 % (TOC < 27 g kg^{-1}) and TOC ≥ 2.7 % (TOC ≥ 27 g kg^{-1}), and multiple linear regressions analysis was done on each group to determine if a stronger relationship could be found to predict soil reduction rates. For soils with TOC < 2.7 % (TOC < 27 g kg^{-1}), TOC and average DOC fit best into a two variable model to predict reduction rate ($R^2 = 0.48$; $p < 0.05$;). For soils with TOC ≥ 2.7 % (TOC ≥ 27 g kg^{-1}), dissolved Fe(II) and TOC gave the best model ($R^2 = 0.54$; $p >0.25$;). The multiple linear regression model for TOC ≥ 2.7 % (TOC ≥ 27 g kg^{-1}) (Table 2) was produced using only six data points resulting in a non-significant model. Results by Smith (2004) showing that time to reduction was faster when TOC > 3.0 % (TOC > 30 g kg^{-1}) correspond to these results.

Results from multiple linear regressions could be applied, along with hydrologic data, in wetland restoration and delineation as an easy, inexpensive method for determining the length of time soils are hydric. Data showing water table fluctuations with time can be used to determine the length of time the soil is saturated in the upper part. Using water table data in conjunction with Figure 10.6, which shows the time required for soil Eh to drop by 500 mV compared to TOC, allows us to predict the frequency and duration of reduced conditions by comparing how long a soil is saturated in the upper part to how long it would take for the soil to become reduced under saturated conditions. An easy method of predicting the frequency and duration that soils meet hydric criteria is very important for large scale wetland delineation because installing redox monitoring systems can be very expensive. Using this linear plateau model in conjunction with water table data could be an easy inexpensive alternative to installing several redox monitoring systems.

Based on our data, TOC along with hydrologic data would provide the best overall estimate for how quickly soils will reduce once saturated (Figure 10.4). Both pH and TOC are readily available or easily measured soil properties, however, different models could be used based on the availability of soil information at restoration sites. Predicting soil reduction rate can serve as a valuable tool for ensuring success of wetland restoration projects.

CONCLUSIONS

Redox potential measurements in incubated soils showed a rapid (typically < 12 h) decline following saturation with water. The reduction rate varied among soil types, indicating variations in soil properties affected reduction rates. Reduction rate was significantly correlated to TOC, DOC, Fe(II) and C/N ratio, but showed the greatest correlation with TOC using a linear plateau model (r = 0.82). Amount of humic acid, DOC, TOC, oxalate to CBD extractable Fe ratio, and C/N ratio were significantly different between soils with TOC < 2.7 % (TOC < 27 g kg^{-1}) and soils with TOC $\geq$ 2.7 % (TOC $\geq$ 27 g kg^{-1}), suggesting that all of these variables in part affected soil reduction rates. A model using TOC and pH ($R^2 = 0.49$) was determined using multiple linear regression analysis. The relationships found between soil properties and reduction rates can be used along with hydrologic data to predict reduction rates for wetland delineation and restoration purposes. The linear plateau model using TOC to predict reduction rate would serve as the most accurate method, although other models such as the multiple linear regression using TOC and pH could be used. Predicting the time to reduction without installing expensive equipment over long time periods can be beneficial to the success and speed of wetland delineation.

REFERENCES

Bartlett, R. J., and B. R. James. 1993. Redox chemistry of soils. Advances in Agronomy. 50:151-208.

Bastviken, S. K., P. G. Eriksson, A. Premrov, and K. Tonderski. 2005. Potential denitrification in wetland sediments with different plant species detritus. Eco. Eng. 25:183-190.

Bochove, E., S. Beauchemin, and G. Theriault. 2002. Continuous Multiple Measurement of Soil Redox Potential Using Platinum Microelectrodes. Soil Sci. Soc. of Am. J. 66:1813-1820.

Caldwell, P. V., M. J. Vepraskas, J. D. Gregory. 2007. Physical properties of natural organic soils in carolina bays of the southeastern United States. Soil Sci. Soc. of Am. J. 71:1051-1057.

Christensen, S., S. Simkins, and J. M. Tiedje. 1990. Temporal patterns of soil denitrification: their stability and causes. Soil Sci. Soc. Am. J. 54:1614-1618.

Clesceri, L. S., A. E. Greenberg, and R.R. Trussell. 1989. Standard methods for examination of water and wastewater. 17th ed. American Public Health Association, Washington DC.

Dahl T. E., 1990. Wetland losses in the United States,1780s to 1980s. U.S. Department of Interior, Fish and Wildlife Service, Washington, DC.

D'Angleo, E. M., and K. R. Reddy. 1999. Regulators of heterotrophic microbial potentials in wetland soils. Soil Biology and Biochemistry. 31:815-830.

Gaunt, J. L., H. U. Neue, J. Bragais, I. F. Grant, and K. E. Giller. 1997. Soil characteristics that regulate soil reduction and methane production in wetland rice soils. Soil Sci. Soc. Am. J. 61:1526-1531.

Hayes, W. A., and M. J. Vepraskas. 2000. Morphological changes in soils produced when hydrology is altered by ditching. Soil Sci. Soc. Am. J. 64:1893-1904.

He, X., M. J. Vepraskas, D. L. Lindbo, and R. W. Skaggs. 2003. A method to predict soil saturation frequency and duration from soil color. Soil Sci. Soc. Am. J. 67:961- 969.

Hill, A. R., K. J. Devito, S. Campagnolo, and K. Sanmugadas. 2000. Subsurface denitrification in a forest riparian zone: Interactions between hydrology and supplies of nitrate and organic carbon. Biogeochemistry. 51:193-223.

Jackson, M. L., C. H. Lim, and L. W. Zelazny. 1986. Oxides, hydroxides, and aluminosilicates. p. 101-150 *In* A. Klute (ed.) Methods of Soil Analysis, Part 1. Physical and mineralogical methods, ASA and SSSA, Madison, WI.

Jenkinson, D. S., J. N. Ladd. 1981. Microbial biomass in soil, measurement and turnover. p. 415-472. *In*. E.A. Paul and J.N. Ladd (ed.) Soil Biochemistry, Vol. 5. Marcel Dekker, Inc., New York.

Johnson, M. D. and A. K. Ward. 1996. Influence of phagotrophic protistan bacterivory in determining the fate of dissolved organic matter (DOM) in a wetland microbial food web. Microb. Ecol. 33:149-162.

Light, T. S. 1973 Standard solutions for redox potential measurements. Analytical Chemistry. 44:1038-1044.

Lindsay, W. L. 1979. Chemical equilibria in soils. John Wiley & Sons, New York, NY.

Loeppert, R. H., and W. P. Inskeep. 1996. Iron. p. 639-664 *In* D. L. Sparks (ed.) Methods of soil analysis, part 3. Chemical methods, ASA and SSSA, Madison, WI.

Lovley, D. R. 1991. Dissimilatory Fe(III) and Mn(IV) reduction. Microbiological Reviews. 55:259-287.

Lovley, D. R., and E. J. Phillips. 1998. Manganese inhibition of microbial iron reduction in anaerobic sediments. Geomicrobiol. J. 6:145-155.

Lowe, K. L., et al. 2000 Microbiological and geochemical characterization of microbial Fe(III) reduction in salt marsh sediments. Geomicrobiol. J. 17:163-178.

Lu, Y. R. Wassmann, H. Neue, and C. Huang. 2000. Dissolved organic carbon and methane emissions from a rice paddy fertilized with ammonium and nitrate. J. Environ. Qual. 29:1733-1740.

Mann, C. J., and R. G. Wetzel. 1996. Loading and utilization of dissolved organic carbon from emergent macrophytes. Aquatic Botany. 53:61-72.

Mitsch, W. J. and J. G. Gosselink. 2000. Wetlands. 3rd ed. John Wiley and Sons, New York, NY.

Nair, V. D., D. A. Graetz, K. R. Reddy, and O. G. Olila. 2001. Soil development in phosphate-mined created wetlands of Florida, USA. Wetlands 21:232-239.

Olson, R. V. and R. Ellis JR. 1982. Iron. p. 301-312. *In* Methods of Soil Analysis Part 2. Chemical and microbiological properties. ASA and SSSA. Madison WI.

Opsahl, S. P. 2005. Organic carbon composition and oxygen metabolism across a gradient of seasonally inundated limesink and riparian wetlands in the southeast coastal plan, USA. Biogeochem. 76:47-68.

Patrick, W. H., R. P. Gambrell, and S.P. Faulkner. 1996. Redox measurements of soils. *In* Methods of Soil Analysis Part 3. Chemical methods. ASA and SSSA Madison, WI.

Ponnamperuma F. N. 1972. The chemistry of submerged soils. Advances in Agronomy. 24:29-96.

Thomas, G. W. 1996. Soil pH and soil acidity. p 475-490 *In* D. L. Sparks (ed.) Methods of soil analysis, part 3. Chemical Methods. ASA and SSSA, Madison, WI.

Richardson, J. L., and M. J. Vepraskas. 2001. Wetland soils: Genesis, hydrology, landscapes, and classification. CRC Press LLC. FL.

Roden, E. E. 2003. Fe(III)-oxide reactivity toward biological versus chemical reduction. Env. Sci. & Tech. 37:1319-1324.

Smith, H. C. 2004. Time required for anaerobic conditions to develop in saturated soils. Master's Thesis, North Carolina State University, Raleigh, NC.

Swift, R. S.1996. Organic matter characterization. p. 1011-1069 *In* D. L. Sparks (ed.) Methods of soil analysis. Part 3. Chemical Methods. ASA and SSSA, Madison, WI.

U.S. Army Corps of Engineers. 1987. Corps of engineers wetland delineation manual. Technical report Y-87-1. Army Corps of Engineers Waterways Experiment Station, Vicksburg, MS.

USDA Soil Conservation Service. 1987. Hydric soils of the United States. In Cooperation with the National Technical Committee for Hydric Soils. Washington, D.C.

Vance, E.C., P.C. Brookes, and D.S. Jenkinson. 1987. An extraction method for measuring soil microbial biomass C. Soil Biol. Biochem. 19:703–707.

Vidon, P., and A. R. Hill. 2004. Denitrification and patterns of electron donors and acceptors in eight riparian zones with contrasting hydrogeology. Biogeochemistry. 71:259-283.

Wafer, C. C., J. B. Richards, and D. L. Osmond. 2004. Construction of platinum-tipped redox probes for determining soil redox potential. J. Env. Qual. 33:2375-2379.

ACKNOWLEDGEMENT

This chapter was as a portion of A.J. Zelasko's M.S. Thesis entitled "Soil Reduction Rates under Water Saturated Conditions in Relation to Soil Properties" that was earned through NC State University and is available through the university's library.

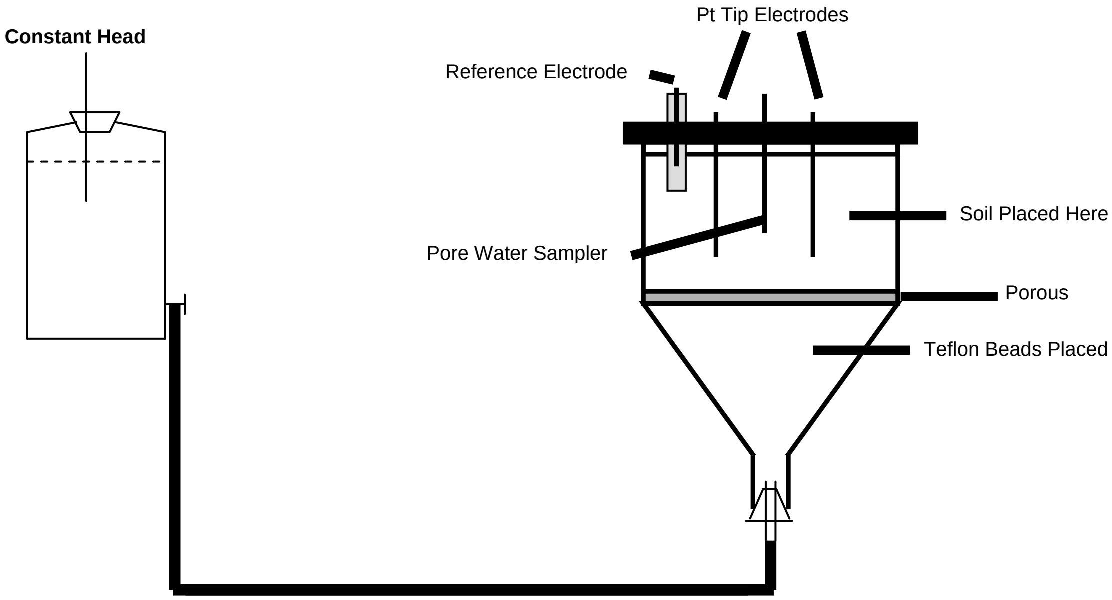

Figure 10.1: Redox incubation system depicting buchner funnel on right with Pt tip electrodes, reference electrode, pore water sampler and salt bridge. Soil was packed above the porous plate and teflon beads were placed below to minimize the amount of water during incubation. A constant head reservoir (left) was used to saturate columns from the bottom upward.

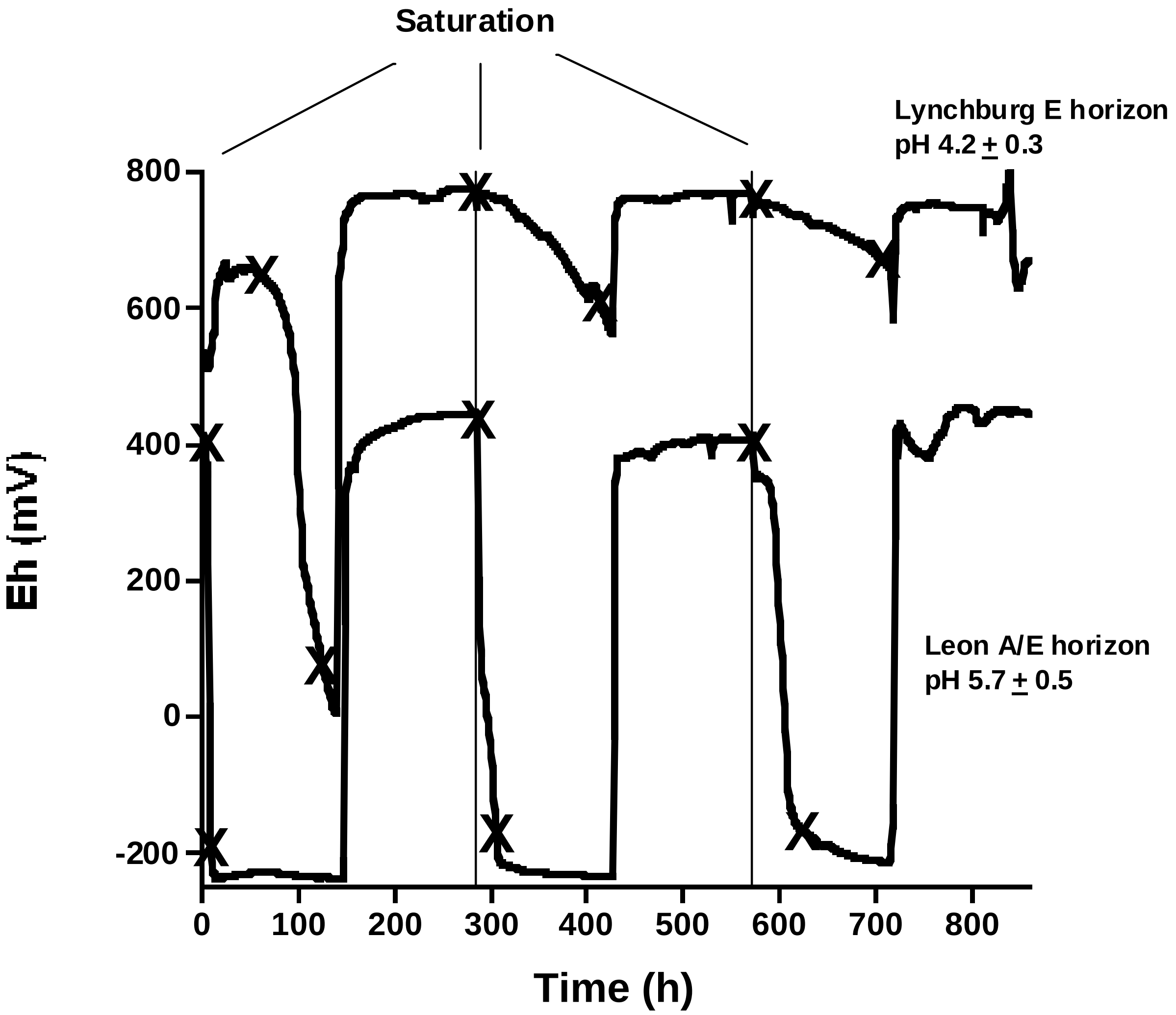

Figure 10.2: Three reduction-oxidation cycles of one replication of two different soil samples: the Lynchburg E horizon, and the Leon A/E horizon. The Y axis and the black vertical lines denote times where the water level was raised to saturate soils. “X” represents the endpoints of data used in the linear regression used to determine reduction rate.

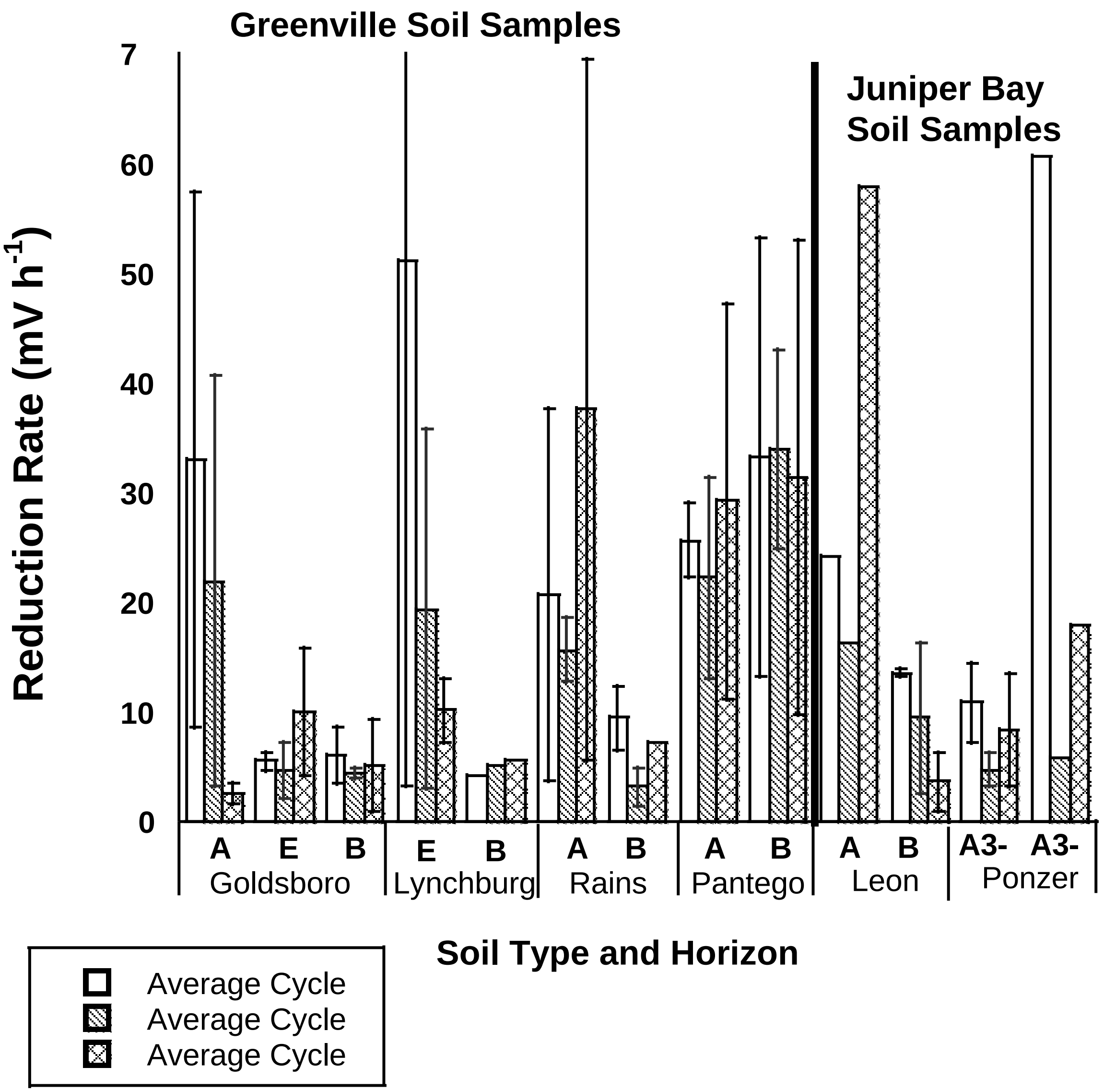

Fig 10.3: Average reduction rates for different soil samples in duplicate. The X axis is arranged by soil series, horizon, location, and landscape position (highest landscape position to left, lowest landscape position to right). Reduction rate was variable in many columns between cycles.

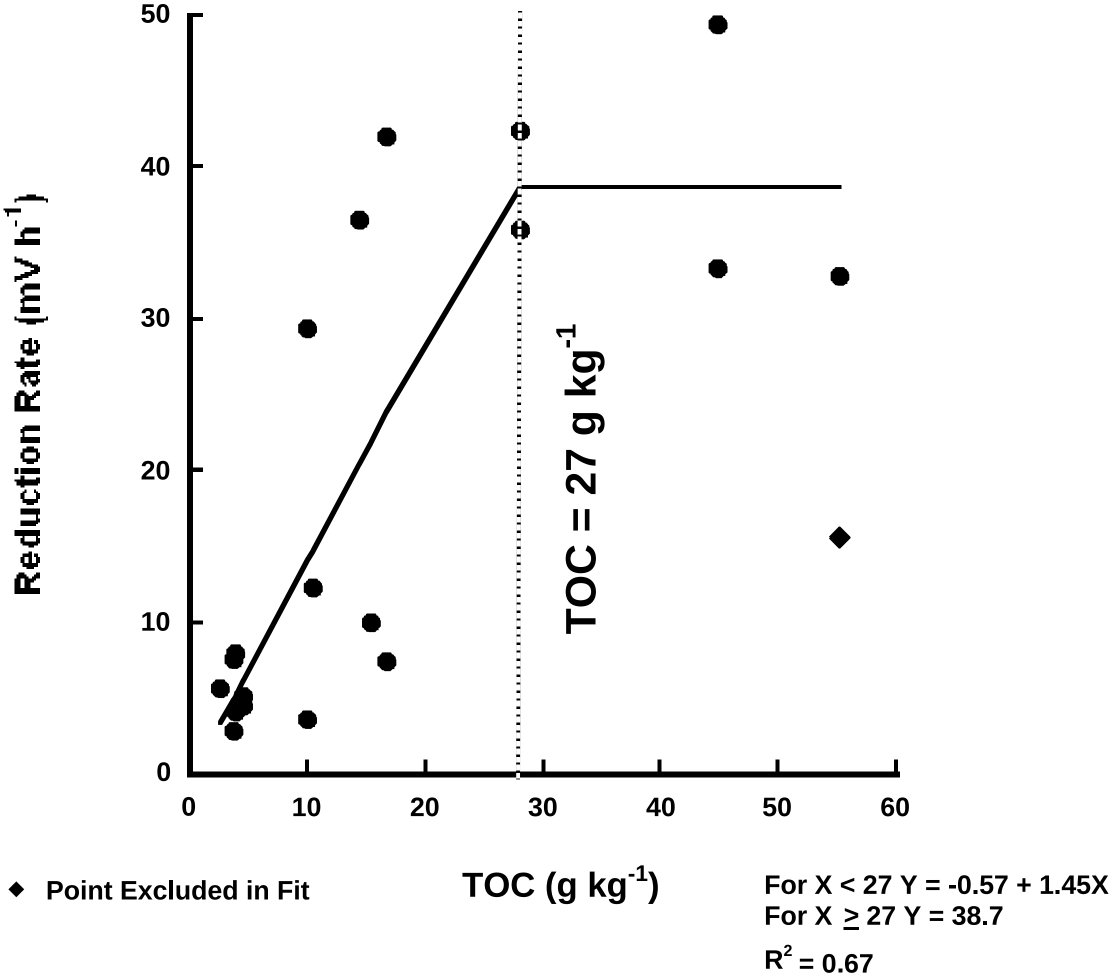

Figure 10.4: Total organic carbon (TOC) concentration in relation to reduction rate. A linear plateau model shows increasing reduction rate with increasing TOC up until TOC = 2.7 % (TOC = 27 g kg^{-1}). One outlying point, pictured as a diamond, was excluded from this fit.

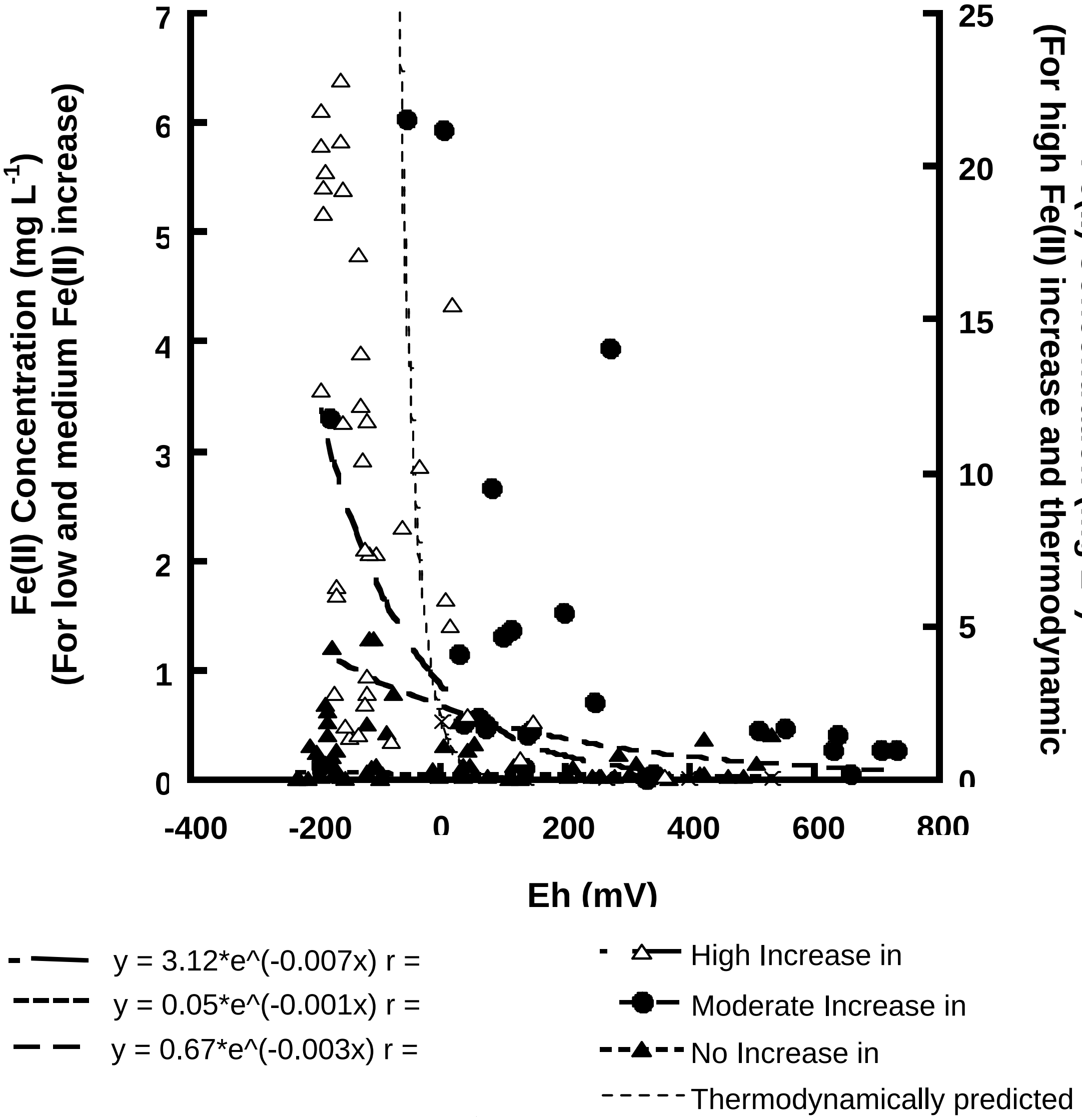

Figure 10.5: Dissolved Fe(II) (mg L^{-1}) vs. Eh for redox incubations. Three groups were denoted: those with high increases in Fe(II) (Pantego A and B horizons, Goldsboro A horizon, and Rains A horizon – right Y axis), those with moderate increases in Fe(II), (Rains E and B horizons, Lynchburg E horizon – left Y axis), and those with no increase in Fe(II), (remaining soils – left Y axis). The smooth curve corresponds to the thermodynamically predicted rate of Fe(II) dissolution from goethite, (right y axis).

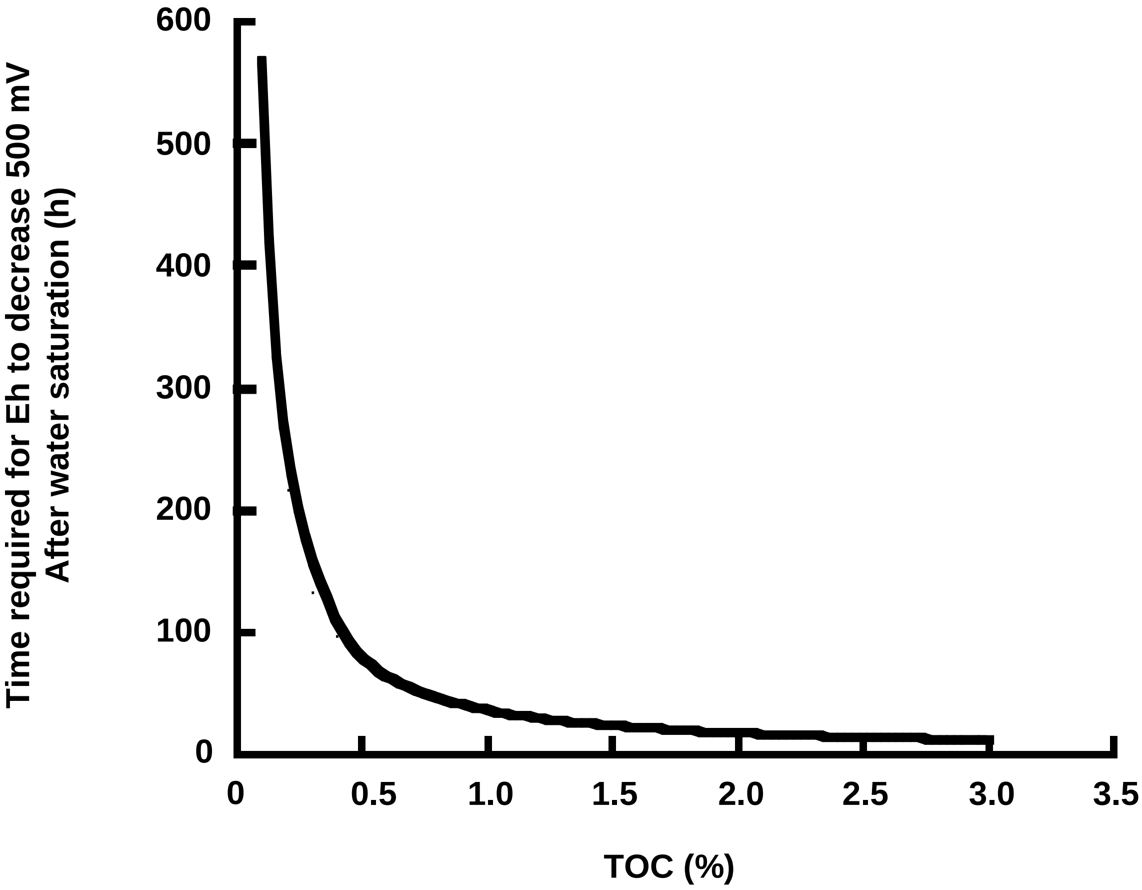

Figure 10.6: Total organic carbon (TOC) compared to the amount of time it would take for soil Eh to decrease by 500 mV after water saturation.

Table 10.1: Selected properties of soil samples used in this study.

Soil	Initial pH	TOC[†]	Total N[§]	C/N Ratio	Fe_{pyr}[*]	Fe_{ox}[‡]	Fe_{CBD}[¶]	Fe_{ox}/Fe_{CBD}[¥]	Al_{CBD}[±]	Final pH
		-------------g kg^{-1}---------------		g C g N^{-1}	----------------------------mg kg^{-1}--------------------------					
Ponzer Oa-1	4.2 ± 0.1	330 ± 24	5.5 ± 0.4	60	3510 ± 191	546 ± 85	634 ± 47	0.85	3530 ± 89	4.0 ± 0.04
Ponzer Oa-2	3.7 ± 0.0	560 ± 3.8	10.5± 0.4	53	3600 ± 165	704 ± 101	582 ± 183	1.21	5420 ± 245	3.8 ± 0.04
Ponzer Oa2-1	4.2 ± 0.3	38 ± 8.5	0.8 ± 0.3	48	558 ± 28	43.8 ± 32	68.4 ± 3	0.64	904 ± 29	4.3 ± 0.03
Ponzer Oa2-2	3.9 ± 0.2	390 ± 16	5.9 ± 0.3	66	1570 ± 161	99.1 ± 41	217 ± 12	0.46	5320 ± 258	3.7 ± 0.08
Leon A/E	5.4 ± 0.3	28 ± 2.2	1.0 ± 0.2	28	1510 ± 88.5	272 ± 43	231 ± 17	1.18	405 ± 26	5.5 ± 0.3
Leon Bhir	4.9 ± 0.2	11 ± 0.3	0.3 ± 0.0	37	296 ± 40	43.8 ± 19	31.3 ± 6	1.40	263 ± 36	5.4 ± 0.2
Goldsboro A	5.0 ± 0.0	45 ± 5.2	1.5 ± 0.2	30	5070 ± 23	2310 ± 7	2630 ± 14	0.88	2850 ± 97	4.9 ± 0.05
Goldsboro B	4.8 ± 0.1	3.7 ± 0.3	≤0.2 ± 0.1	≥19	10200 ± 319	346 ± 68	1480 ± 71	0.23	3520 ± 38	5.0 ± 0.03
Goldsboro E	5.0 ± 0.1	10 ± 1.1	0.3 ± 0.1	33	4980 ± 106	968 ± 20	1590 ± 71	0.61	2500 ± 109	5.0 ± 0.8
Lynchburg B	4.7 ± 0.2	2.7 ± 0.2	≤0.2 ± 0.0	≥14	8400 ± 62	211 ± 73	560 ± 86	0.38	2770 ± 58	4.4 ± 0.2
Lynchburg E	4.7 ± 0.4	4.6 ± 4.5	≤0.3 ± 0.0	≥15	6630 ± 193	422 ± 41	1550 ±58	0.27	2290 ± 157	4.4 ± 0.04
Rains A	4.02 ± 0.4	50 ± 1.2	1.5 ± 0.1	33	3140 ± 200	650 ± 109	512 ± 19	1.27	1090 ± 39	4.2 ± 0.1
Rains B	4.7 ± 0.2	3.9 ± 0.5	≤0.2 ± 0.0	≥20	513 ± 84	23.6 ± 9	43.8 ± 29	0.06	142 ± 23	5.0 ± 0.3
Rains E	4.6 ± 0.1	17 ± 1.1	0.4 ± 0.1	43	1840 ± 294	280 ± 79	252 ± 17	1.11	581 ± 52	4.7 ± 0.1
Pantego A	4.5 ± 0.1	55 ± 6.8	1.5 ± 0.1	37	1990 ± 210	362 ± 90	414 ± 18	0.87	968 ± 25	4.2 ± 0.1
Pantego B	4.7 ± 0.5	15 ± 1.0	0.5 ± 0.00	30	977 ± 94	148 ± 32	173 ± 87	0.56	567 ± 31	4.4 ± 0.2

[†] Total Organic Carbon determined with Perken Elmer PE 2400 CHN elemental analyzer

[§] Total Nitrogen determined by a Perken Elmer PE 2400 CHN elemental analyzer

[*] Sodium Pyrophosphate extractable Fe (Loeppert and Inskeep 1996).

[‡] Oxalate extractable Fe (Jackson et al. 1987)

[¶] Citrate Bicarbonate Dithionate extractable Fe (Jackson et al. 1987)

[¥] Ratio of Oxalate extractable Fe to Citrate Bicarbonate Dithionate extractable Fe

[±] Citrate Bicarbonate Dithionate extractable Al (Jackson et al. 1987)

Table 10.2 Summary of regression models relating reduction rate (RR) to soil properties

Linear Correlation Results

Variable	-------------------Regression Equations---------------		
Mineral Soils	Intercept	Coefficient	r
TOC^{+}	8.00	0.58	0.62*
Average DOC^{a}	8.59	0.32	0.47*
Fe(II)§	13.65	1.66	0.45*
C:N Ratio$^{\Delta}$	-7.40	1.02	0.41**
Humic Acid	30.38	-2.37	0.41**
Initial pH	-42.9	12.7	0.34***
Soils with TOC < 27 g kg^{-1}			
Average DOC	0.006	0.50	0.40*
TOC	-0.51	1.54	0.40*
Soils with TOC $\geq$ 27 g kg^{-1}			
TOC	55.5	-0.48	0.27^{ns}
C:N Ratio	-19.75	2.04	0.19^{ns}

Linear Plateau Mode

	-----------------Regression Equation----------------	r
TOC < 27 g kg^{-1}	RR = -0.57 + 1.45(TOC)	0.82*
TOC $\geq$ 27 g kg^{-1}	RR = 38.7	

Multiple Linear Regression Results

Mineral Soils	**-----------------Regression Equation------------------**	**R^{2}**
TOC and Initial pH	RR=-57.0 + 0.55(TOC) + 13.7(pH)	0.49*
TOC < 27 g kg^{-1}		
DOC and TOC	RR = -2.89+ 0.30(DOC) +0.92(TOC)	0.48*
TOC $\geq$ 27 g kg^{-1}		
TOC and OX:CBD$^{@}$	RR = 47.1 + TOC(-0.55) + 41.5(OX:CBD)	0.54^{ns}

+ Total organic carbon determined with Perken Elmer PE 2400 CHN elemental analyzer. To convert TOC in g kg^{-1} to percent divide by 10.

a Dissolved organic carbon in soil pore water samples

§ Mean dissolved Fe(II) in soil pore water samples

Δ Carbon to nitrogen ratio (g g^{-1})

* p-value < 0.05

** p-value < 0.10

*** p-value < 0.25

@ Oxalate extractable Fe to citrate bicarbonate dithionite extractable Fe (mmol kg^{-1})

ns p-value > 0.25

Table 10.3: Selected soil incubation properties divided into low reduction rate(RR) (< 10 mV h^{-1}) and high reduction rates (> 10 mV h^{-1}) for mineral soils.

	Reduction Slope		Dissolved Fe(II)[§] mg L^{-1}		Final MBC[Δ]		DOC[¥] (mg kg^{-1})		Oxalate to CBD Fe ratio[+]		C/N Ratio[£]		Initial pH		Humic Acid %(g HA / g soil)	
	Mean	Range	Mean	Range	Mean	Range	Mean	Range	Mean	Range	Mean	Range	Mean	Range	Mean	Range
Low TOC[‡]	12.7	39.2	2.7	14.0	60.6	119	25.4	49.5	0.10	0.17	24.8	24.8	4.80	1.1	5.3	9.9
High TOC[a]	34.9	33.7	4.2	10.9	214.3	499	51.3	88.6	0.27	0.28	26.8	26.8	5.0	1.3	4.1	3.2
Difference[@]	-22.2		-1.5		-153.7		-25.9		-0.17		-2.0		-0.2		1.7	
LSD[*]	12.5		3.92		110.6		28.6		0.11		6.00				2.34	
P –Value	< 0.05		0.05		<0.05		< 0.05		< 0.05		< 0.05		0.97		0.13	

‡ Total organic carbon

¥ Total dissolved organic carbon measured from water samples

£ Carbon to nitrogen ratio gC gN^{-1}

[+] Oxalate to citrate bicarbonate dithionate Fe ratio represents poorly crystalline to total Fe in soils.

Δ Final microbial biomass carbon

§ Average dissolved Fe(II) measured from water samples

a Low reduction rate, mV h^{-1}

b High reduction rate, mV h^{-1}

@ Difference between means

*P-value results from paired t-test between low and high means.

Chapter 11

PHOSPHORUS DISSOLUTION IN MINERAL AND ORGANIC SOIL MATERIAL FROM A CAROLINA BAY AS AFFECTED BY REDUCING CONDITIONS

C.S. Brownfield, D.L. Hesterberg, and M.J. Vepraskas

INTRODUCTION

Drained agricultural lands often make convenient sites for wetland restoration projects (Ewing et al., 2004). Because chemical reactions that occur in wetland soils can increase P dissolution (Patrick et al., 1974; Ponnamperuma, 1972), the potential for P to dissolve in restored soils is critically important to water quality (Sallade and Sims, 1997; Shenker et al., 2004; Young and Ross, 2001).

To quantify the potential for P to dissolve when high-P agricultural soils are converted to wetlands, PO_4 chemistry under reducing conditions should be better understood. For decades the reductive dissolution of iron-(hydr)oxide minerals and associated PO_4 has been recognized as a major source of P in lakes (Mortimer, 1941) and in paddy soils used for rice production (Patrick and Mahapatra, 1968; Willet, 1989). More recently, anaerobic incubation studies of Shenker et al. (2004) attributed P dissolution from peat soils in a restored wetland mainly to the reductive dissolution of Fe(III). However, the simple understanding of adsorbed orthophosphate dissolution from Fe(III) mineral surfaces as a consequence of reduction should be challenged for two reasons, described herein.

Phosphate also binds to Al(III) in soils, which is not redox active. Studies suggest that long term P sorption is linked to the presence of Al(III) minerals (Darke and Walbridge; 2000; Richardson, 1985) and Al(III)-humate complexes (Hogan et al., 2004). Under reducing conditions, Al(III) can decrease P dissolution by sorbing P released during reduction (Chacon et al., 2006) and retarding Fe(III) dissolution, probably by blocking electron transfer to Fe(III) mineral surfaces (Murray and Hesterberg, 2006). Long-term P retention in wetlands can also be affected by Fe(III) and Al(III) crystallinity, which are preserved in a poorly ordered state by redox cycling (Kuo and Mikkelsen, 1978).

Soil organic matter also affects PO_4 dissolution under reducing conditions. Research has consistently suggested that P binds to humic substances via Fe- and Al- bridges, which may enhance the ability of a soil to bind P (Gerke, 1993; Gerke and Hermann, 1992; Hermann and Gerke, 1992; Levesque and Schnitzer, 1967; White and Thomas, 1981). Under reducing conditions, however, P has been shown to dissolve from soils that are high in organic matter (Hutchison and Hesterberg, 2004; Young and Ross, 2001). One explanation for this phenomenon is redox-dependent (Ryan et al., 1992) or redox-associated, pH-dependent (Thompson et al, 2006) mobilization of Fe(III)-cemented organic colloids, which can expose organic and occluded P to hydrolysis and reductive dissolution processes, respectively. Mobilization of organic colloids can also result in competition of dissolved organic matter (DOM) with P for adsorption sites on Al(III) and Fe(III) mineral surfaces (Kreller et al., 2003), and in the alteration of Al(III) and Fe(III) solubility through the formation of DOM-metal complexes (Gerke, 1993; Nierop et al., 2002). Jansen et al. (2002) reported that metal binding to DOM decreased in the order Fe(III)>Al(III)>Fe(II), suggesting that in reduced systems, increased competition from DOC for adsorption sites on Al(III) mineral surfaces could enhance the dissolution of Al(III)-bound P.

The goal of this research is to determine the potential for P dissolution to occur in the reduced, organic and organic-rich surface soils in a Robeson County, NC wetland currently undergoing restoration. Dissolution of P there would increase the risk for transport of P to nutrient-sensitive surface waters. Our objectives were to compare the reductive dissolution of P among soil samples that vary in organic matter content, and to measure auxiliary redox-related chemical parameters that would imply possible mechanisms responsible for variations in P dissolution. Knowledge of the chemical processes affecting P dissolution in soils from Robeson County, NC is essential to developing management strategies there and is also useful in predicting the success of related wetland restorations in the future.

MATERIALS AND METHODS

Soil Sampling

In July, 2005, approximately 2 gal soil samples were collected from the surface horizons (0 to 4 in.) at each of six selected locations containing high concentrations of total phosphorus (P_{tot}) and variable organic carbon (TOC) concentrations. Soils at the six sites were mapped as Ponzer (Terric Haplosaprist), Leon (Aeric Alaquod), Pantego (Umbric Paleaquult), or Rutlege (Typic Humaquept) soils. The samples were packed directly into glass jars in the field and transported within 6 h to a refrigerator, where they were stored for < 14 d before being passed through a 0.078” stainless steel (SS) sieve. Sieved samples were mixed by hand for ~ 10 min and subdivided among 1 qt glass mason jars, then frozen in the dark for up to 14 mo before a given sub-sample was thawed for experimentation. Particle size analysis was performed by the pipette method (Gee and Bauder, 1986) after removing organic matter by combustion at 840°F for 24 h.

Static Incubation Experiment

Set up

The purpose of the static incubation experiment was to assess PO_4 dissolution following reduction of whole soil samples. Although the static incubation experiment is presented first in this report, it was actually conducted after other experiments and there remained only enough soil material from four of the six locations sampled in July, 2005. Triplicate, 0.11lb (oven-dry basis) sub-samples from those four locations were water saturated (2.5 lb water per lb solids) and incubated in sealed, 0.53 qt glass mason jars for 2 and 62 d, and concentrations of DRP, Fe(II), and DOC were measured in each sample as described below. Wet soil samples were mixed vigorously with a glass stirring rod to remove entrapped air bubbles. The headspace of each jar was flushed with $N_{2(g)}$ in a glove box and air-tight caps were applied. The samples were randomly positioned in an incubator at 77 ± 0.3°F. Jars were allowed to equilibrate for 2 d in the incubator before the initial sampling. To prevent excessive pressure build-up within jars, their caps were quickly opened twice during the incubation (at 17 and 47 d) in an $N_{2(g)}$-filled glove box, then samples were returned promptly to the incubator.

Sampling

Samples were removed from the incubator at 2 d and at 62 d for measurements and destructive sampling done in an $N_{2(g)}$-filled glove box. Each jar was shaken by hand about 5 to 7 times to mix its contents. The pH and the Eh of the soil suspensions in each jar were measured by placing the electrode in the suspension while flushing the headspace with N_2 gas and lightly swirling the jar's contents. The jars were then re-capped and shaken by hand to suspend all solids. Solids were allowed to settle for 30 seconds, and a portion of the unsettled suspension was transferred to a 3.05 in^3, polycarbonate (PC) centrifuge tube with Teflon taped threads. The sub-samples were capped, removed from the glove box, and centrifuged at 8,100 x g for 10 min. The supernatant was filtered under N_2 gas using 7.87 x 10^{-6} inch Isopore filters and subdivided for aqueous component analysis. The remaining filtrate was transferred to LDPE (2 d samples) or evacuated, borosilicate glass (62 d samples) bottles and refrigerated at 37.4 °F for 60 d before measuring TOC, P, Fe, Al, and Mn.

Continuously Stirred Reactor (CSR) Experiments

Setup

The effect of microbial reduction on PO_4 dissolution from Juniper Bay soil samples was determined using continuously-stirred soil suspensions under aerobic and oxygen-free conditions. The reactor setup is described by Hutchison and Hesterberg (2004) and is based on redox reactors developed by Patrick et al. (1973). Trends in phosphate dissolution were monitored in duplicate suspensions during 25 d of reduction. Aerobic (control) samples were also evaluated to ensure P dissolution was caused by reduction. Either two or four reactors were run concurrently, and samples from all six locations were evaluated in duplicate (one replicate on controls), for a total of 18 experimental units.

To prepare for a reactor experiment, 1 liter of frozen soil material was allowed to thaw for 2-4 h as needed at room temperature (~ 72 °F). The soil material was mixed thoroughly (~ 10 min) by hand with a SS spatula in a 1 gal low density polyethylene (LDPE) bucket and soil moisture contents were determined by oven-drying sub-samples at 221 °F for 24 h. Any thawed soil material was stored in glass jars at 38 °F when not in use. After determining moisture content, the samples were mixed again and each sample was divided evenly between two, tared, 2.1 qt high density polyethylene (HDPE) bottles. De-ionized water was added at 2:1 water:soil by mass. The bottles and their contents were thoroughly mixed by shaking for 1 h at 3.3 s^{-1} to disrupt any aggregates.

The < 0.002" (silt + clay) fractions of the samples were used in stirred reactor experiments to avoid abrasion of reactor vessels. Fractionation involved wet sieving the shaken suspensions through a < 0.002" sieve (No. 270), mixing the silt + clay fractions into 1 gal glass jars. The suspended solids concentrations of the silt + clay suspensions were measured by oven-drying sub-samples of the well mixed suspensions at 221 °F for 24 h.

While continuously stirring a silt+clay suspension, a portion containing 0.05 lbs of solids was quantitatively transferred into a glass reactor vessel (Kimble-Kontes, Vineland, NJ). De-ionized water was added to yield a final solids concentration of 0.033 lbs lb^{-1} in 3.31 lbs of suspension. Suspensions were stirred continuously with a magnetic stirrer at 500 rpm and 77 °C during each redox incubation experiment.

Standardized pH and redox (Eh) electrodes were sealed into rubber-stopperred ports in the lid of the reactor vessel. Each set of Eh and pH electrodes were connected to individual potentiometer and a computer to automatically record measurements at 15-minute intervals, which were later averaged on an hourly basis. A Pt-tip combination redox electrode with a Ag/AgCl reference electrode was used for Eh measurements and all measurements were corrected to the standard hydrogen potential (+ 0.199 V) (Patrick et al., 1996). Redox electrodes were cleaned with de-ionized water and tested for functioning in solutions of hydroquinone in pH 4 and 7 buffers at least every 6 days. The pH electrodes were cleaned and re-standardized (if necessary) at the same time. Aberrant Eh readings for about 1 d following re-immersion of the electrodes into the suspension were omitted.

Carbon dioxide-free air (lab air) (National Welders Supply Company, Charlotte, NC) was bubbled through each suspension at a rate of 0.3 to 0.6 in^3 min^{-1} for 3-5 d to achieve a consistent Eh before reduction was initiated. Gas bubblers (Kimble-Kontes, Vineland, NJ) containing 0.1 N or 0.5 N NaOH solution were placed in the gas flow stream before and after the reactor vessel to trap and measure microbial $CO_{2(g)}$ production during the incubation experiment (Hutchison and Hesterberg, 2004). Data from the Ponzer 1 and Leon 1 samples was lost.

Based on preliminary batch-reduction experiments, a dextrose spike of 0.002 lb lb^{-1} solids was added as a 0.034 fluid ounce aliquot of aqueous solution at t = 0 d to stimulate microbial reduction. Immediately after adding dextrose, CO_2-free air was replaced by 99.99% pure $N_{2\,(g)}$ flowing at 1.2 in^3 min^{-1} to exclude O_2 and induce anaerobic conditions. In control (oxidized) reactor experiments, CO_2-free air was not replaced by $N_{2\,(g)}$, but a dextrose spike was added.

Sampling

Sub-samples of the continuously-stirred suspensions were removed without exposure to oxygen after 0, 1, 2, 3, 4, 6, 8, 10, 12, 15, 18, and 25 d of incubation according to the method used by Hutchison and Hesterberg (2004). A 3.7 cm^3, $N_{2(g)}$-purged glass syringe and stopcock was connected to a sample port installed in the reactor cap, and approximately 1.35 fluid ounces of suspension were withdrawn from the reactor into the syringe. A needle was then attached to the stopcock and the suspension was injected into three evacuated (-25 in Hg), 0.91-in^3 borosilicate glass test tubes fitted with rubber septa. These samples were centrifuged at 8100 x g for 10 min, and the supernatant solutions were filtered through a 7.87 x 10^{-6} inch Isopore polycarbonate filter (Millipore, Billerica, MA) and sub-divided for aqueous component analysis. All filtering and subdivision of filtrate samples was done in a glove box under $N_{2(g)}$ using a red-filtered safe light to prevent exposure to oxygen and ultraviolet radiation (Hutchison, 2003). Cumulative sampling during the entire experiment removed less than 40% of the original suspension mass.

Aqueous Solution Analyses

Dissolved reactive phosphorus (DRP) and Fe(II) were measured colorimetrically in filtrate samples using the modified ascorbic acid method (Kuo, 1996) and the 1,10 phenanthroline method (Loeppert and Inskeep, 1996), respectively. To account for interference from dissolved organic carbon in the Fe(II) analysis, a blank from each filtrate sample was prepared by replacing the phenanthroline reagent with an equal volume of DI water and subtracting absorbance readings of the blanks from those of the samples. Absorbance readings at 3.31 x 10^{-5} inches (810 nm) (for DRP) or 2.00 x 10^{-5} (510 nm) (for Fe(II)) were determined with a UV-210PC UV-Visible Spectrophotometer (Shimadzu Corporation, Kyoto, Japan) within 24 h and 15 d, respectively. If not analyzed immediately, samples were stored at ambient temperature (~ 72 °F) in the dark. Dissolved organic carbon was measured in the filtrate samples using a TOC-5050 total organic carbon analyzer (Shimadzu Corporation, Kyoto, Japan). Prior to analysis, DOC samples were stored for up to 120 d in the dark at 37.4 °F. Total dissolved concentrations of P, Fe, Al and Mn (P_T, Fe_T, Al_T, and Mn_T) were measured by inductively coupled plasma (ICP) emission spectroscopy. Some samples yielded P_T concentrations lower than DRP concentrations; these were digested by adding 0.01 ppm potassium persulfate, autoclaving, and measuring again (Greenberg et al., 1992). Nitrate and SO_4^{2-} concentrations were measured in selected (oxidized) samples by ion chromatography.

Base traps filled with freshly standardized NaOH were titrated for unreacted hydroxide at t = 0 and t = 25 d, and at 4 to 6 d intervals if only 2 reactors were being run. Using a volumetric pipette, triplicate 0.67 ± 0.02 fluid ounce subsamples of NaOH trapping solution were transferred to a 12.2 in^3 Erlenmeyer flask, and 3 to 5 drops of phenolphthalein pH indicator solution were added. The solutions were titrated with standardized 0.1 N HCl until color changed from pink to colorless.

Solids Characterization

The < 0.002” solids from reactor stock suspensions were freeze dried and used to determine P_{tot} and inorganic P (P_i) by the ignition method of Kuo (1996), modified to include filtration of the acid extract through 7.87 x 10^{-6} inch Isopore filters and analysis of dissolved components using ICP emission spectroscopy. Organic P (P_o) was calculated as the difference between P_{tot} and P_i. The freeze-dried solids were also used to determine the amount of Fe and Al extractable with citrate-bicarbonate-dithionite, acid ammonium oxalate, and Na-pyrophosphate solutions according to the methods of Jackson et al. (1986). For each extractant, 3.3 x 10^{-4} lbs of < 0.002” solids were used, and separate extractions were performed on separate samples. The extracts were filtered through 7.87 x 10^{-6} inch (2 micron) Millipore filters and analyzed by atomic absorption spectrometry. Total organic carbon (TOC) concentrations in the < 0.002” freeze-dried solids were determined with a Perkin-Elmer Model 2400 Elemental CN Analyzer (Perkin Elmer Corp., Norwalk, CT).

Total P, P_i, and TOC were also determined in the < 0.078" soil fraction using the above methods.

Statistical Analysis

Statistical analyses were performed with SAS version 9.0 (SAS Institute, Cary, NC, 2005). PROC REG was used for regression analyses. PROC GLM was used to test for differences among solid-phase Fe and Al, using the model:

Extractable Fe/Al = Soil Extractant Soil•Extractant.

PROC GLM was also used to test for differences in P_{tot}, P_o, particle size distribution, TOC, ρ_B, and pH for < 0.078" and < 0.002" solids. PROC TTEST was used to determine differences in mean values for 2 and 62 d aqueous solution measurements in the static incubation experiment.

RESULTS

Soil Characteristics

Table 11.1 shows that P and C were more concentrated in the < 0.002" fraction than in the < 0.078" fraction. Phosphorus concentrations in the < 0.002", freeze-dried subsamples used for laboratory experiments significantly ($p < 0.001$) differed both with respect to soil series and with respect to types of P (P_o vs P_i) within each soil series. The highest concentrations of P_{tot} were in the Leon 1 and Leon 2 solids, which contained 2400 ± 500 ppm P_{tot} and 2600 ± 180 ppm P_{tot}, respectively. The Ponzer 2 sample contained the lowest P_{tot} concentration, 1000 ± 180 ppm P_{tot}, while the Ponzer 1, Rutlege, and Pantego samples had intermediate P_{tot} concentrations. On average, the mineral surface soil fines had twice as much total P (2000 ± 650 ppm P) as the organic surface soil fines (1100 ± 150 ppm P). Organic P constituted between one half and two thirds of P_{tot} in < 0.002" separates from all soils. The bulk densities of the Ponzer 1, Ponzer 2, and Rutlege samples are typical of organic soil material. The bulk densities of the Leon 1, Leon 2, and Pantego samples were lower than typical mineral soil material, probably because they were also rich in organic matter.

Extractable forms of Fe in the < 0.002" samples used for the continuously stirred reactor experiment are shown in Figure 11.1. Concentrations of CBD, oxalate, and pyrophosphate extractable Fe and Al were not significantly different ($p > 0.05$) within each sample. Since pyrophosphate-extractable Fe is thought to be extracted by CBD and oxalate reagents as well (Jackson, 1986), most free Fe within each sample was in pyrophosphate-extractable form, suggesting that it is organically bound. Concentrations of extractable Fe varied significantly ($p < 0.05$) between samples (Fig. 11.1), and ranged from 1710 ± 530 ppm Fe_{cbd} in the Ponzer 2 solids to 5240 ± 300 ppm Fe_{cbd} in the Pantego solids. Comparably, concentrations of Al_{cbd}, Al_{ox}, and Al_{pyr} were approximately three times higher than extractable Fe(III) concentrations. Extractable forms of Al(III) also were not significantly different ($p < 0.05$) in individual samples. Between samples, concentrations of extractable

Al(III) were not significantly different in the Rutlege, Ponzer 1, Ponzer 2, and Pantego samples, while the Leon 1 and Leon 2 solids contained significantly ($p < 0.05$) more extractable Al than other samples.

Static Incubation Experiment

Initial and final concentrations of DRP, Fe(II), and DOC are displayed in Figure 11.2, while trends in all experimental variables are summarized in Table 11.2. At the beginning of the static incubation experiment, the mean Eh of all four samples was 0.38 ± 0.02 V (pH 5.6 ± 0.3) (data not shown). After 62 d of anaerobic incubation, the Eh of all samples significantly ($p < 0.01$) to 0.18 ± 0.3 V, while their pH did not change significantly ($p > 0.05$).

Reducing redox conditions resulted in significant increases in [DRP] ($p < 0.05$) and [DOC] ($p < 0.01$) in all four samples. The greatest increase and highest [DRP] occurred in the Ponzer 1 sample, in which DRP increased about three fold to 2.2 ppm after 62 d. Concentrations of DRP in the Leon 1, Leon 2, and Rutlege samples were 3 to 5–fold lower than in the Ponzer 1 sample after 62 d. Concentrations of DOC after 62 d ranged from 80 ± 3 ppm in the Leon 1 sample to 230 ± 15 ppm in the Ponzer 1 sample. Significant ($p <0.01$) net dissolution of Fe(II) occurred in the Leon 2, Rutlege, and Ponzer 1 samples, but no net Fe(II) dissolution occurred in the Leon 1 sample. Molar $\Delta P:\Delta Fe$ in the Ponzer 1 sample was 2.7 (Table 11.2). As discussed by Hutchison and Hesterberg (2004), molar P:Fe(II) > 1 imply that the congruent dissolution of Fe(III)-bound P cannot account for all PO_4 dissolution.

CSR Experiment

Suspension Reduction

Figure 11.3 shows that the Eh of all suspensions was ~ 0.5 V (mean = 0.48 ± 0.06 V) at t = 0 d. After adding a 0.002 lb dextrose lb^{-1} solids spike at t = 0 to initiate reduction, an Eh of < 0.2 V was achieved within 4 to 5 days and maintained during the remainder of the experiment. The pH of all suspensions changed less than 0.2 units during the experiment with the exception of the “Leon 2” suspension, which decreased by 0.5 pH units. Since all suspensions were undergoing reduction, which typically consumes protons, one or more buffering processes must have been occurring concurrently. Soils that are low in reducible iron may not exhibit a pH greater than 6.5 even after weeks of submergence (Ponnamperuma, 1972), presumably because of the pH buffering capacity of organic matter (Ponnamperuma, 1972; Ruttner, 1963).

Figure 11.4 shows that CO_2 evolution occurred in the reduced treatments, suggesting that reduction was microbially mediated. Furthermore, average CO_2 evolution rates ranged from 20 to 60 µmol d^{-1} in reduced suspensions, and 50 to 130 µmol d^{-1} in control suspensions, consistent with the suppression of microbial respiration that occurs when O_2 is excluded from soil pores (Oades, 1995).

Fe(II) Dissolution

Trends in Fe(II) concentrations in silt + clay suspensions of mineral and organic separates (Fig. 11.5) show that Fe(III) reduction occurred to different degrees during the CSR experiments. During the 25 d experiments, Fe(II) dissolution rates increased in the order Pantego > Leon 1 > Ponzer 1 > Rutlege > Leon 2 > Ponzer 2 and ranged from 3.53×10^{-7} to 1.41×10^{-6} mg d^{-1}. Dissolved [Fe(II)] ranged from 0.4 to 2.6 ppm after 25 d of reduction, depending on soil type.

Phosphorus Dissolution

Figures 11.6 and 11.7 show temporal trends in concentrations of DRP in organic and mineral soil suspensions, respectively, during 25 d of reduction. Either a linear or a quadratic model was used to fit the data, whichever gave the greater coefficient of determination. A quadratic model significantly ($p < 0.01$) fit the Pantego, Ponzer 1, and Ponzer 2 data, while a linear model fit ($p < 0.05$) the Leon 2 and Rutlege soils. Neither model fit data from the Leon 1 soil sample.

After 25 d of reduction, DRP concentrations increased nearly 2-fold in the Ponzer 1 suspension, from 0.6 ppm to 1.1 ppm. No net change in phosphate dissolution was observed in either the other organic suspensions or any of the mineral suspensions. For the solids concentration used in this experiment (15 lb lb^{-1}), up to 6 % (for Ponzer 1) of the total solid-phase P dissolved during reduction. Trends in P_T (data not shown) closely followed DRP trends, indicating that DRP constituted a major fraction of the total dissolved P.

Figure 11.8 shows a correlation between DRP and Fe(II) in the Ponzer 1 suspension, which was the only suspension with notable P dissolution and the only sample in which a significant correlation ($p < 0.05$) was detected. Dissolved Fe(II) after 25 d in the Rutlege, Leon 2, and Ponzer 2 suspensions was 1.25, 1.75, and 2.5-fold higher, respectively, than in the Ponzer 1 suspension; yet no net P dissolution occurred in any of the former suspensions (Figs. 5 and 6). These results indicate that reductive dissolution of organic or oxide-mineral bound Fe(III) did not lead to P dissolution in all but the Ponzer 1 soil sample.

Despite the correlation between DRP and Fe(II) in the Ponzer 1 suspension, Figure 11.9 shows that Fe(II) dissolution alone could not account for all of the P that dissolved. Figure 11.9 shows that the molar P:Fe(II) (at peak [DRP]) in the Ponzer 1 suspension was 2.3, suggesting that Fe(III) reduction alone could not have accounted for all P dissolution in the Ponzer 1 sample.

Concentrations of DOC in the Ponzer 1 suspension were 1.8 fold higher (up to 55 ppm) than in any other suspension and increased concurrently with DRP as a result of reduction in all samples (data not shown). When plotted together, data from all organic samples show a highly significant ($p < 0.01$) positive relationship between DRP and DOC (Fig. 11.10). Data from the Leon 1 and Pantego samples show significant linear relationships between DRP and DOC, while there was no significant relationship identified between DRP and DOC in the Leon 2 sample (data not shown). Based on the strength of the regression analysis shown in Figure 11.10, DOC was a more reliable predictor than Fe(II) for P dissolution.

Oxalate extractable Al was a poor predictor of final DRP concentrations when considering all samples ($p > 0.05$, data not shown). When considering all samples except for the Ponzer 1 sample, however, Al_{ox} significantly ($p = 0.013$) explained 90% of the variability in final DRP concentrations (Fig. 11.11). The high coefficient of determination in Figure 11.10 suggests that poorly crystalline and short-range ordered Al-hydroxides affected PO_4 dissolution in the Ponzer 2, Rutlege, Leon 1, Leon 2, and Pantego samples.

DISCUSSION

The Meaning of Static Incubation and CSR Results

The static incubation experiment and the CSR experiment differed in several key ways. The objective of the static incubation experiment was to determine long term trends in P dissolution in a way that could be used to infer the potential for P to dissolve in reduced soils of a restored wetland. The objective of the CSR experiment was to investigate the causes of P dissolution, and specifically to evaluate the relative importance of Fe(II) and organic carbon dissolution to the dissolution of P. Thus, samples were allowed to react under oxygen-free conditions for 25 d in the CSR experiment and for 62 d in the static incubation experiment.

Diffusive limitations to P dissolution reactions were removed by stirring in the CSR experiment, but were not in the static incubation experiment. Stirring predicated the separation of < 0.002” particles for the CSR experiment, while the entire soil samples (0 to 0.078”) were used in the static incubation experiment. Furthermore, a 19-fold higher solid:suspension was used in the static incubation experiment (285 lb lb^{-1}) than in the CSR experiment (15 lb lb^{-1}) to mimic realistic field conditions in the former and to ensure proper mixing in the latter. In sum, results from the static incubation experiment are more useful for predicting P dissolution from reduced soils in the restored wetland, while results from the stirred reactor experiment provide insight into chemical processes contributing to the dissolution of P.

Differences in P dissolution that occurred in samples evaluated in the static incubation experiment might be explained by a 2- 4-fold higher concentrations of DOC, a 2.5-fold longer incubation time, or a 19-fold higher solids:suspension compared with stirred reactor experiment. However, concentrations of DRP (and DOC) were highest in the Ponzer 1 sample in both experiments. In the CSR experiment, relationships between DRP and dissolved Fe(II), and DRP and DOC, indicate that DOC accounts for trends in P dissolution better than Fe(II).

The dependence of DRP on DOC in reduced suspensions was also reported by Hutchison and Hesterberg (2004), who saw up to sevenfold increases in DRP (from 1.5 up to 10 ppm) after 40 days of microbial reduction of a high-P Umbraquult in a continuously-stirred redox reactor. Their results indicated that DOM produced during soil reduction contributed to the increase in DRP and suggested that this might have been due to competitive adsorption between phosphate and DOM for Fe and Al oxide minerals or to the formation of ternary DOM-Fe-PO_4 or DOM-Al-PO_4 complexes.

Considering both the stirred incubation and CSR experiments, samples in which P dissolution occurred tended to have higher DOC concentrations than samples in which no P dissolution occurred. In fact, no net P dissolution occurred in samples with a final [DOC] of less than 40 ppm. In those samples, final [DRP] was negatively correlated with oxalate-extractable Al, which is consistent with the work of Richardson (1985) reported a dependence of P sorption on Al_{ox} ([DOC] not reported), while Hogan et al. (2004) correlated P dissolution in natural wetlands with Al_{pyr}.

Implications for Wetland Restoration at Juniper Bay

Concentrations of DRP measured in reduced samples from the Ponzer 1 samples were 12 and 22 times more concentrated in P than concentrations known to cause eutrophication in P limited freshwaters. Because the highest concentration of DRP was measured in the Ponzer 1 sample in both the stirred reactor and static incubation experiment, P dissolution is expected to be most pronounced in the center of the Ponzer soil unit at Juniper Bay. However the results of the static incubation experiment suggest that PO_4 dissolution is likely to occur upon reduction of soils at Juniper Bay near the Leon 1, Leon 2, and Rutlege samples, as well. Even so, the impact of P immobilization by plants and long-term (> 62 d) P sorption processes were not evaluated, so a prediction of [DRP] in waters that drain Juniper Bay remains difficult to assess. Rather, results from this study indicate that the organic and organic-rich soils at Juniper Bay present a significant risk for eutrophication after reducing conditions are established. A prudent management strategy would therefore include monitoring of P concentrations at all points where surface water exits the property boundary, and prevention of short-circuits in the drainage network. Short circuits, such as areas where surface water currently ponds near still-open drainages, could potentially conduct dissolved P directly to drainage waters without exposure to plant uptake or long-term sorption processes.

CONCLUSIONS

In the static incubation study, reducing redox conditions resulted in 2- 3-fold increases in DRP after 62 d in all samples. Concentrations of DRP were greatest in the Ponzer 1 sample (max. DRP = 2.2 ppm) and decreased in the order Ponzer 1 >> Leon 1 ≈ Rutlege < Leon 2. In the CSR experiment, which was designed to investigate chemical processes that occurred in the static incubation experiment, an increase in DRP (2-fold, up to 1.1 ppm) was observed for only the Ponzer 1 sample. Dissolved Fe(II) was significantly correlated with DRP in the Ponzer 1 CSR sample, although molar P:Fe implied that congruent dissolution of Fe(III)-bound P could not wholly account for the P that dissolved. A strong ($r^2 = 0.81$) linear relationship between DRP and DOC was found in the organic CSR samples. For CSR samples in which no P dissolution occurred (all except Ponzer 1), final [DRP] after reduction was significantly ($p < 0.05$) negatively correlated with oxalate-extractable Al(III), and the maximum [DOC] was 2- to 8- fold lower than for samples in which P dissolved. These results suggesting that non redox-active Al(III) inhibited the dissolution of PO_4 at low [DOC] (below 40 ppm). Furthermore, these results imply that the P dissolution that occurred was not likely the result of only Fe(III)-bound P dissolution, and that interactions of DOM with PO_4 or minerals that bind PO_4 plays an important role in P dissolution under reducing conditions. Hence, the dissolution of P from reduced, organic-rich soils in restored wetlands presents an environmental concern.

REFERENCES

Chacon, N., S. Flores, and A. Gonzalez. 2006. Implications of iron solubilization on soil phosphorus release in seasonally flooded forests of the lower Orinoco River, Venezuela. Soil Bio. Biochem. 38:1494-1499.

Darke, A., and M.R. Walbridge. 2000. Al and Fe biogeochemistry in a floodplain forest: implications for P retention. Biogeochemistry. 51:1-32.

Ewing, J.M., M.J. Vepraskas, and C.W. Zanner. 2004. Using historical records of land use to improve wetland mitigation. Southeast. Geog. 45:25-43.

Gee, G.W. and J.W. Bauder. 1986. Particle size analysis. *In* A. Klute (Ed.) Methods of Soil Analysis Part 1: Physical and mineralogical methods, 2nd ed. Soil Science Society of America, Inc. Madison, Wisconsin.

Gerke, J. 1993. Phosphate adsorption by humic/Fe-oxide mixtures aged at pH 4 and 7 and by poorly ordered Fe-oxide. Geoderma. 59:279-288.

Gerke, J., and R. Hermann. 1992. Adsorption of orthophosphate to humic-Fe-complexes and to amorphous Fe-oxide. Z Pflanzenernaehr. Bodenkd. 160:427-432.

Greenberg, A., L. Clesceri, A. Eaton, and M. Franson. 1992. Persulfate Digestion Method. *In* Standard methods for the examination of water and wastewater, 18th ed. American Public Health Association, Washington, D.C. p.4-112.

Hermann, R., and J. Gerke. 1992. Complexation of iron (III) to humic substances of a humic podzol at pH 2.5-6.4 – quantification of the organically complexed iron by pyrophosphate extraction. Z. Pflanzernahr. Bodenk. 155:229-232.

Hogan, D.M., T.E. Jordan, and M.R. Walbridge. 2004. Phosphorus retention and soil organic carbon in restored and natural freshwater wetlands. Wetlands. 24(3):573-585.

Hutchison, K.N. 2003. Dissolution of phosphate in a phosphorus-enriched ultisol as affected by microbial reduction. M.S. Thesis. North Carolina State Univ., Raleigh.

Hutchison, K.N., and D. Hesterberg. 2004. Dissolution of phosphate in a phosphorus-enriched ultisol as affected by microbial reduction. J. Environ. Qual. 33:1793-1802.

Jackson, M.L., C.H. Lim, and L.W. Zelazny. 1986. Oxides, hydroxides, and aluminosilicates. *In* A. Klute (Ed.) Methods of Soil Analysis Part 1: Physical and mineralogical methods, 2nd ed. Soil Science Society of America, Inc. Madison, Wisconsin.

Jansen, B., K.G.J. Nierop, and J.M. Verstraten. 2002. Influence of pH and metal/carbon ratios on soluble organic complexation of Fe(II), Fe(III) and Al(III) in soil solutions determined by diffusive gradients in thin films. Anal. Chim. Acta. 454(2):259-270.

Kreller, D.I., G. Gibson, W. Novak, G.W. van Loon, J.H. Horton. 2003. Competitive adsorption of phosphate and carboxylate with natural organic matter on hydrous iron oxides as investigated by chemical force microscopy. Colloids and Surfaces A: Physieochem. Eng. Aspects. 212:249-264.

Kuo, S. 1996. Phosphorus. P.869-919. *In* D.L. Sparks (ed.) Methods of soil analysis. Part 3: Chemical Methods. SSSA, Inc. and ASA, Inc., Madison,WI.

Kuo, S., and D.S. Mikkelsen. 1978. Distribution of iron and phosphorus in flooded and unflooded soil profiles and their relation to phosphorus adsorption. Soil Sci. 127/1:18-25.

Levesque, M. and M. Schnitzer. 1967. Organo-metallic interactions in soils: 6. Preparation and properties of fulvic acid-metal phosphates. Soil Sci. 103:183-190.

Loeppert, R.H., and W.P. Inskeep. 1996. Iron. P. 639-664. *In* D.L. Sparks (ed.) Methods of soil analysis. Part 3 Chemical Methods. SSSA, Inc. and ASA, Inc., Madison, WI.

Mortimer, C.H. 1941. The exchange of dissolved substances between mud and water in lakes. J. Ecol. 29:280-329.

Murray, G.C., and D. Hesterberg. 2006. Iron and phosphate dissolution during abiotic reduction of ferrihydrite-boehmite mixtures. 70:1318-1327.

Nierop, K., B. Jansen, and J. Verstraten. 2002. Dissolved organic matter, aluminium and iron interactions: precipitation induced by metal/carbon ratio, pH and competition. Sci. Tot. Environ. 300:201-211.

Oades, J.M. 1995. An overview of processes affecting the cycling of organic carbon in soils. *In* R.G. Zepp and Ch. Sonntag (Eds.) Role of nonliving organic matter in the Earth's carbon cycle. John Wiley and Sons Ltd., New York.

Patrick, W.H., and I.C. Mahapatra. 1968. Transformations and availability to rice of nitrogen and phosphorus in waterlogged soils. Adv. Agron. 20:323-360.

Patrick, W.H., and R.A. Khalid. 1974. Phosphate release and sorption by soils and sediments: effect of aerobic and anaerobic conditions. Science. 186:53-55.

Patrick, W.H., B.G. Williams, and J.T. Moraghan. 1973. A simple system for controlling redox potential and pH in soil suspensions. Soil Sci. Soc. Am. Proc. 37:331-332.

Patrick, W.H., R.P. Gambrell, and S.P. Faulkner. 1996. Redox measurements of soils. *In* D.L. Sparks (ed.) Methods of soil analysis. Part 3. SSSA Book Ser. 5. SSSA, Madison, WI.

Ponnamperuma, F.N. 1972. The chemistry of submerged soils. Adv. Agron. 24:29-96.

Reddy, K.R., R.H. Kadlec, E. Flaig, and P.M. Gale. 1999. Phosphorus retention in streams and wetlands: a review. Crit. Rev. in Environ. Sci. Tech. 29(1): 83-146.

Richardson, C.J. 1985. Mechanisms controlling phosphorus retenetion capacity in freshwater wetlands. Science. 228:1424-1427.

Ruttner, F. 1963. Fundamentals of limnology, 3rd Ed. University of Toronto Press, Toronto.

Ryan, J.N., and P.M. Gschwend. 1992. Effect of iron diagenesis on the transport of colloidal clay in an unconfined sand aquifer. Geochim. Cosmochim. Acta. 56:1507-1521.

Sallade, Y.E., and J.T. Sims. 1997. Phosphorus transformations in the sediments of Delaware's agricultural drainageways: I. Effect of reducing conditions on phosphorus release. J. Environ. Qual. 26:1579-1588.

SAS Institute. 2005. SAS Version 9.1. SAS Inst., Cary, NC.

Shenker, M., S. Seitelbach, S. Brand, A. Haim, and M.I. Litaor. 2004. Redox reactions and phosphorus release in re-flooded soils of an altered wetland. Eur. J. Soil Sci. 56(4):515-525.

Tadanier C.J., M.E. Schreiber, and J.W. Roller. 2005. Arsenic mobilization through microbially mediated deflocculation of ferrihydrite. Environ. Sci. Tech. 39 (9): 3061-3068.

Thompson, A., O.A. Chadwick, S. Boman, and J. Chorover. 2006. Colloid mobilization during soil iron redox oscillations. Environ. Sci. Tech. 40:5743-5749.

Vollenweider, R.A. 1976. Advances in defining critical loading levels of phosphorus in lake eutrorphication. Mem. 1st. Ital. Idrobiol. 33:53-83.

White, R.E. and G.W. Thomas. 1981. Hydrolysis of aluminum on weakly acidic organic exchanges: implications for phosphate adsorption. Fert. Res. 2:159-167.

Willet, I.R. 1989. Causes and reduction of changes in extractable phosphorus during flooding. Aust. J. Soil Res. 27:45-54.

Young, E.O., and D.S. Ross. 2001. Phosphate release from seasonally flooded soils: a laboratory microcosm study. J. Envrion. Qual. 30:91-101.

ACKNOWLEDGEMENT

This chapter was as a portion of C.S. Brownfield’s M.S. Thesis entitled “Phosphorus Dissolution in a Drained Wetland as affected by Reducing Conditions” that was earned through NC State University and is available through the university’s library.

Table 11.1. Characterization of whole soil and < 0.002” separates used in 62 d static incubation and 25 d continuously stirred reactor experiments, respectively. P_{tot} = Total P, P_0 = Organic P, TOC = Total Organic Carbon, ρ_B = bulk density (oven-dry basis), NA = not applicable. Results within < 0.078” and < 0.002” size fractions that are followed by the same letter are not statistically different at the $p < 0.05$ level. Standard deviations of triplicate measurements are shown in parentheses. Ponzer 1 replicates were combined into one settling column for particle size analysis due to the large sample volume required.

Sample	P_{tot}[‡] (ppm)	P_o/P_{tot}	TOC (‰)	pH	ρ_B (ppm)	Sand (%)	Clay (%)
< 0.078”							
mineral							
Leon 1	400 (100) a	0.68 a	80 (1) a	6.2 (0.06) a	0.99 (0.08) a	94(1) a	1(0.1) a
Leon 2	870 (70) b	0.55 b	70 (1) b	4.9 (0.04) b	1.12 (0.07) b	82(1) b	2(0.3) b
Pantego[†]	390 (24) a	0.60 bc	60 (1) c	6.4 (0.01) c	0.96 (0.01) a	92(1) a	1(0.1) a
Rutlege	350 (30) a	0.80 d	110 (1) d	5.4 (0.03) d	0.81 (0.06) c	81(1) b	3(0.1) b
organic							
Ponzer 1	700 (170) c	0.86 d	470 (1) e	5.2 (0.02) e	0.45 (0.05) d	61 c	7 c
Ponzer 2[†]	770 (30) bc	0.62 ac	350 (1) f	4.5 (0.06) f	0.51 (0.03) d	48(4) d	4(0.8) d
< 0.002”							
mineral							
Leon 1	2400 (500) a	0.51 ab	380 (10) a	5.9 (0.46) a	NA	NA	NA
Leon 2	2600 (180) a	0.49 b	230 (10) b	5.2 (0.03) ab	NA	NA	NA
Pantego	1700 (80) b	0.64 ab	200 (10) b	6.2 (0.12) c	NA	NA	NA
Rutlege	1200 (80) bc	0.63 ab	200 (10) c	4.6 (0.07) d	NA	NA	NA
organic							
Ponzer 1	1200 (70) bc	0.70 a	460 (10) a	5.5 (0.07) a	NA	NA	NA
Ponzer 2	1000 (180) c	0.50 ab	210 (20) c	4.7 (0.17) bd	NA	NA	NA

[†] Samples were not included in static incubation study.

[‡] Results for < 0.078” size class were derived from duplicate samples.

Table 11.2. Changes in pH, Eh DRP, dissolved Fe(II) and DOC concentrations of incubated soil samples after 60 d of anaerobic incubation at 25°C. Standard deviations of triplicate measurements are shown in parentheses. Significance at the $p < 0.01$ and $p < 0.05$ levels are denoted by "**" and "*".

Soil	**pH**	**ΔpH**	**ΔEh**	**ΔDRP**	**ΔFe(II)**	**ΔDOC**
			(V x 10^3)	**(µM) / (ppm)**		**(ppm)**
Leon 1	6.0	0.05 (0.03)	-184 (29)**	10.0 / 0.31**	-1.43 / -0.08	54 (4)**
Leon 2	5.6	0.08 (0.04)	-200 (20)**	6.13 / 0.19*	29.5 / 1.65**	80 (8)**
Rutlege	5.3	0.17 (0.14)	-179 (40)**	13.2 / 0.41**	14.5 / 0.81**	84 (4)**
Ponzer 1	5.5	0.07 (0.04)	-210 (15)**	48.4 / 1.50**	17.7 / 0.99**	118 (12)**

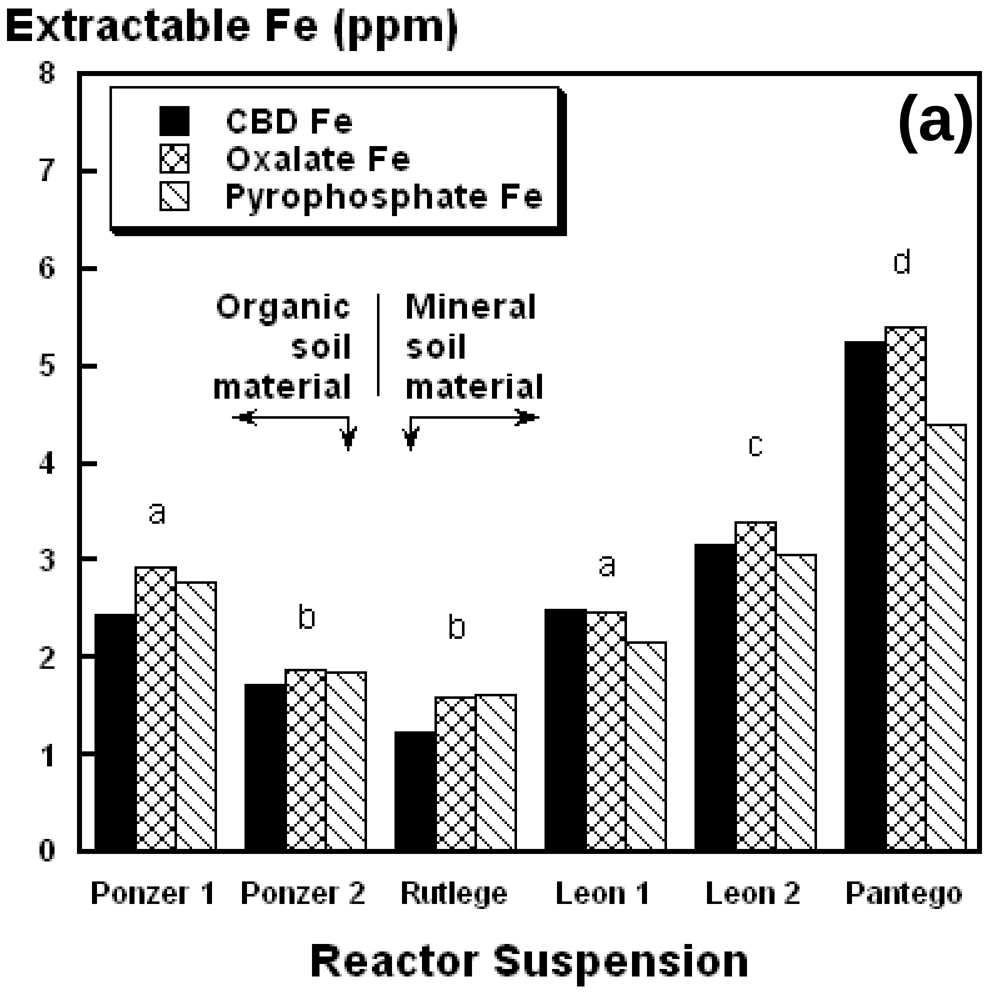

Figure 11.1a. Extractable forms of Fe (mg kg^{-1}) in the < 0.002" solids used in stirred reactor incubation studies. Extractions performed on separate samples. CBD = citrate bicarbonate dithionite.

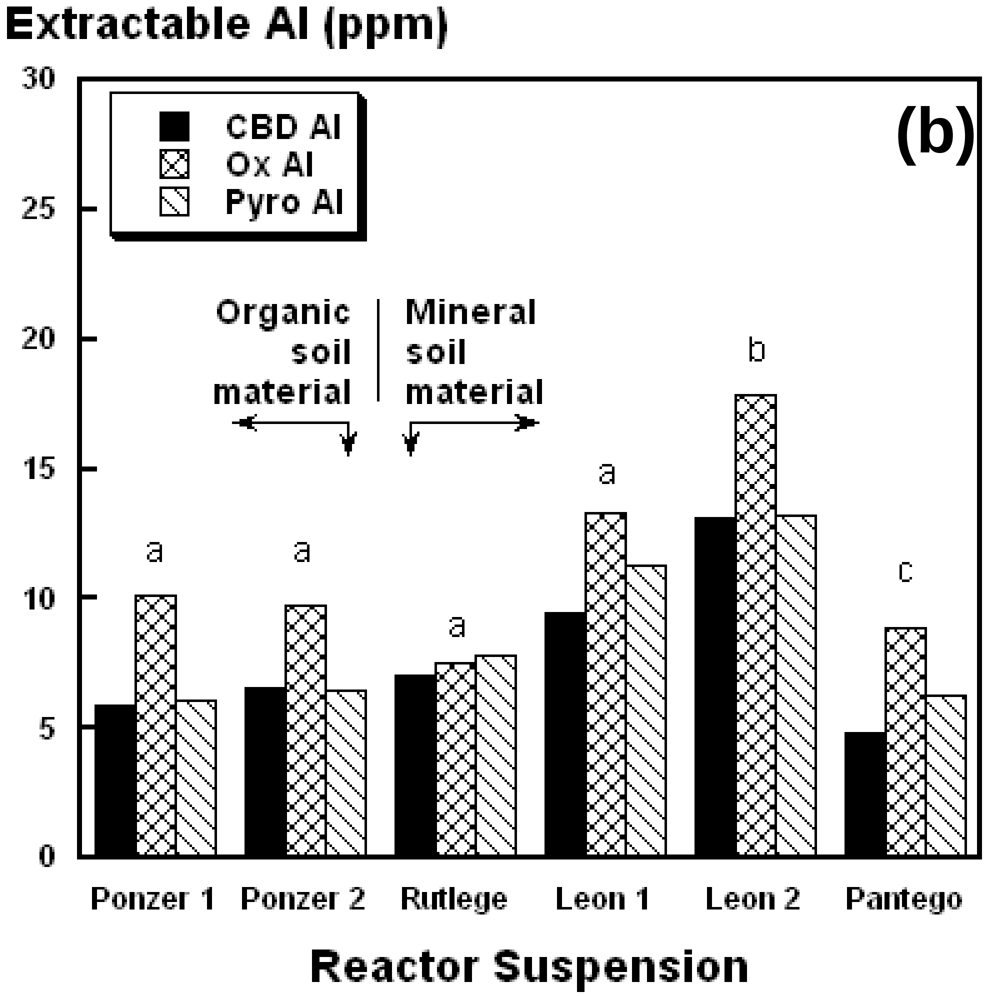

Figure 11.1b. Extractable forms of Al (mg kg^{-1}) in the < 0.002" solids used in stirred reactor incubation studies. Extractions performed on separate samples. CBD = citrate bicarbonate dithionite.

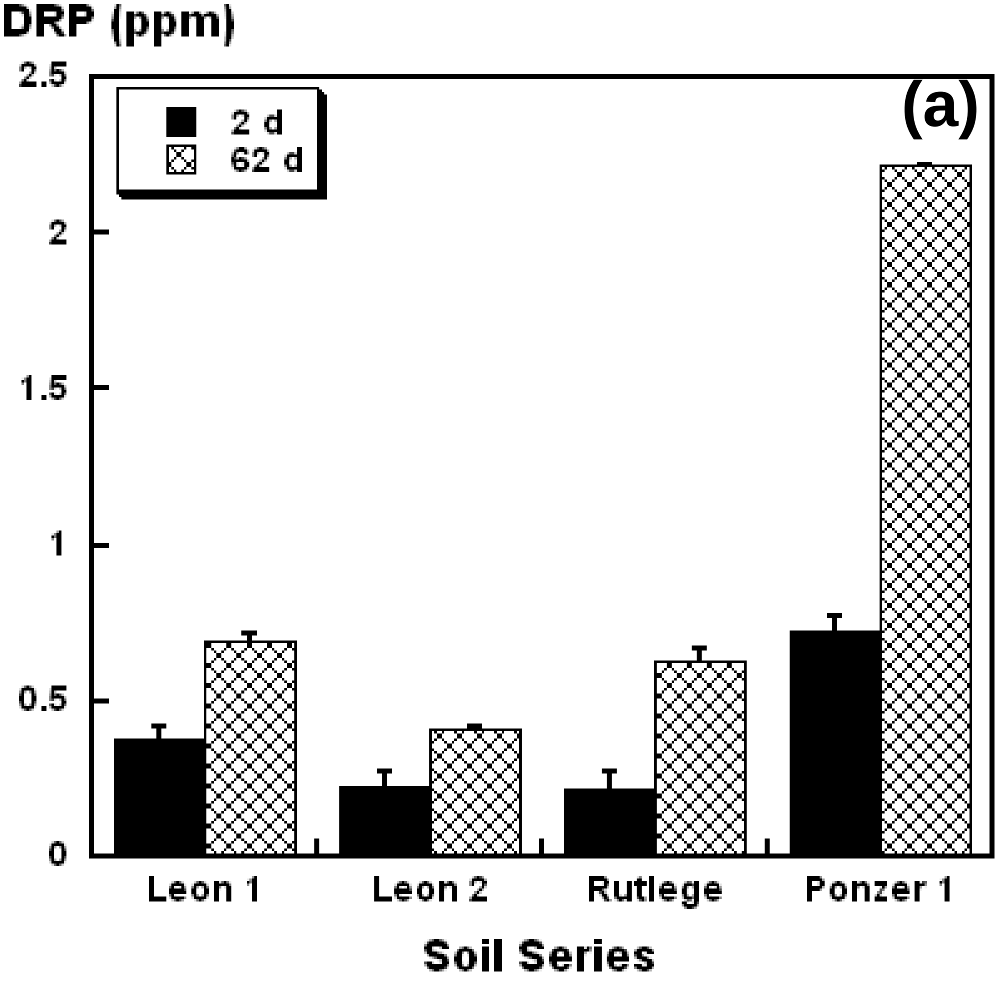

Figure 11.2a. Concentrations of DRP after 2 and 62 d of incubation at 77 °F.

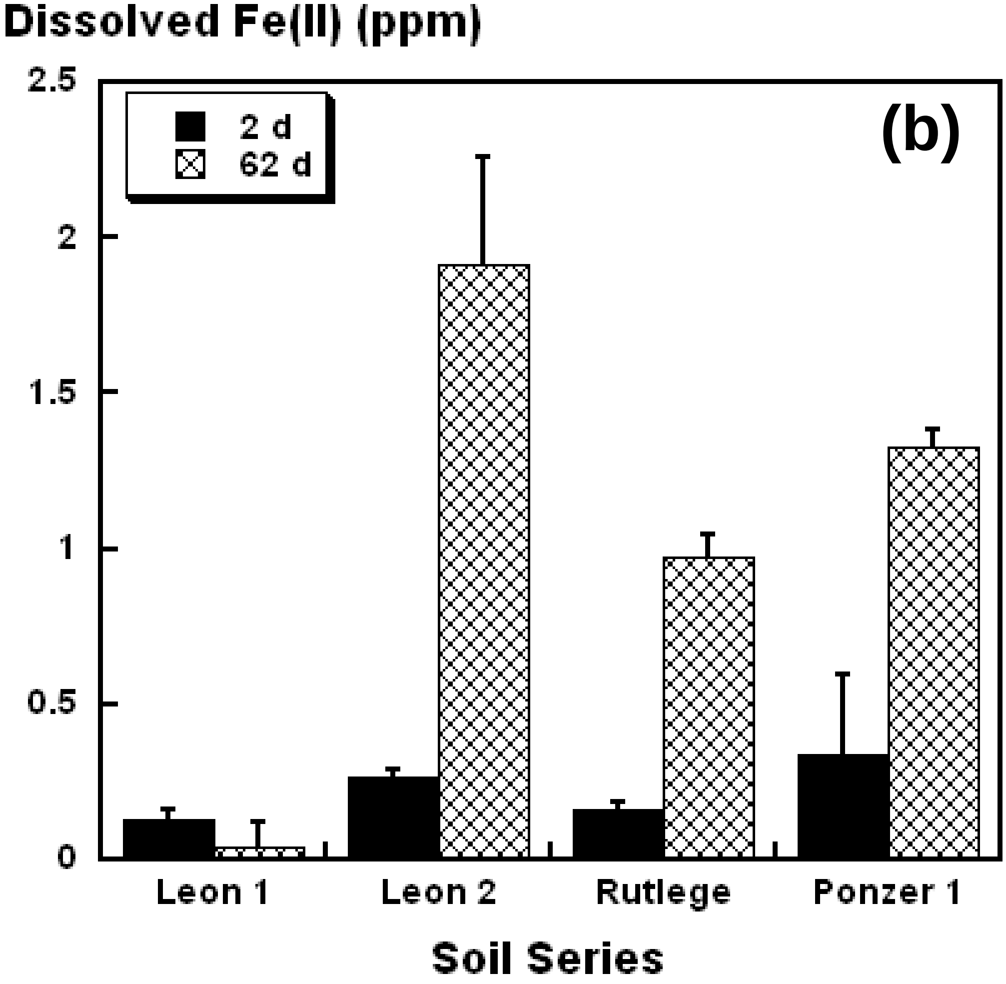

Figure 11.2b. Concentrations of dissolved Fe(II) after 2 and 62 d of incubation at 77 °F.

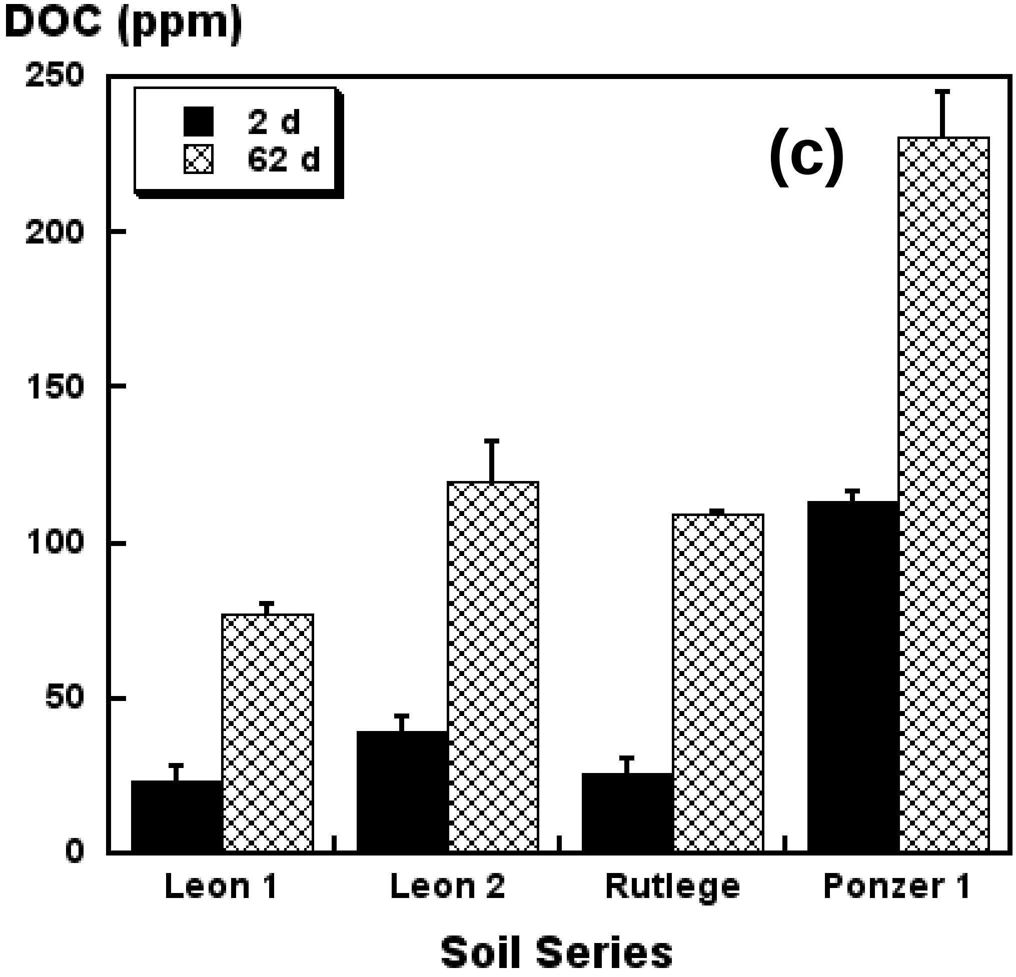

Figure 11.2c. Concentrations of DOC (c) after 2 and 62 d of incubation at 77 °F.

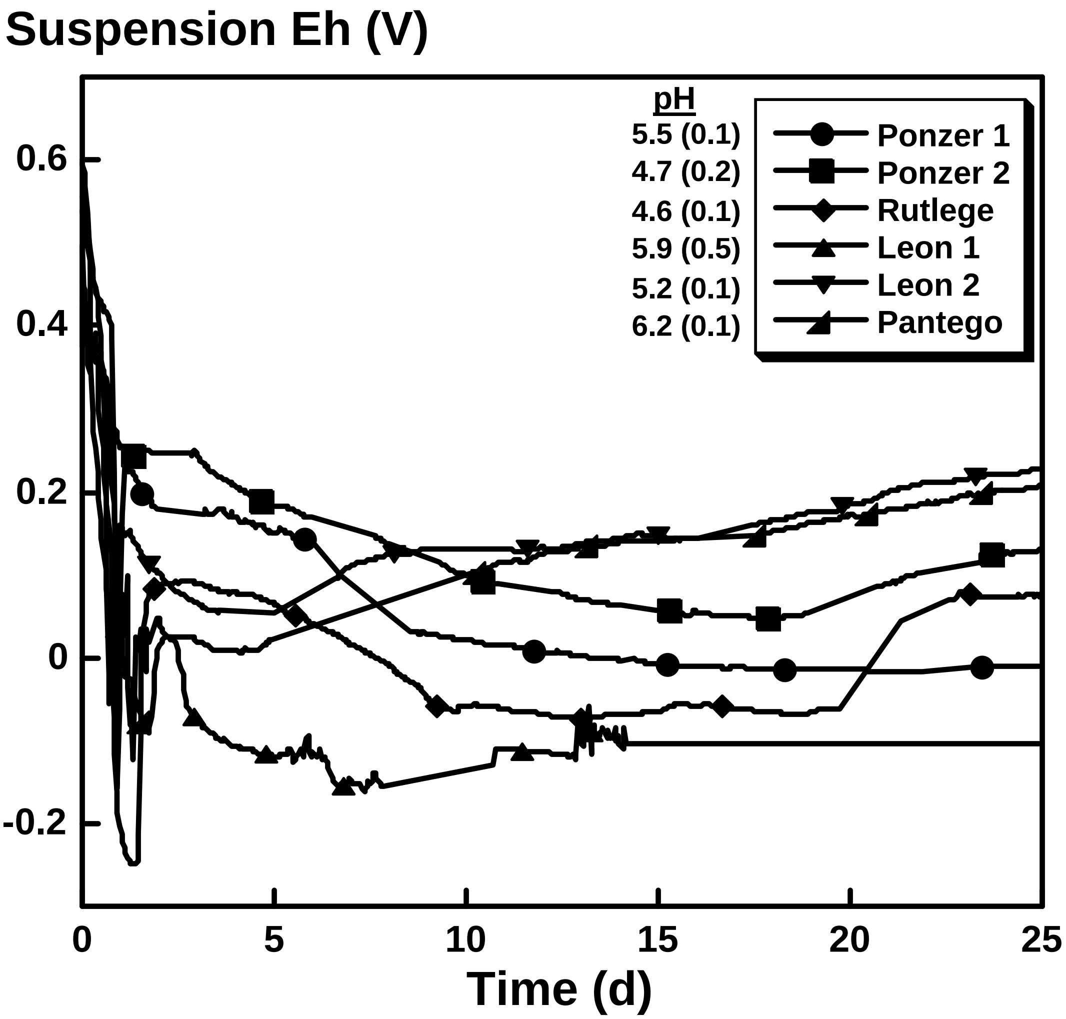

Figure 11.3. Temporal trends in Eh (V) plotted continuously for selected replicates of all suspensions. No significant change in pH occurred, standard deviation of duplicate measurements are shown in parentheses.

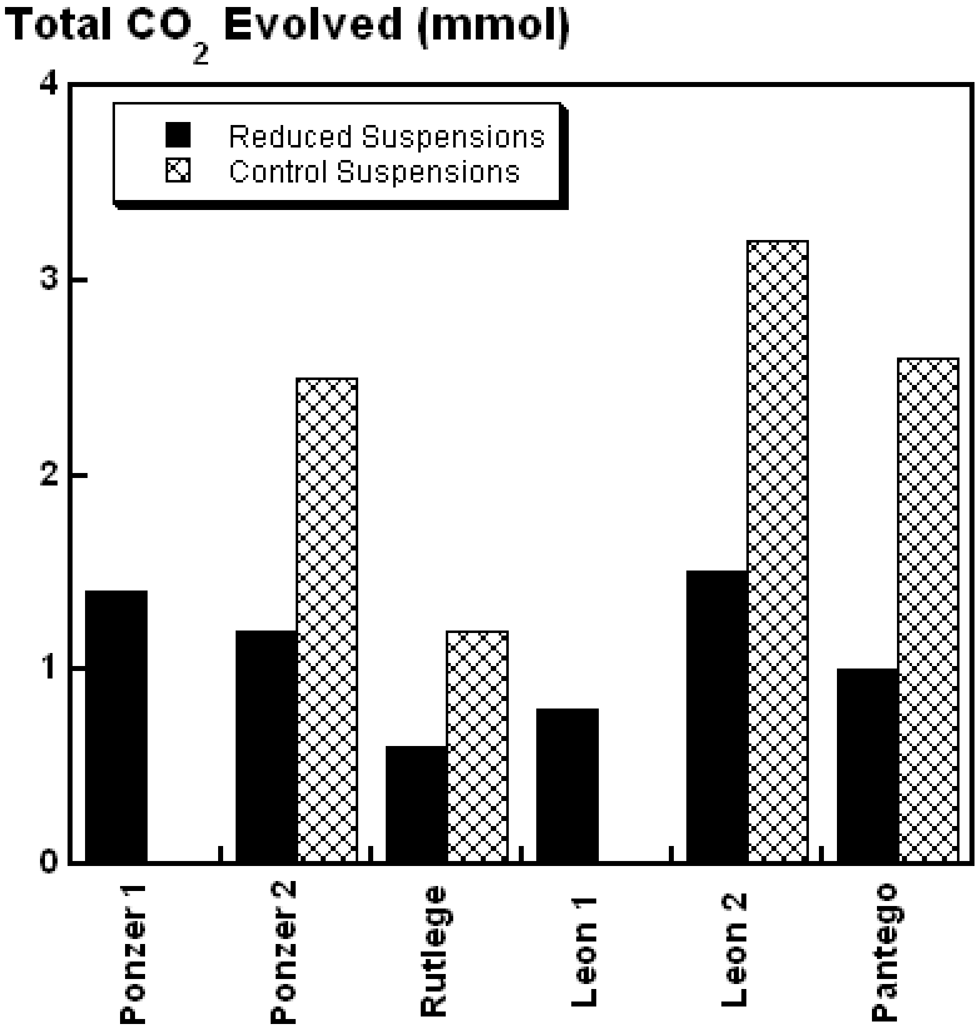

Figure 11.4. Total CO_2 evolved (mmol) from reduced and oxidized suspensions over 25 d. Error bars show standard deviations from duplicate reactors. No error bars are shown for oxidized samples, which were not replicated. Data from Ponzer 1 and Leon 1 oxidized suspensions are not available.

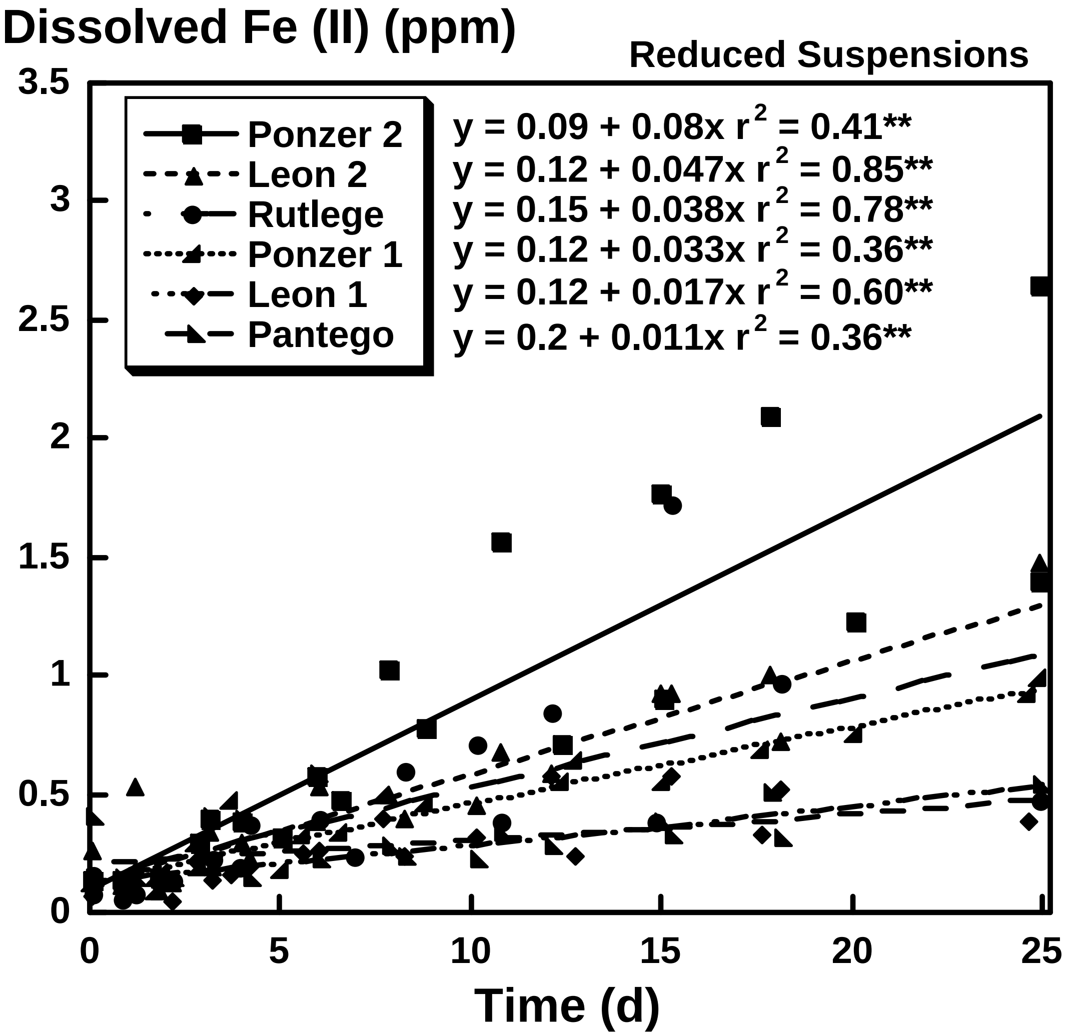

Figure 11.5. Dissolved Fe(II) (ppm) in reactor suspensions. Significant linear trends at the 0.01 level are noted by "**".

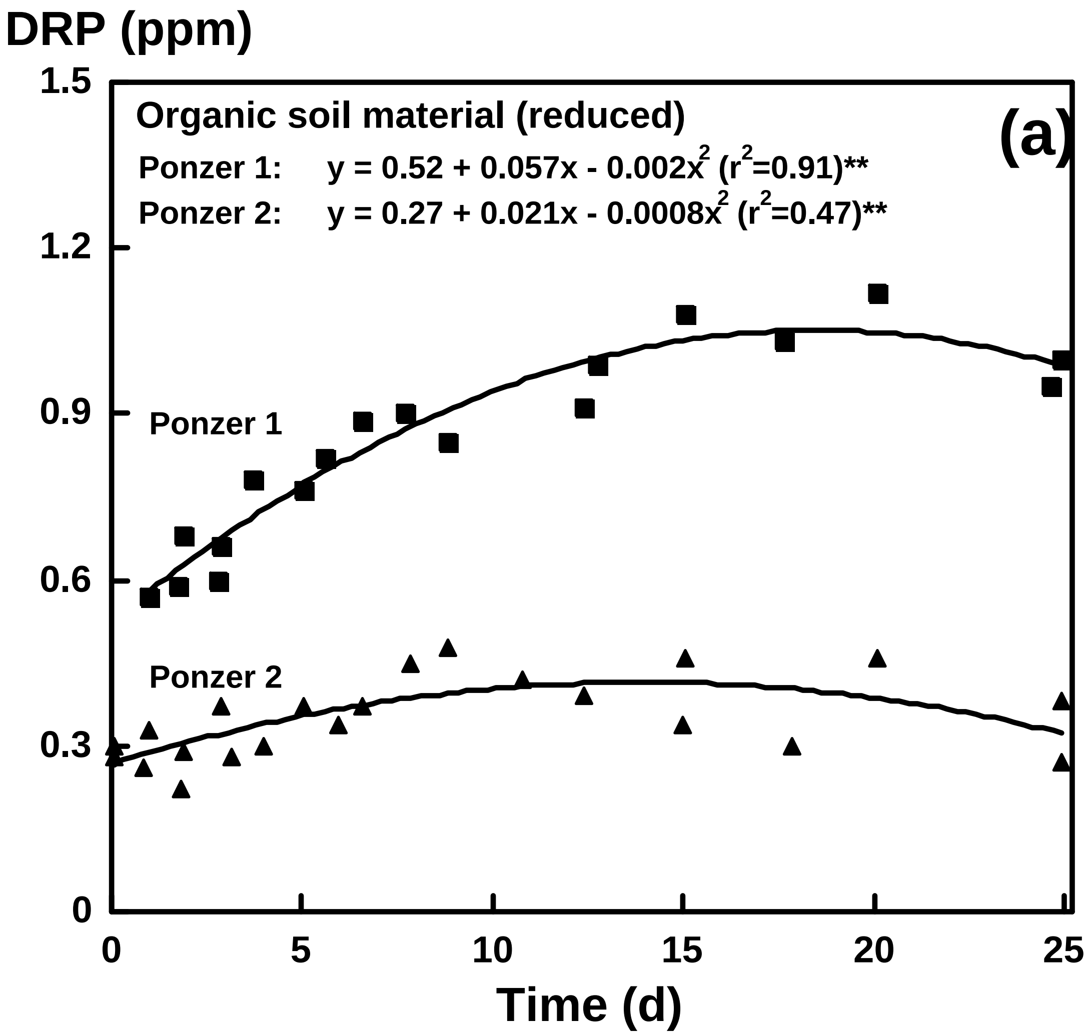

Figure 11.6a. Dissolved reactive phosphorus (DRP) concentrations in reduced suspensions of < 0.002" organic soil separates. Data from reduced treatments were statistically fit by the better of linear and quadratic models. Significance at the 0.01 level is shown by "**". Control treatments were not replicated.

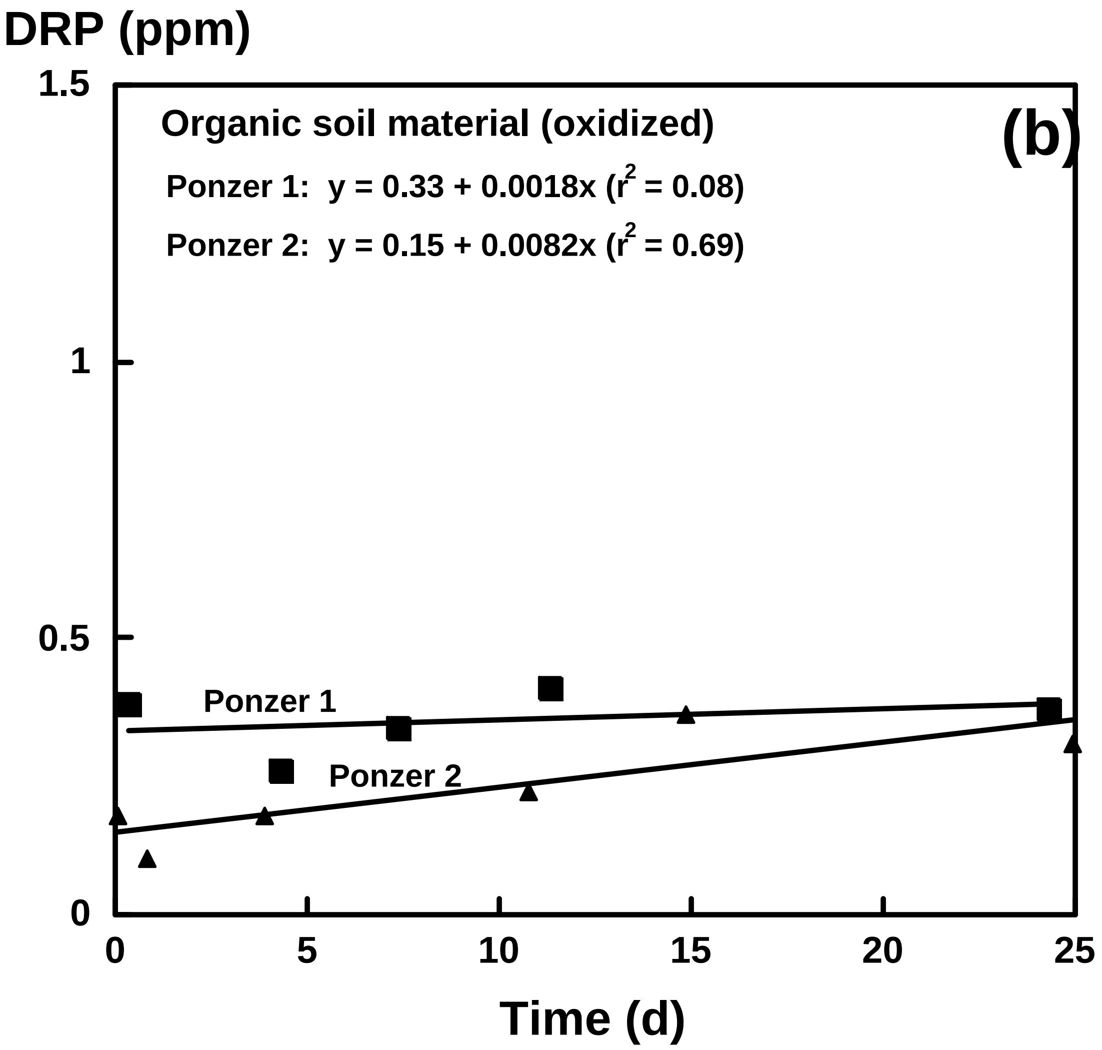

Figure 11.6b. Dissolved reactive phosphorus (DRP) concentrations in oxidized suspensions of < 0.002” organic soil separates. Data from reduced treatments were statistically fit by the better of linear and quadratic models. Significance at the 0.01 level is shown by “**”. Control treatments were not replicated.

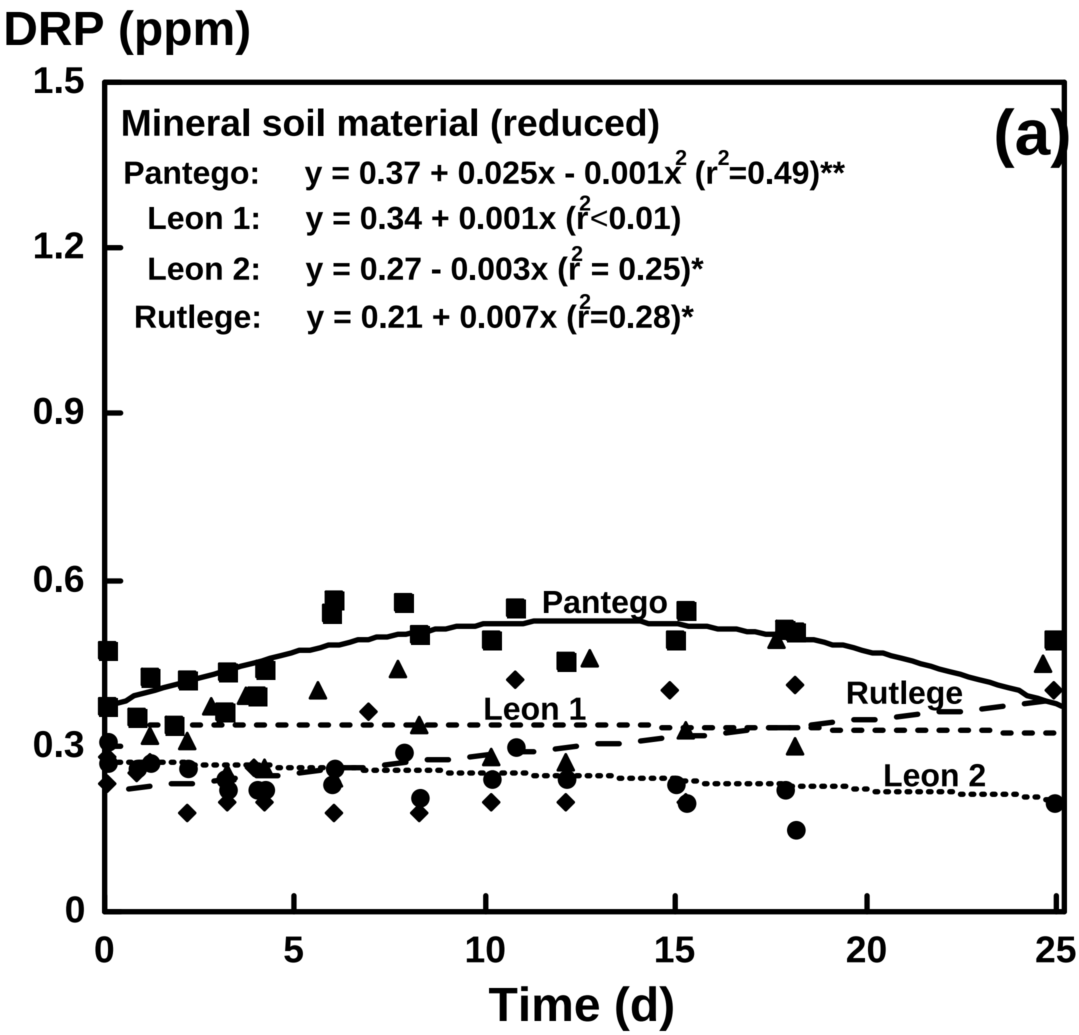

Figure 11.7a. Dissolved reactive phosphorus (DRP) concentrations in reduced suspensions of < 0.002" mineral soil separates. Data from reduced treatments were statistically fit by the better of linear and quadratic models. Significance at the 0.01 and 0.05 level is shown by "**" or "*", respectively. Control treatments were not replicated.

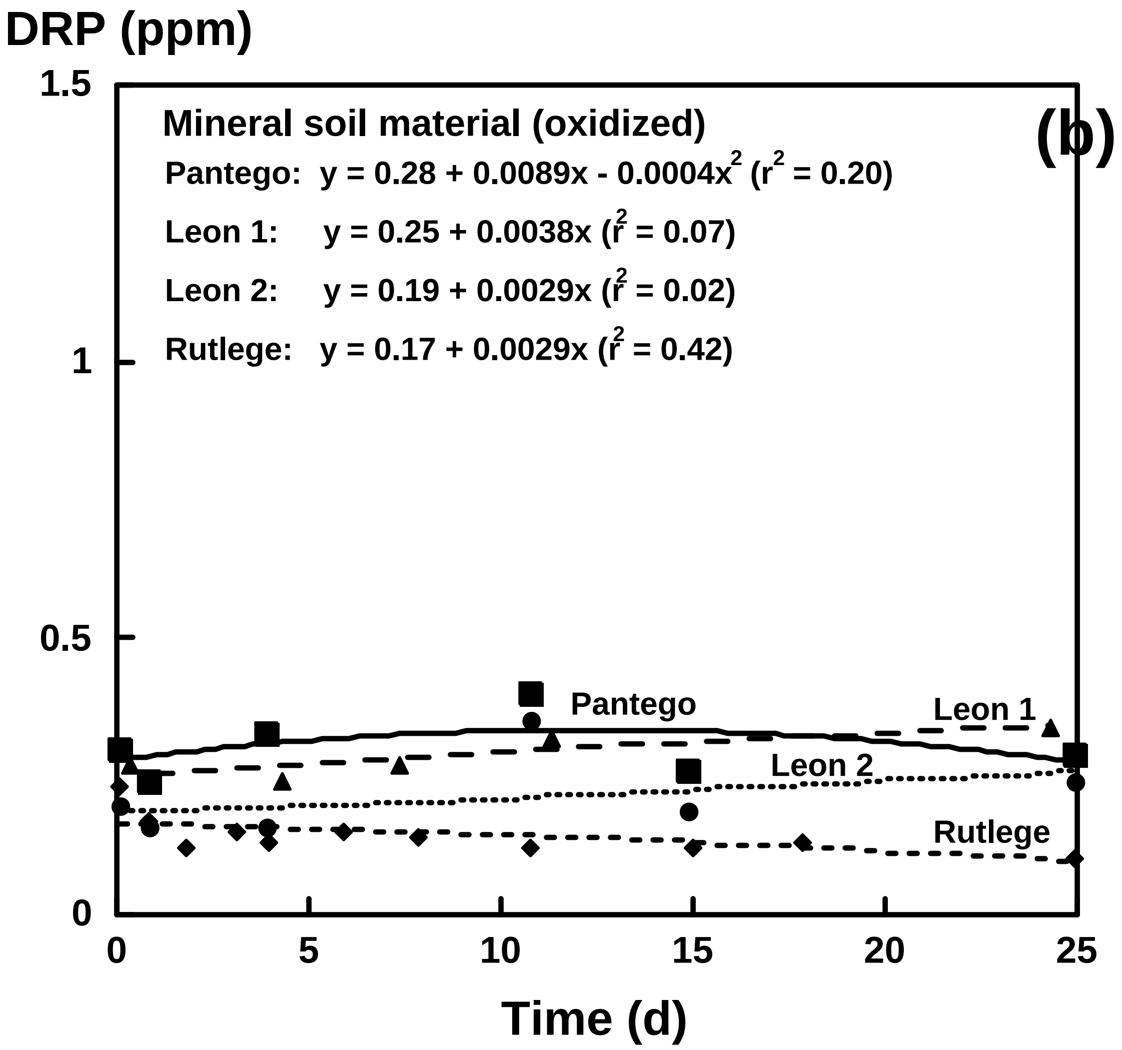

Figure 11.7b. Dissolved reactive phosphorus (DRP) concentrations in oxidized suspensions of < 0.002" mineral soil separates. Data from reduced treatments were statistically fit by the better of linear and quadratic models. Significance at the 0.01 and 0.05 level is shown by "**" or "*", respectively. Control treatments were not replicated.

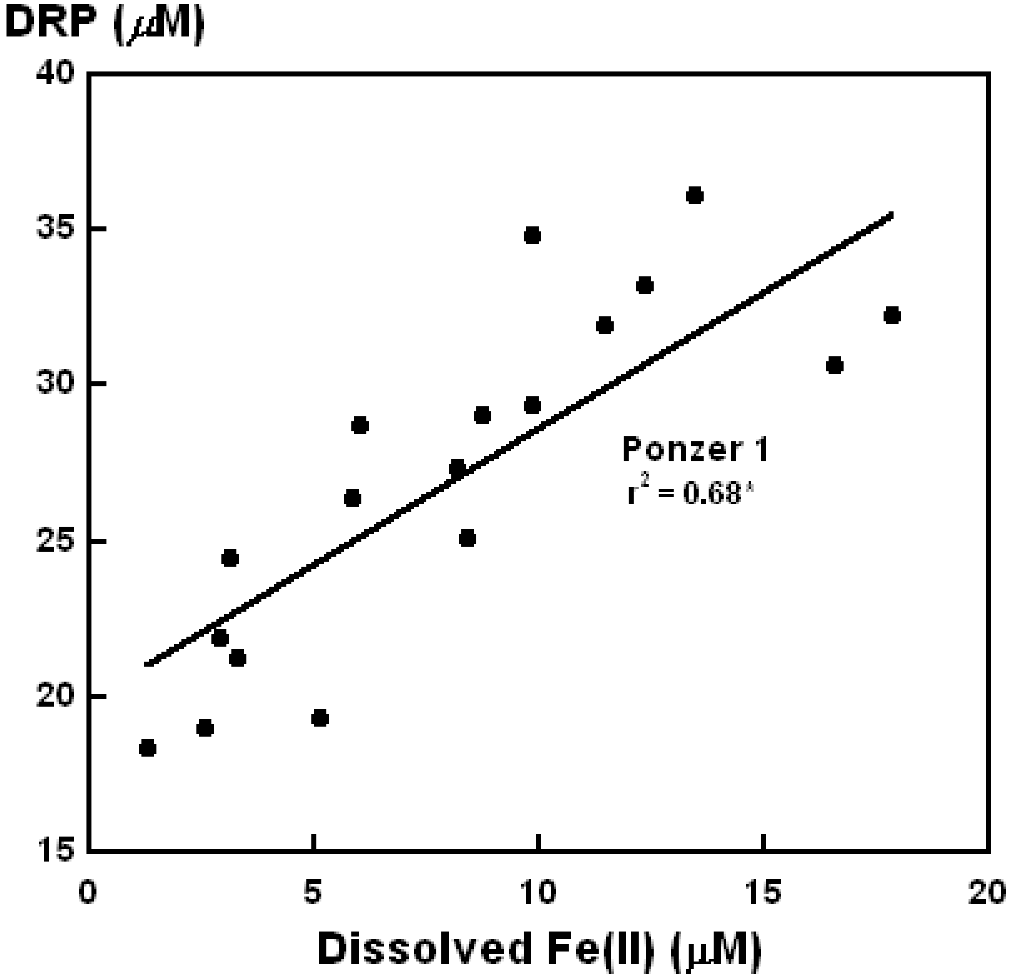

Figure 11.8. Scatter plots of DRP and Fe(II) in the Ponzer 1 soil suspension. Data are presented in μmol L^{-1} for chemical relevance.

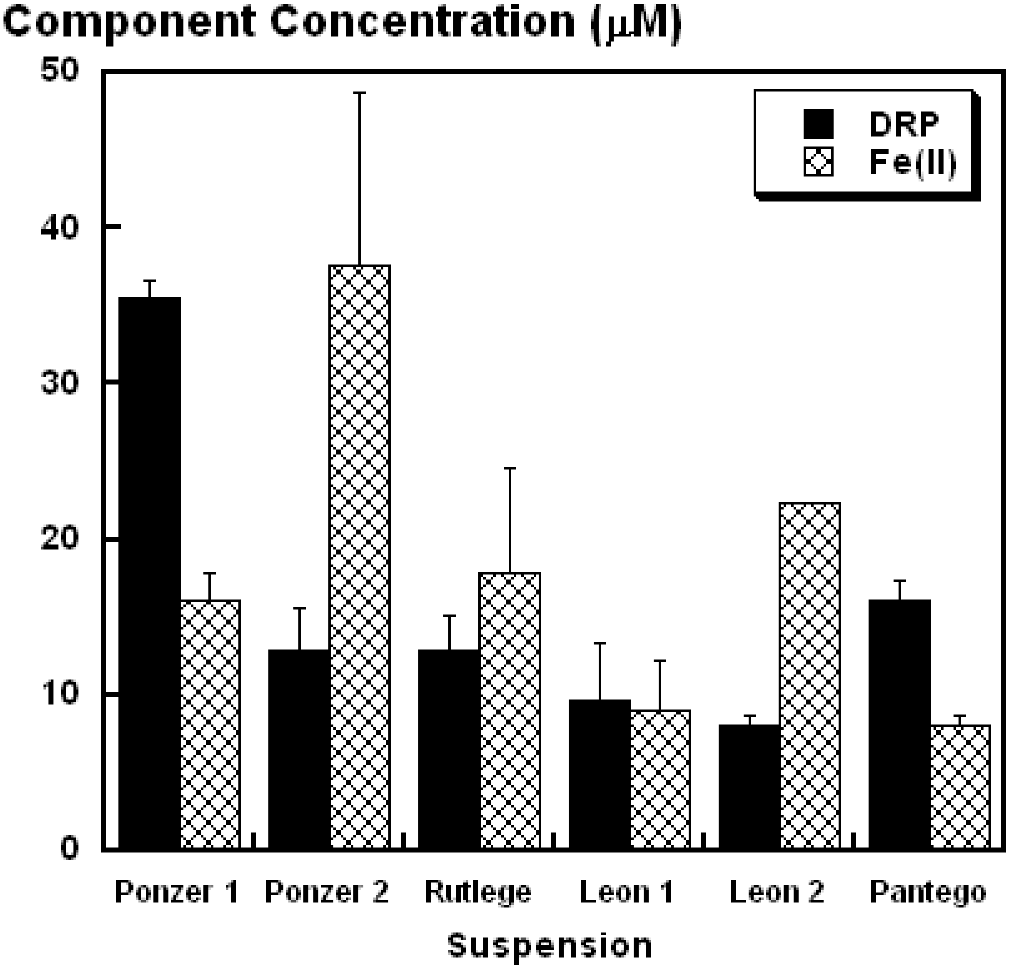

Figure 11.9. Concentrations of DRP and Fe(II) in the reactor solutions at t = 20 d (maximum [DRP]). Data are presented in μmol L^{-1} for chemical relevance.

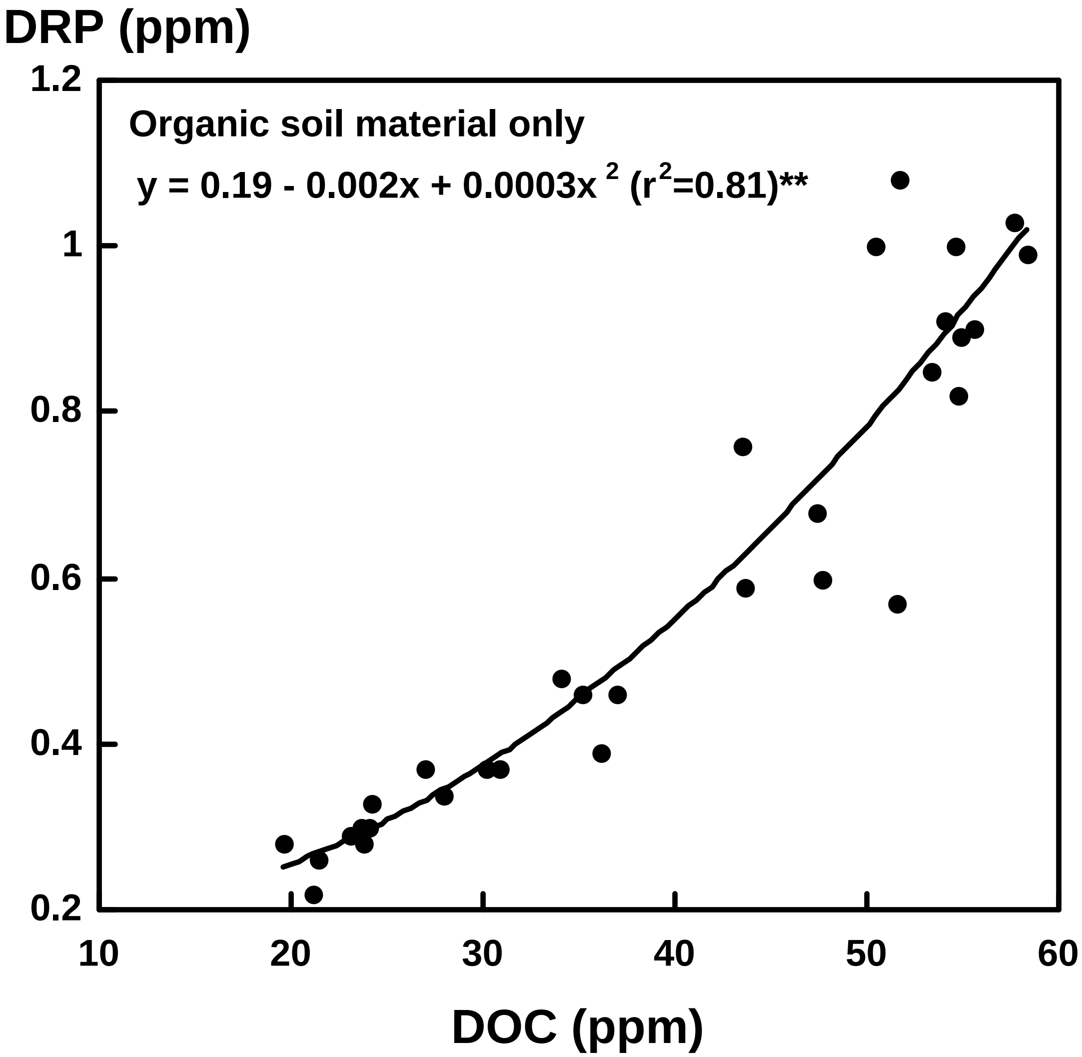

Figure 11.10. Scatter plots of DRP and DOC for the organic samples. Significance at the $p < 0.05$ level is noted by "**".

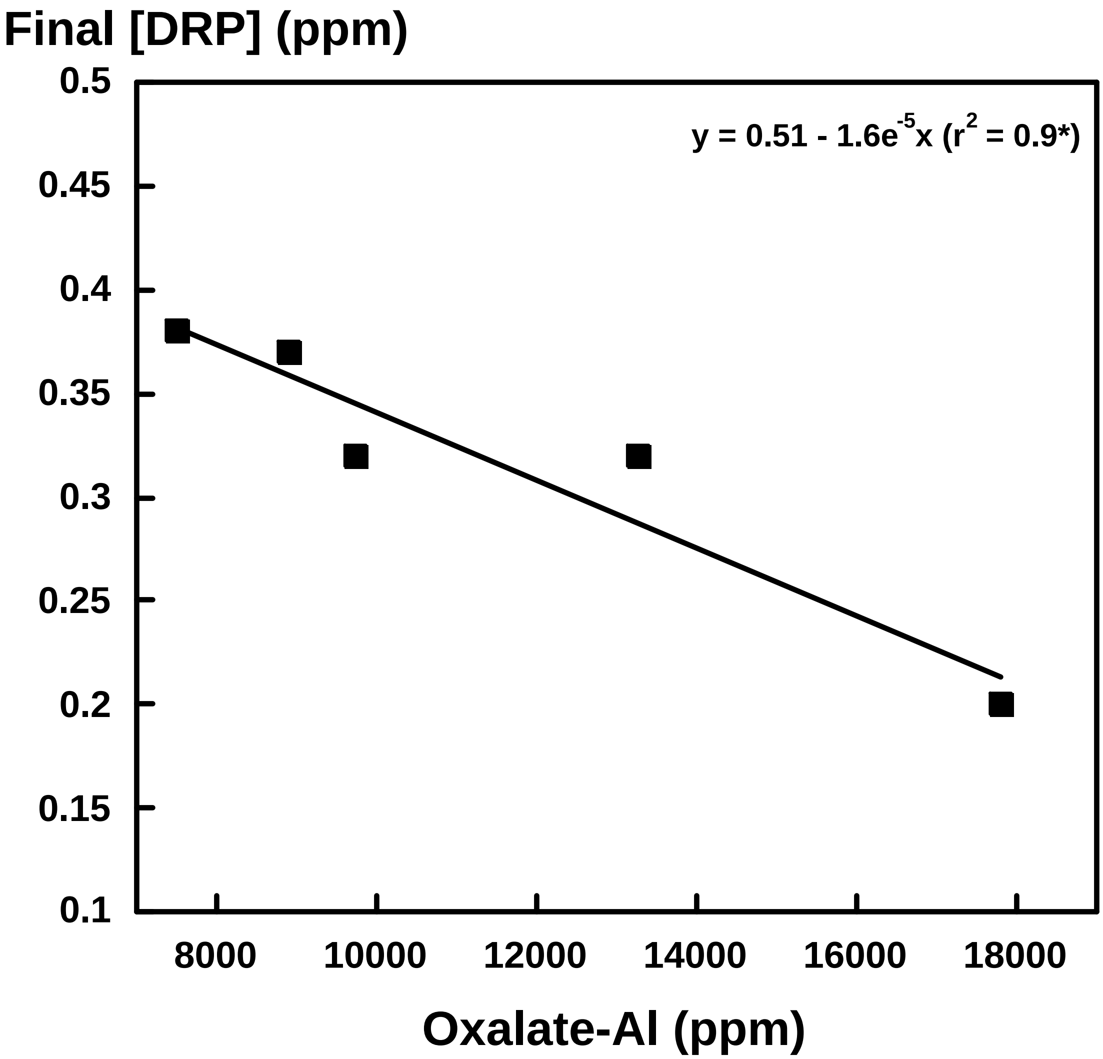

Figure 11.11. Final [DRP] as predicted by Al_{ox} concentrations in the reactor solids. DRP concentrations shown are from best fit models (Figures 6a and 7a) of duplicate reduced suspensions. Ponzer 1 data (x = 10.2 lb 1000 lb^{-1}, y = 0.98 ppm) are not displayed.

Chapter 12

MAJOR FINDINGS AND CONCLUSIONS

M.J. Vepraskas

CONCLUSIONS RELATED TO REFERENCE BAYS

1. Bulk density, total porosity, and particle density values were similar among the Oi, Oe, and Oa horizons of the southeastern organic soils under forest vegetation. The bulk density of the organic soil horizons was approximately 9.98 lb ft^{-3} (0.16 g cm^{-3}). Total porosity values were high (0.90 ft^3 ft^{-3}), and particle densities were approximately 93.6 lb ft^{-3} (1.5 g cm^{-3}). Mean saturated hydraulic conductivity values were significantly different among the horizons, measuring 18, 2.8, and 0.6 in h^{-1} for samples from Oi, Oe, and Oa soil layers, respectively. These results can be used in calibrated hydrologic models to aid in understanding the natural hydrology of Carolina Bay wetlands and in predicting the hydrology of wetland restoration sites with organic soils.

2. DRAINMOD hydrologic models were successful in simulating water table depths at all well locations in the natural (undrained) reference bays over the 2 yr calibration period despite not having regularly spaced drains. Groundwater inflow was observed and was a necessary water budget component to calibrate the hydrologic models for areas near the bay perimeters. This inflow accounted for 16% of total water input on average. The source area for this inflow is not known, but for some locations is believed to originate from a semi-confined aquifer below the bay.

Model simulation results revealed that locations near the perimeters of the bays act as recharge, discharge, or flow through wetlands under various conditions. Groundwater outflow exceeded inflow on an annual basis, but inflow could exceed outflow during periods of low rainfall. On the other hand, locations near the bay centers consistently acted as recharge wetlands. The elevation of the water table in these areas was controlled primarily by rainfall and evapotranspiration. During periods when evapotranspiration exceeded rainfall, the water table depth increased. When rainfall exceeded evapotranspiration, the water table depth decreased.

3. There are distinct differences in the hydrology needed for growth of Pond Pine Woodland plant community as compared to either the Nonriverine Swamp Forest and Bay Forest communities. In addition, roots of trees growing in Pond Pine Woodland and Nonriverine Swamp Forest plant communities could reach mineral soil layers, while trees in the Bay Forest community could not due to very deep organic soil layers on the surface. We believe these differences allow larger trees to grow in the Pond Pine Woodland and Nonriverine Swamp Forest communities than in the Bay Forest community.

Based on observations of reference bay conditions and model results, recommended hydrologies and soil conditions (organic matter content and P concentration) for the plant communities are as follows: If the thickness of organic soil layers is less than 16 in. (40 cm) and the median hydroperiod (i.e. when the water table is above the land surface) is 45-135 days per water year, then tree species typical of the Pond Pine Woodland community should be planted there. For sites with organic soil layers between approximately 8 and 31 in. (20 and 80 cm) thick, phosphorus levels greater than 18 mg dm^{-3}, and a median hydroperiod of 300-320 days per water year, the Nonriverine Swamp Forest community would be a good choice for restoration. For sites with similar hydroperiods, but with organic layer thicknesses greater than 8 in. (20 cm) and phosphorus levels below 18 mg dm^{-3}, the Bay Forest community would be recommended.

CONCLUSIONS RELATED TO JUNIPER BAY

4. Soil electrical conductivity (EC) was measured via electromagnetic induction (EMI). Published work indicated that EC could be used to estimate clay percentage of subsoil layers. It was felt that we could use EC to prepare maps of subsurface clay layers that are critical to restoring wetland hydrology. While a relationship between EC and clay percentage was developed for Juniper Bay, we could not determine exactly the depth that was being measured by the EMI meters tested. Therefore, our conclusion is that EC measured via EMI cannot be used easily to map subsurface clay layers in Coastal Plain sediments. Ground penetrating radar appears to be a better tool for subsurface exploration.

5. Total organic carbon (TOC), PO_4-P, Ca and Mg content in soil solution at various depths close to the surface were observed to be higher following storm events than during baseflow conditions. Monitored subsurface hydraulic gradients also indicate that faster subsurface transport towards drainage ditches of water with high nutrient content is triggered by storm events. This resulted in a higher TOC, PO_4-P, Ca and Mg content in surface water that is carried off-site. This suggests that following a storm event, Juniper Bay could be a source of off-site nutrient pollution.

6. Nitrate (NO_3^-) in the soil solution can be transported horizontally in the capillary fringe (CF) above the water table in Juniper Bay soils. A NO_3^- plume was monitored as it entered the CF from the unsaturated zone and moved horizontally in the CF until it was partially carried below the water table by rain events. Nitrate persisted in the CF, and this allowed it to be transported to greater horizontal distances than in the shallow groundwater. We believe that conditions favoring denitrification were not totally met in the CF due largely to its remaining aerobic for relatively long periods.

It appears that analyzing water chemistry of groundwater samples alone may result in underestimation of the amount of NO_3^- that can travel horizontally through the subsurface from a source. Failure to account for NO_3^- or other pollutants in the CF may underestimate the chances of groundwater contamination.

7. Field studies showed that the time for anaerobic conditions to develop after saturation begins (Lag time) was related to soil organic C percentage but not to average daily temperature. When soil organic carbon was <3%, the Lag values ranged from 3 to 48 d. Soils containing higher soil organic carbon concentrations had Lag values being 5 d or less in

most cases. These results suggest that in created wetlands the minimum amount of soil organic C needed to ensure wetland biogeochemical functions occur is 3%. There appears to be little advantage to having higher organic C levels, although higher levels pose no problems. When soil organic C percentages are below 3%, soils must remain saturated for longer periods for wetland biogeochemical reactions to occur. In short, it is more difficult to restore wetlands when organic C percentages are <3%.

8. Laboratory studies confirmed that the time to develop anaerobic conditions in saturated soils decreases as organic C levels increase, and that at soil organic C levels >3%, the time to develop anaerobic conditions remained constant. The relationships found between soil properties and reduction rates can be used along with hydrologic data to predict durations of anaerobic conditions from water table data.

9. Laboratory experiments showed that saturating and reducing soils will increase amounts of dissolved reactive P in solution. In the experiments, P dissolution was highly correlated with dissolved organic carbon concentrations, possibly because the dissolved organic C displaces P held on soil particles. Therefore, dissolution of P is predicted to be greatest in the organic soils, where dissolved organic carbon concentrations are likely to be highest. The dissolved P concentrations were > 1 ppm and believed to be high enough to contribute to eutrophication of surface waters. This could lead to fish kills in rivers receiving water draining from restored wetlands.

Chapter 13

RECOMMENDATIONS AND TECHNOLOGY TRANSFER PLAN

RECOMMENDATIONS

1. It is important to model restored site hydrology and use the results to choose target vegetation communities to match reference communities. DRAINMOD is a suitable model to use, but there may be others. Drainage ditches need not be present in order to use the DRAINMOD model.

2. Monitor restoration sites for release of P to surface water. Most P will be released during large storms (>2 in. of rainfall) and the impacts of these must be included in measurements. Organic soils will likely be greater sources of P than mineral soils because the amount of P released will increase with the amount of dissolved organic C produced.

3. In constructing wetland restoration sites, topsoil should contain at least 3% soil organic C or 5% organic matter. Less amounts of organic C delay the time a soil becomes anaerobic and reduced.

4. The perimeter ditch at Juniper Bay needs to remain open and functional to avoid surface water ponding to depths that could kill plants. An open perimeter ditch will also lessen the chance of hydrologic trespass occurring.

TECHNOLOGY TRANSFER

The data collected to date comprise one of the largest sets of information on Carolina Bays in the country. This information will be disseminated through research articles, talks at professional meetings, and field trips. Chapters 2 through 11 of this report each represent a scientific article that has been or will be published. In addition, most chapters were used as a part of a student's graduate thesis or dissertation that is available through NC State University's library. Titles of theses and dissertations are included in the Acknowledgements at the end of each chapter in this report. Information in each of the chapters has or will be presented at a scientific meeting.